frontiers | Research Topics

Advances in genetics and molecular diagnosis in colorectal cancer.

Edited by
Jorge Melendez-Zajgla and Farhadul Islam

Published in
Frontiers in Oncology
Frontiers in Medicine
Frontiers in Immunology
Frontiers in Surgery

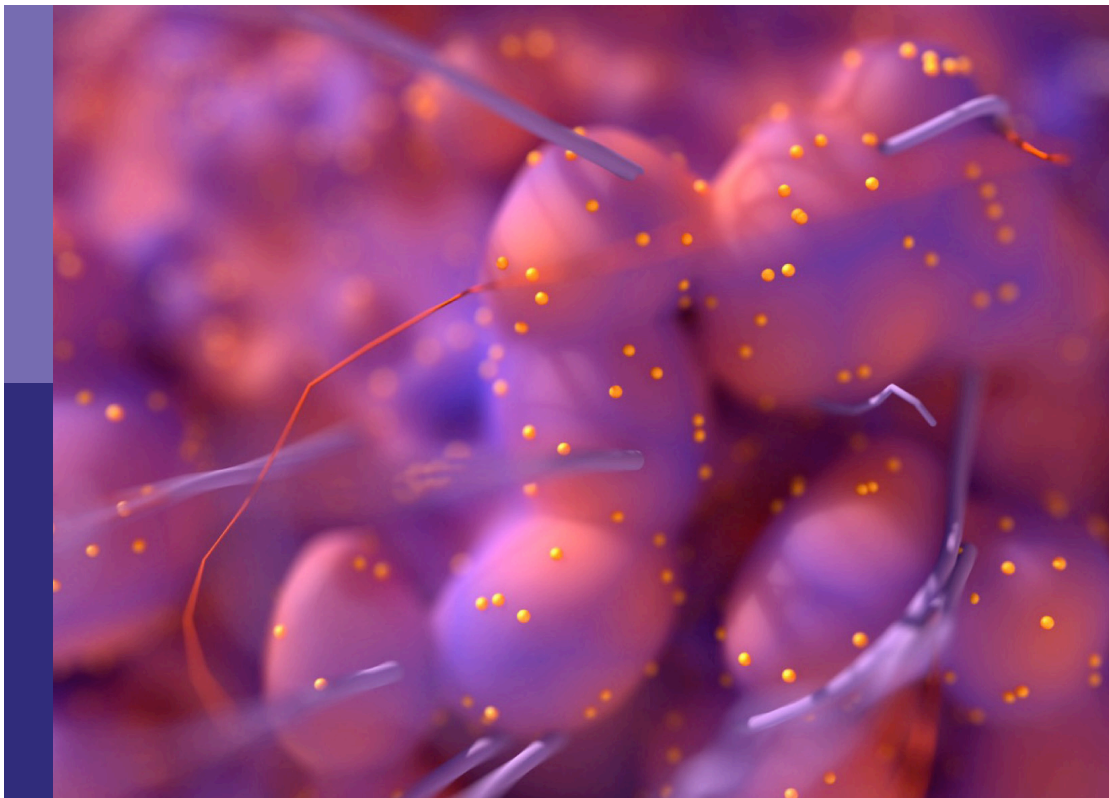

ISSN 1664-8714
ISBN 978-2-8325-3611-7
DOI 10.3389/978-2-8325-3611-7

About Frontiers

Frontiers is more than just an open access publisher of scholarly articles: it is a pioneering approach to the world of academia, radically improving the way scholarly research is managed. The grand vision of Frontiers is a world where all people have an equal opportunity to seek, share and generate knowledge. Frontiers provides immediate and permanent online open access to all its publications, but this alone is not enough to realize our grand goals.

Frontiers journal series

The Frontiers journal series is a multi-tier and interdisciplinary set of open-access, online journals, promising a paradigm shift from the current review, selection and dissemination processes in academic publishing. All Frontiers journals are driven by researchers for researchers; therefore, they constitute a service to the scholarly community. At the same time, the *Frontiers journal series* operates on a revolutionary invention, the tiered publishing system, initially addressing specific communities of scholars, and gradually climbing up to broader public understanding, thus serving the interests of the lay society, too.

Dedication to quality

Each Frontiers article is a landmark of the highest quality, thanks to genuinely collaborative interactions between authors and review editors, who include some of the world's best academicians. Research must be certified by peers before entering a stream of knowledge that may eventually reach the public - and shape society; therefore, Frontiers only applies the most rigorous and unbiased reviews. Frontiers revolutionizes research publishing by freely delivering the most outstanding research, evaluated with no bias from both the academic and social point of view. By applying the most advanced information technologies, Frontiers is catapulting scholarly publishing into a new generation.

What are Frontiers Research Topics?

Frontiers Research Topics are very popular trademarks of the *Frontiers journals series*: they are collections of at least ten articles, all centered on a particular subject. With their unique mix of varied contributions from Original Research to Review Articles, Frontiers Research Topics unify the most influential researchers, the latest key findings and historical advances in a hot research area.

Find out more on how to host your own Frontiers Research Topic or contribute to one as an author by contacting the Frontiers editorial office: frontiersin.org/about/contact

Advances in genetics and molecular diagnosis in colorectal cancer.

Topic editors

Jorge Melendez-Zajgla — National Institute of Genomic Medicine (INMEGEN), Mexico

Farhadul Islam — University of Rajshahi, Bangladesh

Citation

Melendez-Zajgla, J., Islam, F., eds. (2023). *Advances in genetics and molecular diagnosis in colorectal cancer.* Lausanne: Frontiers Media SA. doi: 10.3389/978-2-8325-3611-7

Table of contents

05 Editorial: Advances in genetics and molecular diagnosis in colorectal cancer
Farhadul Islam and Jorge Melendez-Zajgla

07 Benign gallbladder disease is a risk factor for colorectal cancer, but cholecystectomy is not: A propensity score matching analysis
Qiong Qin, Wei Li, Ao Ren, Rong Luo and Shiqiao Luo

16 Tumor genomic profiling and personalized tracking of circulating tumor DNA in Vietnamese colorectal cancer patients
Huu Thinh Nguyen, Trieu Vu Nguyen, Van-Anh Nguyen Hoang, Duc Huy Tran, Ngoc An Le Trinh, Minh Triet Le, Tuan-Anh Nguyen Tran, Thanh Huyen Pham, Thi Cuc Dinh, Tien Sy Nguyen, Ky Cuong Nguyen The, Hoa Mai, Minh Tuan Chu, Dinh Hoang Pham, Xuan Chi Nguyen, Thien My Ngo Ha, Duy Sinh Nguyen, Du Quyen Nguyen, Y-Thanh Lu, Thanh Thuy Do Thi, Dinh Kiet Truong, Quynh Tho Nguyen, Hoai-Nghia Nguyen, Hoa Giang and Lan N. Tu

27 Risk factor analysis of malignant adenomas detected during colonoscopy
Hong Hu, Xiaoyuan Gong, Kai Xu, Shenzheng Luo, Wei Gao, Baiwen Li and Dadao Jing

35 Pan-Cancer analysis and experimental validation identify the oncogenic nature of ESPL1: Potential therapeutic target in colorectal cancer
Yuchen Zhong, Chaojing Zheng, Weiyuan Zhang, Hongyu Wu, Meng Wang, Qian Zhang, Haiyang Feng and Guiyu Wang

52 Association of clinical outcomes and the predictive value of T lymphocyte subsets within colorectal cancer patients
Chaofeng Yuan, Jiannan Huang, Haitao Li, Rongnan Zhai, Jinjing Zhai, Xuedong Fang and Yuanyu Wu

63 Image acquisition as novel colonoscopic quality indicator: a single-center retrospective study
Ke Zhang, Abdiwahid Mohamed Bile, Xinyi Feng, Yemin Xu, Yaoyao Li, Qiang She, Guiqing Li, Jian Wu, Weiming Xiao, Yanbing Ding and Bin Deng

71 The clinical relevance and prediction efficacy from therapy of tumor microenvironment related signature score in colorectal cancer
Xiang Jun, Shengnan Gao, Lei Yu and Guiyu Wang

83 Genomic landscape and expression profile of consensus molecular subtype four of colorectal cancer
Yujie Lu, Dingyi Gu, Chenyi Zhao, Ying Sun, Wenjing Li, Lulu He, Xiaoyan Wang, Zhongyang Kou, Jiang Su and Feng Guo

95 Molecular and genetic targets within metastatic colorectal cancer and associated novel treatment advancements
Christopher G. Cann, Michael B. LaPelusa, Sarah K. Cimino and Cathy Eng

112 Identification and validation of m6A-GPI signatures as a novel prognostic model for colorectal cancer
Bin Ma, Simeng Bao and Yongmin Li

124 Association study between *C10orf90* gene polymorphisms and colorectal cancer
Jian Song, Kaixuan Wang, Zhaowei Chen, Dunjing Zhong, Li Li, Liangliang Guo and Shuyong Yu

frontiers | Frontiers in Oncology

TYPE Editorial
PUBLISHED 19 September 2023
DOI 10.3389/fonc.2023.1279195

OPEN ACCESS

EDITED AND REVIEWED BY
Heather Cunliffe,
University of Otago, New Zealand

*CORRESPONDENCE
Jorge Melendez-Zajgla
jmelendez@inmegen.gob.mx

RECEIVED 17 August 2023
ACCEPTED 08 September 2023
PUBLISHED 19 September 2023

CITATION
Islam F and Melendez-Zajgla J (2023) Editorial: Advances in genetics and molecular diagnosis in colorectal cancer. *Front. Oncol.* 13:1279195. doi: 10.3389/fonc.2023.1279195

Editorial: Advances in genetics and molecular diagnosis in colorectal cancer

Farhadul Islam[1] and Jorge Melendez-Zajgla[2]*

[1]Department of Biochemistry and Molecular Biology, University of Rajshahi, Rajshahi, Bangladesh, [2]Direccion General, Instituto Nacional de Medicina Genomica, Ciudad de Mexico, Mexico

KEYWORDS

colorectal < cancer type, editorial, topic, cancer, advances

Editorial on the Research Topic
Advances in genetics and molecular diagnosis in colorectal cancer

Colorectal cancer (CRC) is the third most common tumor worldwide. Paradoxically, while the global incidence of CRC has been declining over the last decade, cases among patients younger than 55 years have increased from 11% in 1995 to 20% in 2019. Additionally, CRC localization has shifted from the right to the left colon, and unfortunately, it is being diagnosed at later stages. The genomic basis for CRC progression was one of the first to be elucidated. However, our understanding of the molecular heterogeneity in these tumors has been lacking. Thanks to large cancer genomic initiatives such as the TCGA (1) and ICGC (2), most of the somatic mutations in these tumors have been discovered. RNA sequencing of large cohorts of CRC neoplasia has also provided important information about the expression cassettes that drive progression (Zhong et al.). These datasets have been instrumental in exploring new questions, such as new molecular classifications (Lu et al.), the role of microenvironment (Jun et al), including the immune-tumor response (Yuan et al.), and the recent use of expression signatures as prognostic tools. These advancements are offering valuable insights into the nature of CRC and paving the way for improved diagnoses and treatments.

The present Research Topic presents several interesting articles that contribute to these areas. For example, Nguyen et al. took advantage of the known mutated genes in CRC and used a gene panel assay to sequence tumors and create a circulating-free DNA (cfDNA) personalized test that was able more sensitive than carcinoembryonic antigen in detecting neoplasia. This “in house” test could help low-to-medium income countries to provide a surveillance method in CRC or even help to characterize possible actionable mutations.

The extensive genomic characterization of CRC has enabled researchers to search for gene expression signatures that have prognostic and predictive potential. This is done with the goal of stratifying patients. The field is rapidly evolving, as it could lead to a significant shift in cancer treatment approaches. However, currently, only a small number of signatures, primarily in breast cancer, have demonstrated their clinical implications. Jun et al. provide evidence that a novel molecular subtype (TMERSS), based on a tumor

microenvironment signature has not only higher antitumor immune cells number, but also is associated with a better prognosis in patients, associated with a better response to Cetuximab and immunotherapy. Similarly, Ma et al. report a N6-methyladenosine-related gene prognostic index (m6A-GPI) that is associated with a shorter disease-free survival and notable differences in a diverse array of tumor variables, such as copy number alterations and homologous recombination defects.

One of the most intriguing reports in the Topic is the Qin et al. findings that show that benign gallbladder disease was positively correlated with the presence of CRC, especially of the right side. For several years, a controversial association of gallbladder disease and CRC has been proposed. This could be consistent with the known common risk factors for both diseases, such as obesity, smoking, low-fiber diet, etc. A plausible mechanism could be the alterations in bile flow, with would increase inflammation, a known CRC risk factor. In their report, Qin et al. analyzed 7160 CRC cases and showed that patients with gallbladder disease had a higher risk for colon cancer than rectal cancer (20.4% vs 18.2%, p =0.024). These results need to be replicated in other oncologic centers, preferably in additional countries, and a more granular data analysis would help to define new or specific variable associations.

The articles presented in this topic provide a glimpse of the current research trends in CRC. It is noteworthy that most of them are based on the large cancer initiatives that elucidated the mutational landscape of these tumors. Beside generating new hypothesis and a deep understanding of CRC progression, these articles should eventually lead to new diagnostic, prognostic, and therapeutic approaches.

Author contributions

JM-Z: Conceptualization, Writing – original draft, Writing – review & editing. FI: Writing – review & editing.

Funding

JM-Z is funded by CONAHCyT grant A1-S-8462.

Conflict of interest

The authors declare that the research was conducted in the absence of any commercial or financial relationships that could be construed as a potential conflict of interest.

The author(s) declared that they were an editorial board member of Frontiers, at the time of submission. This had no impact on the peer review process and the final decision

Publisher's note

References

1. Cancer Genome Atlas Research N, Weinstein JN, Collisson EA, Mills GB, Shaw KR, Ozenberger BA, et al. The Cancer Genome Atlas Pan-Cancer analysis project. *Nat Genet* (2013) 45(10):1113–20. doi: 10.1038/ng.2764

2. Zhang J, Baran J, Cros A, Guberman JM, Haider S, Hsu J, et al. International Cancer Genome Consortium Data Portal–a one-stop shop for cancer genomics data. *Database (Oxford)* (2011) 2011:bar026. doi: 10.1093/database/bar026

frontiers | Frontiers in Oncology

TYPE Original Research
PUBLISHED 08 December 2022
DOI 10.3389/fonc.2022.1008394

OPEN ACCESS

EDITED BY
Farhadul Islam,
Rajshahi University, Bangladesh

REVIEWED BY
Yen-Chun Peng,
Taichung Veterans General Hospital, Taiwan
Aurel Ottlakan,
University of Szeged, Hungary

*CORRESPONDENCE
Shiqiao Luo
shiqiaoluo@qq.com

SPECIALTY SECTION
This article was submitted to Gastrointestinal Cancers: Colorectal Cancer, a section of the journal Frontiers in Oncology

RECEIVED 31 July 2022
ACCEPTED 21 November 2022
PUBLISHED 08 December 2022

CITATION
Qin Q, Li W, Ren A, Luo R and Luo S (2022) Benign gallbladder disease is a risk factor for colorectal cancer, but cholecystectomy is not: A propensity score matching analysis. *Front. Oncol.* 12:1008394. doi: 10.3389/fonc.2022.1008394

Benign gallbladder disease is a risk factor for colorectal cancer, but cholecystectomy is not: A propensity score matching analysis

Qiong Qin[1], Wei Li[1], Ao Ren[1], Rong Luo[2] and Shiqiao Luo[1]*

[1]Department of Hepatobiliary Surgery, The First Affiliated Hospital of Chongqing Medical University, Chongqing, China, [2]Medical Examination Center, The First Affiliated Hospital of Chongqing Medical University, Chongqing, China

Background: Previous studies reported controversial results on the relationship between cholecystectomy (CHE) and colorectal cancer (CRC). We hypothesized that gallbladder disease (GBD), instead of cholecystectomy, increased the risk of CRC. We aimed to investigate the incidence of benign gallbladder disease (BGBD) and CHE in CRC patients and local adults undergoing annual health examination by analyzing large data from a tertiary hospital in southwest China.

Methods: A propensity score matching (PSM) analyzed, retrospective study from January 1, 2013, to August 31, 2020, including 7,471 pathologically confirmed CRC patients and 860,160 local annual health examination adults in the First Affiliated Hospital of Chongqing Medical University, was conducted. The prevalence of BGBD and the CHE rate were analyzed before and after a 1:1 PSM.

Results: Of the 7,471 CRC patients, 7,160 were eligible for the case group. In addition, 860,160 local health examination adults were included for comparison. The incidence of BGBD was higher in the CRC patients than in the local adults (19.2% vs. 11.3%, $P < 0.001$), but no significant difference in CHE rate existed between the case group and the control group (5.0% vs. 4.8%, $P = 0.340$). In the subgroup analysis, patients with BGBD had a higher risk of colon cancer than rectal cancer (20.4% vs. 18.2%, $P = 0.024$) and more significantly in the right colon ($P = 0.037$). A weakly positive correlation between CHE and right colon cancer was observed before PSM but no longer existed after PSM ($P = 0.168$).

Conclusions: Benign gallbladder disease was positively correlated with colorectal cancer, especially right colon cancer. Cholecystectomy did not increase the risk of colorectal cancer.

KEYWORDS

benign gallbladder disease, cholecystectomy, colorectal cancer, risk factor, propensity score matching analysis

Introduction

Colorectal cancer (CRC) ranks third among lethal cancers worldwide, accounting for nearly 10% of cancer-related deaths each year. It is the second most common cancer in women and the third most common cancer in men (1–4). In China, both the morbidity and mortality of CRC are fifth among cancers (5). Anatomically, based on tumor location, CRC can be divided into right colon cancer (also called proximal colon cancer, including the ascending colon and the front two-thirds of the transverse colon), left colon cancer (also called distal colon cancer, including the posterior third of the transverse colon, descending colon and sigmoid colon) and rectal cancer (4, 6). In general, distal colon cancer is more common than proximal colon cancer, and patients with distal colon cancer are younger than those with proximal colon cancer. In terms of sex distribution, men are more likely to develop CRC than women, possibly due to sex hormone effects. The disparity is more pronounced in older patients. However, there are more women diagnosed in the right colon than men, and the reverse is true in the left colon (6, 7). In 2017, the incidence of CRC was 46.9/100,000 in men and 35.6/100,000 in women in the United States, nearly double that in China (28.64/100,000 in men and 19.33/100,000 in women) (8). CRC patients are getting younger at diagnosis, with the median age of diagnosis dropping from 72years during 1988 and 1989 to 66years during 2015 and 2016. From 2012 to 2016, the prevalence increased by 9% to 10% annually among people 50years old or older, and by up to 24% annually among people under 50years old. From 2008 through 2017, the mortality rate for CRC patients over 65years declined by 35% per year, for those aged 50 years to 64years by 0.6% per year but increased by 1.3% per year for those aged under 50years (6, 9). With the incidence and mortality of CRC increasing annually and patients getting younger, it is crucial to identify the risk factors for CRC prevention and treatment.

Benign gallbladder disease (BGBD) is the most common cause of nonmalignant gastrointestinal death and can severely affect the quality of life (10–13). Clinically, common benign gallbladder diseases include gallstones, cholecystitis, and gallbladder polyps, of which gallstones are referred to as calculous diseases (CD), and cholecystitis and gallbladder polyps are collectively referred to as acalculous disease (ACD) (14). BGBD affects 10%~20% of the global population, 10%~30% in Western countries and 5.9%~21.9% in Asian countries. The prevalence of BGBD differs from 4.2% to 13.11% in different regions of China and varies from 10.45% to 11.64% in the Han population (10, 11, 15–17). In the general population, BGBD prevalence is higher in females than in males (10, 13, 14) and higher in older people than in younger people. The prevalence increases with age (14, 18). Studies by Shaffer (19) and Liu et al. (20) revealed that the incidence rate was 4–10 times and 3.02–3.11 times higher in those over 40 and over 50 than in those under 40 and under 50, respectively. Currently, cholecystectomy (CHE) is the standard treatment for symptomatic BGBD and BGBD with complications, especially gallstones and large gallbladder polyps (21). Because of high incidence of BGBD, cholecystectomy is one of the most performed procedures in surgery. There are approximately 300,000 cholecystectomies performed annually in the United States (22). Although lack of available data, more cholecystectomies may be performed in China, considering similar incidence and more population.

Studies on the relationship between BGBD or CHE and CRC can be traced back to 1978 (23, 24). Some of the current studies suggested a positive correlation with digestive system cancer (25–28), and some believed no correlation existed (29–31). Some studies have shown that the association varies by different tumor sites (32–34). Researchers who proposed a positive correlation believed in the following mechanisms. First, the two diseases shared the same risk factors (11, 33, 35). Risk factors for BGBD, including old age (15, 18), obesity (12), hypercholesterolemia (36, 37), smoking (35), diabetes (13, 38), low-fiber and high-fat diet, and low physical activity (39, 40), are also well-known risk factors for large bowel cancer. Ernst J. Kuipes et al. (4) revealed a 1 unit increased of body mass index (BMI) and a 2–3% increase in CRC risk. Sencond, alterations in bile flow, long-term inflammatory stimulation, and complications caused by BGBD can promote the occurrence of CRC (41–43). Third, Hill, MJ et al. (44) suggested that the gallbladder lost its storage function after CHE and increased secondary bile acids (SBAs), which continued to be secreted into the intestine without food dilution, induced carcinogenesis (45). Elevated levels of bile acids and derivatives have been found in stool from CRC patients and patients who accepted CHE (44). Some studies found that the correlation varied depending on sex and tumor site. A positive relationship in women has been confirmed by many studies, especially in the proximal colon. However, such a relationship has not been proven in men (33, 34). These views were also borne out in some Chinese studies (46). Although many studies suggested a positive correlation, studies that suggested no correlation were not uncommon (29, 31). Despite nearly half a century of exploration, the relationship remains a mystery. Given high frequency of BGBD and CHE worldwide, more evidence is needed to determine whether BGBD and CHE increase the risk of future CRC. A preliminary study in our data indicated there were much more CRC patients with BGBD than CRC patients with history of CHE. Based on a hypothesis that benign gallbladder disease, rather than cholecystectomy, can increase the risk of colorectal cancer, we carry out the analysis to provide more evidence to reveal relationship between benign gallbladder disease or loss of gall bladder and colorecatal cancer.

Materials and methods

Study population

In this large, single-center, retrospective study, a total of 7,471 CRC patients admitted to the First Affiliated Hospital of

Chongqing Medical University between January 1, 2013, and August 31, 2020, were screened, and 7,160 of them were eligible for the case group. A total of 860,160 people who visited the Medical Examination Center in the same period were included in the control group (Figure 1). For the case group, clinicopathological data, including sex, age, body mass index (BMI), tumor location, and time of CRC diagnosis, were collected. By reviewing abdominal ultrasound, computerized tomography (CT), magnetic resonance imaging (MRI), and electronic medical records (EMR), CRC patients with a history of BGBD were identified, including symptomatic and asymptomatic patients. The time of BGBD diagnosis, BGBD type, CHE or not, and time of CHE were included. For the control group, BGBD and CHE information was included through retrieval in the dedicated electronic system of the Medical Examination Center. In this study, BGBD types included gallstones, cholecystitis, and gallbladder polyps. The former subtype was called CD, and the latter two subtypes were collectively referred to as ACD.

Inclusion and exclusion criteria

The inclusion criteria for the case group included: (1) age ≥ 18 years; (2) BMI ≥ 15.0kg/m^2; (3) histologically or cytologically confirmed CRC. The exclusion criteria for the case group included: (1) age < 18 years; (2) BMI < 15kg/m^2; (3) multifocal CRC; (4) other cancer; and (6) incomplete data.

The study population in the control group included an asymptomatic health examination population and a symptomatic physical check-up population during the same period as the case group. The inclusion criteria of the control group were as follows: (1) age ≥18 years and (2) BMI ≥15.0kg/m^2. Exclusion criteria of the control group included (1) age < 18 years; (2) BMI < 15kg/m^2; (3) any cancer; and (4) incomplete data.

Ethical approval

This study was approved by the Clinical Research Ethics Review Committee of The First Affiliated Hospital of Chongqing Medical University (registration number: 2021-770).

Propensity score matching analysis

To decrease the effect of selection bias and confounding factors and increase comparability between subgroups, we performed propensity score matching (PSM) analysis. PSM is a statistical method that can be used to balance interference factors between groups in observational studies, following the law of counterfactual reasoning (47). The PSM consists of the following steps: (1) Use the logistic regression model to calculate propensity scores. (2) Score matching is performed by nearest neighbor matching (NNM), radius matching, or kernel matching. (3) Evaluate the balance after matching. (4) Calculate the average intervention effect (ATT). (5) Conduct sensitivity analysis (48). All steps can be implemented in SPSS software. In our study, we calculated propensity scores by applying the sex, age, and BMI of patients in the case group to a logistic regression model and evaluated the goodness of fit with the caliper value level of 0.002. Finally, one-to-one PSM was achieved (without replacement). Then, we analyzed subgroups before and after 1:1 PSM. The process of PSM was implemented

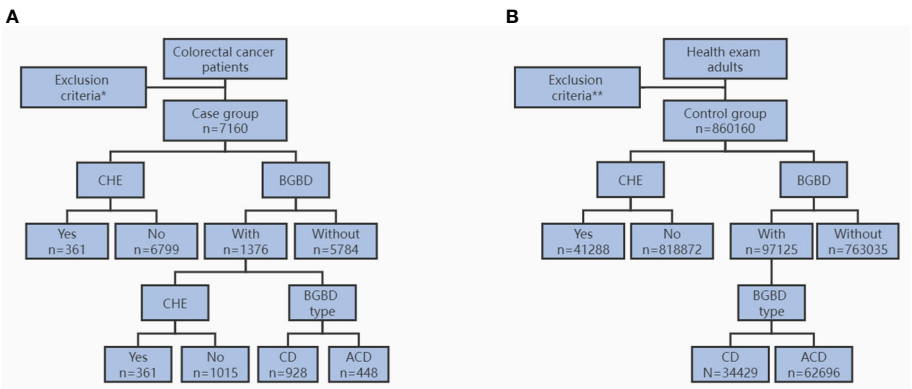

FIGURE 1
Flow diagram for study population of case group **(A)** and control group **(B)**. CHE, cholecystectomy. BGBD, benign gallbladder disease. CD, calculous disease. ACD, acalculous disease. * age < 18 years, BMI < 15.0kg/m^2, multifocal CRC, other cancer, and incomplete data. ** age < 18 years, BMI < 15.0kg/m^2, any cancer, and incomplete data.

in Microsoft Office 2019 and SPSS® version 23.0 (IBM, Armonk, New York, USA).

Statistical analysis

All statistical analyses were performed in SPSS® version 23.0 (IBM, Armonk, New York, USA). The normality of continuous variables was tested using the P-P graph, histogram, and single-sample Kolmogorov–Smirnov test. PSM was used to match the patient's sex, age, and BMI. Continuous variables are presented as the mean values with ranges, and categorical variables are presented as frequencies with percentages. $P < 0.05$ was used to denote a statistically significant difference.

The chi-square test was used to compare all categorical variables. Before PSM, an independent sample t test or one-way analysis of variance was employed to compare normally distributed data, and the Mann–Whitney U test was used to compare nonnormally distributed data. After PSM, the paired sample t test was used for normally distributed variables, and the Wilcoxon test or the Friedman test was used for nonnormally distributed data.

Results

Case and control group analysis

Of the 7,160 CRC patients in the case group, 1,376 (19.2%) had a history of BGBD, and 5,784 (80.8%) did not. Among them, 361 (5.0%) patients had previously undergone cholecystectomy, and 6,799 (95.0%) patients had not. A total of 860,160 local annual health examination adults were enrolled in the control group, of which 97,125 (11.3%) had BGBD and 763,035 (88.7%) did not. Among them, 41,288 (4.8%) accepted cholecystectomy, and 818,872 (95.2%) did not. The prevalence of BGBD in the case group was significantly higher than that in the control group (19.2% vs. 11.3%, $P < 0.001$, Table 1). However, there was no significant difference in the CHE rate between the case and the control groups (5.0% vs. 4.8%, $P = 0.340$, Table 1).

Baseline characteristics of subgroups in the case group

The characteristics of the subgroups based on tumor location showed that the features of right colon cancer were significantly different from those of left colon cancer and rectal cancer. Obvious differences were found in sex, age, and BMI distribution among the three subgroups ($P < 0.001$, Table 2). Generally, CRC was more common in men than women, but right colon cancer was more common in women than left colon cancer and rectal cancer ($P < 0.001$). On average, patients with rectal cancer and left colon cancer were younger than those with right colon cancer (62.6years vs. 63.6years vs. 64.5years, respectively, $P < 0.001$, Table 2). The right colon cancer had a lower BMI than the left colon cancer and rectal cancer (BMI were 21.9kg/m^2 vs. 22.6kg/m^2 vs. 22.5kg/m^2, respectively, $P < 0.001$, Table 2), which was consistent with the clinical phenomenon—right colon cancer with mainly systemic symptoms and left colon cancer with mainly intestinal obstruction symptoms. As shown in Table 2, patients with previous BGBD were more likely to develop right colon cancer ($P = 0.004$), regardless of BGBD subtype ($P = 0.074$). Notably, no difference in CHE rate among the different locations of CRC existed ($P = 0.074$). However, the sex, age, and BMI of the three subgroups were not balanced at baseline, which made the above conclusions inconclusive and required further analysis by PSM.

Subgroup analysis before and after PSM

Information was obtained from the comparison of colon cancer and rectal cancer (Table 3). Before PSM, an imbalance was found at baseline for sex, age, and BMI between the two groups. A higher proportion of BGBD was found in colon cancer patients than in rectal cancer patients (20.9% vs. 17.9%, $P = 0.002$), but no significant difference in CHE rate existed between the two groups (5.5% vs. 4.7%, $P = 0.098$). After PSM, factors including sex, age, and BMI, were reconciled. Statistically significant differences still existed in the prevalence of BGBD

TABLE 1 Incidence of BGBD and CHE between colorectal cancer patients and health examination adults.

	Case group (n = 7160)	Control group (n = 860160)	P value
BGBD*, n (%)			<0.001
with	1376 (19.2)	97125 (11.3)	
without	5784 (80.8)	763035 (88.7)	
CHE*, n (%)			0.340
Yes	361 (5.0)	41288 (4.8)	
No	6799 (95.0)	818872 (95.2)	

*BGBD, benign gallbladder disease. CHE, cholecystectomy.

TABLE 2 Baseline characteristics of different tumor locations in colorectal cancer.

	Right colon = 1473	Left colon = 1716	Rectum = 3971	P value
Sex, n (%)				<0.001
Male	780 (53.0)	1089 (63.5)	2517 (63.4)	
Female	693 (47.0)	627 (36.5)	1454 (36.6)	
Age, median (range), years	64.5 (18-93)	63.6 (21-96)	62.6 (20-96)	<0.001
BMI, median (range), kg/m^2	21.9 (15.0-34.9)	22.6 (15.0-36.1)	22.5 (15.0-41.6)	<0.001
BGBD*, n (%)				0.004
With	318 (21.6)	347 (20.2)	711 (17.9)	
Without	1155 (78.4)	1369 (79.8)	3260 (82.1)	
CHE*, n (%)				0.074
Yes	91 (6.2)	85 (5.0)	185 (4.7)	
No	1382 (93.8)	1631 (95.0)	3786 (95.3)	
BGBD* type, n (%)	318 (100)	347 (100)	711 (100)	0.074
CD*	231 (72.6)	231 (66.6)	466 (65.5)	
ACD*	87 (27.4)	116 (33.4)	245 (34.5)	

*BGBD, benign gallbladder disease. CHE, cholecystectomy. CD, calculous disease. ACD, acalculous disease.

between colon cancer and rectal cancer (20.4% vs. 18.2%, P = 0.024). The CHE rate remained not significantly different (5.2% vs. 4.9%, P = 0.562).

Further analysis was performed before and after PSM 1:1 matching among right colon cancer, left colon cancer, and rectal cancer. As shown in Supplementary Tables 1-3, the three groups of patients were unbalanced at baseline. There was no difference in BGBD prevalence or CHE rate between right and left colon cancer before and after PSM analysis (Supplementary Table 1). Compared with rectal cancer, the prevalence of BGBD and CHE was higher in right colon cancer, but only the difference in BGBD remained after matching, and the difference in CHE disappeared (P = 0.037 and 0.168, respectively, Supplementary Table 2). There was no difference in the incidence of BGBD and CHE between left colon cancer patients and rectal cancer patients after matching (P = 0.126 and 0.523, respectively, Supplementary Table 3).

Discussion

We had investigated association between benign gallbladder disease, cholecystectomy and colorectal cancer in a large sample, PSM-matched, case-control study. Our study revealed that benign gallbladder disease was positively associated with colorectal cancer, and this correlation was more pronounced in right colon cancer, which remained consistent before and after PSM analysis. However, our study did not found an increased risk of colorectal cancer caused by cholecystectomy. Before PSM, cholecystectomy was slightly positively correlated

TABLE 3 Analysis between colon cancer and rectal cancer before and after PSM.

	Before PSM			After PSM		
	Colon = 3189	Rectum = 3971	P value	Colon = 3106	Rectum = 3106	P value
Sex, n (%)			<0.001			0.394
Male	1869 (58.6)	2517 (63.4)		1859 (59.9)	1826 (58.8)	
Female	1320 (41.4)	1454 (36.6)		1247 (40.1)	1280 (41.2)	
Age, median (range), years	64.0 (18-96)	62.6 (20-96)	<0.001	63.6 (18-95)	63.4 (20-96)	0.497
BMI, median (range), kg/m^2	22.3 (15.0-36.1)	22.5 (15.0-41.6)	0.016	22.2 (15.0-36.1)	22.3 (15.0-36.6)	0.461
BGBD*, n (%)			0.002			0.024
With	665 (20.9)	711 (17.9)		634 (20.4)	564 (18.2)	
Without	2524 (79.1)	3260 (82.1)		2472 (79.6)	2542 (81.8)	
CHE*, n (%)			0.098			0.562
Yes	176 (5.5)	185 (4.7)		162 (5.2)	152 (4.9)	
No	3013 (94.5)	3786 (95.3)		2944 (94.8)	2954 (95.1)	

*BGBD, benign gallbladder disease. CHE, cholecystectomy.

with right colon cancer, but this correlation no longer existed after matching the sex, age and BMI. Thus, cholecystectomy itself was not associated with the development of colorectal cancer. This might be explained by the reason that carcinogenic factors were formed as early as the occurrence of BGBD.

Previous studies, mainly case-control studies, cohort studies and inventory surveys, explored the relationship between BGBD, CHE and CRC but the results were controversial. Some studies revealed that both BGBD and CHE were risk factors of CRC and more closely related to proximal colon cancer (30, 49, 50), some studies revealed a positive correlation between BGBD and CRC but no correlation between CHE and CRC (51, 52), while some studies revealed an opposite result (27, 53). There were also studies revealed that neither BGBD nor CHE was associated with CRC (54, 55). Interestingly, Chen et al. (56) revealed a negative association between CHE and CRC through a long-term follow-up cohort study and believed that CHE was a protective factor for CRC. Our results favor that the BGBD, not the CHE, is a risk factor of CRC.

Studies supporting positive correlation between BGBD or CHE and CRC had further explored possible carcinogenic mechanisms.One widely accepted mechanism was that BGBD and CRC shared common risk factors, such as old age (15, 18), obesity (12), hypercholesterolemia (36, 37), smoking (35), diabetes (13, 38), low-fiber and high-fat diet (57), and low physical activity (39). In addition, studies by Almond, HR (45) and Adler et al. (58) revealed that shrinkage of the bile acid pool, changed bile lipid composition, increased secretion of secondary bile acids (SBAs), and increased enterohepatic circulation of bile acids were observed in patients with benign gallbladder disease, which might account for the development of colorectal cancer. It has been confirmed that SBAs in the stool of CRC patients (44), BGBD patients (59) and post-cholecystectomy patients (60) are significantly higher than those in normal people. SBA has been proved with strong carcinogenicity, its carcinogenic activities mainly occur through the following mechanisms. SBA inhibited peripheral blood lymphocytes and colonic mucosa lamina propria lymphocytes, reducing the secretion of secretory immunoglobulin A (SIgA) to weaken intestinal immune function, and the damaged intestinal mucosal barrier had increased permeability and susceptibility to carcinogens (61). SBA interfered with the detoxification of glutathione S-transferase (GST) against exogenous carcinogens (62). SBA promoted carcinogenesis and increased the invasive effect of cancer cells on blood vessels by activating AP21 through the protein kinase C (PKC) signaling pathway (63). SBA activated phosphatidylinositol 3 kinase (PI3K) through the epidermal growth factor receptor (EGFR) signaling pathway, regulating cell proliferation and apoptosis, and inducing carcinogenesis (64). SBA also destroyed the DNA stability of intestinal epithelial cells through oxidation, mutagenesis and transformation activities (65), resulting in biological toxicity. Due to an increase of highly carcinogenic SBAs after BGBD diagonsed or CHE performed and high concentration of SBAs in the stool of CRC patients, scholars had to speculate that BGBD or CHE might promote the occurrence of CRC through secondary bile acids.

However, Simmons (66) and Shaffer et al. (67) found that the bile lipid composition tended to normalize after cholecystectomy. They thought that carcinogenic factors were formed as early as BGBD occurred and cholecystectomy was only a treatment strategy after BGBD diagnosed. Cholecystectomy could not correct the carcinogenic effects of BGBD but itself was not a risk factor for CRC. Researches of Almond (45) and Metzger et al. (58) also revealed that bile acid pools, kinetics and diurnal variation of bile lipid composition did not significantly change before and after cholecystectomy. Thus, we suspected the opinion that cholecystectomy was a risk factor of colorectal cancer. Conversely, based on the bile lipid composition normalizing tendency, we hypothesized that cholecystectomy was a "correction" measure and protective factor for colorectal cancer. Finally, our study successfully provided convincing evidence that cholecystectomy was not a risk factor of colorectal cancer.

There were some obvious strengths of our study. First, this study had a large sample size in both the colorectal cancer group and the local annual health examination group, and the total number of participants was far larger than that in most previous studies. Second, we selected the population undergoing annual health examination as the control group, which could be representative of the local adult population. Some previous studies did not set up a control group, or the control group was not representative enough, such as stomach cancer patients. Inappropriate controls introduced confounding factors in addition to study variables, such as the presence or absence of gastric cancer. Both the lack of a control group and the weak representation of the control group could undermine the validity of their findings. Third, we used PSM analysis in subgroups, which could eliminate or reduce the selection bias or error brought by confounding factors. The BGBD in our study included clinically common subtypes: gallstones, cholecystitis, and gallbladder polyps. Most previous studies used cholelithiasis, cholecystitis, or cholecystectomy as a complete substitute for gallbladder disease and did not conduct PSM analysis.

Our research also had some shortcomings that need to be overcome. As a single-center retrospective study, selection bias and confounding factors could not be avoided, although large sample size and PSM analysis ameliorated part of the bias. In addition, due to lack of information on gender, age, BMI, and comorbidities of control group, we were unable to achieve PSM analysis between case and control groups and only performed PSM analysis in subgroups of case group. We failed to achieve a direct PSM analysis among three subgroups, which is an undisputed shortcoming that might reduce the validity of our results. However, methods supporting direct PSM analysis of the

three subgroups were limited at present, and we tried repeatedly, but it was still difficult to achieve. Although the best PSM analysis was not achieved, we believed that results obtained from PSM analysis of the two groups were still convincing. We believe that with the maturity of PSM analysis, multisubgroup direct PSM analysis will eventually be realized. Furthermore, we could not identify whether patients with BGBD and CRC share the same oncogene mutation, because BGBD was not routinely tested for genes. Therefore, although BGBD occurred before CRC in our study, we could not completely rule out effect of causal inversion. To solve this disturbance, Mendelian randomization studies should be needed.

Conclusion

In conclusion, our study showed benign gallbladder disease was associated with increased risk of colorectal cancer, particularly with right colon cancer. Cholecystectomy was weakly positive with right colon cancer before PSM, but the association disappeared after PSM.

Data availability statement

The raw data supporting the conclusions of this article will be made available by the authors, without undue reservation.

Ethics statement

The studies involving human participants were reviewed and approved by the Clinical Research Ethics Review Committee of The First Affiliated Hospital of Chongqing Medical University. The patients/participants provided their written informed consent to participate in this study.

Author contributions

All authors were instrumental in creation of the study, data analysis, manuscript writing and editing. All authors read and approved the final manuscript.

Acknowledgments

Thanks to Dr. Rong Luo's team at the Medical Examination Center for providing the control group data for this study. Thanks to Dr. Shiqiao Luo for his guidance of this study.

Conflict of interest

The authors declare that the research was conducted in the absence of any commercial or financial relationships that could be construed as a potential conflict of interest.

Publisher's note

All claims expressed in this article are solely those of the authors and do not necessarily represent those of their affiliated organizations, or those of the publisher, the editors and the reviewers. Any product that may be evaluated in this article, or claim that may be made by its manufacturer, is not guaranteed or endorsed by the publisher.

Supplementary material

The Supplementary Material for this article can be found online at: https://www.frontiersin.org/articles/10.3389/fonc.2022.1008394/full#supplementary-material

References

1. Arnold M, Sierra MS, Laversanne M, Soerjomataram I, Jemal A, Bray F, et al. Global patterns and trends in colorectal cancer incidence and mortality. *Gut* (2017) 66(4):683–91. doi: 10.1136/gutjnl-2015-310912

2. Bray F, Ferlay J, Soerjomataram I, Siegel RL, Torre LA, Jemal A, et al. Global cancer statistics 2018: GLOBOCAN estimates of incidence and mortality worldwide for 36 cancers in 185 countries. *CA: Cancer J Clin* (2018) 68(6):394–424. doi: 10.3322/caac.21492

3. Fitzmaurice C, Abate D, Abbasi N, Abbastabar H, Abd-Allah F, Abdel-Rahman O, et al. Global, regional, and national cancer incidence, mortality, years of life lost, years lived with disability, and disability-adjusted life-years for 29 cancer groups, 1990 to 2017: A systematic analysis for the global burden of disease study. *JAMA Oncol* (2019) 5(12):1749–68. doi: 10.1001/jamaoncol.2019.2996

4. Kuipers EJ, Grady WM, Lieberman D, Seufferlein T, Sung JJ, Boelens PG, et al. Colorectal cancer. *Nat Rev Dis Primers* (2015) 1:15065. doi: 10.1038/nrdp.2015.65

5. Chen W, Sun K, Zheng R, Zeng H, Zhang S, Xia C, et al. Report of cancer incidence and mortality in China, 2014. *Chin J Oncol* (2018) 40(1):5–13. doi: 10.3760/cma.j.issn.0253-3766.2018.01.002

6. Dekker E, Tanis PJ, Vleugels JLA, Kasi PM, Wallace MB. Colorectal cancer. *Lancet* (2019) - 1474-547X(Electronic):1467–80. doi: 10.1016/S0140-6736(19)32319-0

7. Chen H, Li N, Ren J, Feng X, Lyu Z, Wei L, et al. Participation and yield of a population-based colorectal cancer screening programme in China. *Gut* (2019) 68(8):1450–7. doi: 10.1136/gutjnl-2018-317124

8. Siegel RL, Miller KD, Fedewa SA, Ahnen DJ, Meester RGS, Barzi A, et al. Colorectal cancer statistics, 2017. *CA: Cancer J Clin* (2017) 67(3):177–93. doi: 10.3322/caac.21395

9. Siegel RL, Miller KD, Sauer AG, Fedewa SA, Butterly LF, Anderson JC, et al. Colorectal cancer statistics, 2020. *CA: Cancer J Clin* (2020) 70(3):145–64. doi: 10.3322/caac.21601

10. Everhart JE, Khare M, Hill M, Maurer KR. Prevalence and ethnic differences in gallbladder disease in the united states. *Gastroenterology* (1999) 117(3):632–9. doi: 10.1016/S0016-5085(99)70456-7

11. Lammert F, Gurusamy K, Ko CW, Miquel J-F, Méndez-Sánchez N, Portincasa P, et al. Gallstones. *Nat Rev Dis Primers* (2016) 2:16024. doi: 10.1038/nrdp.2016.24

12. Aune D, Norat T, Vatten L. Body mass index, abdominal fatness and the risk of gallbladder disease. *Eur J Epidemiol* (2015) 30(9):1009–19. doi: 10.1007/s10654-015-0081-y

13. Ruhl C, Everhart J. Association of diabetes, serum insulin, and c-peptide with gallbladder disease. *Hepatol (Baltimore Md.)* (2000) 31(2):299–303. doi: 10.1002/hep.510310206

14. Einarsson K, Hellström K, Kallner M. Gallbladder disease in hyperlipoproteinaemia. *Lancet* (1975) 1(7905):484–7. doi: 10.1016/S0140-6736(75)92831-7

15. Zhu L, Aili A, Zhang C, Saiding A, Abudureyimu K. Prevalence of and risk factors for gallstones in uighur and han Chinese. *World J Gastroenterol* (2014) 20(40):14942–9. doi: 10.3748/wjg.v20.i40.14942

16. Aerts R, Penninckx F. The burden of gallstone disease in Europe. *Alimentary Pharmacol Ther* (2003) 18(Suppl 3):49–53. doi: 10.1046/j.0953-0673.2003.01721.x

17. Xu Q, Tao L-Y, Wu Q, Gao F, Zhang F-L, Yuan L, et al. Prevalences of and risk factors for biliary stones and gallbladder polyps in a large Chinese population. *HPB Off J Int Hepato Pancreato Biliary Assoc* (2012) 14(6):373–81. doi: 10.1111/j.1477-2574.2012.00457.x

18. Bateson M. Fortnightly review: gallbladder disease. *BMJ (Clinical Res ed.)* (1999) 318(7200):1745–8. doi: 10.1136/bmj.318.7200.1745

19. Shaffer E. Epidemiology and risk factors for gallstone disease: has the paradigm changed in the 21st century? *Curr Gastroenterol Rep* (2005) 7(2):132–40. doi: 10.1007/s11894-005-0051-8

20. Liu C-M, Tung T-H, Chou P, Chen VT-K, Hsu C-T, Chien W-S, et al. Clinical correlation of gallstone disease in a Chinese population in Taiwan: experience at Cheng hsin general hospital. *World J Gastroenterol* (2006) 12(8):1281–6. doi: 10.3748/wjg.v12.i8.1281

21. Kim SS, Donahue TR. Laparoscopic cholecystectomy. *Jama* (2018) 319(17):1834. doi: 10.1001/jama.2018.3438

22. Hassler KR, Collins JT, Philip K, Jones MW. *Laparoscopic cholecystectomy*. Treasure Island (FL: StatPearls Publishing (2022).

23. Capron JP, Delamarre J, Canarelli JP, Brousse N, Dupas JL. Does cholecystectomy predispose to colo-rectal cancer? *Gastroenterol Clin Biol* (1978) 2(4):383–9.

24. Hager J, Riedler L. Correlation between cholecystectomy and colonic carcinoma? *ZFA (Stuttgart)* (1978) 54(31):1607–9.

25. GBD 2017 Causes of Death Collaborators. Global, regional, and national age-sex-specific mortality for 282 causes of death in 195 countries and territories, 1980-2017: a systematic analysis for the global burden of disease study 2017. *Lancet (London England)* (2018) 392(10159):1736–88. doi: 10.1016/S0140-6736(18)32203-7

26. Zhou M, Wang H, Zeng X, Yin P, Zhu J, Chen W, et al. Mortality, morbidity, and risk factors in China and its provinces, 1990-2017: a systematic analysis for the global burden of disease study 2017. *Lancet (London England)* (2019) 394(10204):1145–58. doi: 10.1016/S0140-6736(19)30427-1

27. Jung YK, Yoon J, Lee KG, Kim HJ, Park B, Choi D, et al. De Novo cancer incidence after cholecystectomy in Korean population. *J Clin Med* (2021) 10(7):1445. doi: 10.3390/jcm10071445

28. Hindson J. Digestive Disease Week 2022. Nat Rev Gastroenterol Hepatol. (2022) 19(8):487. doi: 10.1038/s41575-022-00659-x

29. Maringhini A, Maringhini M. Gallstones and colon cancer: A result of a wrong study revived. *Gastroenterology* (2017) 153(5):1453–4. doi: 10.1053/j.gastro.2017.08.068

30. Nogueira L, Freedman ND, Engels EA, Warren JL, Castro F, Koshiol J, et al. Gallstones, cholecystectomy, and risk of digestive system cancers. *Am J Epidemiol* (2014) 179(6):731–9. doi: 10.1093/aje/kwt322

31. Maringhini A, Moreau JA, Melton LJ 3rd, Hench VS, Zinsmeister AR, DiMagno EP, et al. Gallstones, gallbladder cancer, and other gastrointestinal malignancies. an epidemiologic study in Rochester, Minnesota. *Ann Internal Med* (1987) 107(1):30–5. doi: 10.7326/0003-4819-107-1-30

32. Shabanzadeh D, Sørensen L, Jørgensen T. Association between screen-detected gallstone disease and cancer in a cohort study. *Gastroenterology* (2017) 152(8):1965–1974.e1. doi: 10.1053/j.gastro.2017.02.013

33. Ward HA, Murphy N, Weiderpass E, Leitzmann MF, Aglago E, Gunter MJ, et al. Gallstones and incident colorectal cancer in a large pan-European cohort study. *Int J Cancer* (2019) 145(6):1510–6. doi: 10.1002/ijc.32090

34. McFarlane M, Welch K. Gallstones, cholecystectomy, and colorectal cancer. *Am J Gastroenterol* (1993) 88(12):1994–9.

35. Lieberman DA, Prindiville S, Weiss DG, Willett WVA Cooperative Study Group 380. Risk factors for advanced colonic neoplasia and hyperplastic polyps in asymptomatic individuals. *JAMA* (2003) 290(22):2959–67. doi: 10.1001/jama.290.22.2959

36. Neugut A. Relation between the frequency of colorectal adenoma and the serum cholesterol level. *New Engl J Med* (1987) 317(1):55–6. doi: 10.1056/nejm198707023170117

37. Törnberg SA, Holm LE, Carstensen JM, Eklund GA. Risks of cancer of the colon and rectum in relation to serum cholesterol and beta-lipoprotein. *New Engl J Med* (1986) 315(26):1629–33. doi: 10.1056/NEJM198612253152601

38. Tsilidis KK, Kasimis JC, Lopez DS, Ntzani EE, Ioannidis JPA. Type 2 diabetes and cancer: umbrella review of meta-analyses of observational studies. *BMJ (Clinical Res ed.)* (2015) 350:g7607. doi: 10.1136/bmj.g7607

39. Giovannucci E, Ascherio A, Rimm EB, Colditz GA, Stampfer MJ, Willett WC, et al. Physical activity, obesity, and risk for colon cancer and adenoma in men. *Ann Internal Med* (1995) 122(5):327–34. doi: 10.7326/0003-4819-122-5-199503010-00002

40. Lee I, Paffenbarger R. Quetelet's index and risk of colon cancer in college alumni. *J Natl Cancer Institute* (1992) 84(17):1326–31. doi: 10.1093/jnci/84.17.1326

41. Mantovani A, Allavena P, Sica A, Balkwill F. Cancer-related inflammation. *Nature* (2008) 454(7203):436–44. doi: 10.1038/nature07205

42. Grivennikov S, Greten F, Karin M. Immunity, inflammation, and cancer. *Cell* (2010) 140(6):883–99. doi: 10.1016/j.cell.2010.01.025

43. Aune D, Vatten L, Boffetta P. Tobacco smoking and the risk of gallbladder disease. *Eur J Epidemiol* (2016) 31(7):643–53. doi: 10.1007/s10654-016-0124-z

44. Hill MJ, Drasar BS, Williams RE, Meade TW, Cox AG, Simpson JE, et al. Faecal bile-acids and clostridia in patients with cancer of the large bowel. *Lancet (London England)* (1975) 1(7906):535–9. doi: 10.1016/S0140-6736(75)91556-1

45. Almond HR, Vlahcevic ZR, Bell CC Jr, Gregory DH, Swell L. Bile acid pools, kinetics and biliary lipid composition before and after cholecystectomy. *New Engl J Med* (1973) 289(23):1213–6. doi: 10.1056/NEJM197312062892302

46. Xu Y-K, Zhang F-L, Feng T, Li J, Wang Y-H. [Meta-analysis on the correlation of cholecystectomy or cholecystolithiasis to risk of colorectal cancer in Chinese population]. *Ai zheng = Aizheng = Chin J Cancer* (2009) 28(7):749–55. doi: 10.5732/cjc.008.10829

47. Rosenbaum PR, Rubin DB. The central role of the propensity score in observational studies for causal effects. *Biometrika* (1983) 70:41–55. doi: 10.1093/biomet/70.1.41

48. Benedetto U, Head SJ, Angelini GD, Blackstone EH. Statistical primer: propensity score matching and its alternatives. *Eur J Cardiothorac Surg* (2018) 53(6):1112–7. doi: 10.1093/ejcts/ezy167

49. Pan Z, Lin Z, Fu S, Tian Y. Preliminary establishment of colorectal cancer screening model for patients with chronic enteritis in Zhoushan area. *Laboratory Medicine* (2021) 36(05):510–3. doi: 10.3969/j.issn.1673-8640.2021.05.010

50. Luo H, Yang Z. Study on the correlation between cholecystolithiasis, cholecystectomy and colorectal cancer[D]. *Kunming Medical University* (2019). doi: 10.27202/d.cnki.gkmyc.2019.000515

51. Li W, Chen S. The related risk factors and clinical analysis of colorectal cancer[D]. *Fujian Medical University* (2019). doi: 10.27020/d.cnki.gfjyu.2019.000574

52. Gosavi S, Mishra RR, Kumar VP. Study on the relation between colorectal cancer and gall bladder disease. *J Clin Diagn Res* (2017) 11(3):Oc25–oc27. doi: 10.7860/JCDR/2017/22954.9485

53. Mándi M, Keleti G, Juhász M. The role of appendectomy and cholecystectomy in the pathogenesis of colorectal carcinomas. *Ann Med Surg (Lond)* (2021) 72:102991. doi: 10.1016/j.amsu.2021.102991

54. Yan P, Yao P. Analysis of risk factors and establishment of risk scoring system for colorectal adenoma[D]. *Xinjiang Medical University* (2021). doi: 10.27433/d.cnki.gxyku.2021.000569.

55. Polychronidis G, Wang K, Lo C-H, Wang L, He M, Knudsen MD, et al. Gallstone disease and risk of conventional adenomas and serrated polyps: A prospective study. *Cancer Epidemiol Biomarkers Prev* (2021) 30(12):2346–9. doi: 10.1158/1055-9965.EPI-21-0515

56. Chen C, Lin C, Kao C. The effect of cholecystectomy on the risk of colorectal cancer in patients with gallbladder stones. *Cancers* (2020) 12(3):550. doi: 10.3390/cancers12030550

57. Song M, Chan AT, Sun J. Influence of the gut microbiome, diet, and environment on risk of colorectal cancer. *Gastroenterology* (2020) 158(2):322–40. doi: 10.1053/j.gastro.2019.06.048

58. Metzger AL, Adler R, Heymsfield S, Grundy SM. Diurnal variation in biliary lipid composition. possible role in cholesterol gallstone formation. *New Engl J Med* (1973) 288(7):333–6. doi: 10.1056/NEJM197302152880702

59. Hu H, Shao W, Liu Q, Liu N, Wang Q, Xu J, et al. Gut microbiota promotes cholesterol gallstone formation by modulating bile acid composition and biliary cholesterol secretion. *Nat Commun* (2022) 13(1):252. doi: 10.1038/s41467-021-27758-8

60. Shiha MG, Ashgar Z, Fraser EM, Kurien M, Aziz I. High prevalence of primary bile acid diarrhoea in patients with functional diarrhoea and irritable bowel syndrome-diarrhoea, based on Rome III and Rome IV criteria. *EClinicalMedicine* (2020) 25:100465. doi: 10.1016/j.eclinm.2020.100465

61. Rey J, Garin N, Spertini F, Corthésy B. Targeting of secretory IgA to peyer's patch dendritic and T cells after transport by intestinal m cells. *J Immunol (Baltimore Md 1950)* (2004) 172(5):3026–33. doi: 10.4049/jimmunol.172.5.3026

62. Baijal P, Fitzpatrick D, Bird R. Modulation of colonic xenobiotic metabolizing enzymes by feeding bile acids: comparative effects of cholic, deoxycholic, lithocholic and ursodeoxycholic acids. *Food Chem Toxicol* (1998) 36 (7):601–7. doi: 10.1016/S0278-6915(98)00020-9

63. Tsujii M, DuBois R. Alterations in cellular adhesion and apoptosis in epithelial cells overexpressing prostaglandin endoperoxide synthase 2. *Cell* (1995) 83(3):493–501. doi: 10.1016/0092-8674(95)90127-2

64. Raufman J-P, Shant J, Guo CY, Roy S, Cheng K. Deoxycholyltaurine rescues human colon cancer cells from apoptosis by activating EGFR-dependent PI3K/Akt signaling. *J Cell Physiol* (2008) 215(2):538–49. doi: 10.1002/jcp.21332

65. Qiao D, Gaitonde SV, Qi W, Martinez JD. Deoxycholic acid suppresses p53 by stimulating proteasome-mediated p53 protein degradation. *Carcinogenesis* (2001) 22(6):957–64. doi: 10.1093/carcin/22.6.957

66. Simmons F, Ross A, Bouchier I. Alterations in hepatic bile composition after cholecystectomy. *Gastroenterology* (1972) 63(3):466–71. doi: 10.1016/S0016-5085 (19)33295-0

67. Shaffer E, Braasch J, Small D. Bile composition at and after surgery in normal persons and patients with gallstones. influence of cholecystectomy. *New Engl J Med* (1972) 287(26):1317–22. doi: 10.1056/NEJM1972122 82872603

frontiers | Frontiers in Oncology

TYPE Original Research
PUBLISHED 12 December 2022
DOI 10.3389/fonc.2022.1069296

OPEN ACCESS

EDITED BY
Jorge Melendez-Zajgla,
Instituto Nacional de Medicina Genómica (INMEGEN), Mexico

REVIEWED BY
Erika Hissong,
NewYork-Presbyterian, United States
Linda Erlina,
University of Indonesia, Indonesia

*CORRESPONDENCE
Lan N. Tu
lantu@genesolutions.vn

SPECIALTY SECTION
This article was submitted to Cancer Genetics, a section of the journal Frontiers in Oncology

RECEIVED 13 October 2022
ACCEPTED 23 November 2022
PUBLISHED 12 December 2022

CITATION
Nguyen HT, Nguyen TV, Nguyen Hoang V-A, Tran DH, Le Trinh NA, Le MT, Nguyen Tran T-A, Pham TH, Dinh TC, Nguyen TS, Nguyen The KC, Mai H, Chu MT, Pham DH, Nguyen XC, Ngo Ha TM, Nguyen DS, Nguyen DQ, Lu Y-T, Do Thi TT, Truong DK, Nguyen QT, Nguyen H-N, Giang H and Tu LN (2022) Tumor genomic profiling and personalized tracking of circulating tumor DNA in Vietnamese colorectal cancer patients.
Front. Oncol. 12:1069296.
doi: 10.3389/fonc.2022.1069296

Tumor genomic profiling and personalized tracking of circulating tumor DNA in Vietnamese colorectal cancer patients

Huu Thinh Nguyen[1], Trieu Vu Nguyen[2], Van-Anh Nguyen Hoang[3,4], Duc Huy Tran[1], Ngoc An Le Trinh[1], Minh Triet Le[1], Tuan-Anh Nguyen Tran[3,4], Thanh Huyen Pham[2], Thi Cuc Dinh[2], Tien Sy Nguyen[2], Ky Cuong Nguyen The[2], Hoa Mai[2], Minh Tuan Chu[2], Dinh Hoang Pham[2], Xuan Chi Nguyen[2], Thien My Ngo Ha[3,4], Duy Sinh Nguyen[5], Du Quyen Nguyen[3,4], Y-Thanh Lu[3,4], Thanh Thuy Do Thi[3], Dinh Kiet Truong[3], Quynh Tho Nguyen[3], Hoai-Nghia Nguyen[3,4], Hoa Giang[3,4] and Lan N. Tu[3,4]*

[1]University Medical Center, Ho Chi Minh City, Vietnam, [2]Thu Duc City Hospital, Ho Chi Minh City, Vietnam, [3]Medical Genetics Institute, Ho Chi Minh City, Vietnam, [4]Gene Solutions, Ho Chi Minh City, Vietnam, [5]Department of Oncology, Faculty of Medicine, Nguyen Tat Thanh University, Ho Chi Minh City, Vietnam

Background: Colorectal cancer (CRC) is the fifth most common cancer with rising prevalence in Vietnam. However, there is no data about the mutational landscape and actionable alterations in the Vietnamese patients. During post-operative surveillance, clinical tools are limited to stratify risk of recurrence and detect residual disease.

Method: In this prospective multi-center study, 103 CRC patients eligible for curative-intent surgery were recruited. Genomic DNA from tumor tissue and paired white blood cells were sequenced to profile all tumor-derived somatic mutations in 95 cancer-associated genes. Our bioinformatic algorithm identified top mutations unique for individual patient, which were then used to monitor the presence of circulating tumor DNA (ctDNA) in serial plasma samples.

Results: The top mutated genes in our cohort were *APC*, *TP53* and *KRAS*. 41.7% of the patients harbored *KRAS* and *NRAS* mutations predictive of resistance to Cetuximab and Panitumumab respectively; 41.7% had mutations targeted by either approved or experimental drugs. Using a personalized subset of top ranked mutations, we detected ctDNA in 90.5% of the pre-operative plasma samples, whereas carcinoembryonic antigen (CEA) was elevated in only 41.3% of them. Interim analysis after 16-month follow-up revealed post-operative detection of ctDNA in two patients that had recurrence, with the lead time of 4-

10.5 months ahead of clinical diagnosis. CEA failed to predict recurrence in both cases.

Conclusion: Our assay showed promising dual clinical utilities in residual cancer surveillance and actionable mutation profiling for targeted therapies in CRC patients. This could lay foundation to empower precision cancer medicine in Vietnam and other developing countries.

KEYWORDS

mutational landscape, somatic mutation, minimal residual disease (MRD), circulating tumor (ctDNA), next-generation sequencing (NGS)

Introduction

Colorectal cancer (CRC) is the third most commonly diagnosed and the second leading cause of cancer death worldwide (1). In Vietnam, CRC accounts for 9.0% of all cancer cases in both women and men, with 16,426 new cases and 8,203 deaths in 2020 (1). Recent advances in next generation sequencing (NGS) have enabled genetic data-driven decision making in clinical oncology. For example, the discovery that *KRAS* mutations are predictive of primary resistance to the EGFR inhibitor Erbitux® has changed the clinical use of this drug for metastatic CRC. In developing countries like Vietnam, however, access to genetic testing is still limited due to high cost and lack of trained laboratories. Therefore, the mutational landscape of CRC in Vietnam and its translational potential for precision medicine are currently unknown.

Together with the rising incidence of CRC, the 5-year survival rate of Vietnamese patients was reported at only 45.0% (2), lower than that in other countries (3, 4). A major cause of cancer death is metastatic recurrence, potentially due to residual cancer cells remaining after curative-intent treatment including surgery and adjuvant therapies. Currently, there are limited clinical tools to help identify patients with post-operative residual disease that may benefit from additional or more intensive systemic therapy. Imaging methods and blood test to detect the biomarker carcinoembryonic antigen (CEA) both have limited sensitivity and specificity to detect residual tumor burden and hence often fail to identify patients at risk for relapse early (5, 6).

Circulating tumor DNA (ctDNA) is a type of cell-free DNA (cfDNA) released from cancer cells into the bloodstream. ctDNA can be distinguished from normal cfDNA based on different alterations such as somatic mutations and epigenetic changes. Several longitudinal clinical trials have demonstrated that residual tumor monitoring by ctDNA in liquid biopsy is effective for many solid tumors particularly CRC. Patients who had post-operative ctDNA positive had a significantly higher risk of recurrence and metastasis compared to those negative for ctDNA (7, 8). In addition to the prognostic value, ctDNA monitoring allowed detection of CRC relapse earlier than conventional methods by an average lead time of 4-10.9 months (3, 7), allowing for opportune intervention to improve overall survival. Currently, ctDNA monitoring technology is only available in developed countries and remains unaffordable for majority of the patients.

With the goal of making precision medicine accessible and affordable to the Vietnamese, we established K-Track®, a streamlined and affordable assay with dual clinical utilities in residual cancer surveillance and actionable mutation profiling for targeted therapies. Our interim analysis showed that the assay could stratify patients based on post-treatment ctDNA status and detect relapse early ahead of clinical diagnosis.

Materials and method

Patients and sample collection

In this prospective multicenter cohort study, 103 patients diagnosed with stage I-IV CRC were recruited at the University Medical Center, Thu Duc city Hospital, and Medical Genetics Institute in Ho Chi Minh city, Vietnam from April 2021 to June 2022. Patients must be at least 18 years old, eligible for curative-intent surgery and had not received any cancer treatment, or experienced recurrence prior to the time of study entry. 10 mL of peripheral blood was serially collected: less than 14 days before surgery, 30 days after surgery and then at scheduled follow-up visits every 6 months. 6-8 sections of formalin-fixed paraffin-embedded (FFPE) tumor samples with at least 60% tumor cellularity were also collected. CEA level was measured at each visit by the diagnostic laboratory at the participating site and CEA level of less than 5 ng/mL was considered normal. All

patients received treatment according to standard-of-care; clinicopathological and treatment information was provided by physicians in a standardized format. Clinical recurrence and/or metastasis was confirmed by either imaging or biopsy result. Patient demographics were listed in Table 1; study design and sample analysis workflow were in Figure 1 (created with BioRender.com).

All patients provided written informed consent to participate in the study and to the anonymous use of their samples, clinical and genomic data for this study. All genomic data were de-identified and aggregated for the genetic analysis of the cohort.

Tumor sample processing

Genomic DNA was isolated from FFPE and matching white blood cells (WBC) samples by the QIAamp DNA FFPE Tissue Kit (Qiagen, USA) and the MagMAX™ DNA Multi-Sample Ultra 2.0 kit (ThermoFisher, USA) respectively according to manufacturers' instructions. 150-200 ng of gDNA was used for library preparation. Specifically, DNA fragmentation and library preparation for both FFPE and WBC samples were performed using the NEBNext Ultra II FS DNA library prep kit (New England Biolabs, USA). Libraries were hybridized with predesigned probes for a gene panel of 95 targeted genes (Integrated DNA Technologies, USA). This panel includes the top 20 most frequently mutated genes in CRC and other solid tumors as reported in the Catalogue of Somatic Mutations in Cancer (COSMIC) database (Table S1). DNA libraries were sequenced on the DNBSEQ-G400 sequencer (MGI, China) with an average target coverage of 200X. A sample passed quality control when the percentage of target regions that did not reach coverage = 1 over any base was less than 1% and the percentage of all target bases achieving 20X or greater coverage depth was over 98%.

TABLE 1 Patient demographics.

Characteristic	N = 103
Median age at diagnosis (range), year	60 (27 – 85)
Gender, N (%)	
Female	45 (43.7)
Male	58 (56.3)
Size of tumor, mean (range), cm	4.9 (2 – 15)
Number of tumors, mean (range)	1 (1 – 2)
Tumor site, N (%)	
Colon	*68 (66.0)*
Left	28 (27.2)
Right	23 (22.3)
Transverse	4 (3.9)
Sigmoid	7 (6.8)
Unknown	6 (5.8)
Rectal	*26 (25.2)*
Not available	*9 (8.8)*
Clinical nodal status, N (%)	
Negative	47 (45.6)
Positive	35 (34.0)
Not available	21 (20.4)
Histological grade, N (%)	
1	0 (0.0)
2	72 (69.9)
3	8 (7.8)
Not available	23 (22.3)
TNM stage, N (%)	
I	13 (12.6)
II	41 (39.9)
III	40 (38.8)
IV	3 (2.9)
Not available	6 (5.8)

Tumor variant calling and ranking

Sequencing data were processed based on best practices workflows from Genome Analysis Tool Kit (GATK) for somatic variant calling (9). First, both read 1 and read 2 in paired-end Fastq files were assessed using FastQC (10) for total number of reads, quality score distribution across all bases, quantification of contaminants, and estimates of duplication rate. Reads were then aligned to the human reference genome (GRCh38) by BWA-MEM (v0.7.15) (11). Post-alignment procedures including sorting, marking duplicated reads and assessing alignment quality was done by Picard (v2.25.6) (12). Somatic variants were called by GATK MuTect2 (v4.0.12.0) (13) in the tumor-normal mode for paired FFPE and WBC samples with the use of a panel of normals and the population allele frequency from The Genome Aggregation Database (gnomAD). This step was to remove sequencing noise, germline variants and clonal hematopoiesis of intermediate potential (CHIP) variants. All filtered variants were further assessed for their functional impact using Variant Effect Predictor with the data from COSMIC and Clinvar databases. For mutational spectrum analysis, a minimum Variant allele frequency (VAF) of 5% in FFPE was applied for additional filtering. The annotated Variant Call Format (VCF) was then converted to the Mutation Annotation File (MAF) format using vcf2maf (doi:10.5281/zenodo.593251). The MAF data were analyzed and visualized by the 'maftools' in R package v3.4.2 (14).

All non-synonymous alterations were ranked by our K-Track® scoring algorithm to identify the most potential tumor-derived mutations to track. Ranking criteria include 1) VAF in FFPE; 2) being predicted as pathogenic/deleterious in the Clinvar and COSMIC databases or by SIFT and Polyphen; 3) being a stop-gained mutation in a tumor suppressor gene (by

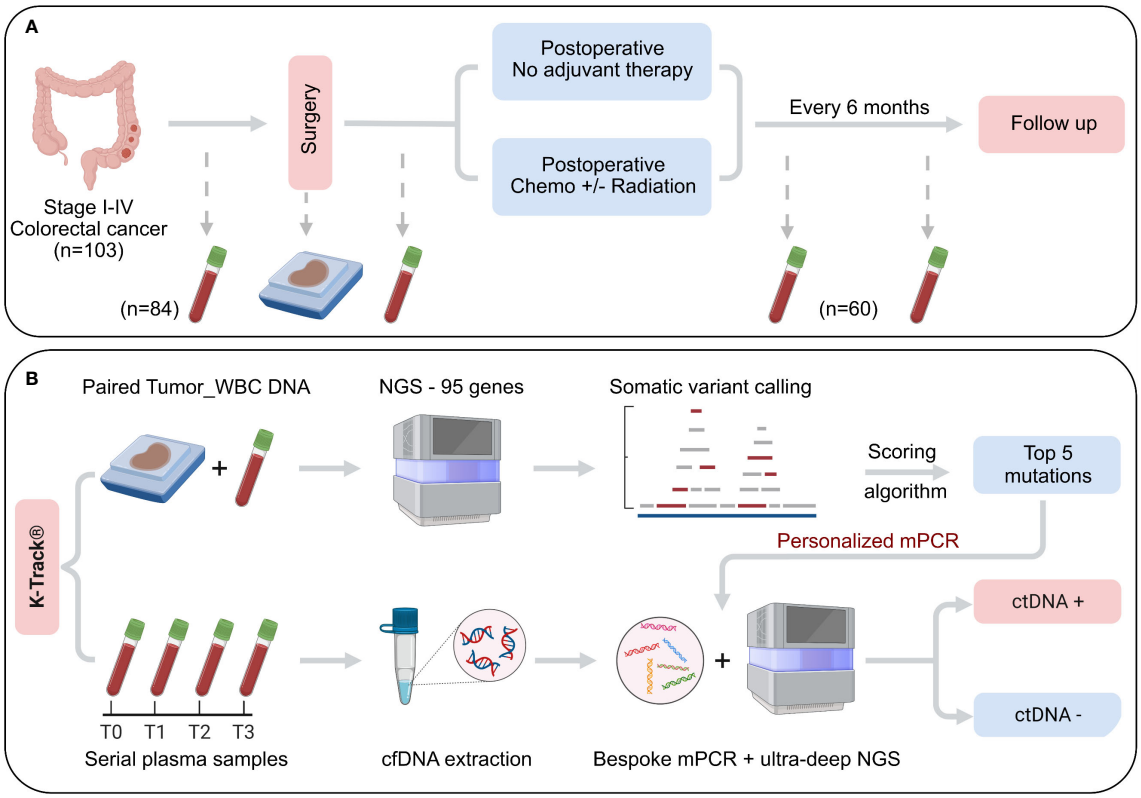

FIGURE 1
Schematic of study design and K-Track® assay. **(A)** 103 patients with primary colorectal cancer stage I-IV, eligible for curative-intent surgery were enrolled. Serial plasma samples were collected before surgery and at scheduled visits after surgery. FFPE samples of surgically removed tumors were also collected. Clinical outcomes were recorded at each visit. **(B)** Genomic DNA of paired FFPE and WBC were sequenced to profile all tumor-specific somatic alterations in 95 cancer-associated genes. Top 5 mutations were selected by our K-Track® scoring algorithm and then used to monitor ctDNA presence in plasma samples by a bespoke multiplex PCR assay and ultra-deep sequencing at an average of 100,000X.

COSMIC classification); 4) being a mutation in an oncogene (by COSMIC classification) with reported frequency of more than 3 times in COSMIC; 5) validated as a tumor-derived mutation in our in-house database. Exclusion criteria included mutations being located in low complexity regions. The top mutations unique to each patient were selected to design bespoke multiplex PCR assays in plasma.

Plasma sample processing and multiplex PCR

cfDNA was extracted from plasma samples using the MagMAX™ Cell-Free DNA Isolation Kit (ThermoFisher, USA). cfDNA concentration was quantified using the QuantiFluor® dsDNA system (Promega, USA). A concentration of ≥ 0.1 ng/uL or total of ≥ 3 ng of cfDNA was required. An average cfDNA input for mPCR assay was 6.9 ng (range 3-20 ng). Compatible primers were designed by Primer3Plus software and synthesized by PhuSa Biochem, Vietnam. cfDNA fragments carrying the selected mutation sites were amplified in a PCR reaction containing designed primer pairs and enzyme KAPA HiFi DNA Polymerase (Roche, USA). Amplified cfDNA fragments were indexed and sequenced on the NextSeq 2000 system (Illumina, USA) with an average depth of 100,000X per amplicon. Amplicons with less than 10,000X coverage were considered failed.

Plasma variant calling and ctDNA analysis

The raw fastq data of amplicons were removed adapters with Trimmomatic (v0.39) (15), mapped to the human reference genome (GRCh38) using BWA-MEM (v0.7.15), sorted and marked duplicates using Picard (v2.25.6). Variant calling was performed using mpileup from Samtools (v1.11) (16).

To determine limit of detection (LOD), we used commercial reference standards Tru-Q1 and Tru-Q0 (Horizon Discovery,

USA) and titrate the somatic mutations at average VAFs of 3%, 0.5%, 0.1%, 0.05% and 0% based on DNA input. The mixtures were fragmented to mimic cfDNA length and then processed through the mPCR workflow as above. The observed VAF was compared with the expected VAF for each mutation to determine the LOD of the assay. In addition, negative cfDNA samples isolated from 150 plasma samples of healthy donors were also subject to the same workflow to determine the false-positive rate of the assay.

A sample was called positive for ctDNA if at least one tracked mutation was detected with VAF ≥ LOD. Mean VAF of a sample was calculated as mean of all positive mutations if present. If no mutations were found positive, mean VAF was the mean of all tracked mutations.

Statistical analysis

For continuous variables including the number of mutations, VAF, cfDNA, ctDNA and CEA levels, Mann-Whitney U test was performed for comparison between 2 groups; Kruskal-Wallis with *post hoc* Dunn's test was performed for more than 2 groups. For the categorical variable of the ctDNA detection rate, Chi-squared test and Fisher's exact test were used. All statistical tests were performed in Graphpad Prism and considered significant at $p < 0.05$.

Results

Study design and participants

Among 103 Vietnamese CRC patients recruited, the median age of the patients was 60 (range: 27 – 85) years old with a balanced ratio of males (56.3%) and females (43.7%) (Table 1). All patients had carcinoma at TNM stage I (12.6%), II (39.9%), III (38.8%), and IV (2.9%). 66.0% of them had colon cancer while 25.2% had rectal cancer. Majority had 1 tumor with an average tumor size of 4.9 cm and intermediate histological grade (69.9%). 34.0% of the cases had spread to lymph nodes (Table 1).

In our K-Track® assay, FFPE tumor and serial plasma samples were collected before and after surgery at scheduled visits (Figure 1A). FFPE samples were collected for all 103 patients; 84 of them provided pre-operative blood samples and until June 2022, 60 patients had post-operative blood samples collected (Figure 1A). Genomic DNA from paired FFPE and WBC were hybridized to the predesigned 95-gene panel to identify all tumor-derived alterations. Our scoring algorithm described in the Method was used to rank and select top mutations for each patient, which were then used to track ctDNA in the plasma. The detection of ctDNA was then compared with clinical outcomes at each visit (Figure 1B).

Mutational landscape

Sequencing results of paired FFPE-WBC showed that 99.0% of the patients had at least 1 somatic mutation in the 95 examined genes. We observed a wide range of 2 to 237 somatic mutations, with an average of 7 mutations per patient (Figure 2A). The mutation burden was not affected by the TNM stage or the tumor site (Figures 2A, B). Majority of the mutations were missense (72.3%), followed by frameshift (13.5%) and nonsense (12.3%) mutations (Figure 2C).

The most frequently mutated genes in our cohort were *APC* (69.9%), *TP53* (63.1%) and *KRAS* (39.8%) (Figure 2D). While missense mutations were dominant for most of the highly mutated genes, *APC* was the exception with primarily nonsense mutations (51.7%) (Figure 2D). We then compared the mutation frequency in our cohort with published CRC datasets from the Caucasian cohorts: TCGA (n=981) (17, 18) and DFCI (n=619) (19); as well as the Asian cohorts: China (n=630) (20) and Korea (n=145) (21). The frequency of *TP53* mutations in the Vietnamese seemed to be slightly higher than the Caucasian and more comparable with the Asian (Figure 2E). Interestingly, *FAT4* mutations (27.2%) followed the opposite trend that the mutation frequency in the Vietnamese was more similar to the Caucasian, which was twice more prevalent than the Chinese (Figure 2E).

When examining the pattern of mutual exclusivity and co-occurrence of all mutations, we found that multiple gene pairs had co-occurring mutations (Figure 2F). Mutual exclusivity was less abundant and the most significant mutually exclusive genes were *TP53* with either *TRRAP*, *RNF213*, *KRAS* or *PIK3CA* (Figure 2F). Besides, among the 95 examined genes, *KRAS* showed a prominent mutation hotspot at amino acid Glycine 12, as G12D/S/V/C/A mutations accounted for 56.8% of all *KRAS* mutated cases (Figure S1).

Actionable alterations

The top three signaling pathways being altered in our CRC cohort were Wnt/β-catenin signaling (*APC*, *TCF7L2*, *AMER1*, *RNF43*), genome integrity (*TP53, ATR*), and mitogen-activated protein kinase – MAPK signaling (*KRAS, NF1*) with the mutation frequency of 85.3%, 83.3% and 55.9% respectively (Figure 3A). We then characterized actionable alterations in our cohort who might benefit from genetic sequencing. The OncoKB database (22), an expert-curated precision oncology knowledge base, was used to classify somatic alterations with treatment implications stratified by different levels of evidence (22). The list of alterations and corresponding drugs for CRC were listed in Table S2. In total, 1.9% of patients had *BRAF* V600E mutation predictive of response to the approved drug Encorafenib. 41.7% of the patients had at least 1 somatic mutation predictive of resistance to the level 1

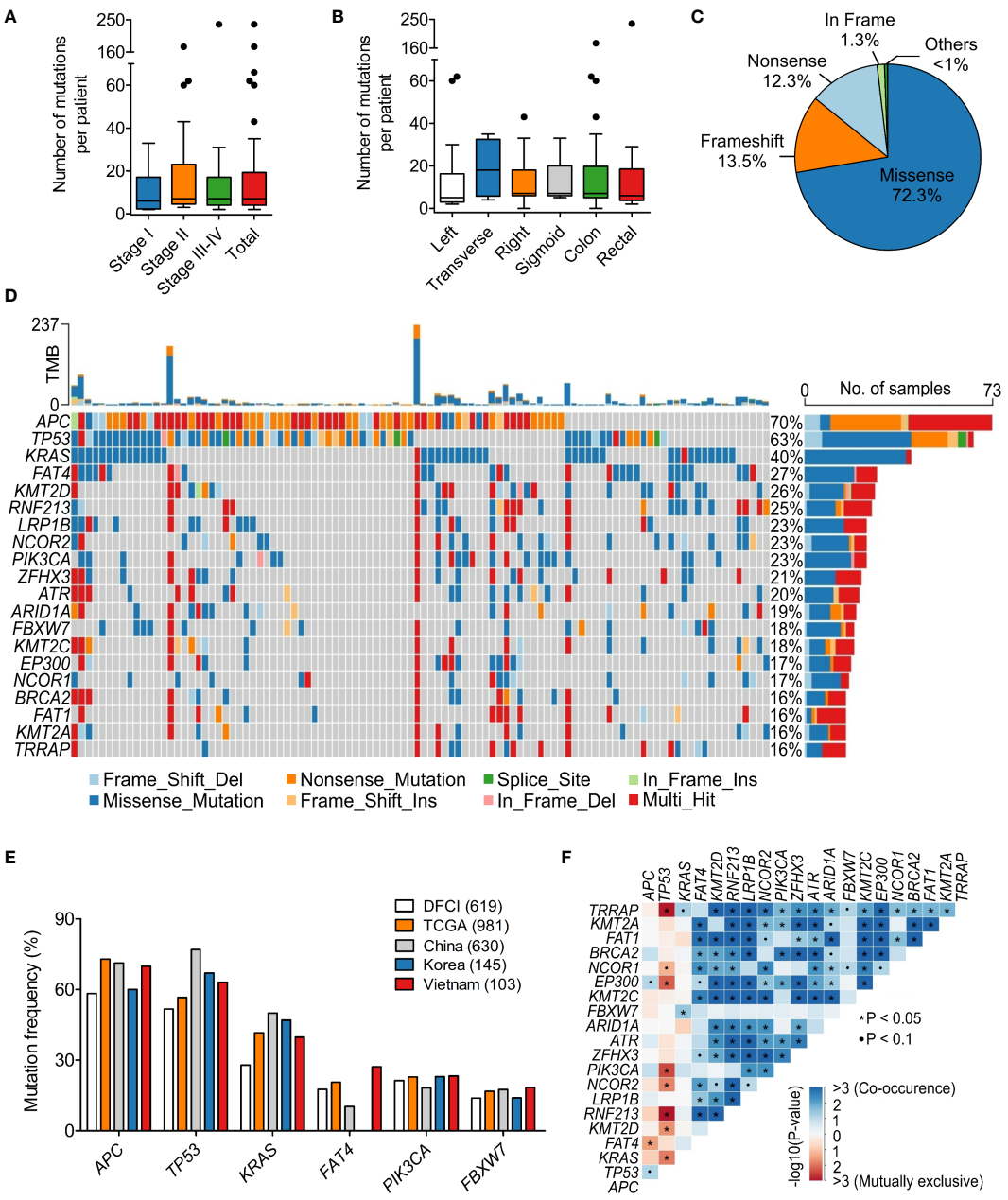

FIGURE 2
Mutational spectrum of 95 genes in the Vietnamese colorectal cancer patients. **(A)** The average number of tumor-derived mutations was 7 mutations per patient and not different by stage. **(B)** The mutation burden was not different by the tumor site. **(C)** Pie chart showing the distribution of mutation classes identified in 95 genes. **(D)** The top 25 significantly mutated genes in our cohort. **(E)** Mutation frequency of top mutated genes in our cohort was compared with published datasets of Caucasian and Asian cohorts. **(F)** Mutually exclusive and co-occurring mutated genes in our dataset. *P < 0.05; Kruskal-Wallis and *post hoc* Dunn's test for **(A, B)**.

FDA-approved drugs (Figure 3B). Majority (39.8%) of them were *KRAS* resistance mutations to Cetuximab (Table S2), with G12/13 being the most common site (33.0%). 1.9% of the patients had *NRAS* Q61 mutation associated with resistance to Panitumumab (Figure 3B). Besides FDA-approved drugs, a few experimental drugs have demonstrated therapeutic effects either in clinical studies (level 3 drug - Adagrasib) or biological research (level 4 drugs – Table S2) and they might benefit about 1.9% and 37.9% respectively of the Vietnamese CRC patients in the future (Figure 3C).

Personalized tracking of ctDNA in plasma

The set of somatic mutations identified in the tumor FFPE was subjected to our developed algorithm for ranking based on several criteria (described in Methods). Those with the highest score and highest VAF in FFPE were selected for tracking. Based on our analysis, VAF of a mutation in FFPE was a critical factor for its likelihood of detection in plasma because mutations with VAF less than 10% in FFPE had a much lower detection rate in plasma compared to those with VAF ≥ 10% (Figure S2A). On average, we selected 5 (range 2-10) mutations per patient regardless of the TNM stage (Figure 4A).

Personalized multiplex PCR and ultra-deep sequencing were performed to detect ctDNA in plasma samples with an average read depth of 100,000X per amplicon. In this dataset, 3.8% amplicons with less than 10,000X coverage were considered failed and removed from downstream analysis (Figure S2B). In our LOD assay, mutations at frequency below 0.05% could still be detected but false-positive signals from healthy plasma samples were also recorded with VAF < 0.05% (Figure S2C). Therefore, we chose the cut-off of 0.05% to keep the false-positive rate below 1% (Figure S2D). Any mutation with VAF ≥ 0.05% in plasma samples was called "positive".

The average number of positive mutations detected in the plasma was 2 (range 1-9) mutations per patient, accounting for ≥ 50% of tracked mutations in most cases. A plasma sample was called "positive" for ctDNA when at least 1 tracked mutation was positive. The overall detection rate in pre-operative plasma samples was 90.5% (Figure 4B). This rate was found to be associated with the TNM stage as the ctDNA detection rate in stage I cancer was significantly lower than stage II-IV (Figure 4C). Other clinicopathological variables such as nodal involvement, tumor histological grade and CEA level status did not affect ctDNA detection (Figure 4C). Furthermore, pre-operative CEA measurement showed that only 41.3% of the patients had elevated CEA levels, lower than the ctDNA detection rate (Figure 4D).

We next compared the dynamics of cfDNA, ctDNA, and CEA levels after surgery. The results showed that total level of

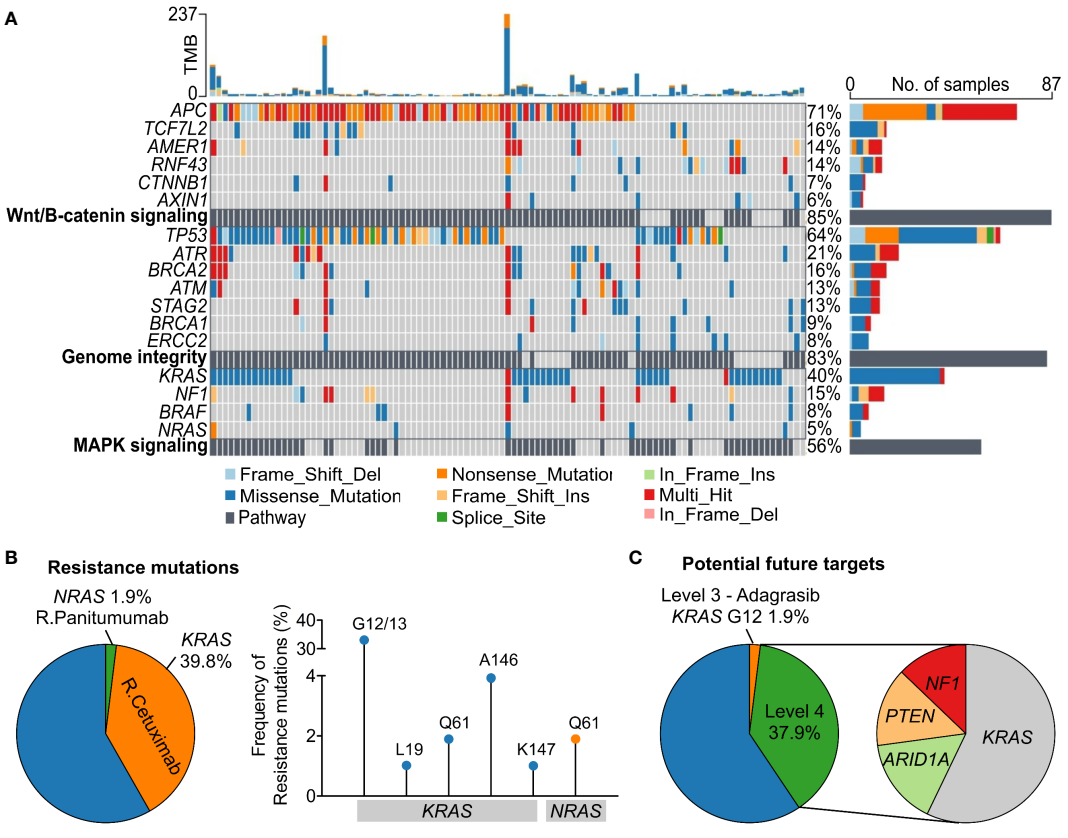

FIGURE 3
Oncogenic signaling pathways and actionable alterations in the Vietnamese colorectal cancer patients. **(A)** The top three signaling pathways with frequent oncogenic alterations in our cohort were Wnt/β-catenin signaling, genome integrity, and MAPK signaling. **(B)** Proportions of patients harboring mutations in *KRAS* and *NRAS* predictive of resistance to Cetuximab and Panitumumab respectively. Frequency of the specific resistance mutations was also illustrated. **(C)** Proportions of patients carrying mutations that are candidate biomarkers for response to drugs with compelling clinical evidence (level 3) or laboratory evidence (level 4) as classified by the OncoKB database.

cfDNA was not different between pre-operative and post-operative samples. Meanwhile, the ctDNA level, measured as the mean VAF of the tracked mutations, and the CEA level significantly reduced after surgery, correlating with the clinical removal of tumor burden (Figure 4E). The result of ctDNA clearance was then compared with the clinical outcomes of patients who had been followed up for at least 16 months. Out of 19 patients, two were diagnosed with relapse and both of them had ctDNA detected in the plasma 4.0 and 10.5 months earlier than clinical diagnosis (Figure 5A). Two case studies were illustrated in more detail. Patient ZMC002 with stage II colon cancer had pre-operative ctDNA(+) but normal CEA level; after surgery, ctDNA was undetected in all follow-up plasma samples, aligning with the clinical evaluation of full remission (Figure 5B). Patient ZMC006 also with stage II colon cancer, had ctDNA detected in the plasma sample at 6 months after surgery but was clinically stable at that point. He was later diagnosed with liver and lung metastasis at 10 months after surgery by CT scan. CEA level remained normal both before surgery and at the time point when ctDNA was positive (Figure 5C).

Discussion

In this study, we generated the first somatic variant dataset for Vietnamese CRC patients and evaluated the clinical actionability of the alterations. Using our panel of 95 cancer-associated genes, we found that the mutational burden varied greatly among patients (0-237 mutations), with an average of 7 mutations per patient. This data is consistent with the reported wide range of tumor mutational burden in CRC and also suggested that some hypermutated cases in our cohort could have microsatellite instability (23).

The most frequently mutated genes in our Vietnamese cohort were *APC, TP53* and *KRAS*, agreeing with the well documented data in other Asian and Caucasian cohorts (17–21). *FAT4* was among the top mutated genes in CRC but our mutation frequency seemed to be higher than the Asian (20, 24) and more similar to the Caucasian. *FAT4* mutations were reported to have good prognosis and be a predictive biomarker for better response to immunotherapy (25, 26). Furthermore, our mutual exclusivity analysis showed several major driver genes such as *TP53* with *KRAS*, *TP53* with *PIK3CA*, similar to

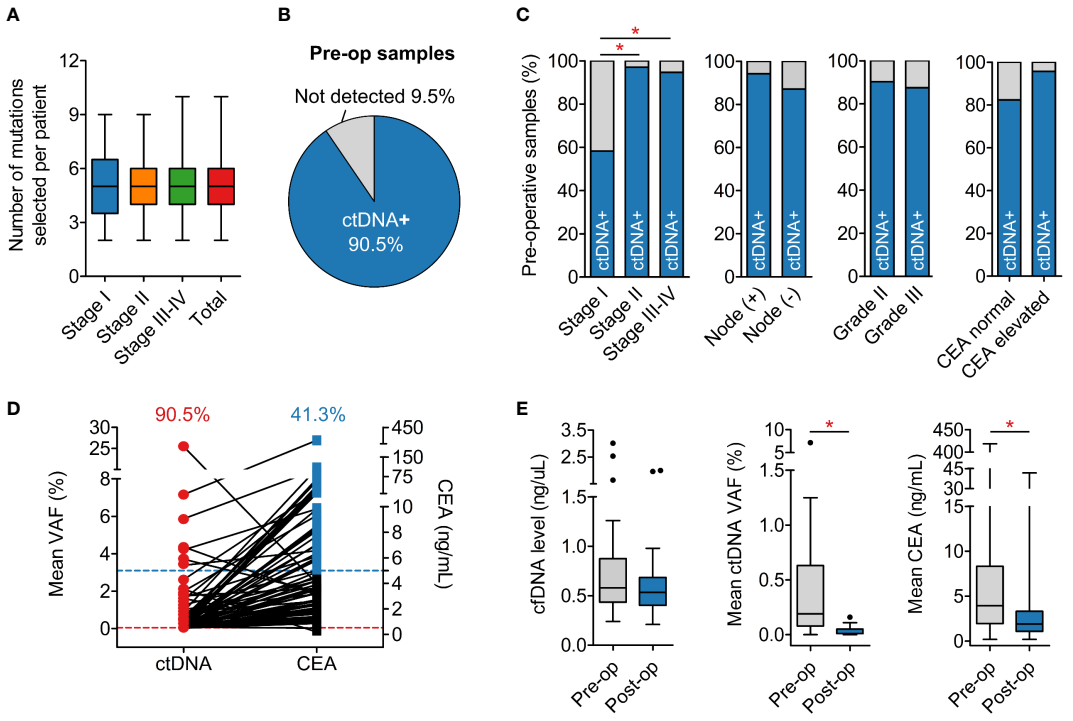

FIGURE 4
Detection of ctDNA in plasma samples. **(A)** The average number of mutations selected to track was 5 mutations per patient regardless of cancer stage. **(B)** Detection rate of ctDNA in pre-operative plasma samples was 90.5%. **(C)** Pre-operative ctDNA detection rate was associated with TNM stage, as the rate in stage I was significantly lower than in stage II and III. Nodal involvement, histological grade and CEA level status did not affect the detection rate. **(D)** Pre-operative CEA level was found elevated (≥5 ng/mL) in only 41.3% patients. **(E)** Total levels of cfDNA were not different between pre-operative and post-operative plasma samples while ctDNA and CEA levels significantly reduced after surgery. *P < 0.05; Kruskal-Wallis and *post hoc* Dunn's test for **(A)**; Chi-squared test and Fisher's exact test for **(C)**; Mann-Whitney U test for **(E)**.

several other cohorts (17, 18, 21), but not *APC* and *PIK3CA* as reported in the Taiwanese (24). This result could be affected by the gene panel used and the sample number in different studies, but might also suggest potential discrepancy in the carcinogenic pathways among different ethnicities.

Our data showed that up to 41.7% of the Vietnamese patients harbored a resistance mutation in either *KRAS* or *NRAS* that could affect their response to Cetuximab and Panitumumab respectively. This result strongly highlights the necessity of comprehensive genetic analysis to help physicians select appropriate treatment plan for individual CRC patient. Moreover, Wnt/β-catenin, genome integrity and MAPK signaling were found the most commonly altered pathways in our cohort, similar to previous reports (27). There are currently a few experimental drugs in both clinical studies and laboratory research (Table S2) targeting alterations in the MAPK signaling in CRC. This could hopefully translate to future access to more tailored therapies for CRC patients.

Our K-Track® assay utilized tumor-derived mutations in 95 genes to design a personalized 5-plex mPCR assay to detect ctDNA in liquid biopsy. This approach is fairly simplified compared to multiple studies using tumor whole exome sequencing and mPCR for 16 amplicons (Table S3). Using a small gene panel focusing only on strong cancer-associated genes has advantages of lower background noise, reduced data workload and lower sequencing cost compared to whole exome sequencing. This ultimately makes the assay more high-throughput and affordable for routine testing in Vietnam and probably other developing countries. Interestingly, although reducing the number of mutations to track was reported to modestly compromise the sensitivity of the assay (28), a recent report from Henriksen et al. argued that tracking 1 mutation was as sensitive as 16 mutations in CRC relapse detection (29). In this study, despite using a small gene panel, we detected somatic mutations in 99.0% of patients. The analytical validation of K-Track® mPCR NGS platform allowed for the limit of detection at 0.05% and the specificity of > 99%. This LOD is lower than a few platforms achieving LOD at 0.01% (28, 30) but outperformed several others with LOD of ≥ 0.1% (31–33).

The pre-operative ctDNA detection rate for all patients was 90.5%, higher than the 63.8-74.0% rates in similar assays using gene panels (8, 34, 35); and comparable to the 88.5-96.0% rates in studies using whole exome sequencing approach (7, 29, 36, 37) (details in Table S3). The non-inferior performance of our K-Track® again supported both the clinical and economic values of the assay. Furthermore, consistent with previous publications (7, 36), we observed that TNM stage was associated with the pre-operative ctDNA detection rate, that stage I tumors seemed to release less ctDNA into the bloodstream than the stage II-IV tumors. CEA, the primary biomarker for CRC, had fairly low pre-operative detection rate of only 41.3%, as also reported previously (7, 35). Even in

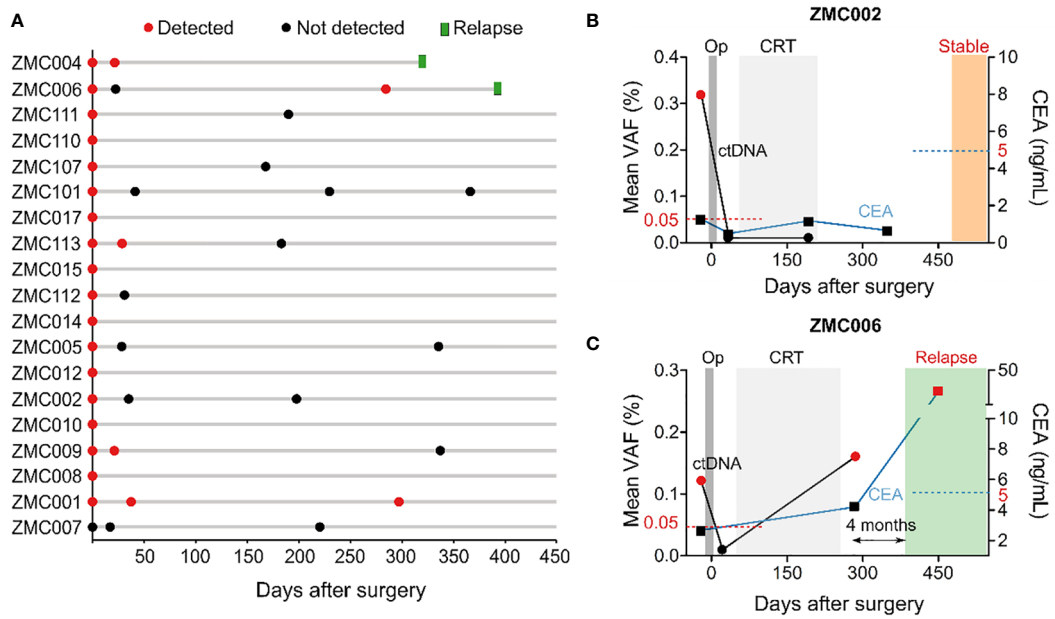

FIGURE 5
Longitudinal monitoring of ctDNA and clinical outcomes of patients. **(A)** Swimmer plot depicting ctDNA results over time and incidence of relapse in 19 patients that had been followed up for at least 16 months. This was an interim analysis as the study is on-going. **(B, C)** Longitudinal plot showing the mean VAF of ctDNA, CEA level, treatment and clinical status over time of patients ZMC002 and ZMC006. Molecular relapse detection was 4 months earlier than clinically diagnosed relapse in patient ZMC006. CEA level was still normal at the time point when ctDNA was found positive. Op, operation, CRT, chemoradiotherapy.

patients with elevated CEA level before surgery, the drop in CEA level following total tumor excision was less pronounced than that in ctDNA. Therefore, we conclude that ctDNA appeared to be a more sensitive and reliable signal than CEA to reflect the dynamics of tumor burden.

After 16-month follow up, 2 cases that were clinically diagnosed with metastasis or relapse had post-operative ctDNA(+) with the lead time of 4-10.5 months, comparable with the median lead time of 4-11.5 months in other assays (Table S3). Meanwhile, in both patients who relapsed, the CEA level remained normal at the time points when ctDNA was positive. Our findings agreed with Reinert et al. (7) that ctDNA could be a more effective monitoring tool than CEA for CRC patients during post-operative surveillance.

The major limitation of this report was that the clinical data was not yet mature as the study is on-going. A more comprehensive assessment to conclude the sensitivity and specificity of the K-Track® assay in relapse detection is warranted upon study completion. Besides that, the current design for K-Track® assay was tumor-guided, making its accuracy highly dependent on tumor sample availability, FFPE quality and sampling location. A blood-only design that bypasses tumor requirement appears to be more convenient, and has been shown to achieve comparable accuracy with tumor-guided approach in CRC patients (3, 38). We are investigating the feasibility of this approach both technically and economically as these studies also had to combine assays on epigenomic features together with mutations to identify ctDNA (3, 38).

In conclusion, we provided the first somatic variant landscape of the Vietnamese CRC patients that contributes to the knowledge base of the genetic complexity of colorectal cancer. We also developed a streamlined K-Track® assay that showed promising dual clinical utilities in residual cancer surveillance and actionable mutation profiling for targeted therapies. Although the performance of the assay needs to be fully evaluated after study completion, this report supports that K-Track® could be the affordable approach to precision oncology in Vietnam and possibly other developing countries.

Data availability statement

The data presented in the study are deposited in the BioProject repository, accession number PRJNA902849 https://www.ncbi.nlm.nih.gov/bioproject/PRJNA902849.

Ethics statement

The studies involving human participants were reviewed and approved by the institutional ethics committees of the Thu Duc city Hospital (approval number 17/HDDD) and the University of Medicine and Pharmacy, Ho Chi Minh city (approval number 14/GCN-HDDD for the study at University Medical Center and approval number 164/HDDD for the study at the Medical Genetics Institute). The patients/participants provided their written informed consent to participate in this study.

Author contributions

HN, TVN, DT, NT, ML, TP, TD, TSN, KT, HM, MC, DP, XN, DSN, DQN, Y-TL, QN recruited patients and performed clinical analysis. V-AH, T-AT, TH, TT, DT, H-NN, HG processed samples and analyzed genetic data. LT designed experiments, analyzed data and wrote the manuscript. All authors contributed to the article and approved the submitted version.

Funding

This study was funded by Gene Solutions, Vietnam. The funder did not have any role in the study design, data collection and analysis, or preparation of the manuscript.

Conflict of interest

V-AH, T-AT, TH, DQN, Y-TL, H-NN, HG and LT are current employees of Gene Solutions, Vietnam.

The remaining authors declare that the research was conducted in the absence of any commercial or financial relationships that could be construed as a potential conflict of interest.

Publisher's note

Supplementary material

The Supplementary Material for this article can be found online at: https://www.frontiersin.org/articles/10.3389/fonc.2022.1069296/full#supplementary-material

References

1. Sung H, Ferlay J, Siegel RL, Laversanne M, Soerjomataram I, Jemal A, et al. Global cancer statistics 2020: GLOBOCAN estimates of incidence and mortality worldwide for 36 cancers in 185 countries. *CA Cancer J Clin* (2021) 71:209–49. doi: 10.3322/caac.21660

2. Le DD, Vo TV, Sarakarn P. Overall survival rate of Vietnamese patients with colorectal cancer: A hospital-based cohort study in the central region of Vietnam. *Asian Pac J Cancer Prev* (2021) 22:3569–75. doi: 10.31557/APJCP.2021.22.11.3569

3. Parikh AR, Van Seventer EE, Siravegna G, Hartwig AV, Jaimovich A, He Y, et al. Minimal residual disease detection using a plasma-only circulating tumor DNA assay in patients with colorectal cancer. *Clin Cancer Res* (2021) 27:5586–94. doi: 10.1158/1078-0432.CCR-21-0410

4. Fang L, Yang Z, Zhang M, Meng M, Feng J, Chen C. Clinical characteristics and survival analysis of colorectal cancer in China: a retrospective cohort study with 13,328 patients from southern China. *Gastroenterol Rep (Oxf)* (2021) 9:571–82. doi: 10.1093/gastro/goab048

5. Duffy MJ. Carcinoembryonic antigen as a marker for colorectal cancer: is it clinically useful? *Clin Chem* (2001) 47:624–30. doi: 10.1093/clinchem/47.4.624

6. Sørensen CG, Karlsson WK, Pommergaard HC, Burcharth J, Rosenberg J. The diagnostic accuracy of carcinoembryonic antigen to detect colorectal cancer recurrence - a systematic review. *Int J Surg* (2016) 25:134–44. doi: 10.1016/j.ijsu.2015.11.065

7. Reinert T, Henriksen TV, Christensen E, Sharma S, Salari R, Sethi H, et al. Analysis of plasma cell-free DNA by ultradeep sequencing in patients with stages I to III colorectal cancer. *JAMA Oncol* (2019) 5:1124–31. doi: 10.1001/jamaoncol.2019.0528

8. Tie J, Cohen JD, Wang Y, Christie M, Simons K, Lee M, et al. Circulating tumor DNA analyses as markers of recurrence risk and benefit of adjuvant therapy for stage III colon cancer. *JAMA Oncol* (2019) 5:1710–7. doi: 10.1001/jamaoncol.2019.3616

9. DePristo MA, Banks E, Poplin R, Garimella KV, Maguire JR, Hartl C, et al. A framework for variation discovery and genotyping using next-generation DNA sequencing data. *Nat Genet* (2011) 43:491–8. doi: 10.1038/ng.806

10. Andrews S. *FastQC: A quality control tool for high throughput sequence data* (2010). Available at: https://www.bioinformatics.babraham.ac.uk/projects/fastqc/.

11. Li H. Aligning sequence reads, clone sequences and assembly contigs with BWA-MEM. *arXiv: Genomics* (2013). Available at: https://arxiv.org/abs/1303.3997.

12. *Picard*. Broad Institute. Available at: http://broadinstitute.github.io/picard/.

13. McKenna A, Hanna M, Banks E, Sivachenko A, Cibulskis K, Kernytsky A, et al. The genome analysis toolkit: a MapReduce framework for analyzing next-generation DNA sequencing data. *Genome Res* (2010) 20:1297–303. doi: 10.1101/gr.107524.110

14. Mayakonda A, Lin DC, Assenov Y, Plass C, Koeffler HP. Maftools: efficient and comprehensive analysis of somatic variants in cancer. *Genome Res* (2018) 28:1747–56. doi: 10.1101/gr.239244.118

15. Bolger AM, Lohse M, Usadel B. Trimmomatic: a flexible trimmer for illumina sequence data. *Bioinformatics* (2014) 30:2114–20. doi: 10.1093/bioinformatics/btu170

16. Li H, Handsaker B, Wysoker A, Fennell T, Ruan J, Homer N, et al. The sequence Alignment/Map format and SAMtools. *Bioinformatics* (2009) 25:2078–9. doi: 10.1093/bioinformatics/btp352

17. Cancer Genome Atlas Network. Comprehensive molecular characterization of human colon and rectal cancer. *Nature* (2012) 487:330–7. doi: 10.1038/nature11252

18. Ellrott K, Bailey MH, Saksena G, Covington KR, Kandoth C, Stewart C, et al. Scalable open science approach for mutation calling of tumor exomes using multiple genomic pipelines. *Cell Syst* (2018) 6:271–281.e7. doi: 10.1016/j.cels.2018.03.002

19. Giannakis M, Mu XJ, Shukla SA, Qian ZR, Cohen O, Nishihara R, et al. Genomic correlates of immune-cell infiltrates in colorectal carcinoma. *Cell Rep* (2016) 15:857–65. doi: 10.1016/j.celrep.2016.03.075

20. Huang W, Li H, Shi X, Lin M, Liao C, Zhang S, et al. Characterization of genomic alterations in Chinese colorectal cancer patients. *Jpn J Clin Oncol* (2021) 51:120–9. doi: 10.1093/jjco/hyaa182

21. Lee CS, Song IH, Lee A, Kang J, Lee YS, Lee IK, et al. Enhancing the landscape of colorectal cancer using targeted deep sequencing. *Sci Rep* (2021) 11:8154. doi: 10.1038/s41598-021-87486-3

22. Chakravarty D, Gao J, Phillips S, Kundra R, Zhang H, Wang J, et al. OncoKB: a precision oncology knowledge base. *JCO Precis Oncol* (2017) 1:1–16. doi: 10.1200/PO.17.00011

23. Zhao Q, Wang F, Chen YX, Chen S, Yao YC, Zeng ZL, et al. Comprehensive profiling of 1015 patients' exomes reveals genomic-clinical associations in colorectal cancer. *Nat Commun* (2022) 13:2342. doi: 10.1038/s41467-022-30062-8

24. Su MW, Chang CK, Lin CW, Chu HW, Tsai TN, Su WC, et al. Genomic and metabolomic landscape of right-sided and left-sided colorectal cancer: Potential preventive biomarkers. *Cells* (2022) 11(3):527. doi: 10.3390/cells11030527

25. Zhuang Y, Wang H, Jiang D, Li Y, Feng L, Tian C, et al. Multi gene mutation signatures in colorectal cancer patients: predict for the diagnosis, pathological classification, staging and prognosis. *BMC Cancer* (2021) 21:380. doi: 10.1186/s12885-021-08108-9

26. Chen M, Zhang Q, Chen H, Wang Z, Xu T, QI C, et al. FAT4 mutation as a potential predictive biomarker for immunotherapy combined with anti-angiogenic therapy in MSS metastatic colorectal cancer. *J Clin Oncol* (2022) 40:e15504–4. doi: 10.1200/JCO.2022.40.16_suppl.e15504

27. Sanchez-Vega F, Mina M, Armenia J, Chatila WK, Luna A, La KC, et al. Oncogenic signaling pathways in the cancer genome atlas. *Cell* (2018) 173:321–337.e10. doi: 10.1016/j.cell.2018.03.035

28. Abbosh C, Birkbak NJ, Wilson GA, Jamal-Hanjani M, Constantin T, Salari R, et al. Phylogenetic ctDNA analysis depicts early-stage lung cancer evolution. *Nature* (2017) 545:446–51. doi: 10.1038/nature22364

29. Henriksen TV, Reinert T, Rasmussen MH, Demuth C, Løve US, Madsen AH, et al. Comparing single-target and multitarget approaches for postoperative circulating tumour DNA detection in stage II-III colorectal cancer patients. *Mol Oncol* (2022) 16(20):3654–65. doi: 10.1002/1878-0261.13294

30. Newman AM, Bratman SV, To J, Wynne JF, Eclov NC, Modlin LA, et al. An ultrasensitive method for quantitating circulating tumor DNA with broad patient coverage. *Nat Med* (2014) 20:548–54. doi: 10.1038/nm.3519

31. Diefenbach RJ, Lee JH, Stewart A, Menzies AM, Carlino MS, Saw RPM, et al. Anchored multiplex PCR custom melanoma next generation sequencing panel for analysis of circulating tumor DNA. *Front Oncol* (2022) 12:820510. doi: 10.3389/fonc.2022.820510

32. Poh J, Ngeow KC, Pek M, Tan KH, Lim JS, Chen H, et al. Analytical and clinical validation of an amplicon-based next generation sequencing assay for ultrasensitive detection of circulating tumor DNA. *PloS One* (2022) 17:e0267389. doi: 10.1371/journal.pone.0267389

33. Watanabe K, Nakamura Y, Low SK. Clinical implementation and current advancement of blood liquid biopsy in cancer. *J Hum Genet* (2021) 66:909–26. doi: 10.1038/s10038-021-00939-5

34. Tarazona N, Gimeno-Valiente F, Gambardella V, Zuñiga S, Rentero-Garrido P, Huerta M, et al. Targeted next-generation sequencing of circulating-tumor DNA for tracking minimal residual disease in localized colon cancer. *Ann Oncol* (2019) 30:1804–12. doi: 10.1093/annonc/mdz390

35. Schøler LV, Reinert T, Ørntoft MW, Kassentoft CG, Árnadóttir SS, Vang S, et al. Clinical implications of monitoring circulating tumor DNA in patients with colorectal cancer. *Clin Cancer Res* (2017) 23:5437–45. doi: 10.1158/1078-0432.CCR-17-0510

36. Shirasu H, Taniguchi H, Watanabe J, Kotaka M, Yamazaki K, Hirata K, et al. O-11 monitoring molecular residual disease by circulating tumor DNA in resectable colorectal cancer: Molecular subgroup analyses of a prospective observational study GALAXY in CIRCULATE-Japan. *Ann Oncol* (2021) 32:S222–3. doi: 10.1016/j.annonc.2021.05.015

37. Henriksen TV, Tarazona N, Frydendahl A, Reinert T, Gimeno-Valiente F, Carbonell-Asins JA, et al. Circulating tumor DNA in stage III colorectal cancer, beyond minimal residual disease detection, toward assessment of adjuvant therapy efficacy and clinical behavior of recurrences. *Clin Cancer Res* (2022) 28:507–17. doi: 10.1158/1078-0432.CCR-21-2404

38. Vidal J, Casadevall D, Bellosillo B, Pericay C, Garcia-Carbonero R, Losa F, et al. Clinical impact of presurgery circulating tumor DNA after total neoadjuvant treatment in locally advanced rectal cancer: A biomarker study from the GEMCAD 1402 trial. *Clin Cancer Res* (2021) 27:2890–8. doi: 10.1158/1078-0432.CCR-20-4769

frontiers | Frontiers in Medicine

TYPE Original Research
PUBLISHED 08 February 2023
DOI 10.3389/fmed.2023.1106272

OPEN ACCESS

EDITED BY
Jacopo Troisi,
University of Salerno, Italy

REVIEWED BY
Lee-Ching Zhu,
University of North Carolina at Chapel Hill, United States
Jorge Melendez-Zajgla,
Instituto Nacional de Medicina Genómica (INMEGEN), Mexico

*CORRESPONDENCE
Dadao Jing
✉ dadaojing@126.com

SPECIALTY SECTION
This article was submitted to Gastroenterology, a section of the journal Frontiers in Medicine

RECEIVED 23 November 2022
ACCEPTED 13 January 2023
PUBLISHED 08 February 2023

CITATION
Hu H, Gong X, Xu K, Luo S, Gao W, Li B and Jing D (2023) Risk factor analysis of malignant adenomas detected during colonoscopy. *Front. Med.* 10:1106272. doi: 10.3389/fmed.2023.1106272

Risk factor analysis of malignant adenomas detected during colonoscopy

Hong Hu[1], Xiaoyuan Gong[1], Kai Xu[1], Shenzheng Luo[1], Wei Gao[2], Baiwen Li[1] and Dadao Jing[1]*

[1]Department of Gastroenterology, Shanghai General Hospital, Shanghai Jiao Tong University School of Medicine, Shanghai, China, [2]Department of General Surgery, Shanghai General Hospital, Shanghai Jiao Tong University School of Medicine, Shanghai, China

Background: Several studies have shown that colorectal adenomas are the most important precancerous lesions. The colonoscopic identification of groups with the high risk of malignant colorectal adenomas remains a controversial issue for clinicians.

Aims: To evaluate the basic characteristics of colorectal adenomas with malignancy risk using high-grade dysplasia (HGD) as an alternative marker for malignant transformation.

Methods: Data from Shanghai General Hospital between January 2017 and December 2021 were retrospectively analyzed. The primary outcome was the incidence of HGD in adenomas, which was used as a surrogate marker for the risk of malignancy. Odds ratios (ORs) for the HGD rate in adenomas were analyzed in relation to adenoma-related factors.

Results: A total of 9,646 patients identified with polyps during 57,445 screening colonoscopies were included in the study. Patients with flat polyps, sessile polyps, and pedunculated polyps represented 27.3% (N = 2,638), 42.7% (N = 4,114), and 30.0% (N = 2,894) of the total number, respectively. HGD was found in 2.41% (N = 97), 0.92% (N = 24), and 3.51% (N = 98) of sessile adenomas, flat adenomas, and pedunculated adenomas, respectively ($P < 0.001$). Multivariable logistic regression showed that polyp size ($P < 0.001$) but not shape ($P > 0.8$), was an independent predictor of HGD. Contrast to the diameter ≤1 cm, the OR value for diameters 1–2, 2–3, and >3 cm was 13.9, 49.3, and 161.6, respectively. The HGD incidence also increased in multiple adenomas (>3 vs. >1, ORs 1.582) and distal adenomas (distal vs. proximal adenomas, OR 2.252). Adenoma morphology (pedunculated vs. flat) was statistically significant in univariate analysis but not when size was included in the multivariate analysis. Besides, the incidence of HGD was also significantly higher in older patients (>64 vs. <50 years old, OR = 2.129). Sex (P = 0.681) was not statistically significant. All these associations were statistically significant ($P < 0.05$).

Conclusion: The malignant potential of polyps is mostly affected by their size but not by their shape. In addition, distal location, multiple adenomas, and advanced age were also correlated with malignant transformation.

KEYWORDS

colonoscopy, colorectal adenomas, colorectal cancer, risk factors, screening

Introduction

Colorectal cancer (CRC) is the third most common cancer and fourth most common cause of death globally, accounting for roughly 1.2 million new cases and 600,000 deaths per year. This trend is further increasing as the world grows richer and humans switch to a Western diet. Treatments for CRC are improving, but they are still far from ideal, and identifying and preventing precancerous lesions remains critical. In contrast to sporadic inflammatory and hereditary CRCs, the adenoma-carcinoma pathway underlies the development of most CRCs (1–4). More than 70% of colorectal adenomas progressed to adenomatous carcinoma through a series of gene mutations. Adenomas are considered precursors in most cases of CRC (5). Patients with advanced adenoma are significantly more likely to develop CRC and are at a significantly increased risk of CRC death compared to patients without adenoma (6–8).

Endoscopy is still the most significant examination for the prevention and detection of early colon cancer because it can detect the size, shape, location, and activity of tumors and can take a biopsy of suspicious lesions under a directional microscope (9). When endoscopists perform colonoscopy, the early identification of high-risk adenomas and high-risk groups is of great significance for the selection of treatment methods and follow-up time.

This study aimed to evaluate the effect of the shape, size, location, and number of endoscopically detected adenomas on malignant transformation based on the adenoma-carcinoma progression hypothesis, using high-grade dysplasia (HGD) as a surrogate marker for CRC, combined with age and sex distribution, to provide a theoretical basis for early identification of high-risk adenomas.

Materials and methods

Patients

We recorded the results of colonoscopies performed at the Shanghai General Hospital from January 2017 to December 2021. A total of 57,445 colonoscopies were documented, of which 12,442 detected polyps. A total of 2,526 pathologically suggested non-adenomatous polyps, 169 patients diagnosed with colon cancer, and 101 patients without detailed information records were excluded. The inclusion and exclusion criteria are shown in Figure 1. Finally, 9,646 patients were included in the study. If more than one polyp was found, only the adenoma with the most advanced histology or the largest polyp was recorded in detail as the target adenoma.

Documented data used for this analysis are as follows

Patients were men and women divided into age groups of <50 years, 50–64 years, and ≥65 years. The number of polyps was divided into the following categories: 1, 2–3, and >3; polyp size was distinguished according to the following categories: <1, 1–2, 2–3, and >3 cm. Shape: pedunculated/sessile/flat. Lesion morphology was classified according to the Paris classification: pedunculated (Paris Ip), sessile (Paris Is), and flat (Paris IIa, IIb, and IIc). Location categories included distal locations (i.e., descending colon, rectum, and sigmoid colon) and proximal locations (above the descending colon). Histology (shown in Figure 2): tubular, villous, tubulovillous, serrated adenomas, and the category of HGD, with the latter including carcinoma *in situ* in accordance with the World Health Organization definition.

Statistical analysis

All statistical tests were conducted using SPSS version 26.0 (IBM Corporation, Armonk, NY, USA). Continuous variables were expressed as mean ± standard deviation (±SD) or median ± interquartile range (Md ± IQR). Normally distributed data were analyzed using a 2-tailed *t*-test, whereas non-normally distributed data were analyzed using the Mann–Whitney *U*-test. Categorical variables are indicated as proportions and analyzed using the χ^2 test. If >20% of the expected value was less than 5, Fisher's exact test was used. To control for potential confounding between predictor variables, binary logistic regression was performed to calculate the odds ratios (ORs) with 95% confidence intervals (CIs). Statistical significance was defined as $P < 0.05$.

Results

Patient and polyp characteristics

Details of the included patients and the adenomas detected are shown in Table 1. In total, 9,646 patients with adenomas were identified. The adenomas were ≤5 mm in size in 29.3% of cases, and only 22.6% were >1 cm. HGD was found in 2.3% of adenomas ($N = 219$).

Univariate and multivariate analysis of risk factors for high-grade dysplasia in adenomas

Univariate analysis

According to the presence or absence of HGD, 9,646 patients with adenoma were divided into the adenoma group (9,427 cases) and the HGD group (219 cases). There was no difference in sex ($P = 0.681$) between the two groups; however, there were significant differences in age, adenoma location, adenoma number, adenoma morphology, and adenoma size ($P < 0.001$), as shown in Table 2.

Multivariate analysis

The Table 3 shows the percentages of adenoma sizes and HGD with different morphologies. Table 3 also shows the distribution of HGD in adenomas of different morphologies: flat, sessile, or pedunculated. The overall risk of HGD diagnosis in patients with pedunculated lesions was 3.39% ($N = 98$), compared to 2.41% ($N = 97$) in patients with sessile lesions and 0.92% in patients with flat lesions ($P < 0.05$).

In addition, there was a significant difference in the prevalence of HGD in different sizes of the three types of adenomas. Table 3 shows that adenomas ≤10 mm were less likely to develop HGD regardless

Abbreviations: CRC, colorectal cancer; HGD, high-grade dysplasia; OR, odds ratio.

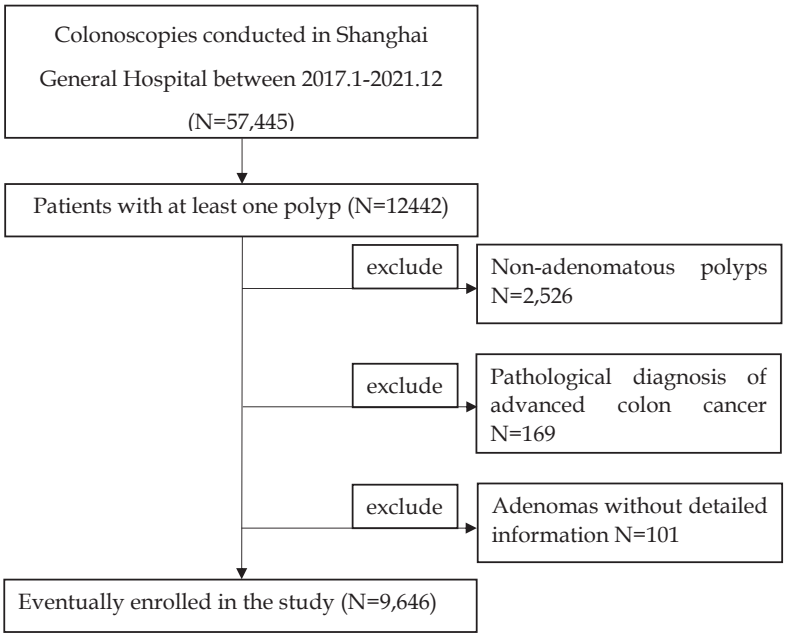

FIGURE 1
Flowchart of the patients included in the study.

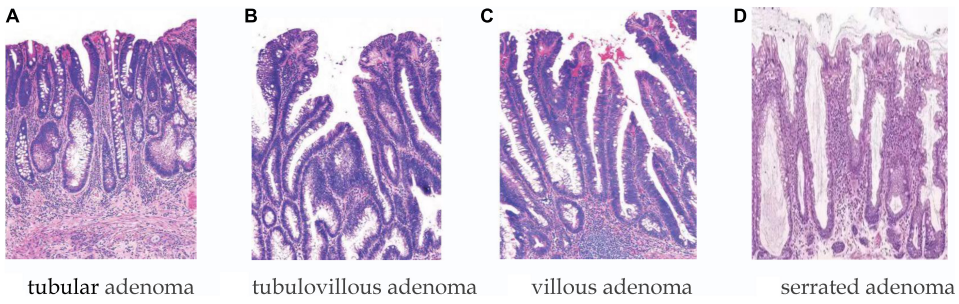

FIGURE 2
Histology: **(A)** Tubular, **(B)** tubulovillous, **(C)** villous, and **(D)** serrated adenomas.

of whether they were pedunculated or sessile adenomas (≤1 cm, pedunculated vs. sessile vs. flat, 0.73% vs. 0.48% vs. 0.52%, $P < 0.05$).

To confirm these findings, we performed multivariable logistic regression analyses for polyp size and shape with additional adjustments for age, number of adenomas, and adenoma location. Regression analysis showed that polyp size, age, and location were statistically significant independent risk factors for HGD ($P < 0.001$).

Polyp shape was a statistically significant risk factor for HGD in the univariate model ($P < 0.0001$). However, polyp shape was no longer a statistical risk factor for HGD when polyp size was included in the multivariate model ($P > 0.8$), as detailed in Table 4.

Age distribution

Table 5 shows the age distribution of the adenomas. The patients were divided into two groups: <60 years and ≥60 years. Compared with non-elderly patients, elderly patients had a higher proportion of proximal adenomas (47.26% vs. 41.32%), multiple adenomas (54.26% vs. 38.45%), more macroadenomas (25.82% vs. 20.12%), and a higher malignant transformation rate than young patients (3.11% vs. 1.60%). The morphological distribution was not significantly worse (pedunculated vs. sessile, 29.89% vs. 30.10%), all of which were statistically significant ($P < 0.05$).

Sex distribution

Table 6 shows the sex distribution of the adenomas. The incidence of pedunculated adenoma was higher in men than in women (31.01% vs. 28.19%, $P < 0.05$), but the incidence of distal adenoma was lower (54.25% vs. 59.29%, $P < 0.05$). However, there was no significant difference in the incidence of HGD between men and women (2.35% vs. 2.22%, $P = 0.681$).

Discussion

The identification of groups at high risk of colorectal adenoma remains a controversial issue for clinicians.

TABLE 1 Basic characteristics of patient and polyp.

Characteristic	Study population (N = 9,646)	
Patient age, mean (SD), range	57.35 (11.827)	17–92
Patient sex, male: female (%)	Male 6,205, 64.3%	Female 3,441, 35.7%
	N	%
Adenoma size		
<0.5 cm	2,827	29.3
0.5–1 cm	4,634	48.0
1–1.5 cm	1,321	13.7
1.5–2 cm	485	5.0
2–3 cm	260	2.7
>3 cm	119	1.2
Adenoma shape		
Pedunculated	2,894	30.0
Sessile	4,114	42.7
Flat	2,638	27.3
Adenoma histology		
Tubular	8,877	92.0
Tubulovillous	304	3.2
Villous	15	0.2
Serrated	231	2.4
HGD	219	2.3
Adenoma location		
Proximal	4,240	44.0
Distal	5,406	56.0

Adenomas reported are target adenomas (i.e., those with the most severe histology or maximum size). HGD, high-grade dysplasia. Distal = descending colon, rectum, and sigmoid colon; proximal = above the descending colon.

TABLE 2 Univariate analysis of adenoma factors relative to the occurrence of HGD.

	Adenoma (N = 9,427)	HGD (N = 219)		P-value
	N (%)	N (%)		
Sex			X^2 = 0.168	0.681
Male	6,067 (62.9)	138 (1.4)		
Female	3,360 (34.8)	81 (0.8)		
Age			X^2 = 27.192	<0.001
<50	2,320 (24.1)	24 (0.3)		
50–64	4,266 (44.2)	102 (1.1)		
≥65	2,934 (30.4)	93 (1.0)		
Size			X^2 = 1,275.171	<0.001
≤1 cm	7,435 (77.1)	26 (0.3)		
1–2 cm	1,708 (17.7)	98 (1.0)		
2–3 cm	213 (2.2)	47 (0.5)		
>3 cm	71 (0.7)	48 (0.5)		
Amount			X^2 = 58.958	<0.001
1	5,187 (53.8)	73 (0.8)		
2–3	2,622 (27.2)	69 (0.7)		
>3	1,618 (16.8)	77 (0.8)		
Morphology			X^2 = 38.394	<0.001
Sessile	4,017 (41.6)	97 (1.0)		
Flat	2,614 (27.1)	24 (0.2)		
Pedunculated	2,796 (29.0)	98 (1.0)		
Location			X^2 = 46.030	<0.001
Proximal	4,193 (43.5)	47 (0.5)		
Distal	5,234 (54.3)	172 (1.8)		

HGD, high-grade dysplasia. Distal = descending colon, rectum, and sigmoid colon; proximal = above the descending colon.

The use of HGD as a surrogate marker for the risk of cancer development from adenomas seems to be accepted, based on the concept of the adenoma-carcinoma sequence, although it is not fully known how long HGD persists before it develops into carcinoma or to what extent this is related to other risk factors (10–12). There is evidence of an increased risk of cancer development from HGD in the upper gastrointestinal tract (13). Besides, HGD is also associated with an increased risk of colon cancer in patients with inflammatory bowel disease (14, 15).

Research on the location of adenoma and the risk of cancer has also been controversial. The question of the "biology" of the left colon vs. the right colon has puzzled many scholars. Recent

TABLE 3 Size distribution of adenoma shape.

Polyp	Polyp shape								
	Pedunculated			Sessile			Flat		
	N	Of those, HGDs	HGD (%)	N	Of those, HGDs	HGD (%)	N	Of those, HGDs	HGD (%)
Size									
<0.5	256	0	0.00	1,254	1	0.08	1,317	1	0.08
0.5–1	1,507	11	0.73	1,982	8	0.40	1,145	5	0.44
1–1.5	676	22	3.25	521	22	4.22	124	2	1.61
1.5–2	276	30	10.87	178	18	10.11	31	4	12.90
2–3	139	25	17.99	111	18	16.22	10	4	40.0
>3	40	10	25.00	68	30	44.12	11	8	72.73
All cases	2,894	98	3.39	4,017	97	2.41	2,614	24	0.92

HGD, high-grade dysplasia. Distal = descending colon, rectum, and sigmoid colon; proximal = above the descending colon.

10.3389/fmed.2023.1106272

TABLE 4 Comparison of univariate and multivariate analysis of adenoma factors relative to the occurrence of HGD.

	Univariate	Multivariate
Size		
P	<0.001	<0.001
OR (95% CI)		
≤1 cm	1	
1–2 cm	16.408 (10.614–25.363)	13.890 (8.756–22.034)
2–3 cm	63.099 (38.347–103.829)	48.684 (28.641–82.755)
>3 cm	193.326 (113.632–328.913)	165.599 (95.244–287.923)
Morphology		
P	<0.001	>0.800
OR (95% CI)		
Sessile	2.630 (1.678–4.123)	0.957 (0.580–1.579)
Pedunculated	3.818 (2.435–5.984)	0.946 (0.568–1.575)
Flat	1	
Amount		
P	<0.001	<0.05
OR (95% CI)		
1	1	
2–3	2.131 (1.559–2.914)	1.261 (0.893–1.781)
>3	3.182 (2.238–4.523)	1.582 (1.070–2.339)
Age		
P	<0.001	<0.05
OR (95% CI)		
<50	1	
50–64	2.311 (1.477–3.166)	1.866 (1.152–3.022)
>64	3.164 (2.014–4.973)	2.129 (1.300–3.487)
Location		
P	<0.001	<0.001
OR (95% CI)		
Proximal	1	
Distal	2.932 (2.118–4.059)	2.252 (1.589–3.190)

HGD, high-grade dysplasia, CI, confidence interval. Distal = descending colon, rectum, and sigmoid colon; proximal = above the descending colon.

TABLE 5 Age distribution of adenoma location, amount, size, and shape.

	<60 years old	Of those, HGD (%)	≥60 years old	Of those, HGD (%)
Location	<0.001			
Proximal	2,216, 41.32%	16, 0.72	2,024, 47.26%	31, 1.53
Distal	3,147, 58.68%	70, 2.22	2,259, 52.74%	102, 4.52
Amount	<0.001			
1	3,301, 61.55%	36, 1.09	1,959, 45.74%	37, 1.89
>1	2,062, 38.45%	50, 2.42	2,324, 54.26%	96, 4.13
Size	<0.001			
≤1 cm	4,284, 79.88%	11, 0.26	3,177, 74.18%	15, 0.47
1–2 cm	913, 17.02%	41, 4.49	893, 20.85%	57, 6.38
2–3 cm	118, 2.20%	18, 15.25	142, 3.32%	29, 20.42
>3 cm	48, 0.90%	16, 33.33	71, 1.66%	32, 45.07
Morphology	<0.001			
Pedunculated	1,614	46, 2.85	1,280	52, 4.06
Sessile	3,749	40, 1.07	3,003	81, 2.70
Flat	5,363	86, 1.60	4,283	133, 3.11

retrospective analyses have noted that a significantly smaller volume but a proximal location of proximal adenomas is associated with a higher incidence of malignancy (16–19). In addition, CRC mortality after polypectomy was lower in patients with right-sided adenomas in the Norwegian Cancer Registry (12, 20). There is also a significant difference in the location of adenoma between the elderly and the young. Statistical data show that the incidence of colorectal tumors in the young has increased year by year in recent years, and the main incidence is concentrated in the left colon and rectum (21). At present, advanced colon cancer has entered the era of precision treatment under the guidance of the primary site (left and right colon). Solving the problem of the location of colorectal adenoma is of guiding significance for precision treatment. HGD was significantly more common in distal adenomas than in proximal adenomas in this study. The location of the adenoma does not fully account for this contradiction (22, 23). This may be partly due to the earlier appearance of clinical symptoms such as blood in the stool and changes in stool shape and bowel habits in patients with distant adenomas, which prompt people to seek more medical advice (24).

The role of adenoma shape has been debated for many years. Some studies have shown that sessile lesions have a higher risk of malignancy (25, 26); however, there is also evidence to support the higher HGD rate of pedunculated adenomas (27). In the present study, the incidence of HGD was higher in pedunculated adenomas than in flat adenomas in the univariate analysis. This is partly due to the higher proportion of large pedunculated adenomas than flat adenomas (>1 cm, pedicled vs. flat, 39.08% vs. 6.81%). However, this difference was lost when size was included in the multivariate analysis, which is consistent with the findings of Reinhart et al. (28). The influence of adenoma morphology is still controversial, but our results suggest that it is not an independent risk factor for malignant transformation of adenomas. The Paris classification was used for adenoma morphology in this paper, but no morphological significance could be observed. More detailed morphological classification further studies may be needed to confirm this conclusion. Some studies have suggested that villous components are closely related to the malignant potential of adenomas, but whether this is also affected by the factor of adenoma size is unknown. We cannot verify this point due to the small number of villous adenoma samples in this study. We look forward to further studies to analyze the role of villous components in adenomas of similar size in the future.

Other risk factors such as adenoma size and patient age were confirmed in this study. Both large size and advanced age were positively correlated with HGD (29). In this study, compared with adenomas <1 cm, the OR for polyps 2 cm and 2–3 cm were 13.890 (8.756, 22.034) and 48.684 (28.641, 82.755), respectively, and the OR for polyps >3 cm was 165.599 (95.244, 287.923). The large CIs were due to the low total number of HGDs. However, a high OR clearly indicated the effect of size on HGD incidence. The effect of size on the prevalence of advanced cancer was consistent with the data from

TABLE 6 Sex distribution of adenoma location and shape.

	All cases (mean age, 57.35 years)		Men (mean age, 56.79 years)		Women (mean age, 58.35 years)	
	N	%	*N*	%	*N*	%
All patients with adenomas	9,646	100%	6,205	64.3%	3,441	35.7%
Adenoma location						
Proximal	4,240	44.0	2,839	45.75	1,401	40.71
Of those, HGD	47	1.11	28	0.99	29	2.07
Distal	5,406	56.0	3,366	54.25	2,040	59.29
Of those, HGD	172	3.18	110	3.27	62	3.04
Adenoma shape						
Pedunculated	2,894	30.00	1,924	31.01	970	28.19
Of those, HGD	98	3.39	67	3.48	31	3.20
Sessile	6,752	70.00	4,281	68.99	2,471	71.81
Of those, HGD	121	1.79	71	1.66	50	2.02
Adenoma shape and location						
Proximal pedunculated	1,178	12.21	794	12.80	384	11.16
Of those, HGD	17	1.44	10	1.26	7	1.82
Distal pedunculated	1,716	17.79	1,130	18.21	586	17.03
Of those, HGD	81	6.88	57	5.04	24	4.10
Proximal sessile	3,062	31.74	2,045	32.96	1,017	29.56
Of those, HGD	30	0.98	18	0.88	12	1.18
Distal sessile	3,690	38.25	2,236	36.04	1,454	42.26
Of those, HGD	91	2.47	53	2.37	35	2.41

HGD, high-grade dysplasia. Distal = descending, rectum, and sigmoid colon; proximal = above the descending colon.

other studies. Nearly all studies reported a risk of severe dysplasia of less than 1% in small (<10 mm) adenomas, and our results fall within this range (0.59%) (27, 28).

Related studies have shown that the recurrence rate of multiple adenomas after colonoscopic resection is significantly higher than that of single adenomas, and adenoma recurrence is considered to be one of the main risk factors for malignant transformation. At the same time, our analysis found that the incidence of HGD in patients with multiple adenomas was significantly higher than those with single adenomas (>3 vs. 1, OR 1.582) (30–32). Patients with familial adenomatous polyposis have a high rate of malignant transformation, and we speculate that patients with multiple polyps may have a higher genetic susceptibility (33, 34).

Many studies have shown that age is associated with the development of CRC (35). Some studies have found that patients <50 years of age are more likely to have distal CRC, while older patients are more likely to have proximal CRC (36). In this study, the elderly and non-elderly groups were divided using 60 years as the baseline, and there was no significant difference in the morphological distribution between the two groups (pedicled vs. sessile, 29.89% vs. 30.10%). In the elderly group, the proportion of proximal adenomas was higher (> 60 vs. ≤60 years, 47.26% vs. 41.32%), multiple adenomas were more common (> 60 vs. ≤60 years, 54.26% vs. 38.45%), and large adenomas >1 cm were more frequent (>60 vs. ≤60 years, 25.82% vs. 20.12%). The rate of HGD in the elderly group was higher than that in the non-elderly group (>60 vs. ≤60 years, 3.11% vs. 1.60%), and the OR value was 1.539 (95% CI: 1.139–2.080). Our results suggest that adenomas in elderly patients had more features of high-risk, and more active treatment measures should be taken in patients with adenomas >60 years.

In some studies, men and women had different risks of CRC, which may be related to smoking, alcohol consumption, obesity, and other factors (37–39). No effect of sex difference on HGD incidence was observed in the present study, which is in line with the findings of Rösch et al. (27).

This study had some limitations. (1) This was a retrospective study, and there was a selection and information biases in the data collection process due to the possibility of convenient sampling and incomplete or missing patient records. (2) The sample population selection and construction process were all conducted in the same medical institution, which was a single-center study with certain limitations. In the future, a multicentre study should be conducted for further verification. (3) Data from only one adenoma per patient, the one that was most important in terms of histology or size, were analyzed. This may have introduced some bias, particularly in patients with multiple polyps, which may have diluted some of the observed effects.

Conclusion

In conclusion, this study shows that when HGD is used as a surrogate marker for CRC, the effect of sex and morphology on malignancy is controversial, but adenoma size is the most important

factor in the development of HGD in all morphologic adenomas. Adenomas detected in the distal colon had a higher incidence of HGD than those detected in the proximal colon. Patients with multiple adenomas have a higher incidence of HGD. Adenomas in elderly patients had more features of high-risk, more active treatment and follow-up should be performed in patients with high-risk adenomas.

Data availability statement

The original contributions presented in this study are included in the article/supplementary material, further inquiries can be directed to the corresponding author.

Ethics statement

The studies involving human participants were reviewed and approved by the Ethics Committee of Shanghai General Hospital, Shanghai Jiao Tong University School of Medicine (IRB No. 021KY049). The patients/participants provided their written informed consent to participate in this study. The respondents were informed about the aim of the study. This study was conducted in accordance with the declaration of Helsinki. The confidentiality and anonymity of the data was also ensured.

Author contributions

All authors made a significant contribution to the work reported, whether that is in the conception, study design, execution, acquisition of data, analysis and interpretation, or in all these areas, took part in drafting and revising or critically reviewing the article, gave final approval of the version to be published, have agreed on the journal to which the article has been submitted, and agreed to be accountable for all aspects of the work.

Acknowledgments

We thank the Departments of Gastroenterology and Pathology of Shanghai General Hospital for their participation in data collection and case recruitment for this study.

Conflict of interest

The authors declare that the research was conducted in the absence of any commercial or financial relationships that could be construed as a potential conflict of interest.

Publisher's note

References

1. Brenner H, Kloor M, Pox CP. Colorectal cancer. *Lancet.* (2014) 383:1490–502. doi: 10.1016/S0140-6736(13)61649-9

2. Weitz J, Koch M, Debus J, Höhler T, Galle PR, Büchler MW. Colorectal cancer. *Lancet.* (2005) 365:153–65.

3. Brody H. Colorectal cancer. *Nature.* (2015) 521:S1. doi: 10.1038/521S1a

4. Dekker E, Tanis PJ, Vleugels JL, Kasi PM, Wallace MB. Colorectal cancer. *Lancet.* (2019) 394:1467–80. doi: 10.1016/S0140-6736(19)32319-0

5. Komor MA, Bosch LJ, Bounova G, Bolijn AS, Diemen PM, Rausch C, et al. Consensus molecular subtype classification of colorectal adenomas. *J Pathol.* (2018) 246:266–76.

6. Click B, Pinsky PF, Hickey T, Doroudi M, Schoen RE. Association of colonoscopy adenoma findings with long-term colorectal cancer incidence. *JAMA.* (2018) 319:2021–31. doi: 10.1001/jama.2018.5809

7. Miller EA, Pinsky PF, Schoen RE, Prorok PC, Church TR. Effect of flexible sigmoidoscopy screening on colorectal cancer incidence and mortality: long-term follow-up of the randomised US PLCO cancer screening trial. *Lancet Gastroenterol Hepatol.* (2019) 4:101–10. doi: 10.1016/S2468-1253(18)30358-3

8. Cottet V, Jooste V, Fournel I, Bouvier A, Faivre J, Bonithon-Kopp C. Long-term risk of colorectal cancer after adenoma removal: a population-based cohort study. *Gut.* (2012) 61:1180–6. doi: 10.1136/gutjnl-2011-300295

9. Lin JS, Piper MA, Perdue LA, Rutter CM, Webber EM, Connor E, et al. Screening for colorectal cancer: updated evidence report and systematic review for the US preventive services task force. *JAMA.* (2016) 315:2576–94. doi: 10.1001/jama.2016.3332

10. Leslie A, Carey FA, Pratt NR, Steele RJ. The colorectal adenoma-carcinoma sequence. *Br J Surg.* (2002) 89:845–60. doi: 10.1046/j.1365-2168.2002.02120.x

11. Nakamura F, Sato Y, Okamoto K, Fujino Y, Mitsui Y, Kagemoto K, et al. Colorectal carcinoma occurring via the adenoma-carcinoma pathway in patients with serrated polyposis syndrome. *J Gastroenterol.* (2022) 57:286–99. doi: 10.1007/s00535-022-01858-8

12. Calderwood AH, Lasser KE, Roy HK. Colon adenoma features and their impact on risk of future advanced adenomas and colorectal cancer. *World J Gastrointest Oncol.* (2016) 8:826–34. doi: 10.4251/wjgo.v8.i12.826

13. Conio M, Cameron AJ, Chak A, Blanchi S, Filiberti R. Endoscopic treatment of high-grade dysplasia and early cancer in Barrett's oesophagus. *Lancet Oncol.* (2005) 6:311–21. doi: 10.1016/S1470-2045(05)70167-4

14. Pulusu SS, Lawrance IC. Dysplasia and colorectal cancer surveillance in inflammatory bowel disease. *Expert Rev Gastroenterol Hepatol.* (2017) 11:711–22. doi: 10.1080/17474124.2017.1327347

15. Murthy SK, Feuerstein JD, Nguyen GC, Velayos F. AGA clinical practice update on endoscopic surveillance and management of colorectal dysplasia in inflammatory bowel diseases: expert review. *Gastroenterology.* (2021) 161:1043–51.e4. doi: 10.1053/j.gastro.2021.05.063

16. Sawhney MS, Dickstein J, LeClair J, Lembo C, Yee E. Adenomas with high-grade dysplasia and early adenocarcinoma are more likely to be sessile in the proximal colon. *Colorectal Dis.* (2015) 17:682–8. doi: 10.1111/codi.12911

17. Benedix F, Kube R, Meyer F, Schmidt U, Gastinger I, Lippert H, et al. Comparison of 17,641 patients with right- and left-sided colon cancer: differences in epidemiology, perioperative course, histology, and survival. *Dis Colon Rectum.* (2010) 53:57–64. doi: 10.1007/DCR.0b013e3181c703a4

18. Klein JL, Okcu M, Preisegger KH, Hammer HF. Distribution, size and shape of colorectal adenomas as determined by a colonoscopist with a high lesion detection rate: influence of age, sex and colonoscopy indication. *United European Gastroenterol J.* (2016) 4:438–48. doi: 10.1177/2050640615610266

19. Loree JM, Pereira AA, Lam M, Willauer AN, Raghav K, Dasari A, et al. Classifying colorectal cancer by Tumor location rather than sidedness highlights a continuum in mutation profiles and consensus molecular subtypes. *Clin Cancer Res.* (2018) 24:1062–72. doi: 10.1158/1078-0432.CCR-17-2484

20. de Jonge V, Nicolaas JS, Leerdam ME, Kuipers EJ, Zanten SJ. Systematic literature review and pooled analyses of risk factors for finding adenomas at surveillance colonoscopy. *Endoscopy.* (2011) 43:560–72. doi: 10.1055/s-0030-1256306

21. Ouakrim DA, Pizot C, Boniol M, Malvezzi M, Boniol M, Negri E, et al. Trends in colorectal cancer mortality in Europe: retrospective analysis of the WHO mortality database. *BMJ.* (2015) 351:h4970. doi: 10.1136/bmj.h4970

22. Xiang L, Zhan Q, Zhao X, Wang Y, An S, Xu Y, et al. Risk factors associated with missed colorectal flat adenoma: a multicenter retrospective tandem colonoscopy study. *World J Gastroenterol.* (2014) 20:10927–37. doi: 10.3748/wjg.v20.i31.10927

23. Xiang L, Zhan Q, Wang X, Zhao X, Zhou Y, An S, et al. Risk factors associated with the detection and missed diagnosis of colorectal flat adenoma: a Chinese multicenter observational study. *Scand J Gastroenterol.* (2018) 53:1519–25. doi: 10.1080/00365521.2018.1533581

24. Nawa T, Kato J, Kawamoto H, Okada H, Yamamoto H, Kohno H, et al. Differences between right- and left-sided colon cancer in patient characteristics, cancer morphology and histology. *J Gastroenterol Hepatol.* (2008) 23:418–23.

25. Rembacken BJ, Fujii T, Cairns A, Dixon MF, Yoshida S, Chalmers DM, et al. Flat and depressed colonic neoplasms: a prospective study of 1000 colonoscopies in the UK. *Lancet.* (2000) 355:1211–4.

26. Hart AR, Kudo S, Mackay EH, Mayberry JF, Atkin WS. Flat adenomas exist in asymptomatic people: important implications for colorectal cancer screening programmes. *Gut.* (1998) 43:229–31.

27. Rösch T, Altenhofen L, Kretschmann J, Hagen B, Brenner H, Pox C, et al. Risk of malignancy in adenomas detected during screening colonoscopy. *Clin Gastroenterol Hepatol.* (2018) 16:1754–61.

28. Reinhart K, Bannert C, Dunkler D, Salzl P, Trauner M, Renner F, et al. Prevalence of flat lesions in a large screening population and their role in colonoscopy quality improvement. *Endoscopy.* (2013) 45:350–6.

29. Pommergaard H, Burcharth J, Rosenberg J, Raskov H. The association between location, age and advanced colorectal adenoma characteristics: a propensity-matched analysis. *Scand J Gastroenterol.* (2017) 52:1–4. doi: 10.1080/00365521.2016.1218929

30. Facciorusso A, Maso MD, Serviddio G, Vendemiale G, Muscatiello N. Development and validation of a risk score for advanced colorectal adenoma recurrence after endoscopic resection. *World J Gastroenterol.* (2016) 22:6049–56. doi: 10.3748/wjg.v22.i26.6049

31. Bonithon-Kopp C, Piard F, Fenger C, Cabeza E, Morain C, Kronborg O, et al. Colorectal adenoma characteristics as predictors of recurrence. *Dis Colon Rectum.* (2004) 47:323–33.

32. Nusko G, Hahn EG, Mansmann U. Characteristics of metachronous colorectal adenomas found during long-term follow-up: analysis of four subsequent generations of adenoma recurrence. *Scand J Gastroenterol.* (2009) 44:736–44.

33. Galiatsatos P, Foulkes WD. Familial adenomatous polyposis. *Am J Gastroenterol.* (2006) 101:385–98.

34. Half E, Bercovich D, Rozen P. Familial adenomatous polyposis. *Orphanet J Rare Dis.* (2009) 4:22.

35. Laish I, Mizrahi J, Naftali T, Konikoff FM. Diabetes mellitus and age are risk factors of interval colon cancer: a case-control study. *Dig Dis.* (2019) 37:291–6.

36. Weinberg BA, Marshall JL. Colon cancer in young adults: trends and their implications. *Curr Oncol Rep.* (2019) 21:3.

37. Cho S, Shin A. Population attributable fraction of established modifiable risk factors on colorectal cancer in Korea. *Cancer Res Treat.* (2021) 53:480–6. doi: 10.4143/crt.2019.742

38. Jodal HC, Klotz D, Herfindal M, Barua I, Tag P, Helsingen LM, et al. Long-term colorectal cancer incidence and mortality after adenoma removal in women and men. *Aliment Pharmacol Ther.* (2022) 55:412–21.

39. Schmuck R, Gerken M, Teegen E, Krebs I, Klinkhammer-Schalke M, Aigner F, et al. Gender comparison of clinical, histopathological, therapeutic and outcome factors in 185,967 colon cancer patients. *Langenbecks Arch Surg.* (2020) 405:71–80. doi: 10.1007/s00423-019-01850-6

frontiers | Frontiers in Immunology

TYPE Original Research
PUBLISHED 16 March 2023
DOI 10.3389/fimmu.2023.1138077

OPEN ACCESS

EDITED BY
Wei Guo,
Qilu Hospital, Shandong University, China

REVIEWED BY
Jorge Melendez-Zajgla,
National Institute of Genomic Medicine (INMEGEN), Mexico
Wentao Dai,
Shanghai Center For Bioinformation Technology, China

*CORRESPONDENCE
Haiyang Feng
haiyangf9@126.com
Guiyu Wang
guiywang@hrbmu.edu.cn

†These authors have contributed equally to this work

SPECIALTY SECTION
This article was submitted to Cancer Immunity and Immunotherapy, a section of the journal Frontiers in Immunology

RECEIVED 05 January 2023
ACCEPTED 06 March 2023
PUBLISHED 16 March 2023

CITATION
Zhong Y, Zheng C, Zhang W, Wu H, Wang M, Zhang Q, Feng H and Wang G (2023) Pan-Cancer analysis and experimental validation identify the oncogenic nature of ESPL1: Potential therapeutic target in colorectal cancer. *Front. Immunol.* 14:1138077. doi: 10.3389/fimmu.2023.1138077

Pan-Cancer analysis and experimental validation identify the oncogenic nature of ESPL1: Potential therapeutic target in colorectal cancer

Yuchen Zhong[1,2†], Chaojing Zheng[1†], Weiyuan Zhang[1], Hongyu Wu[2], Meng Wang[2], Qian Zhang[2], Haiyang Feng[2*] and Guiyu Wang[1*]

[1]Cancer Center/Department of Colorectal Cancer Surgery, The Second Affiliated Hospital of Harbin Medical University, Harbin, Heilongjiang, China, [2]Department of Colorectal Cancer Surgery, The Cancer Hospital of University of Chinese Academy of Sciences (Zhejiang Cancer Hospital), Institute of Basic Medicine and Cancer (IBMC), Chinese Academy of Science, Hangzhou, Zhejiang, China

Introduction: Extra spindle pole bodies like 1 (ESPL1) are required to continue the cell cycle, and its primary role is to initiate the final segregation of sister chromatids. Although prior research has revealed a link between ESPL1 and the development of cancer, no systematic pan-cancer analysis has been conducted. Combining multi-omics data with bioinformatics, we have thoroughly described the function of ESPL1 in cancer. In addition, we examined the impact of ESPL1 on the proliferation of numerous cancer cell lines. In addition, the connection between ESPL1 and medication sensitivity was verified using organoids obtained from colorectal cancer patients. All these results confirm the oncogene nature of ESPL1.

Methods: Herein, we downloaded raw data from numerous publicly available databases and then applied R software and online tools to explore the association of ESPL1 expression with prognosis, survival, tumor microenvironment, tumor heterogeneity, and mutational profiles. To validate the oncogene nature of ESPL1, we have performed a knockdown of the target gene in various cancer cell lines to verify the effect of ESPL1 on proliferation and migration. In addition, patients' derived organoids were used to verify drug sensitivity.

Results: The study found that ESPL1 expression was markedly upregulated in tumorous tissues compared to normal tissues, and high expression of ESPL1 was significantly associated with poor prognosis in a range of cancers. Furthermore, the study revealed that tumors with high ESPL1 expression tended to be more heterogeneous based on various tumor heterogeneity indicators. Enrichment analysis showed that ESPL1 is involved in mediating multiple cancer-related

pathways. Notably, the study found that interference with ESPL1 expression significantly inhibited the proliferation of tumor cells. Additionally, the higher the expression of ESPL1 in organoids, the greater the sensitivity to PHA-793887, PAC-1, and AZD7762.

Discussion: Taken together, our study provides evidence that ESPL1 may implicate tumorigenesis and disease progression across multiple cancer types, highlighting its potential utility as both a prognostic indicator and therapeutic target.

KEYWORDS

cell cycle, ESPL1, pan-cancer, patient derived organoids, cancer therapy

1 Introduction

It is well known that cancer incidence is significantly associated with age. To date, cancer remains the second leading cause of human death (1). Despite the advances in medical technology and the increasing number of cancer treatment options, a large number of patients are still diagnosed at an advanced stage when treatment approaches are often not feasible, eventually resulting in cancer-related death. Given that surgery and chemotherapy alone are not enough to save cancer patients, there is a need to develop more cancer treatment options. Therefore, this calls for studies to explore the mechanisms of cancer development at the molecular level for effective diagnosis and treatment.

ESPL1 (extra spindle pole bodies like 1) is a protein-coding gene whose related pathways are mitotic G1-G1/S phases and cell cycle. Notably, ESPL1 is regulated by at least two independent mechanisms. First, it is inactivated *via* interaction with securin/PTTG1, which probably covers its active site (2). It should be noted that its association with PTTG1 is not only inhibitory since PTTG1 is also required for ESPL1 activation, and thus the enzyme is inactive in cells in which PTTG1 is absent. Therefore, degradation of PTTG1 at anaphase liberates ESPL1 and triggers RAD21 cleavage. Second, phosphorylation at Ser-1126 inactivates it. The complete phosphorylation during mitosis is removed when cells undergo anaphase. Studies have proposed that activating the enzyme at the metaphase-anaphase transition requires the removal of both securin and inhibitory phosphate (3–5). A previous cancer study discovered frequent alterations in STAG2 and ESPL1 in bladder cancer, which suggests that it may be involved in bladder tumorigenesis through sister chromatid cohesion and segregation process (6). In addition, two other previous studies concluded that ESPL1 might be a prognostic biomarker in malignant glioma and endometrial cancer (7, 8).

Considering that ESPL1 is still inadequately studied in cancer and there are no relevant pan-cancer analyses, the main aim of this study was to perform a systematic full-scale pan-cancer analysis of tumor samples from public databases. Specifically, we explored the expression and prognostic significance of ESPL1 in various human malignancies using data from The Cancer Genome Atlas (TCGA). Furthermore, we evaluated the association of ESPL1 expression with tumor-infiltrating immune cells and immune-related genes, and then explored the association between ESPL1 expression and tumor mutational load (TMB), microsatellite instability (MSI), mutant-allele tumor heterogeneity (MATH), and homologous recombination deficiency (HRD). Moreover, we identified ESPL1 specific genes and signaling pathways that regulate cancer progression and finally performed a drug correlation analysis. Collectively, the findings of this study reveal that ESPL1 is associated with tumorigenesis and progression in a variety of cancers, which suggests that it is a potential prognostic marker.

2 Materials and methods

2.1 Data collection and processing

Standardized pan-cancer dataset was downloaded from the Xena functional genomics explorer (https://xenabrowser.net/) database, followed by extraction of the expression data of ENSG00000135476 (ESPL1) gene in each sample. Next, log2(x+1) transformations were performed for each expression value. Notably, the expression data of 33 cancer species were obtained. Due to the small sample size of normal tissues from the TCGA database, we further retrieved normal tissue expression data from the GTEX database (9). The abbreviations for the names of the cancers are in Supplementary Table 1. For colorectal cancer, liver cancer, lung cancer, and cervical cancer, we also compared gene expression levels using GEO data. These eight GEO datasets are GSE39001 and GSE6791 for cervical cancer (10, 11), GSE112790 and GSE45267 for liver cancer (12, 13), GSE68571 and GSE75037 for lung cancer (14, 15), and GSE24550 and GSE21815 for colorectal cancer (16, 17). To ensure data comparability, we performed normalization of the data using the "preprocessCore" package. For batch effects, we utilized the "removeBatchEffect" function from the "limma" package for removal.

2.2 Gene expression and clinical and survival analysis

The tumor cell line expression matrix was obtained from the CCLE dataset (https://portals.broadinstitute.org/ccle/about), and analysis was conducted using "ggplot2" R package (v3.3.3) (18, 19).

Next, we obtained a high-quality prognostic dataset from the TCGA prognostic study previously reported by Liu J et al (20). The Cox proportional hazards regression model was then built using the "coxph" function of the "survival" R package (version 3.2-7) to analyze the relationship between gene expression and prognosis in each tumor. The function "surv_cutpoint" calculates the optimal cut point for survival analysis and restricts the group proportion such that a subgroup cannot exceed 60% of the total sample size.

Univariate Cox regression analysis and forest plots generated through the "forestplot" R package were used to display the P value, HR, and 95% CI of each variable. For the multivariate analysis, we utilized the R package "coxph" for data processing and incorporated various factors such as TNM staging, clinical staging, tumor grade, tumor location, pathological type, age, and sex for different cancer types. Finally, the "survminer" package was used to visualize the results of the multivariate analysis.

For receiver operating characteristic (ROC) analysis, we performed the analysis using the "timeROC" package (version 0.4) in R language and generated the graphs using the "pdf" and "plot" functions. The ROC was constructed based on three primary parameters: survival status, survival time, and ESPL1 expression level. The training and testing sets were randomly partitioned using the "caret" package, with a ratio of 70:30 for the partitioning. Specifically, the "createDataPartition" function was employed for random partitioning, with the survival outcome as the sampling parameter. 70% of the samples were designated as the training set and the remaining 30% as the testing set.

For age comparison, we divided the samples into high and low expression groups based on the median ESPL1 expression level and compared the age distribution between the two groups. For comparison between genders, we directly compared the ESPL1 expression levels between males and females in each cancer type.

2.3 Genetic heterogeneity analysis

Homologous recombination deficiency (HRD) data for each tumor was obtained from previous studies (21). We then integrated the HRD and gene expression data of the samples, and then log2(x +1) was further used to transform each expression value.

MuTect2 software processed the level 4 simple nucleotide variation dataset downloaded from TCGA, calculated the tumor mutation burden (TMB) and mutant-allele tumor heterogeneity (MATH) for each tumor using the TMB and inferHeterogeneity function of the R package maftools (version 2.8.05), and combined the TMB and MATH score with gene expression data (22). A log2(x +1) transformation was further applied to each expression value.

The microsatellite instability (MSI) scores for each tumor were obtained from previous studies and integrated with the available data, and finally log2(x+1) transformations were performed (23).

2.4 Immune analysis

The expression data of two types of immune checkpoint pathway genes [inhibitory (24) and stimulatory (25)] and five types of immune pathway genes [chemokine (26), receptor (18), MHC (21), immuno-inhibitor (24), and immuno-stimulator (27)] in each sample were extracted from the downloaded TCGA dataset, and all normal samples were filtered. Log2(x+1) transformation was performed on each expression value, and the Pearson correlation between ENSG00000135476 (ESPL1) and marker genes was calculated. Next, the deconvo_xCell method of the R package IOBR (version 0.99.9) was used to analyze the relationship between immune cells and the expression of ESPL1 (24, 28). We used the false discovery rate (FDR) method to correct the p-values when performing the correlation analysis to ensure statistical accuracy. In more detail, the 'corr.test' function in the R package 'psych' is used for correlation analysis, with the 'adjust' parameter set to 'fdr'.

Notably, the ESTIMATE algorithm includes three scores: immune score (assessment of immune cell infiltration level); stromal score (assessment of immunity of stromal components); and ESTIMATE score. The "Estimate" R package evaluates the above three scores for each TCGA sample (29).

2.5 Protein–protein interaction analysis

The protein-protein interaction (PPI) network was established using the Search Tool for the Retrieval of Interacting Genes (STRING) (https://cn.string-db.org/) with the following input parameters: "evidence", "experiments", and "low confidence level". A total of 31 nodes were finally obtained and subjected to enrichment analysis. The Kyoto Encyclopedia of Genes and Genomes (KEGG) results were replotted by http://www.bioinformatics.com.cn, a free online platform for data analysis and visualization.

2.6 Enrichment analyses and similar genes

The GEPIA2 (http://gepia2.cancer-pku.cn/#index) database was used to obtain the top 200 genes similar to ESPL1 based on the TCGA dataset using the "Similar Gene" function (30). The heat map of similar genes and ESPL1 correlation was also obtained using the "Gene_Corr" function of TIMER2.0 database (http://timer.cistrome.org/) (31–33). The ESPL1 negatively correlated genes were identified using the "psych" package in R.

Next, Webgestalt (http://www.webgestalt.org/) and "clusterprofile" package in R were used for enrichment analysis of the 200 similar genes (34, 35). The basic parameters were Homo sapiens, ORA, and pathway-KEGG, whereas the reference set was genome encoding-protein. In addition, the advanced parameters were set to FDR < 0.05.

2.7 Drug sensitivity analysis

The Genomics of Drug Sensitivity in Cancer (GDSC) (https://www.cancerrxgene.org/) and Cancer Therapeutics Response Portal (CTRP) (https://portals.broadinstitute.org/ctrp/) databases were used

for drug sensitivity analysis (25, 36–40). Finally, the two sub-datasets were pooled, and Pearson's correlation analyses were performed.

2.8 Cell culture

The present study used eight cell lines from four cancers for *in vitro* experiments. Three colorectal cancer cell lines (SW620, LOVO, and HCT116), two lung carcinoma cell lines (A549 and PC9), two liver cancer cell lines (HepG2 and Hep3B), and the cervical cancer cell line Hela are included. HeLa, Hep3B, HepG2, SW620, LOVO, and A549 cells were grown in 10% FBS-supplemented DMEM media. PC9 was grown in 1640 medium containing 10% FBS. HCT116 was grown on McCoy's 5A medium supplemented with 10% FBS. The cultures were incubated at 37°C with 5% CO2.

2.9 Organoids culture

The study was approved by the Ethics Committee of Zhejiang Cancer Hospital, and samples were taken from colorectal cancer patients who underwent surgery at the hospital. After surgery, colorectal samples were sent to the pathology department for pathological examination as part of routine clinical care for cancer patients. Harvesting the tissues had no impact on the patients' surgical procedures, post-operative radiotherapy or chemotherapy, diagnosis, or the cost of treatment, and therefore the patients' informed consent was non-mandatory.

A total of 12 colorectal cancer organoids were harvested. Briefly, after obtaining the cancer tissue, the tissue is first thoroughly washed using a washing buffer. The tissue is then cut up and added to the tissue digestion solution. The tumor cells were filtered using a 70 μM filter, resuspended again using the washing buffer, and centrifuged three times. After the removal of the supernatant, the Matrigel (BD, 356234) was added for resuspension. Finally, the cell suspension was inoculated into 48-well plates (Corning 3300). Organoid culture medium purchased from STEMCELL (IntestiCult™ Organoid Growth Medium (Human), Cat.06010).

2.10 Drug sensitivity assay

PHA-793887 (HY-11001), PAC-1 (HY-13523), and AZD-7762 (HY-10992) were purchased from MCE (https://www.medchemexpress.com/). DMSO is used as a solvent, and the maximum concentration of DMSO during cell culture does not exceed 0.5%. Organoid viability assay using the CellTiter-Glo® 3D Cell Viability Assay (Promega, G9681). All drug sensitivity verifications were carried out on the third day after the drug was delivered.

2.11 Cell viability assay

CCK-8 Cell Counting Kit (A311-01) was purchased from Vazyme (www.vazyme.com/) to assess the proliferative assay. The assay protocol is carried out in accordance with the manufacturer's manual. The absorbance was measured at 450 nM by a microplate reader (Tecan, Switzerland).

2.12 Total RNA extraction and qRT-PCR

FastPure Cell/Tissue Total RNA Isolation Kit V2 (RC112) from Vazyme® used to extract RNA from cell. HiScript® II Q RT SuperMix for qPCR (+gDNA wiper) (R223) from Vazyme® used to reverse transcription. ChamQ Universal SYBR qPCR Master Mix (Q711) from Vazyme® used for qPCR validation.

Primer of ESPL1 sequences (5'→3'): F: GAAGACTCA GCCTCAGGTG, R: TAGAAAGACCAGTGGCTACG.

Primer of GAPDH sequences (5'→3'): CAGGAGGCAT TGCTGATGAT, R: GAAGGCTGGGGCTCATTT.

2.13 Cell transfects

siRNA transfect was performed using Lipofectamine 2000 reagent (Invitrogen) according to the manufacturer's instruction. siRNA-1 sequences: Sense: 5'-AAAGUUGACUCUUUUGAAGCU-3', Antisense: 5'-CUUCAAAAGAGUCAACUUUGG-3'. siRNA-2 sequences: Sense: 5'-AGACAAAGAGAAUUCGUUCCA-3', Antisense: 5'-GAACGAAUUCUCUUUGUCUUA-3'.

3 Results

3.1 Aberrant expression of ESPL1 in cancer tissues

We first compared the difference in expression of ESPL1 between cancer and normal tissues and found that ESPL1 was commonly highly expressed in cancers (Figure 1A). Given the insufficient number of normal samples, the data of normal samples from the GTEx database was added for comparison. Results showed that ESPL1 was significantly highly expressed in ACC, BLCA, BRCA, CECS, CHOL, COAD, ESCA, GBM, KIRP, LAML, KICH, LGG, LIHC, LUAD, LUSC, OV, PAAD, PRAD, READ, SKCM, TGCT, STAD, USC and UCEC (Figure 1B). We also used the CCLE database to verify cell line-level expression. We found that the highest expression of ESPL1 was in lymphoma, leukemia, neuroblastoma, and liver cancer cell lines (Figure 1C). Moreover, the expression of ESPL1 was low in liposarcoma, bile duct cancer, and head and neck cancer cell lines.

Next, we evaluated the level of ESPL1 expression in multiple cancer types at different pathological stages. As shown in Supplementary Figure 1, we divided all samples into early (Stage I and II) and late (Stage III and IV) groups based on pathological staging. This type of grouping is more commonly used in clinical trials. We found significantly higher expression of ESPL1 in stage III and IV samples in ACC, CESC, KIPAN, KIRC, KIRP, LIHC, LUAD, UCEC and UCS. In contrast, a different result emerged in THYM and OV, where expression was lower in advanced-stage samples.

Finally, we further validated the dysregulated expression of ESPL1 by comparing it with eight independent GEO datasets, including cervical cancer, lung cancer, liver cancer, and colorectal cancer. Consistently, ESPL1 expression was significantly elevated in cancer samples across all eight datasets (Supplementary Figure 2).

We hypothesized that the expression level of ESPL1 may vary in different patients with the same cancer type. Thus, we combined ESPL1 expression with clinical information and found that ESPL1 expression levels showed statistical differences with age and sex in some cancers. As shown in Supplementary Figure 3A, the high expression group of ESPL1 had a higher average age in BLCA, KICH, LGG, PRAD, and UCEC, while in BRCA, ESCA, LUSC, LAML, PCPG, and THYM, the high expression group had a lower average age. Similarly, there were gender differences in ESPL1 expression levels, with higher expression levels observed in females in KIRP, LIHC, and SARC, and males had higher expression levels in LAML and LUAD (Supplementary Figure 3B).3.2 ESPL1 has potential as a tumor prognostic marker.

Considering that numerous genes highly expressed in cancer tissues affect patient prognosis, we speculated that ESPL1 also impacts patient survival. Therefore, we separated the patients into high and low expression groups for survival analysis based on ESPL1 expression, with the cut-off value by the median of expression.

As shown in Figure 2, a univariate analysis was performed with patient death as the event endpoint. Results showed that the prognosis of patients was worse in the ESPL1 high expression group in ACC, KIRP, LGG, MESO, KIRC, KICH, UCEC, PAAD, LUAD, PCPG, SKCM, LIHC, and SARC. Conversely, a positive correlation was found between high ESPL1 expression and improved prognosis in THYM. In addition, it was found that ESPL1 was highly expressed in ACC, CHOL, KIRC, KIRP, LGG, LUAD, SKCM, and UCEC cancerous tissues, and it shortened the survival of patients. Figure 2B demonstrates the relationship between ESPL1 expression and Progression Free Interval (PFI), where we found that in 18 types of cancer, high expression of ESPL1 was associated with poorer PFI.

Multivariate analysis is a statistical technique that analyzes the relationships between multiple variables in a dataset. It is used to determine the strength and direction of the relationships between variables, and to identify patterns and trends in the data. We combined ESPL1 expression with various clinical information and verified the effect of ESPL1 on patient prognosis through multivariate analysis. As shown in Supplementary Figure 4, ESPL1 remained a prognostic risk factor (HR>1 and p<0.05) for ACC, KICH, LUAD, MESO, PAAD, PCPG, SKCM, SARC, and LGG, further suggesting that ESPL1 may play an oncogenic role.

We postulated that ESPL1 could potentially serve as a marker for predicting cancer development. We constructed a receiver operating characteristic curve based on ESPL1 expression to test this. As shown in Figure 2C, the heat map demonstrates the area under the curve (AUC) for predicting patient OS for ESPL1 in 32 tumors. In ACC, MESO, KICH, KIRP, LGG, and PCPG, the AUC were determined with high precision to be greater than 0.70

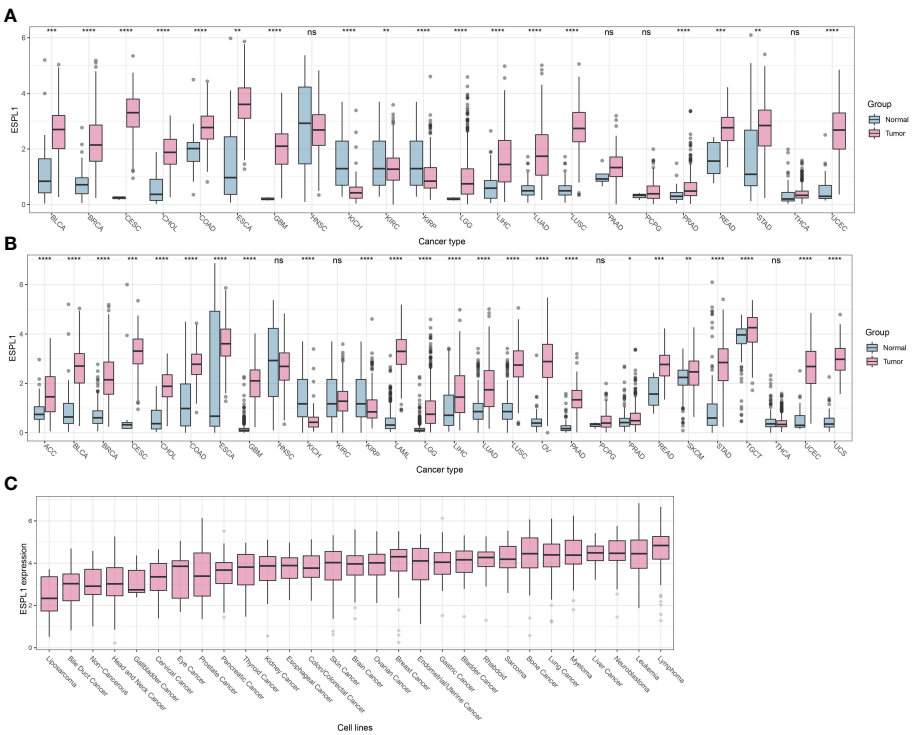

FIGURE 1
ESPL1 is aberrantly expressed in tumor tissue. **(A)** Expression profile of ESPL1 in TCGA cohorts. **(B)** Expression analysis of ESPL1 in tumor tissues from TCGA database and matched normal tissues from the GTEx database. **(C)** Expression of ESPL1 in different types of cell lines. *P<0.05, **P<0.01; ***P<0.001, ****P<0.0001; ns, Not Significant. GTEx, Data of Genotype-Tissue Expression; TCGA, The Cancer Genome Atlas.

10.3389/fimmu.2023.1138077

(Figure 2D). Specifically, in ACC, the AUC of ESPL1 predicted prognosis with a value between 0.83 and 0.94. In GBM and UVM, the AUC for predicting 5-year survival reached 0.74 and 0.87, respectively, although the accuracy of predicting 1-4 year prognosis was poor.

Finally, we plotted Kaplan-Meier survival curves grouped according to ESPL1 expression based on the best cut-off value method. As shown in Figure 3, the survival time was shorter for high expression of ESPL1 in the 18 tumors.

Based on these findings, we conclude that ESPL1 may have oncogenic characteristics, and high expression is associated with poorer prognosis in cancer patients. We believe that, following validation through further prospective clinical studies, ESPL1 has the potential to become a prognostic biomarker in various malignancies.

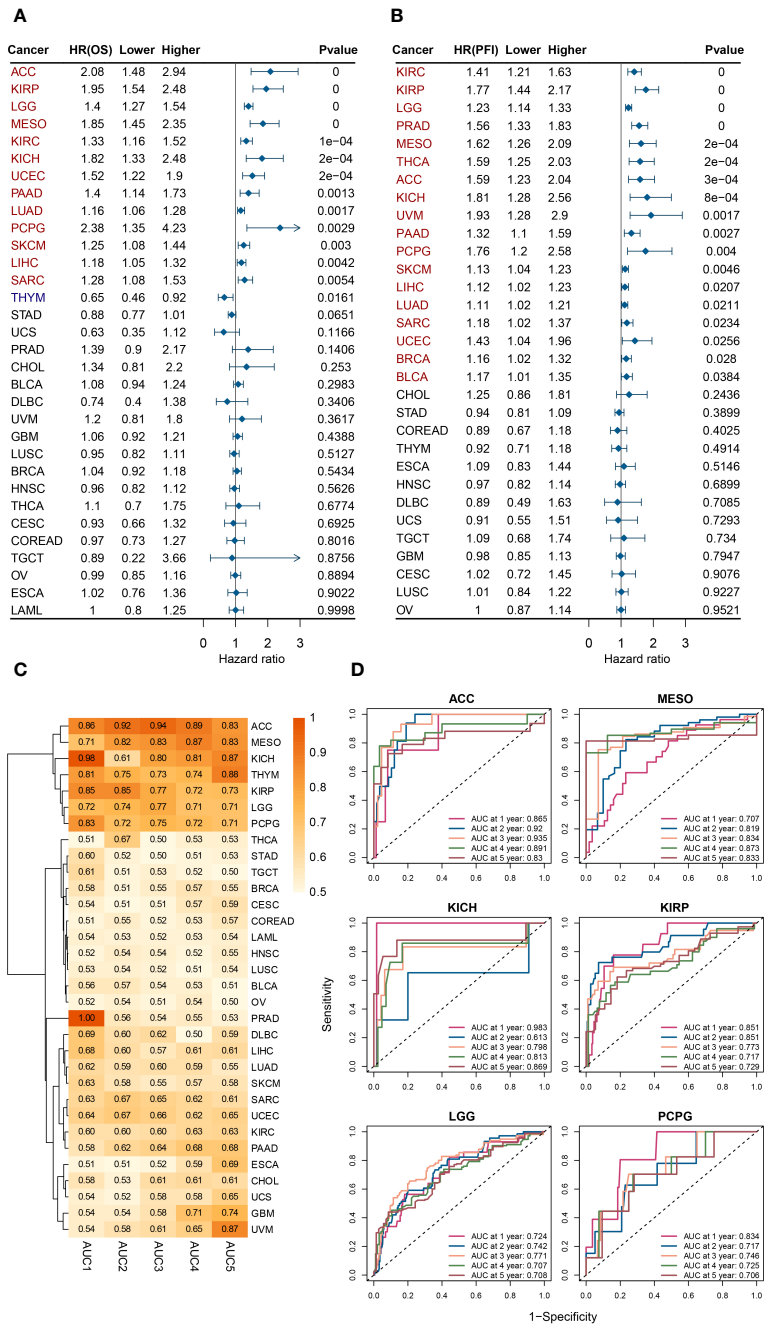

FIGURE 2
ESPL1 expression correlates with patient prognosis. Forest plot of associations between ESPL1 expression and **(A)** OS and **(B)** PFI. **(C)** Heat map of AUC of ESPL1 expression to predict patient prognosis from 1 to 5 years. **(D)** ROC of ESPL1 expression to predict prognosis in ACC, MESO, KICH, KIRP, LGG and PCPG. OS, overall survival; PFI, Progression Free Interval; AUC, Area Under Curve; ROC, Receiver Operating Characteristic.

3.3 Correlation between ESPL1 and tumor microenvironment

The tumor microenvironment (TME) is critical for tumor growth and is directly associated with tumor progression and metastasis. Therefore, we analyzed the correlation between ESPL1 expression in various cancers and the immune cells/scores using the XCELL algorithm (Figure 4A). We found that THYM and THCA correlated extremely well with ESPL1 expression. In particular, in THYM, there was a strong correlation with a variety of T cells. In contrast, in THCA, ESPL1 expression was positively correlated with immune cells and stromal cells. LUAD, PAAD, STAD, LIHC, COAD, LUSC, ESCA, UCEC, BLCA, and SARC negatively correlated with immune microenvironment cells. This result gives us a hint that ESPL1 may play different roles in the immune microenvironment in different cancers.

We also calculated the immune, stromal, and ESTIMATE scores using the ESTIMATE algorithm. It was found that the expression of ESPL1 was negatively correlated with these scores in most cancers. However, THCA, KIPAN, GBMLGG, and KIRC were positively correlated with immune scores (Figure 4B; Supplementary Table 2). Similarly, THCA, KIPAN, and GBMLGG were positively correlated with stromal scores (Figure 4C; Supplementary Table 2). The same results were also found about the estimate scores. Moreover, the expression of ESPL1 was positively correlated with the ESTIMATE score in THCA, KIPAN, GBMLGG, and KIRC (Figure 4D; Supplementary Table 2). In THYM, ESPL1 was significantly positively correlated with the

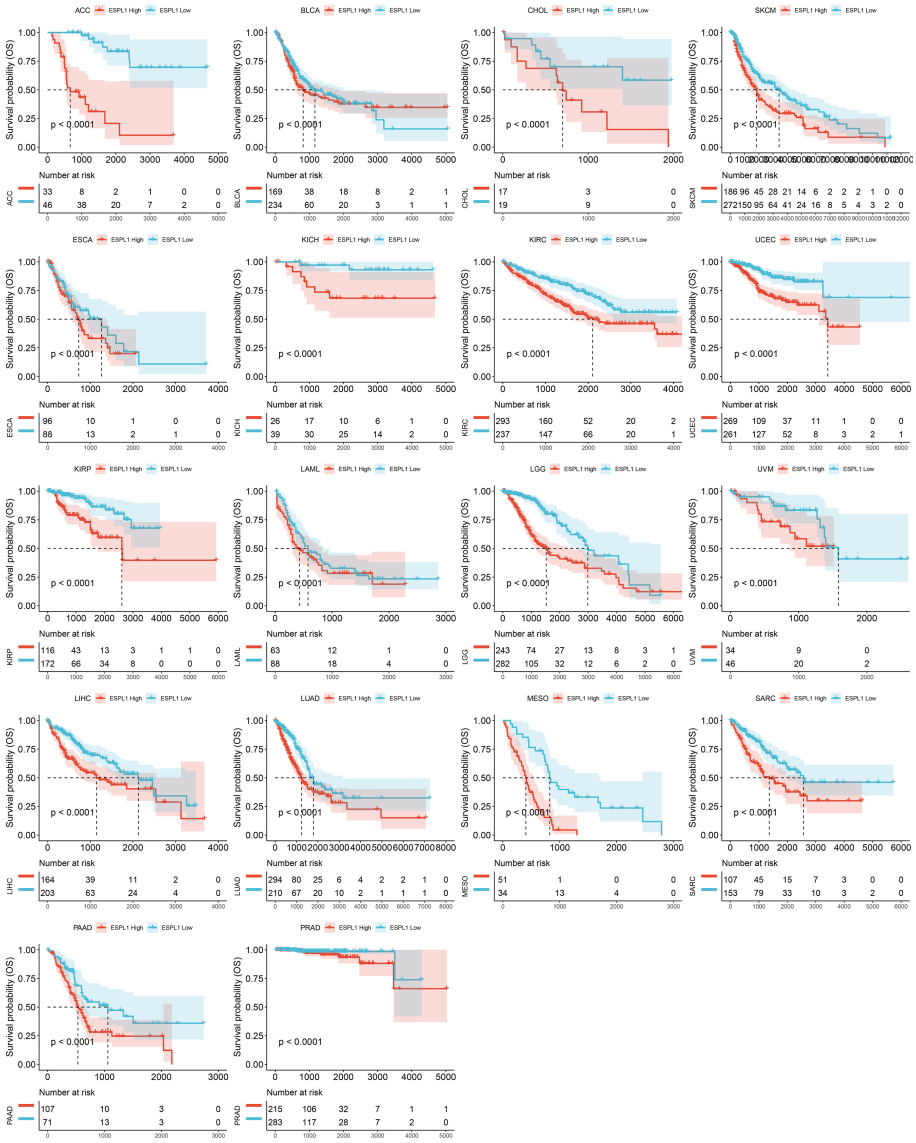

FIGURE 3
Kaplan-Meier plots with statistically significant differences in overall survival analysis by best-cut off value method for ESPL1.

10.3389/fimmu.2023.1138077

immune score but negatively correlated with the ESTIMATE score. This finding is consistent with xCell results, which show that ESPL1 expression significantly correlates with T and B cells, increasing the immune score. However, the correlation with stromal cells is negative or not significant, resulting in a negative correlation in stromal score. In LUAD, PAAD, STAD, LIHC, COAD, READ, LUSC, ESCA, UCEC, BLCA, SARC, and ACC, the xCell results demonstrated a negative correlation trend between various T cells, B cells, macrophages, and ESPL1 expression, which is consistent with the immune score in ESTIMATE. Overall, the three immune scores showed a significant negative trend in GBM, ESCA, STES, SARC, STAD, UCEC, SKCM, PAAD, OV, BLCA, and ACC. In KIPAN, THCA, there was a significant positive correlation. No statistically significant correlations existed in MESO, READ, KIRP, LAML, UVM, UCS, CHOL, and DLBC. This indicates that the function of ESPL1 may differ significantly among different types of tumors.

3.4 Correlation between ESPL1 expression and immune markers

Given that immunoregulatory genes are closely associated with cancer development, we evaluated the expression data of 150 immunoregulatory genes in each sample and correlated them with the expression of ESPL1 (Figures 5A–E). Figure 5A shows the heatmap of immunostimulatory genes with ESPL1 expression. Through clustering, we found high positive correlations in DLBC, KIPAN, and THCA. While in PRAD, READ, LIHC, OV, KIRC, LAML, HNSC, UVM, MESO, and GBMLGG, there is a predominantly positive correlation trend. An extremely strong correlation emerged in THYM. This trend switched to a negative correlation in LUAD, LUSC, and STES. Notably, CD276, MICB, PVR, and ULBP1 showed statistically significant correlations with ESPL1 in most tumors, suggesting that these genes may be essential to unlocking the influence of ESPL1 on tumor development.

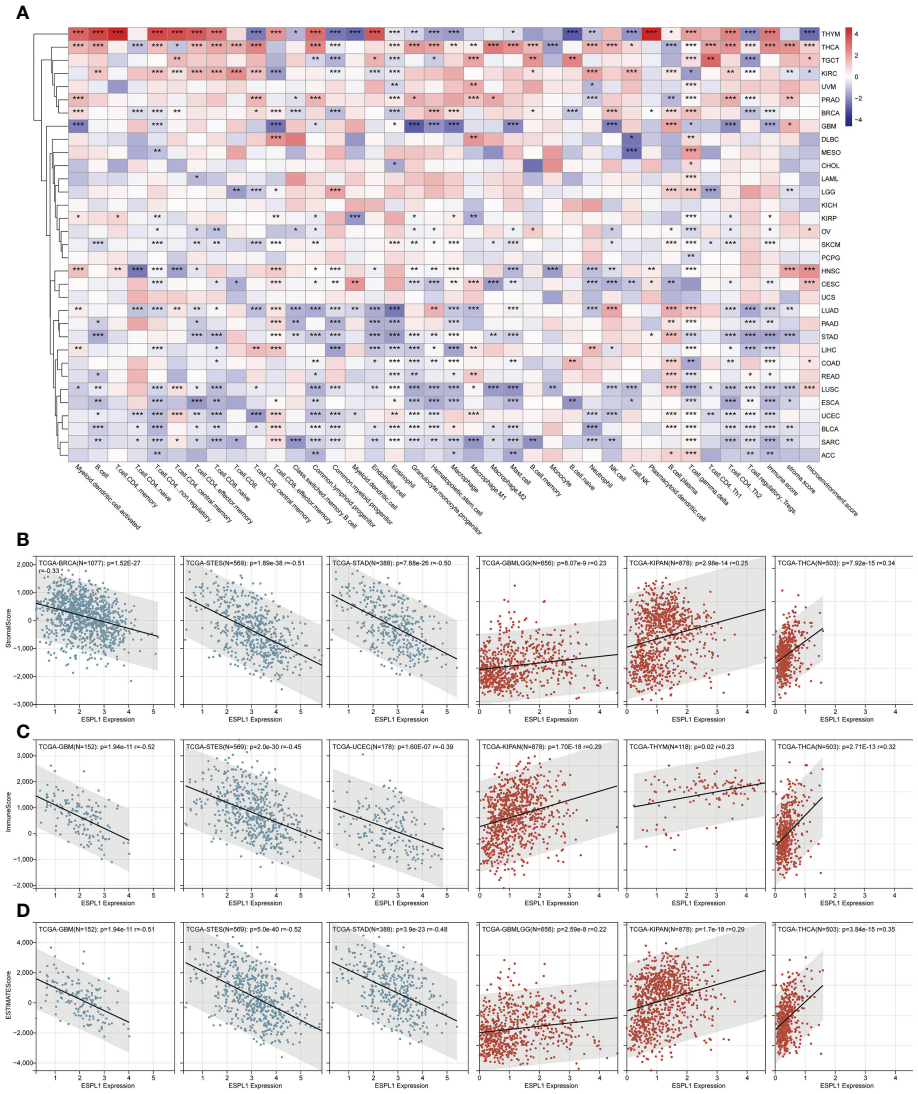

FIGURE 4
The effect of ESPL1 on TME in pan-cancers. **(A)** Correlation between ESPL1 and TME cells by xCELL algorithm. Representative results of correlation analysis between ESPL1 expression and immune score **(B)**, stromal score **(C)** and ESTIMATE score **(D)** by ESTIMATE algorithm (Three most positive correlations versus three most negative correlations). *p<0.05, **p<0.01, ***p<0.001. TME, tumor microenvironment.

Chemokines are very powerful and can impact tumor migration and immune cell infiltration. Through Figure 5B, we explored the correlation between chemokines and ESPL1. Similarly, the correlations showed a divergent trend, with the expression of chemokine genes increasing with the expression of ESPL1 in KIPAN, KIRC, THCA and, conversely, a statistically negative correlation in TGCT, GBM, LUSC and THYM. Figures 5C–E shows the correlation results of ESPL1 with receptor, immunoinhibitor and MHC, respectively. The bifurcation trend was again observed, with STES, STAD, and LUSC showing a negative trend among receptor-related genes, while GBMLGG, KIPAN, THCA, PRAD, KIRC, LIHC, and HNSC showed a positive trend. In the correlation analysis with MHC, significant positive correlations were also found in KIRC, LGG, GBMLGG, KIPAN, THCA, and PRAD. These results suggest that the correlation between ESPL1 and immunity is extremely strong in KIPAN, GBMLGG, and THCA; in these tumors, more immune-related validation is needed.

3.5 Correlation between ESPL1 expression and tumor heterogeneity

Considering that TMB and MSI correlated with immunotherapy efficacy, we further assessed the correlation between ESPL1 expression and TMB and MSI. Immune checkpoint inhibitor sensitivity is associated with high tumor mutational burden (TMB), Figure 6A shows the information of TMB with ESPL1 expression in each cancer. The results indicated that TMB positively correlated with ESPL1 expression in DLBC, CHOL, ACC, LUAD, KICH, PRAD, LGG, STAD, PADD, BRCA, SARC, and READ. Surprisingly, there was a statistically negative correlation between the expression of ESPL1 and TMB in THYM, with high expression of ESPL1 being associated with a better prognosis. The instability of microsatellites results from defects in the mismatch repair system, resulting in hypermutation patterns. MSI is often used to guide treatment, such as in colorectal cancer, where immune

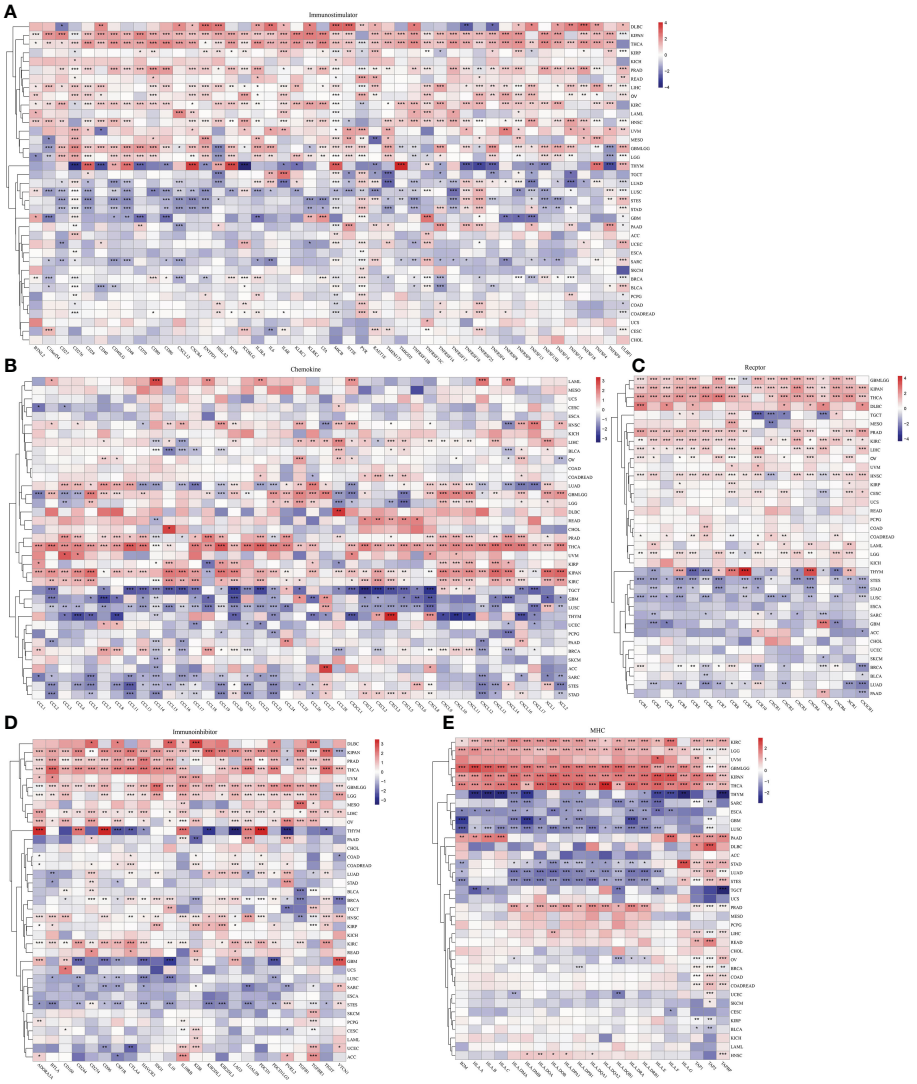

FIGURE 5
The effect of ESPL1 on immunological genes in pan-cancers. Correlation between ESPL1 and **(A)** immunostimulators, **(B)** chemokines, **(C)** receptors, **(D)** Immunoinhibitor and **(E)** MHC. *p<0.05, **p<0.01, ***p<0.001.

checkpoint blockade treatment decisions are made based on a patient's MSI status. From Figure 6B, we can find that MSI showed a significant negative correlation with the expression of ESPL1 in DLBC and a positive trend in LUSC, ACC, and STAD. Previous studies have reported that homologous recombination deficiency will produce specific and quantifiable genomic changes, and the HRD status is a key indicator of treatment and prognosis in many tumors (21, 41, 42). After analyzing the relationship between HRD and ESPL1 expression, we found that HRD increased with the increase of ESPL1 expression in 22 types of tumors (Figure 6C). Mutant-allele tumor heterogeneity (MATH) is an algorithm for assessing tumor heterogeneity, with higher MATH values indicating higher tumor heterogeneity (26, 43). This study explored the relationship between MATH and ESPL1 expression and found a significant correlation in 14 tumors, with a positive correlation in 10 tumors and a negative correlation in four tumors (GBMLGG, LGG, KIPAN, and THCA) (Figure 6D).

3.6 Enrichment analysis of ESPL1

To further explore the molecular mechanisms and functions of the ESPL1 gene in tumorigenesis, enrichment analysis was performed to screen for ESPL1-related proteins and pathways. First, protein–protein interaction (PPI) network analysis was performed using STRING, and the top 30 genes associated with ESPL1 were obtained (Figure 7A). After KEGG analysis of these genes and drawing Sangchi map, it was found that the pathways significantly associated with tumor were enriched in cell cycle, the AMPK signaling pathway, and the PI3K Akt signaling pathway (Figure 7B). Next, we performed gene ontology (GO) enrichment

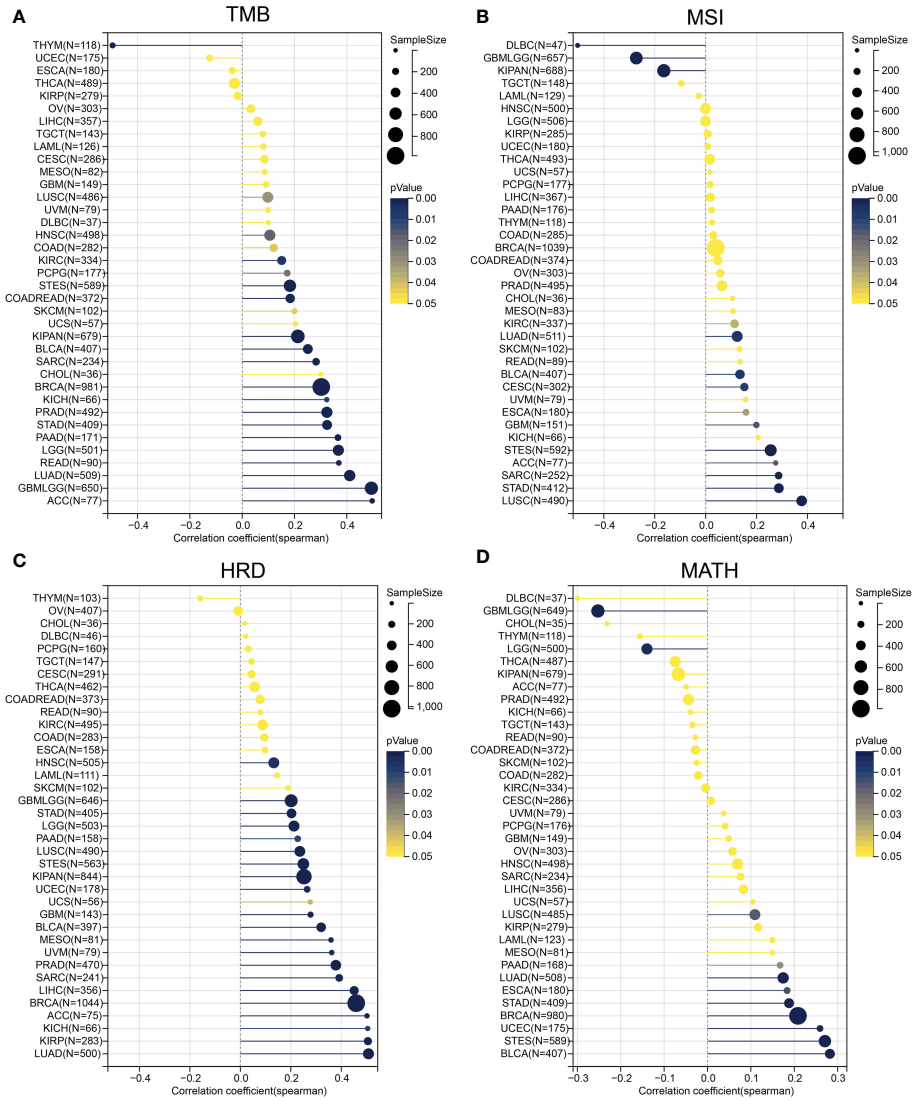

FIGURE 6
Correlation of ESPL1 with tumor heterogeneity. Correlation between ESPL1 expression and **(A)** TMB, **(B)** MSI, **(C)** HRD and **(D)** MATH. TMB, tumor mutational burden; MSI, microsatellite instability; HRD, homologous recombination deficiency; MATH, mutant-allele tumor heterogeneity.

analysis with regard to biological processes, cell components, and molecular functions (Figure 7C). In addition, we combined the expression data of all TCGA tumors and identified the top 200 genes most related to ESPL1 expression (the list of the top 200 similar genes is provided in Supplementary Table 3). We then analyzed the correlation between the first ten similar genes and ESPL1 and found that all were significantly positively correlated with ESPL1 expression (Figure 7D). Moreover, the KEGG enrichment results showed that the 200 genes were mainly associated with cancer-related pathways, including cycle, DNA replication, and mismatch repair (Figure 7E). To further explore the biological functions of down-regulated ESPL1-related proteins, we obtained the top 200 genes negatively correlated with the expression level of ESPL1. We performed enrichment analysis on these genes (Supplementary Tables 4, 5). However, these 200 genes showed no statistically significant enrichment in the terms or pathways identified in the KEGG or GO analyses. No terms with an FDR<0.05 were enriched for BP, MF, and CC. This set of 200 genes may have lacked annotations in the enrichment analysis or may not be involved in any specific biological functions.

3.7 Drug sensitive analyses of ESPL1

Furthermore, GDSC and CTRP, two of the largest tumor-related drug databases, were utilized to discover drugs that target

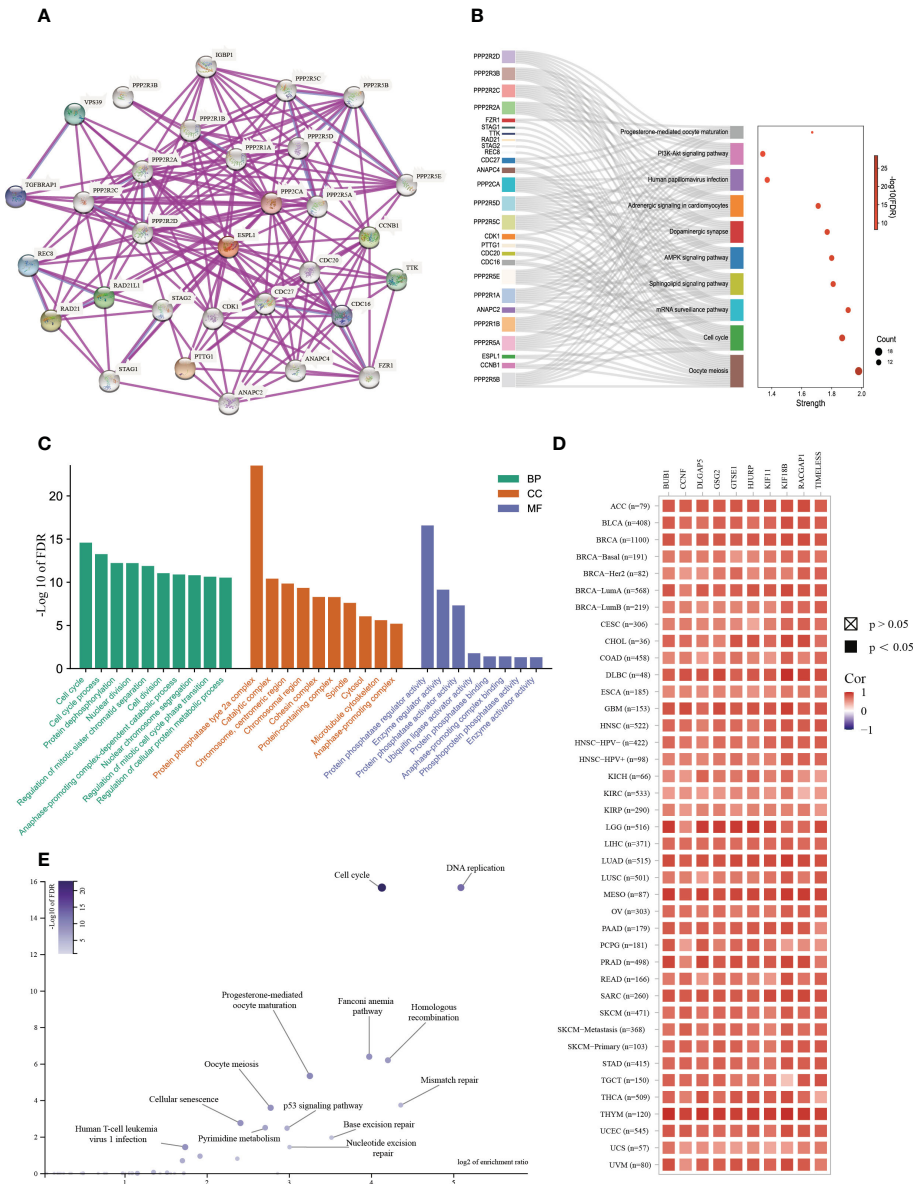

FIGURE 7
Enrichment analysis of ESPL1-related partners. **(A)** PPI analysis of ESPL1. **(B)** Sankey diagram of KEGG pathway analysis results. **(C)** GO functional classification. **(D)** Heat map of ESPL1 correlations with the top 10 similar genes in different cancer types. **(E)** Volcano plot of KEGG results for 200 similar genes. PPI, protein-protein interaction; KEGG, Kyoto Encyclopedia of Genes and Genomes. BP, biological process. CC, cellular component. MF, molecular function. FDR, false discovery rate.

tumors with high ESPL1 expression. the CTRP database indicated that GSK-J4 (R= -0.471) and BRD-K30748066 (R= -0.469) were the most negatively correlated with ESPL1 expression (Figure 8A). Figure 8B shows the top 20 drugs negatively correlated with high ESPL1 expression *via* GDSC, with NPK76-II-72-1 (R= -0.318) being the most negatively correlated. Using the intersection, we identified twelve medicines that appeared in both datasets (Figure 8C). Three medications that impede the cell cycle or induce apoptosis are among the most remarkable findings from comparing the data. PHA-793887 is a strong CDK inhibitor with anti-cancer effects on the cell cycle (44). The activation of procaspase-3, which promotes apoptosis, is the approach through which Procaspase activating compound 1 (PAC1) kills cancer cells (45). AZD-7762 is a checkpoint kinase inhibitor that inhibits tumor proliferation and growth by targeting Chk1 and Chk2 (46). Coincidentally, ESPL1 is a critical cell cycle regulator, and as ESPL1 expression rises, so does the drug sensitivity of the cell cycle inhibitors list above.

Therefore, we determined the connection between ESPL1 expression and these three small molecule inhibitors using colorectal cancer patient-derived organoids. Figures 8D–F show the molecular structures from PubChem of PHA-793887, PAC1, and AZD-7762, respectively. Figure 8G depicts images of the organoids in normal culture before and two days after adding the drugs (days 0 and 2). The normal growth of the organoid had a circular form with a maximum diameter of 200 μM; however, the addition of drugs resulted in a considerable reduction in roundness, fragmentation, and darkening. Figure 8H shows the distribution of the expression of ESPL1 in 12 cases of organoid. The expression of ESPL1 varied greatly, with the maximum expression of PDO#6 being 57 times higher than the lowest expression. By analyzing the link between drug sensitivity and ESPL1 expression in the organoids, we determined that the IC50 of the three drugs reduced dramatically with increasing ESPL1 expression (Figures 8I–K). We also discovered that the IC50 of PHA-793887 varied widely between organoids, with the greatest IC50 reaching 179 μM (PDO#10) and the lowest reaching only 6.6 μM (PDO#06).

To investigate whether ESPL1 is a direct target of PAC1, AZD-7762, and PHA-793887, we performed IC50 assays after knocking down ESPL1 expression in HCT116 and SW620 cell lines. As shown in the Supplementary Figure 5, there was no significant change in the IC50 values of the three drugs after ESPL1 knockdown. Only in SW620, the IC50 of AZD7762 was reduced after knockdown using si1, which was unexpected and may contradict our initial hypothesis.

3.8 Knockdown of ESPL1 impact on proliferation *in vitro*

A total of 8 types of cell lines, including colorectal, liver, lung, and cervical cancer, were used to verify the impact of knockdown ESPL1. ESPL1 is highly expressed in these cancers, and the prognosis is worse for high expression. Initially, we inhibited the expression of ESPL1 in these cell lines using siRNA and confirmed the results at the mRNA level (Figure 9A). We found that cell proliferation in both cancer cell lines was significantly inhibited following interference with ESPL1 expression (Figure 9B). This conclusion is consistent with expectations, as ESPL1 is a critical gene involved in cell division, and its suppression has a definite effect on cell proliferation.

4 Discussion

The cell cycle represents a series of tightly integrated events that allow the cell to grow and proliferate (27). Notably, cancer represents a dysregulation of the cell cycle so cells that overexpress cyclins or do not express the CDK inhibitors continue to undergo unregulated cell growth (27, 47). ESPL1 encodes separase, a protein that regulates the cell cycle and plays an important role in the process of chromosome segregation. Previous studies have confirmed that ESPL1 is an oncogene that is overexpressed in many human cancers of breast, bone, brain, and prostate (48, 49). However, although researchers have gained some insight into the cell cycle regulation by ESPL1, more is needed to know whether and how it drives tumorigenesis, progression, and metastasis.There are no relevant pan-cancer analyses to date. Overall, as a key cell cycle-associated gene, the potential role of ESPL1 in carcinogenesis and cancer development is worth investigating.

First, we investigate the relationship between ESPL1 expression and the prognosis for survival of common cancers. Comparing cancer tissues to normal tissues revealed that ESPL1 was highly elevated in a number of malignancies. This could be due to the fact that upregulation of ESPL1 promotes cell cycle progression, resulting in a rapid increase in cell proliferation. Moreover, by comparing the expression of ESPL1 in various clinical stages, we discovered that ESPL1 expression increased as pathological stages progressed. Interestingly, as the disease advanced in SKCM and OV, ESPL1 expression decreased, particularly in SKCM, where patients with high ESPL1 expression had a poorer prognosis. However, the tumor stage was negatively correlated with the expression of ESPL1, a phenomenon that deserves further study. Kaplan-Meier and univariate Cox regression analyses revealed that upregulation of ESPL1 expression was associated with poor prognosis. Using the optimal cutoff value, we found that high expression of ESPL1 was significantly associated with poor prognosis in 18 different types of cancer. To avoid sample size imbalance, we ensured that the sample size of each group was at most 60% of the total sample size after grouping, thus ensuring comparability and statistical significance between the two groups. However, high ESPL1 expression was associated with better OS prognosis in THYM patients, implying that ESPL1 may be protective in this cancer. However, the PFI of THYM predicted by ESPL1 did not statistically distinguish a better prognosis, suggesting that additional confounding factors influenced the prediction of OS by ESPL1 in THYM. Through

multivariate analysis that integrates clinical information, ESPL1 remains a prognostic risk factor in multiple types of cancer. We hypothesized that ESPL1 expression is a reliable indicator of prognosis. Using ROC, we obtained an AUC of 0.7+ in ACC, MESO, KICH, KIRP, LGG, PCPG, GBM, THYM, and UVM for predicting 5-year survival.

It is worth noting that cancers develop in complex tissue environments, the tumor microenvironment, which they depend upon for sustained growth, invasion, and metastasis (50). TME consists of three critical components: tumor cells, stromal cells, and ECM (51). This study also integrated, for the first time, the correlation between ESPL1 expression and the tumor microenvironment. Results demonstrated that high expression of ESPL1 in THYM showed a positive correlation with various CD4+ T cells, and a negative correlation with epithelial cells and macrophages. However, most other cancers showed a negative correlation with CD4+ T cells, which may be one of the reasons why the high expression of ESPL1 in THYM exhibited a better

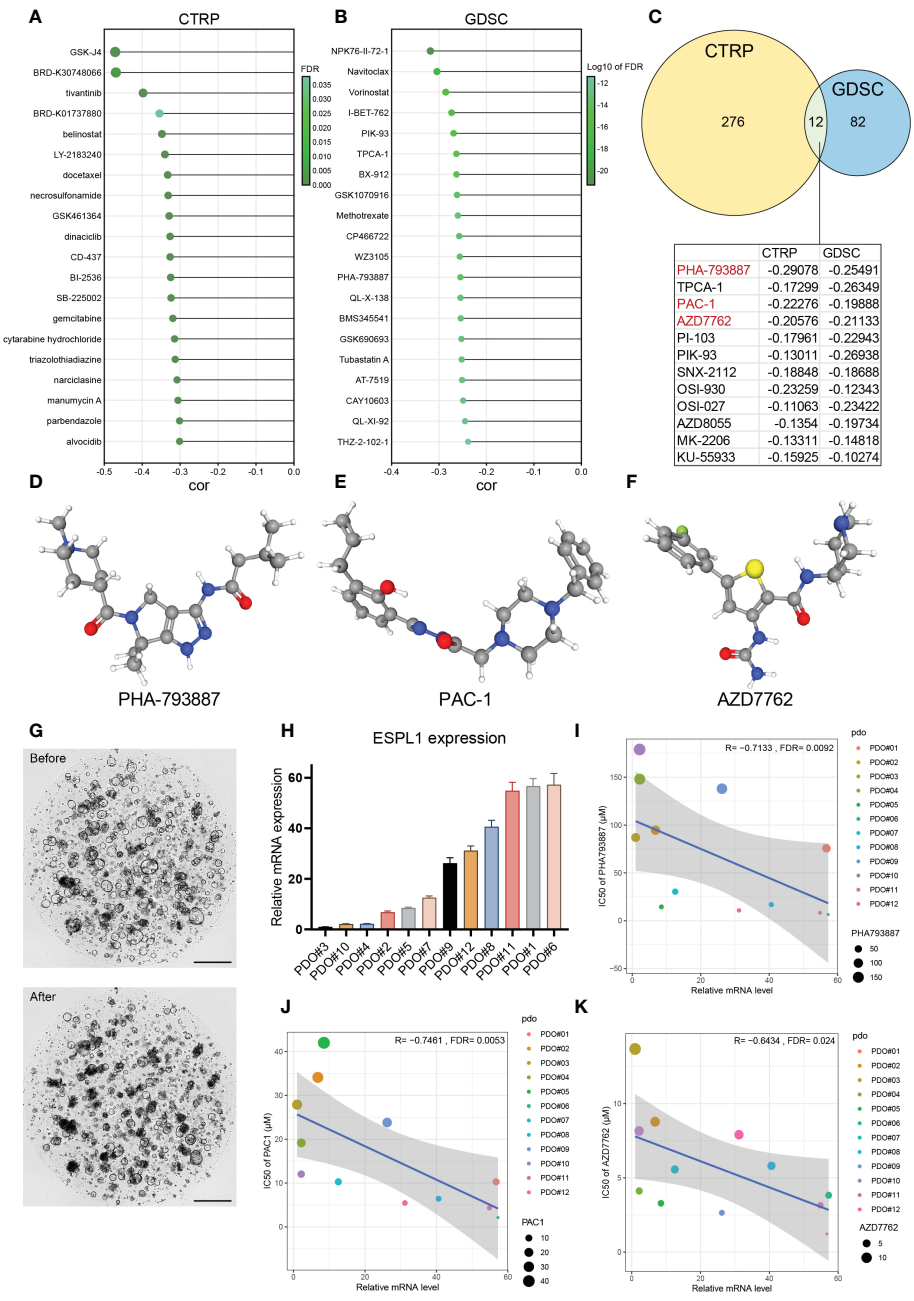

FIGURE 8
The relationship between ESPL1 and drug sensitivity. The drugs with the strongest correlation in ESPL1 expression were in the **(A)** CTRP and **(B)** GDSC databases. **(C)** Venn diagram of the results of the two databases. **(D-F)** The three-dimensional structure of drugs in PubChem. **(G)** Patient derived organoids (PDO) before and after coculture with drugs. Scale with 500 μM. **(H)** Expression level of ESPL1 in 12 PDOs. Correlation of ESPL1 expression in organoids with IC50 of **(I)** PHA793887, **(J)** PAC-1 and **(K)** AZD7762.

prognosis. Moreover, we found that Th2 cell was positively correlated with ESPL1 expression in the majority of tumors.

The ESTIMATE algorithm has been shown to predict tumor purity and reflects the characteristics of TME. Most tumor scores decreased with the increase in expression of ESPL1, but the opposite was true for THCA. The three scores were positively correlated with ESPL1 expression, and most cells in the TME were positively correlated with ESPL1 expression; in THCA, ESPL1 may affect immunity through a different mechanism. The immune score reflects the number and functional status of immune cells infiltrating the tumor microenvironment, including T cells, B cells, plasma cells, natural killer cells, and others. By using Immune Score, we can obtain information about the immune infiltration in the tumor microenvironment. XCELL, on the other hand, provides a detailed evaluation of each type of immune cell present in the microenvironment. In summary, these two algorithms can help us understand the relationship between ESPL1 and the tumor microenvironment from a macro and cellular level.

A slight association between TME cells and ESPL1 expression was found in UCS and CHOL, which implies that ESPL1 is not a suitable TME therapeutic target in these two tumors.

The same conclusion was obtained in the pan-correlation analysis, which explored the association between immune-related genes and ESPL1. The analysis showed that the correlation between ESPL1 and immune-related genes in USC and CHOL was not strong, suggesting that the effect of ESPL1 on these two cancers is not through the immune function. CD276 belongs to the immunoglobulin superfamily and participates in the regulation of T-cell-mediated immune response. We found that CD276 is statistically correlated with ESPL1 in a variety of tumors and that there may be an intrinsic link between them. ULBP1 is a ligand of NKG2D, an immune system-activating receptor on NK cells and T-cells. here was also a significant co-expression relationship between ESPL1 and ULBP1; ESPL1 could be involved in the immune regulation of tumors. Notably, ESPL1 was negatively correlated with immune-related genes in LUAD, LUSC, STAD, THYM, SARC,

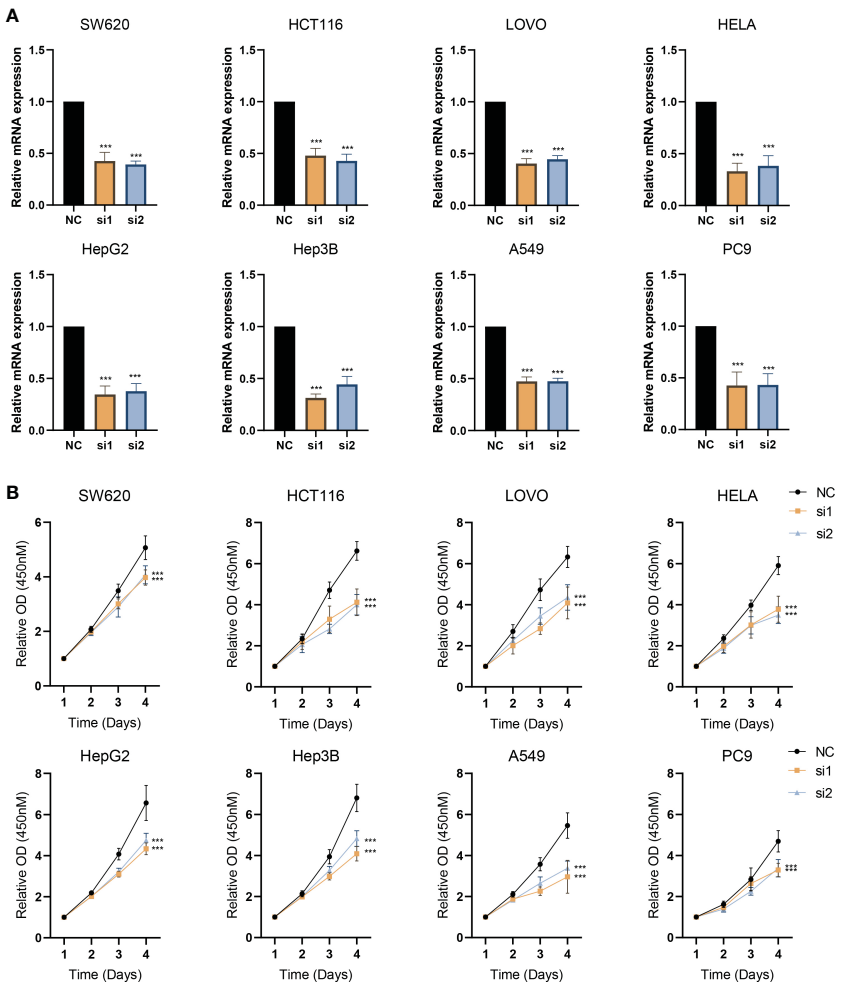

FIGURE 9
Interference with ESPL1 expression inhibits cell proliferation in a variety of cell lines. **(A)** Validation of siRNA interference efficiency. **(B)** Cell proliferation curves following interference with ESPL1 expression in eight different cell lines.

GBM, and TGCT. High expression of ESPL1 was associated with better survival in THYM, suggesting that ESPL1 may influence patient prognosis by affecting immunity.

The TMB, MSI, MATH, and HRD are indicators of tumor heterogeneity and can be used to guide application of tumor immunotherapy. In THYM, the expression of ESPL1 was negatively correlated with TMB, while high expression of ESPL1 was coincidentally associated with a better prognosis. This may indicate that ESPL1 could decrease TMB and thus improve patient survival, but further validation is required. In BLCA, STAD, and LUSC, ESPL1 expression was positively correlated with TMB and MSI, suggesting that these tumors may show good response to immunotherapy. In LUSC and BLCA, ESPL1 was also positively correlated with MATH, HRD, and all the four indicators suggesting that target ESPL1-targeted treatments may be effective in LUSC and BLCA.

Analysis of GDSC and CTRP databases identified drugs negatively correlated with ESPL1, suggesting that tumor cells with high ESPL1 expression are likely to be more sensitive to these drugs. GSK-J4 is a potent dual inhibitor of H3K27me3/me2-demethylases JMJD3/KDM6B and UTX/KDM6A. GSK-J4 inhibits LPS-induced TNF-α production in human primary macrophages and can induce endoplasmic reticulum stress-associated apoptosis. GSK-J4 is thought to be effective in diffuse intrinsic pontine glioma (DIPG) (52), and the drug sensitivity of GSK-J4 is enhanced with increased expression of ESPL1. Perhaps it is feasible to use ESPL1 as an indication for GSK-J4 in DIPG. BRD-K30748066 is a CDK9 inhibitor, a member of the cyclin-dependent protein kinase (CDK) family. This correlation is consistent with the function of ESPL1. A total of 12 drugs were shown to be more sensitive in cancer cell lines with high ESPL1 by correlation analysis of the two drug databases. Interestingly, a variety of mTOR inhibitors were involved, including AZD-8055, OSI-027 and PI-103. In addition, pro-apoptotic and cell cycle inhibiting drugs are also listed, including PHA-793887, PAC-1 and AZD-7762. Through organoid drug sensitivity testing, we confirmed that the expression of ESPL1 was statistically linked with PHA-793887, PAC-1, and AZD-7762, and that the expression of ESPL1 in colorectal cancer patient tissues may indicate the use of these drugs. In patients with high ESPL1 expression, certain drugs may be more effective. However, interference with ESPL1 expression in cell lines should lead to increased drug resistance. The absence of this trend may indicate that ESPL1 does not directly affect the response to these three drugs. The relationship and mechanisms between ESPL1 expression levels and PAC1, AZD7762, and PHA793887 deserve further investigation and discussion.

Finally, through *in vitro* studies, we demonstrated that ESPL1 can impact the proliferation, which is concordant with the bioinformatics results.

In conclusion, this study demonstrates the potential of ESPL1 as a cancer biomarker in various malignancies, with high expression of ESPL1 associated with worse prognosis in multiple cancer types and immune infiltration. Additionally, ESPL1 expression is associated with TMB, MSI, MATH, and HRD in several cancer types, suggesting a connection with tumor heterogeneity. We assessed drug sensitivity using organoids and found that those with high ESPL1 expression were more vulnerable to cell cycle inhibitors. Therefore, ESPL1 could serve as a marker for cancer therapy. *In vitro* assays confirmed that interference with ESPL1 can affect cell proliferation. Nonetheless, the study has some limitations, including the small sample size for organoid drug sensitivity tests, which may lead to bias. Future research should further investigate ESPL1 in other malignancies.

5 Conclusions

Through the use of public data mining, we were able to confirm that ESPL1 is an oncogene, that it can serve as a prognostic marker for several cancers, that it can be used to direct cancer medication therapy in patient derived organoids, and that ESPL1 knockdown can limit cell growth *in vitro*.

Data availability statement

The original contributions presented in the study are included in the article/Supplementary Material. Further inquiries can be directed to the corresponding authors.

Ethics statement

The studies involving human participants were reviewed and approved by the Ethics Committee of Zhejiang Cancer Hospital. Written informed consent for participation was not required for this study in accordance with the national legislation and the institutional requirements.

Author contributions

YZ conceived the idea, analyzed the data, and drafted the work. CZ and YZ analyzed the data and performed the visualization. WZ, HW, MW, and QZ collected the data and participated in the revision. HF and GW supervised the study. HF and GW provide funding support. All authors contributed to the article and approved the submitted version.

Funding

National Natural Science Foundation of China (No. 62276084), Major Health and Medicine Projects in Zhejiang Province (No.2022503044), Zhejiang Health Medicine Clinical Research Application Project (No. 2022483926), and Zhejiang Provincial Basic Public Welfare Research Program (No. LGD22C040016).

Acknowledgments

We are grateful to the Institute of Basic Medicine and Cancer, Chinese Academy of Sciences for providing the cell lines and research environment.

Conflict of interest

The authors declare that the research was conducted in the absence of any commercial or financial relationships that could be construed as a potential conflict of interest.

Publisher's note

All claims expressed in this article are solely those of the authors and do not necessarily represent those of their affiliated organizations, or those of the publisher, the editors and the reviewers. Any product that may be evaluated in this article, or claim that may be made by its manufacturer, is not guaranteed or endorsed by the publisher.

Supplementary material

The Supplementary Material for this article can be found online at: https://www.frontiersin.org/articles/10.3389/fimmu.2023.1138077/full#supplementary-material

SUPPLEMENTARY FIGURE 1
Relationship between ESPL1 expression and pathological staging. ns. not significant; *, p<0.05; **, p<0.01; ***, p<0.001.

SUPPLEMENTARY FIGURE 2
Validating the aberrant expression of ESPL1 through GEO. **(A, B)** Cervical cancer. **(C, D)** Liver cancer, **(E, F)** Lung cancer, **(G, H)** Colorectal cancer.

SUPPLEMENTARY FIGURE 3
Relationship between ESPL1 expression and clinical information. **(A)** Box plots showing the relationship between ESPL1 expression and age. **(B)** Box plots showing the relationship between ESPL1 expression and gender.

SUPPLEMENTARY FIGURE 4
Multivariate survival analysis based on ESPL1 expression and multiple clinical information.

SUPPLEMENTARY FIGURE 5
The IC50 values of HCT116 and SW620 cells after siRNA-mediated interference of ESPL1 expression. (A and C) IC50 curves of three drugs in HCT116 and SW620 cells. (B and D) Column chart comparing IC50 values.

References

1. Sung H, Ferlay J, Siegel RL, Laversanne M, Soerjomataram I, Jemal A, et al. Global cancer statistics 2020: GLOBOCAN estimates of incidence and mortality worldwide for 36 cancers in 185 countries. *CA: Cancer J Clin* (2021) 71(3):209–49. doi: 10.3322/caac.21660

2. Sun Y, Kucej M, Fan HY, Yu H, Sun QY, Zou H. Separase is recruited to mitotic chromosomes to dissolve sister chromatid cohesion in a DNA-dependent manner. *Cell* (2009) 137(1):123–32. doi: 10.1016/j.cell.2009.01.040

3. Waizenegger I, Giménez-Abián JF, Wernic D, Peters JM. Regulation of human separase by securin binding and autocleavage. *Curr Biol CB.* (2002) 12(16):1368–78. doi: 10.1016/S0960-9822(02)01073-4

4. Stemmann O, Zou H, Gerber SA, Gygi SP, Kirschner MW. Dual inhibition of sister chromatid separation at metaphase. *Cell* (2001) 107(6):715–26. doi: 10.1016/S0092-8674(01)00603-1

5. Zou H, Stemman O, Anderson JS, Mann M, Kirschner MW. Anaphase specific auto-cleavage of separase. *FEBS Lett* (2002) 528(1-3):246–50. doi: 10.1016/S0014-5793(02)03238-6

6. Guo G, Sun X, Chen C, Wu S, Huang P, Li Z, et al. Whole-genome and whole-exome sequencing of bladder cancer identifies frequent alterations in genes involved in sister chromatid cohesion and segregation. *Nat Genet* (2013) 45(12):1459–63. doi: 10.1038/ng.2798

7. Yang Q, Yu B, Sun JTTK. CDC25A, and ESPL1 as prognostic biomarkers for endometrial cancer. *BioMed Res Int* (2020) 2020:4625123. doi: 10.1155/2020/4625123

8. Liu Z, Lian X, Zhang X, Zhu Y, Zhang W, Wang J, et al. ESPL1 is a novel prognostic biomarker associated with the malignant features of glioma. *Front Genet* (2021) 12:666106. doi: 10.3389/fgene.2021.666106

9. GTEx Consortium. The genotype-tissue expression (GTEx) project. *Nat Genet* (2013) 45(6):580–5. doi: 10.1038/ng.2653

10. Espinosa AM, Alfaro A, Roman-Basaure E, Guardado-Estrada M, Palma Í, Serralde C, et al. Mitosis is a source of potential markers for screening and survival and therapeutic targets in cervical cancer. *PloS One* (2013) 8(2):e55975. doi: 10.1371/journal.pone.0055975

11. Pyeon D, Newton MA, Lambert PF, den Boon JA, Sengupta S, Marsit CJ, et al. Fundamental differences in cell cycle deregulation in human papillomavirus-positive and human papillomavirus-negative head/neck and cervical cancers. *Cancer Res* (2007) 67(10):4605–19. doi: 10.1158/0008-5472.CAN-06-3619

12. Shimada S, Mogushi K, Akiyama Y, Furuyama T, Watanabe S, Ogura T, et al. Comprehensive molecular and immunological characterization of hepatocellular carcinoma. *EBioMedicine* (2019) 40:457–70. doi: 10.1016/j.ebiom.2018.12.058

13. Wang HW, Hsieh TH, Huang SY, Chau GY, Tung CY, Su CW, et al. Forfeited hepatogenesis program and increased embryonic stem cell traits in young hepatocellular carcinoma (HCC) comparing to elderly HCC. *BMC Genomics* (2013) 14:736. doi: 10.1186/1471-2164-14-736

14. Beer DG, Kardia SL, Huang CC, Giordano TJ, Levin AM, Misek DE, et al. Gene-expression profiles predict survival of patients with lung adenocarcinoma. *Nat Med* (2002) 8(8):816–24. doi: 10.1038/nm733

15. Girard L, Rodriguez-Canales J, Behrens C, Thompson DM, Botros IW, Tang H, et al. An expression signature as an aid to the histologic classification of non-small cell lung cancer. *Clin Cancer Res* (2016) 22(19):4880–9. doi: 10.1158/1078-0432.CCR-15-2900

16. Sveen A, Agesen TH, Nesbakken A, Rognum TO, Lothe RA, Skotheim RI. Transcriptome instability in colorectal cancer identified by exon microarray analyses: Associations with splicing factor expression levels and patient survival. *Genome Med* (2011) 3(5):32. doi: 10.1186/gm248

17. Iwaya T, Yokobori T, Nishida N, Kogo R, Sudo T, Tanaka F, et al. Downregulation of miR-144 is associated with colorectal cancer progression *via* activation of mTOR signaling pathway. *Carcinogenesis* (2012) 33(12):2391–7. doi: 10.1093/carcin/bgs288

18. Ghandi M, Huang FW, Jané-Valbuena J, Kryukov GV, Lo CC, McDonald ER3rd, et al. Next-generation characterization of the cancer cell line encyclopedia. *Nature* (2019) 569(7757):503–8. doi: 10.1038/s41586-019-1186-3

19. Zhou T, Cai Z, Ma N, Xie W, Gao C, Huang M, et al. A novel ten-gene signature predicting prognosis in hepatocellular carcinoma. *Front Cell Dev Biol* (2020) 8:629. doi: 10.3389/fcell.2020.00629

20. Liu J, Lichtenberg T, Hoadley KA, Poisson LM, Lazar AJ, Cherniack AD, et al. An integrated TCGA pan-cancer clinical data resource to drive high-quality survival outcome analytics. *Cell* (2018) 173(2):400–16.e11. doi: 10.1016/j.cell.2018.02.052

21. Thorsson V, Gibbs DL, Brown SD, Wolf D, Bortone DS, Ou Yang TH, et al. The immune landscape of cancer. *Immunity* (2018) 48(4):812–30.e14. doi: 10.1016/j.immuni.2018.03.023

22. Beroukhim R, Mermel CH, Porter D, Wei G, Raychaudhuri S, Donovan J, et al. The landscape of somatic copy-number alteration across human cancers. *Nature* (2010) 463(7283):899–905. doi: 10.1038/nature08822

23. Bonneville R, Krook MA, Kautto EA, Miya J, Wing MR, Chen HZ, et al. Landscape of microsatellite instability across 39 cancer types. *JCO Precis Oncol* (2017) 2017:PO.17.00073. doi: 10.1200/PO.17.00073

24. Zeng D, Ye Z, Shen R, Yu G, Wu J, Xiong Y, et al. IOBR: Multi-omics immuno-oncology biological research to decode tumor microenvironment and signatures. *Front Immunol* (2021) 12:687975. doi: 10.3389/fimmu.2021.687975

25. Rees MG, Seashore-Ludlow B, Cheah JH, Adams DJ, Price EV, Gill S, et al. Correlating chemical sensitivity and basal gene expression reveals mechanism of action. *Nat Chem Biol* (2016) 12(2):109–16. doi: 10.1038/nchembio.1986

26. Mroz EA, Tward AD, Pickering CR, Myers JN, Ferris RL, Rocco JW. High intratumor genetic heterogeneity is related to worse outcome in patients with head and neck squamous cell carcinoma. *Cancer* (2013) 119(16):3034–42. doi: 10.1002/cncr.28150

27. Schwartz GK, Shah MA. Targeting the cell cycle: a new approach to cancer therapy. *J Clin Oncol* (2005) 23(36):9408–21. doi: 10.1200/JCO.2005.01.5594

28. Aran D, Hu Z, Butte AJ. xCell: digitally portraying the tissue cellular heterogeneity landscape. *Genome Biol* (2017) 18(1):220. doi: 10.1186/s13059-017-1349-1

29. Yoshihara K, Shahmoradgoli M, Martínez E, Vegesna R, Kim H, Torres-Garcia W, et al. Inferring tumour purity and stromal and immune cell admixture from expression data. *Nat Commun* (2013) 4:2612. doi: 10.1038/ncomms3612

30. Tang Z, Kang B, Li C, Chen T, Zhang Z. GEPIA2: an enhanced web server for large-scale expression profiling and interactive analysis. *Nucleic Acids Res* (2019) 47(W1):W556–w60. doi: 10.1093/nar/gkz430

31. Li B, Severson E, Pignon JC, Zhao H, Li T, Novak J, et al. Comprehensive analyses of tumor immunity: implications for cancer immunotherapy. *Genome Biol* (2016) 17(1):174. doi: 10.1186/s13059-016-1028-7

32. Li T, Fu J, Zeng Z, Cohen D, Li J, Chen Q, et al. TIMER2.0 for analysis of tumor-infiltrating immune cells. *Nucleic Acids Res* (2020) 48(W1):W509–w14. doi: 10.1093/nar/gkaa407

33. Li T, Fan J, Wang B, Traugh N, Chen Q, Liu JS, et al. TIMER: A web server for comprehensive analysis of tumor-infiltrating immune cells. *Cancer Res* (2017) 77(21):e108–e10. doi: 10.1158/0008-5472.CAN-17-0307

34. Liao Y, Wang J, Jaehnig EJ, Shi Z, Zhang B. WebGestalt 2019: gene set analysis toolkit with revamped UIs and APIs. *Nucleic Acids Res* (2019) 47(W1):W199–w205. doi: 10.1093/nar/gkz401

35. Yu G, Wang LG, Han Y, He QY. clusterProfiler: an r package for comparing biological themes among gene clusters. *Omics* (2012) 16(5):284–7. doi: 10.1089/omi.2011.0118

36. Yang W, Soares J, Greninger P, Edelman EJ, Lightfoot H, Forbes S, et al. Genomics of drug sensitivity in cancer (GDSC): a resource for therapeutic biomarker discovery in cancer cells. *Nucleic Acids Res* (2013) 41(Database issue):D955–61. doi: 10.1093/nar/gks1111

37. Iorio F, Knijnenburg TA, Vis DJ, Bignell GR, Menden MP, Schubert M, et al. A landscape of pharmacogenomic interactions in cancer. *Cell* (2016) 166(3):740–54. doi: 10.1016/j.cell.2016.06.017

38. Garnett MJ, Edelman EJ, Heidorn SJ, Greenman CD, Dastur A, Lau KW, et al. Systematic identification of genomic markers of drug sensitivity in cancer cells. *Nature* (2012) 483(7391):570–5. doi: 10.1038/nature11005

39. Seashore-Ludlow B, Rees MG, Cheah JH, Cokol M, Price EV, Coletti ME, et al. Harnessing connectivity in a Large-scale small-molecule sensitivity dataset. *Cancer discovery.* (2015) 5(11):1210–23. doi: 10.1158/2159-8290.CD-15-0235

40. Basu A, Bodycombe NE, Cheah JH, Price EV, Liu K, Schaefer GI, et al. An interactive resource to identify cancer genetic and lineage dependencies targeted by small molecules. *Cell* (2013) 154(5):1151–61. doi: 10.1016/j.cell.2013.08.003

41. Casolino R, Paiella S, Azzolina D, Beer PA, Corbo V, Lorenzoni G, et al. Homologous recombination deficiency in pancreatic cancer: A systematic review and prevalence meta-analysis. *J Clin Oncol* (2021) 39(23):2617–31. doi: 10.1200/JCO.20.03238

42. Vergote I, González-Martín A, Ray-Coquard I, Harter P, Colombo N, Pujol P, et al. European Experts consensus: BRCA/homologous recombination deficiency testing in first-line ovarian cancer. *Ann Oncol* (2022) 33(3):276–87. doi: 10.1016/j.annonc.2021.11.013

43. Mroz EA, Rocco JW. MATH, a novel measure of intratumor genetic heterogeneity, is high in poor-outcome classes of head and neck squamous cell carcinoma. *Oral Oncol* (2013) 49(3):211–5. doi: 10.1016/j.oraloncology.2012.09.007

44. Brasca MG, Albanese C, Alzani R, Amici R, Avanzi N, Ballinari D, et al. Optimization of 6,6-dimethyl pyrrolo[3,4-c]pyrazoles: Identification of PHA-793887, a potent CDK inhibitor suitable for intravenous dosing. *Bioorganic medicinal Chem* (2010) 18(5):1844–53. doi: 10.1016/j.bmc.2010.01.042

45. Putt KS, Chen GW, Pearson JM, Sandhorst JS, Hoagland MS, Kwon JT, et al. Small-molecule activation of procaspase-3 to caspase-3 as a personalized anticancer strategy. *Nat Chem Biol* (2006) 2(10):543–50. doi: 10.1038/nchembio814

46. Zabludoff SD, Deng C, Grondine MR, Sheehy AM, Ashwell S, Caleb BL, et al. AZD7762, a novel checkpoint kinase inhibitor, drives checkpoint abrogation and potentiates DNA-targeted therapies. *Mol Cancer Ther* (2008) 7(9):2955–66. doi: 10.1158/1535-7163.MCT-08-0492

47. Evan GI, Vousden KH. Proliferation, cell cycle and apoptosis in cancer. *Nature* (2001) 411(6835):342–8. doi: 10.1038/35077213

48. Zhang N, Pati D. Biology and insights into the role of cohesin protease separase in human malignancies. *Biol Rev Cambridge Philos Society.* (2017) 92(4):2070–83. doi: 10.1111/brv.12321

49. Meyer R, Fofanov V, Panigrahi A, Merchant F, Zhang N, Pati D. Overexpression and mislocalization of the chromosomal segregation protein separase in multiple human cancers. *Clin Cancer Res* (2009) 15(8):2703–10. doi: 10.1158/1078-0432.CCR-08-2454

50. Quail DF, Joyce JA. Microenvironmental regulation of tumor progression and metastasis. *Nat Med* (2013) 19(11):1423–37. doi: 10.1038/nm.3394

51. Yin SY, Jian FY, Chen YH, Chien SC, Hsieh MC, Hsiao PW, et al. Induction of IL-25 secretion from tumour-associated fibroblasts suppresses mammary tumour metastasis. *Nat Commun* (2016) 7:11311. doi: 10.1038/ncomms11311

52. Grasso CS, Tang Y, Truffaux N, Berlow NE, Liu L, Debily MA, et al. Functionally defined therapeutic targets in diffuse intrinsic pontine glioma. *Nat Med* (2015) 21(6):555–9. doi: 10.1038/nm.3855

frontiers | Frontiers in Surgery

TYPE Original Research
PUBLISHED 03 May 2023
DOI 10.3389/fsurg.2023.1102545

OPEN ACCESS

EDITED BY
Jorge Melendez-Zajgla,
National Institute of Genomic Medicine (INMEGEN), Mexico

REVIEWED BY
Hao Wang,
Second Military Medical University, China
Yen-Chun Peng,
Taichung Veterans General Hospital, Taiwan

*CORRESPONDENCE
Xuedong Fang
fangxd1961@163.com
Yuanyu Wu
wyy511@jlu.edu.cn

†These authors have contributed equally to this work

RECEIVED 19 November 2022
ACCEPTED 14 April 2023
PUBLISHED 03 May 2023

CITATION
Yuan C, Huang J, Li H, Zhai R, Zhai J, Fang X and Wu Y (2023) Association of clinical outcomes and the predictive value of T lymphocyte subsets within colorectal cancer patients. Front. Surg. 10:1102545. doi: 10.3389/fsurg.2023.1102545

Association of clinical outcomes and the predictive value of T lymphocyte subsets within colorectal cancer patients

Chaofeng Yuan[1], Jiannan Huang[1], Haitao Li[2], Rongnan Zhai[1], Jinjing Zhai[1], Xuedong Fang[1*†] and Yuanyu Wu[1*†]

[1]Department of Gastrointestinal Colorectal Surgery, China-Japan Union Hospital of Jilin University, Changchun, China, [2]Department of Orthopedics, China-Japan Union Hospital of Jilin University, Changchun, China

Introduction: Tumor immunity is a hot topic in tumor research today, and human immunity is closely related to tumor progression. T lymphocyte is an important component of human immune system, and the changes in their subsets may influence the progression of colorectal cancer (CRC) to some extent. This clinical study systematically describes and analyzes the association of $CD4^+$ and $CD8^+$ T-lymphocyte content and $CD4^+/CD8^+$ T-lymphocyte ratio with CRC differentiation, clinical pathological stage, Ki67 expression, T-stage, N-stage, carcinoembryonic antigen (CEA) content, nerve and vascular infiltration, and other clinical features, as well as preoperative and postoperative trends. Furthermore, a predictive model is constructed to evaluate the predictive value of T-lymphocyte subsets for CRC clinical features.

Methods: Strict inclusion and exclusion criterion were formulated to screen patients, preoperative and postoperative flow cytometry and postoperative pathology reports from standard laparoscopic surgery were assessed. PASS and SPSS software, R packages were invoked to calculate and analyze.

Results: We found that a high $CD4^+$ T-lymphocyte content in peripheral blood and a high $CD4^+/CD8^+$ ratio were associated with better tumor differentiation, an earlier clinical pathological stage, lower Ki67 expression, shallower tumor infiltration, a smaller number of lymph node metastases, a lower CEA content, and a lower likelihood of nerve or vascular infiltration ($P < 0.05$). However, a high $CD8^+$ T-lymphocyte content indicated an unpromising clinical profile. After effective surgical treatment, the $CD4^+$ T-lymphocyte content and $CD4^+/CD8^+$ ratio increased significantly ($P < 0.05$), while the $CD8^+$ T-lymphocyte content decreased significantly ($P < 0.05$). Further, we comprehensively compared the merits of $CD4^+$ T-lymphocyte content, $CD8^+$ T-lymphocyte content, and $CD4^+/CD8^+$ ratio in predicting the clinical features of CRC. We then combined the $CD4^+$ and $CD8^+$ T-lymphocyte content to build models and predict major clinical characteristics. We compared these models with the $CD4^+/CD8^+$ ratio to explore their advantages and disadvantages in predicting the clinical features of CRC.

Discussion: Our results provide a theoretical basis for the future screening of effective markers in reflecting and predicting the progression of CRC. Changes in T lymphocyte subsets affect the progression of CRC to a certain extent, while their changes also reflect variations in the human immune system.

KEYWORDS

colorectal cancer, flow cytometry, laparoscopy, tumor markers, immunity

Introduction

CRC is the third most common malignancy worldwide and has the second highest mortality rate (1). The morbidity and mortality rates continue to increase each year. Moreover, there is a trend toward a younger age in the incidence of CRC. Early diagnosis and treatment are paramount for malignant tumors; however, early-stage CRC often has no clinical symptoms. Moreover, in most cases, conventional screening tests, such as serum tumor marker tests, are not abnormal, which gives CRC the opportunity to infiltrate and grow further. When there are abnormalities in the relevant tests, CRC is considered to have reached an advanced stage. Even after effective surgical treatment, adjuvant chemotherapy, targeted therapy, and immunotherapy, there are varying degrees of recurrence and metastasis. Therefore, screening for valid and accurate markers that are closely associated with CRC to reflect and predict the progression of CRC is of great importance in current clinical management.

Tumor immunity has become a hot topic of research. Many researchers believe that tumor development is closely related to human immunity. The immune strength of the host can directly influence tumor development, and T lymphocytes play an indispensable role in the fight against tumors. T lymphocytes are classified into cytotoxic T cells and helper T cells according to the expression of cluster differentiation on the cell surface. The content of T lymphocytes subsets can reflect the level of immunity. $CD4^+$ T lymphocytes can activate $CD8^+$ T lymphocytes and promote the secretion of cytotoxic granules to kill tumor cells by modulating antigen presenting cells(APC) to provide stronger antigenic signals, or by providing co-stimulatory signals *via* dendritic cells (2, 3). Maintaining a dynamic balance in the content and ratio of $CD4^+$ and $CD8^+$ T lymphocytes is important for immune homeostasis, and any increase or decrease in the ratio of T lymphocytes can affect the immunity. Therefore, measuring the number of T-lymphocyte subsets in peripheral blood might predict tumor development and clinical features.

Previous studies have shown that the levels of $CD4^+$ and $CD8^+$ T lymphocytes are closely related to the clinical characteristics and prognosis of various malignancies, such as pancreatic cancer (4), bladder cancer (5), and breast cancer (6). However, studies on T-lymphocyte subset alterations in CRC are still scarce. In a clinical prognostic study of rectal cancer, Naito et al. (7) found that $CD8^+$ T-lymphocyte content could be a valid independent indicator of CRC prognosis. Kuwahara et al. (8) predicted the prognosis of patients with CRC by integrating $CD4^+$ and $FOX3^+$ cells and concluded that a low proportion of $CD4^+$ and $FOX3^+$ cells suggests a poor prognosis. The studies mentioned above have shown the potential of changes in T-lymphocyte subsets to predict the prognosis and clinical features of CRC.

The present study specifically analyzed the association between changes in T-lymphocyte subsets and the clinical features of CRC. Furthermore, we predicted the level of development and malignancy of CRC based on changes in T-lymphocyte subsets. Ultimately, we combined $CD4^+$ and $CD8^+$ T-lymphocyte counts and used logistic regression to build models to better predict the major clinical characteristics of CRC.

Materials and methods

Selection of clinical patients

To reduce the influence of confounding factors and improve the accuracy of clinical trials, we formulated a series of criteria for patient screening. The inclusion criteria were as follows: (1) a preoperative cytological or pathological diagnosis of CRC; (2) no anti-tumor treatments after diagnosis of CRC; (3) no high-risk factors, such as CRC enterocutaneous fistula, intestinal obstruction, and gastrointestinal hemorrhage; (4) a Karnofsky score of >60; and (5) stable vital signs and normal consciousness. The exclusion criteria were as follows: (1) severe mental disorders; (2) use of immunosuppressive or immune-enhancing agents; (3) severe hematological disorders, autoimmune diseases, cardiovascular diseases, respiratory diseases, or sepsis; (4) pregnancy or breastfeeding; (5) allergies to biological products; (6) abnormal bone marrow function; (7) primary malignancy other than CRC; and (8) severe diabetes mellitus, hypertension, or obesity.

According to the above inclusion and exclusion criteria, postoperative pathology reports of 86 patients with pathologically confirmed CRC after standard laparoscopic resection at the China-Japan Union Hospital of Jilin University were collected from September 2021 to September 2022, with pathological staging according to the 8th American Joint Committee on Cancer criteria(AJCC). There were 55 male patients (mean age: 64.1 ± 10.8 years) and 31 female patients (mean age: 62.2 ± 9.8 years). The ethics committee approved the study, and all patients provided written informed consent. This study was conducted in accordance with the principles of the Declaration of Helsinki.

Options for CRC surgery

To ensure consistency in the surgical procedure, we used standard minimally invasive laparoscopic surgery to resect colorectal malignancies. For malignant tumors of the right hemicolon, we used laparoscopic radical right hemicolectomy. In cases of malignant tumors of the left hemicolon, we used laparoscopic radical left hemicolectomy. For rectal cancer, we used either the laparoscopic Dixon or Miles procedure.

Application of flow cytometry

To reduce the impact of surgical stress on immune function, we chose to collect peripheral blood on the day before surgery and on the tenth postoperative day. All patients had 200 μl of fresh peripheral blood drawn in the morning in the condition of

limosis. $CD4^+$ and $CD8^+$ antibodies (40 µl each) were added within 4 h, mixed thoroughly, and protected from light for 30 min at room temperature. Red blood cell lysate (2.0 ml) was then added, mixed, and protected from light for 20 min at room temperature. After centrifugation (2,500 r/min for 5 min), the supernatant was removed, and 20 ml of 0.1% sodium azide phosphate buffer was added, mixed thoroughly, and centrifuged again (1,500 r/min for 5 min). $CD4^+$ T-lymphocyte content, $CD8^+$ T-lymphocyte content, and $CD4^+/CD8^+$ ratio were obtained by flow cytometry.

Statistical analysis and data visualization

We used SPSS 22.0 software for statistical analysis and applied the Wilcoxon or Kruskal–Wallis rank-sum test to analyze the relationship between clinical pathological characteristics and T-lymphocyte subsets. The association between the main clinical features, T-lymphocyte subsets and the TNM stage was analyzed using the Chi-square test. The relationship between T-lymphocyte subsets and CEA was analyzed using Spearman's correlation test. For preoperative and postoperative changes in T-lymphocyte subsets, the paired Wilcoxon rank-sum test was used. The ggplot2 package of R software was then applied to visualize the results of the above data analysis and plot the combined comparison, scatter, and pairwise plots. The pROC package was used for the analysis of the receiver operating characteristic (ROC) curves of the independent and joint indicators, while the ggplot2 package was used to visualize the graphs. To facilitate a visual depiction of the relationships between the major clinical features of the 86 patients, we used the ggalluvial package to delineate alluvial plots.

Efficacy analysis of sample size

To test the efficacy of this clinical trial, we used PASS software to analyze the statistical efficacy of the sample size required for the trial. The final estimated sample sizes are shown in Table 1. Table 1 shows that the vast majority of the clinical sample sizes that were collected were larger than the estimated sample sizes, which reflects the high statistical validity of our experiment.

TABLE 1 Estimated sample size required for each of the major clinical features.

Clinical characteristics	$CD4^+$	$CD8^+$	$CD4^+/CD8^+$ ratio
Ki67 expression	30	30	24
Organization differentiation	81	54	21
Clinical stage	51	30	18
T-stage	36	24	20
N-stage	42	32	27
CEA expression	118	50	61
Perineural invasion	50	84	52
Vascular invasion	88	26	30
Preoperative and postoperative trends	66	107	39

CEA, Carcinoembryonic antigen.

Results

General distribution of clinical pathological features of patients with CRC

The alluvial plot visualizes the relationship between Ki67 expression, clinical pathological stage, degree of tumor differentiation, nerve invasion, and vascular invasion in all patients (Figure 1). The majority of patients with advanced colorectal cancer had high Ki67 expression. Correspondingly, a large proportion of patients with high Ki67 expression had poorly differentiated tumor tissue. Simultaneously, the majority of patients with nerve and vascular invasion had poorly differentiated tumors and a late clinical pathological stage, as well as high Ki67 expression. We applied the Chi-square test and presented the distribution of the main features of CRC patients in a clear and visual way in Table 2.

Comparison of clinical pathological features

We analyzed the differences in T-lymphocyte subsets between major clinical pathological features. As Ki67 expression increased, the $CD4^+$ T-lymphocyte content and $CD4^+/CD8^+$ ratio gradually decreased, while CD8+ T-lymphocyte content continued to increase (Figures 2A1–3). With the increase in clinical pathological stage (Figures 2B1–3), T-stage (Figures 2D1–3), N-stage (Figures 2E1–3), vascular invasion (Figures 2F1–3), and perineural invasion (Figures 2G1–3); the decrease in tumor tissue differentiation (Figures 2C1–3), the $CD4^+$ T-lymphocyte content and the $CD4^+/CD8^+$ ratio significantly decreased, while the $CD8^+$ T-lymphocyte content significantly increased. There was no significant difference in T-lymphocyte subsets by age, sex, or tumor site ($P > 0.05$) (Figures 2H1–J3). The results suggest that T-lymphocyte subsets have strong association with major clinical pathological features. Thus, T lymphocyte subsets have the potential to fully reflect changes in clinical features.

Correlation between CEA and T-lymphocyte subsets

To further explore the correlation between CEA and T-lymphocyte subsets, we used Spearman's correlation analysis and depicted scatter plots. Figures 3A,C show a significant negative correlation of $CD4^+$ T-lymphocyte content and $CD4^+/CD8^+$ ratio with CEA, while Figure 3B shows a significant positive correlation between $CD8^+$ T-lymphocyte content and CEA. Based on the absolute magnitude of r, the $CD4^+/CD8^+$ ratio correlated most strongly with CEA, followed by $CD8^+$ T-lymphocyte content and $CD4^+$ T-lymphocyte content.

Trends in preoperative and postoperative T-lymphocyte subsets

In order to reduce the effect of confounding factors, such as surgical stress and the postoperative inflammatory response on

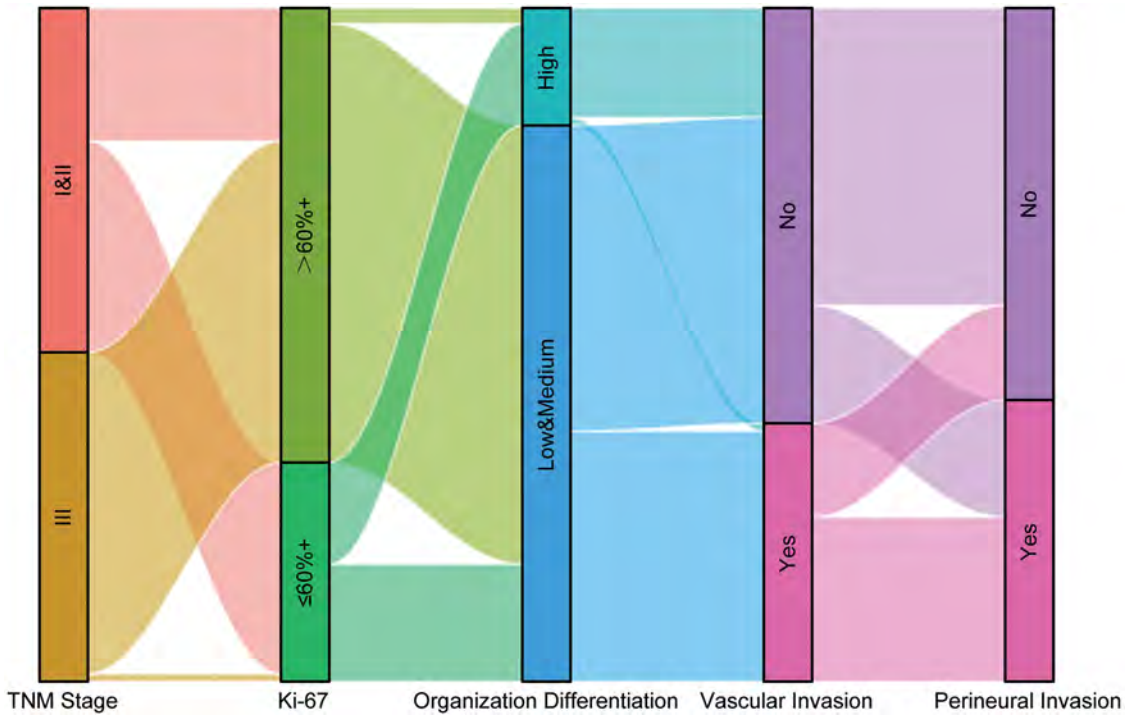

FIGURE 1
Overview of the distribution of clinical pathological features.

postoperative immunity, we drew peripheral blood for flow cytometry analysis on the tenth postoperative day after normalization of leukocytes and neutrophils. Postoperatively, we routinely administered anti-inflammatory, acid-suppressive, analgesic, and anti-emetic medications, and we did not administer immunosuppressive or immune-enhancing agents. After effective treatment with laparoscopic surgery, the $CD4^+$ T-lymphocyte content and the $CD4^+/CD8^+$ ratio increased significantly, while the $CD8^+$ T-lymphocyte content decreased significantly (Figures 4A–C).

Prediction of different clinical features by T-lymphocyte subset

For testing the ability of T-lymphocyte subsets to predict clinical features, we plotted ROC curves to judge the predictive performance of different indicators and found the best cut-off value. The DeLong test was then applied to identify significant differences between the predictive merits of these indicators. Based on the fact that a Ki67 positivity of 60% is often used as the dividing line in daily clinical practice, we classified Ki67 positivity of ≤60% as low expression and Ki67 positivity of >60% as high expression. A comparison of the predictive efficacy of T-lymphocyte subsets is depicted in the ROC curves in Figure 5A. All three indicators had high predictive performance. The difference in predictive performance between the $CD4^+/CD8^+$ ratio and $1/CD8^+$ was not statistically significant. Based on the situation of lymph node metastasis, we classified clinical pathological stages I and II as early colorectal cancer and stage III as advanced colorectal cancer. Using the DeLong test, we found the best predictive efficacy for the $CD4^+/CD8^+$ ratio (Figure 5B). We then divided the moderately and poorly differentiated adenocarcinomas into one group and the highly differentiated adenocarcinomas into another. Figure 5C clearly shows that the $CD4^+/CD8^+$ ratio had the best predictive performance. We further classified T1 and T2 as the low tumor infiltration group, T3 and T4 as the high tumor infiltration group (Figure 5D). After applying the DeLong test, the $CD4^+/CD8^+$ ratio continued to have the best predictive performance. Comparisons of the predictive efficacy of the T-lymphocyte subsets for vascular invasion and perineural invasion are shown in Figures 5E,F. Finally, we tabulated the best cut-off values and corresponding sensitivity, specificity of the three indicators for the prediction of major clinical features (Tables 3, 4).

Model indicators predicting different clinical features

Applying the logistic regression analysis, we combined $CD4^+$ and $CD8^+$ T lymphocytes to build models for various clinical characteristics to identify more accurate indicators. Figures 6A–C shows the predictive efficacy of the model indicators for Ki67 expression, tumor differentiation, and vascular invasion in the form of ROC curves. After applying the DeLong test, we found that the predictive efficacy of the

TABLE 2 The characteristics and T cell subsets in colorectal patients according to TNM stage.

Clinical Features	TNM Stage I & II	TNM stage III	Total	*P* Value
Sex				
Male	33	22	55	0.029
Female	11	20	31	
Age (years)				
≤65	21	21	42	0.83
>65	23	21	44	
Tumor organization differentiation				
High Differentiation	15	0	15	3.17×10^{-8}
Medium Differentiation	25	15	40	
Low Differentiation	4	27	31	
Tumor location				
Right Hemicolon	15	10	25	0.11
Left Hemicolon	7	15	22	
Rectum	22	17	39	
Ki-67 expression				
≤60%+	27	1	28	5.38×10^{-9}
>60%+	17	41	58	
Vascular invasion				
Yes	6	27	33	1.38×10^{-6}
No	38	15	53	
Perineural invasion				
Yes	8	28	36	5.22×10^{-6}
No	36	14	50	
T-lymphocyte subsets				
$CD4^+$% > optimal cut-off value (38.5)	36	9	45	2.08×10^{-8}
$CD4^+$% < optimal cut-off value (38.5)	8	33	41	
$CD8^+$% > optimal cut-off value (24.4)	6	39	45	1.94×10^{-13}
$CD8^+$% < optimal cut-off value (24.4)	38	3	41	
$CD4^+/CD8^+$ > optimal cut-off value (1.625)	36	1	37	1.03×10^{-13}
$CD4^+/CD8^+$ < optimal cut-off value (1.625)	8	41	49	

The Chi-square test is applied in Table 2.

model indicators was better than that of the $CD4^+/CD8^+$ ratio. The model indicators predicting clinical pathological stage, T-stage, and perineural invasion are depicted in **Figures 6D–F** in the forms of ROC. The model indicators did not show better predictive efficacy than the $CD4^+/CD8^+$ ratio after applying the DeLong test. The relevant data for each model indicator are presented in **Table 5**.

Discussion

CRC development is a multifactorial, multistep process involving a wide range of mechanisms. Tumor immune escape, low body immune surveillance, and an altered tumor microenvironment are all involved (9). During the body's anti-tumor process, T lymphocytes kill tumor cells at the primary site and reduce the risk of tumor spread and distant metastasis. However, when cytotoxic T cells and helper T cells are hypofunctional, the release of cytotoxic granules is significantly reduced. As a result, the immune response to tumor antigens decreases (10). Thus, T-lymphocyte subsets in peripheral blood might have association with progression of malignant tumor, and as such, they have the potential to reflect and predict major clinical pathological characteristics of CRC.

The results of this study suggest that T-lymphocyte subsets in peripheral blood are closely associated with the major clinical features of CRC. Increased expression of Ki67, which a proliferating cell-associated antigen, implies a strong proliferative capacity of tumor cells and a poorer prognosis for patients (11). We found that $CD4^+$ T-lymphocyte content and $CD4^+/CD8^+$ ratio decreased with an increase in Ki67 expression, while $CD8^+$ T-lymphocyte content gradually increased. This means that the decrease in $CD4^+$ T-lymphocyte content and $CD4^+/CD8^+$ ratio suggest a progressive state and accelerated proliferation of CRC. A high $CD8^+$ T-lymphocyte content may be associated with poor clinical outcomes. Clinical stage is a comprehensive evaluation of malignancy, and an advanced stage equates to a higher probability of tumor recurrence and metastasis after surgery (12). In this study, $CD4^+$ T-lymphocyte content and $CD4^+/CD8^+$ ratio were significantly negatively correlated with clinical stage, while $CD8^+$ T-lymphocyte content was significantly positively correlated with clinical stage. This implies that T-lymphocyte subsets are predictive of clinical stage. An increase in $CD4^+$ T-lymphocyte content and $CD4^+/CD8^+$ ratio means that the tumor is still in an early clinical stage, while an increase in $CD8^+$ T-lymphocyte content means that the tumor has escalated to an advanced stage. The degree of tumor differentiation is often an important risk factor that affects the prognosis of patients (13). Our results found significant correlations of reduced $CD4^+$ T-lymphocyte content, reduced $CD4^+/CD8^+$ ratio, and increased $CD8^+$ T-lymphocyte content with poorer tumor tissue differentiation. This further illustrates that the alteration in T-lymphocyte subsets influences tumor progression.

It is known that a later T-stage represents deeper tumor tissue infiltration, while a later N-stage suggests a higher number of lymph node metastases. The progression of both stages suggests a worrying outcome for patient survival (14). The changes in T-lymphocyte subsets all showed similar trends when combined with clinical stage, T-stage, and N-stage in our current study. This implies that a decrease in $CD4^+$ T-lymphocyte content, a decrease in $CD4^+/CD8^+$ ratio, and an increase in $CD8^+$ T-lymphocyte content indicate disappointing clinical pathological features.

Vascular and nerve invasion, as high-risk factors for CRC, imply an increased risk of distant tumor metastasis. Our findings clearly demonstrate that a decrease in $CD4^+$ T-lymphocyte content, a decrease in $CD4^+/CD8^+$ ratio, and an increase in $CD8^+$ T-lymphocyte content may increase the risk of vascular and nerve invasion of CRC. As one of the most commonly used tumor markers that is associated with CRC in clinical practice, although the sensitivity and specificity of CEA are not ideal, to a certain degree, increase of CEA can reflect the progression, postoperative recurrence and metastasis of CRC (15). Spearman's correlation analysis showed that all

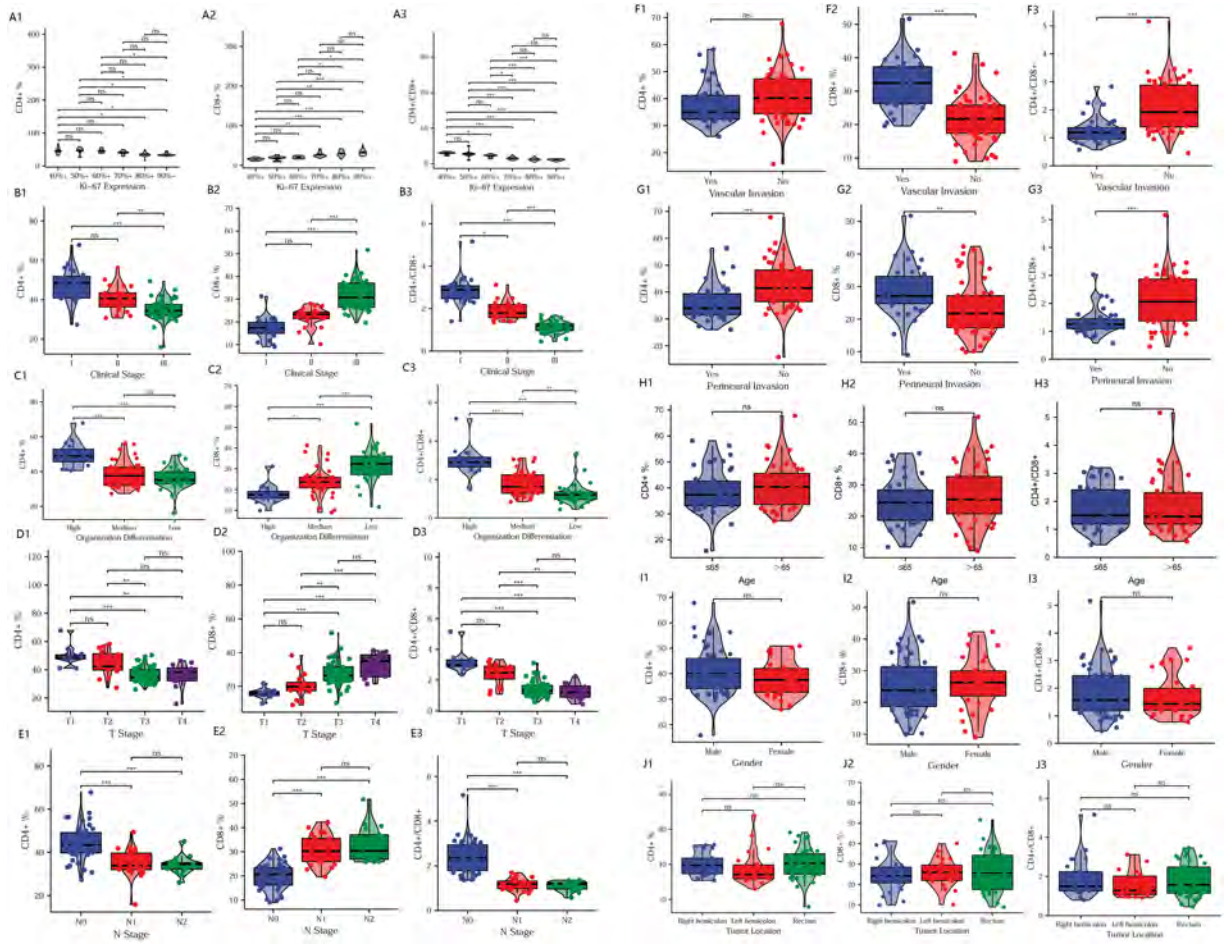

FIGURE 2
Comparison of clinical pathological features. Relationship between T-lymphocyte subsets and Ki67 expression (A1–A3), clinical pathological stage (B1–B3), tumor differentiation (C1–C3), T-stage (D1–D3), N-stage (E1–E3), vascular invasion (F1–F3), perineural invasion (G1–G3), age (H1–H3), sex (I1–I3), and tumor site (J1–J3). *$P < 0.05$; **$P < 0.01$; ***$P < 0.001$; ns, not significant.

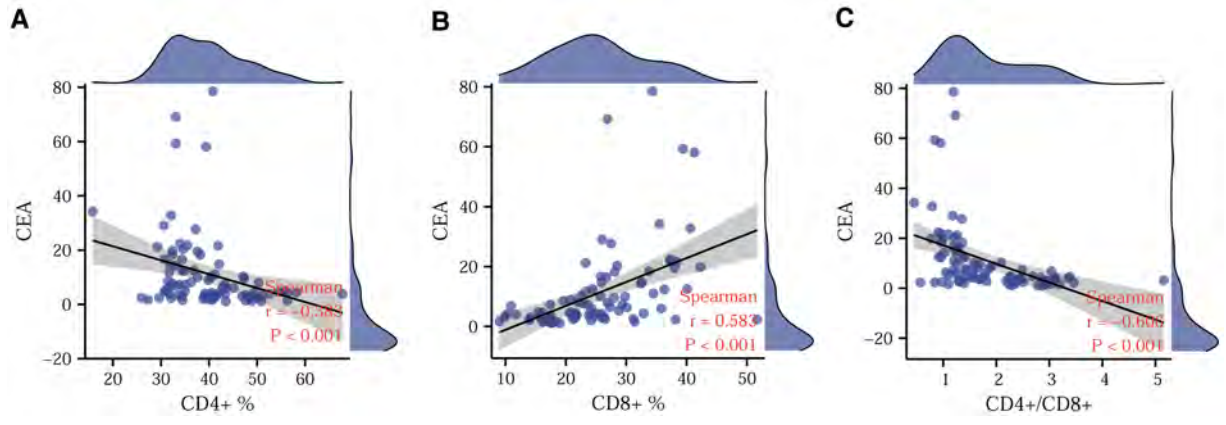

FIGURE 3
Correlation between CEA and T-lymphocyte subsets. Correlations of $CD4^+$ (**A**), $CD8^+$ (**B**), and $CD4^+/CD8^+$ ratio (**C**) with CEA. CEA. Carcinoembryonic antigen.

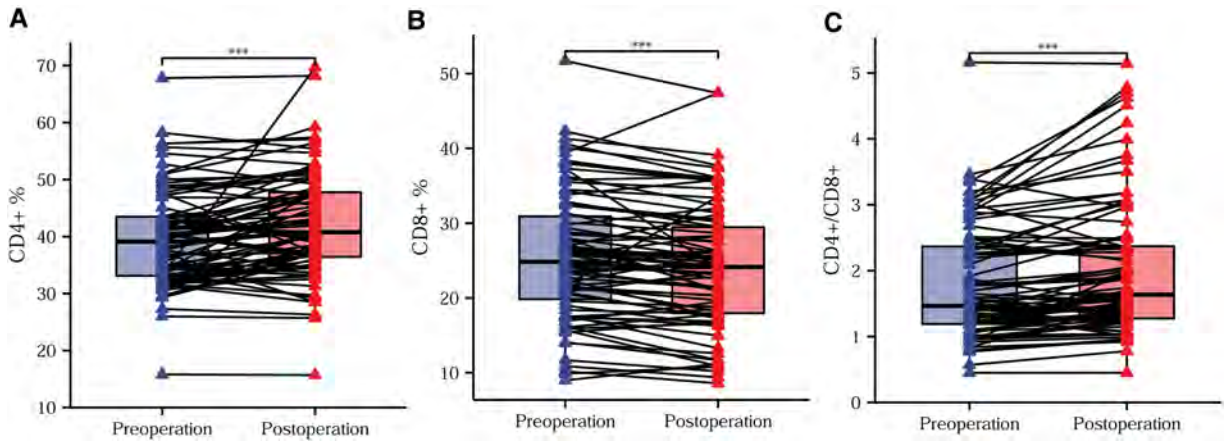

FIGURE 4
Trends in preoperative and postoperative T-lymphocyte subsets. Differences in the $CD4^+$ T-lymphocyte content (A), $CD8^+$ T-lymphocyte content (B), and $CD4^+/CD8^+$ ratio (C) before compared with after surgery. $^*P < 0.05$; $^{**}P < 0.01$; $^{***}P < 0.001$; ns, not significant.

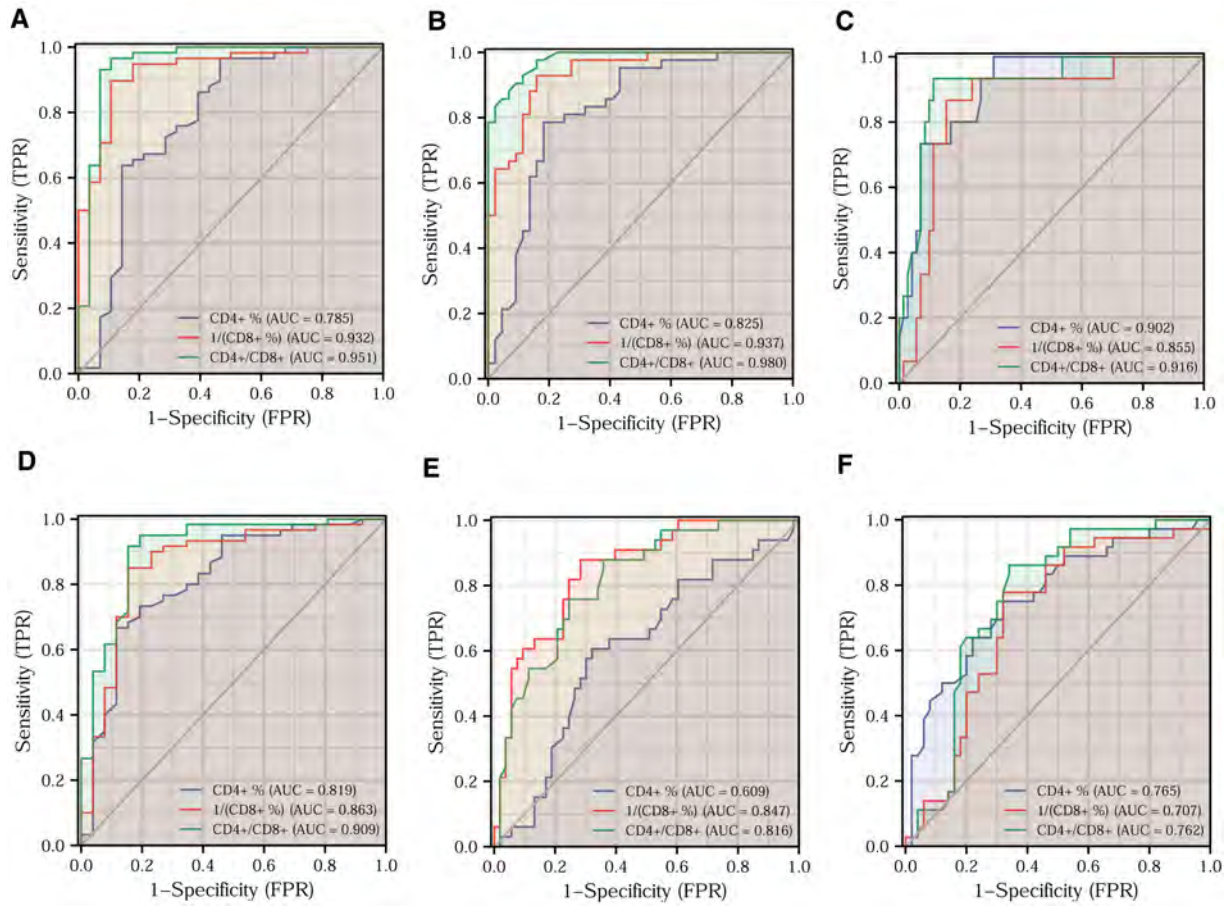

FIGURE 5
Prediction of different clinical features by T-lymphocyte subset. Efficacy of T-lymphocyte subsets for predicting Ki67 expression (A), clinical pathological stage (B), tumor differentiation (C), T-stage (D), vascular invasion (E), and perineural invasion (F).

T-lymphocyte subsets were significantly correlated with CEA. This further proves that a decrease in $CD4^+$ T-lymphocyte content and $CD4^+/CD8^+$ ratio and an increase in $CD8^+$ T-lymphocyte content are closely associated with a desperate clinical profile and an unpromising outcome. Conversely, T-lymphocyte subsets were unrelated to age, sex and tumor

site. Taken together, these results suggest that T-lymphocyte subsets have a high degree of confidence in reflecting the clinical features of CRC.

TABLE 3 Optimal cut-off values for T-lymphocyte subsets to predict the major clinical features of colorectal cancer.

Clinical characteristics	$CD4^+$ (%)	1/($CD8^+$ %)	$CD4^+/CD8^+$ ratio
Ki67 expression	47.45	0.046	1.895
Clinical stage	38.50	0.041	1.625
Organization differentiation	40.45	0.048	2.365
T-stage	39.10	0.046	2.215
Vascular invasion	37.05	0.040	1.625
Perineural invasion	39.10	0.040	1.625

The preoperative and postoperative changes in T-lymphocyte subsets suggest that the body's immune response was enhanced after the primary malignant lesion was removed by effective surgical intervention. Malignant tumors and the immune system are always in a process of resistance. The greater the tumor malignancy, the more aggressive it is and the stronger its suppressive effect on the body's immunity, with a consequent decrease in immune function. When the malignant tumor was eradicated, the suppression of immunity vanished and immune function gradually returned to normal. Therefore, alterations in T-lymphocyte subsets have the potential to be used in postoperative monitoring of tumor metastasis and recurrence, as well as in evaluating drug efficacy. Further analysis can be formulated by tracking the patient's postoperative survival.

TABLE 4 Sensitivity and specificity of the best Cut-off values of T-lymphocyte subsets.

Clinical characteristics	$CD4^+$ (%)		1/($CD8^+$ %)		$CD4^+/CD8^+$ ratio	
	Sensitivity	Specificity	Sensitivity	Specificity	Sensitivity	Specificity
Ki-67 expression	96.6%	53.6%	89.7%	89.3%	93.1%	92.9%
Clinical stage	78.6%	81.8%	92.9%	84.1%	97.6%	84.1%
Organization differentiation	98.6%	69.0%	86.7%	84.5%	93.3%	88.7%
T stage	66.7%	88.5%	85.0%	84.6%	91.7%	84.6%
Vascular invasion	60.6%	67.9%	87.9%	71.7%	87.9%	64.2%
Perineural invasion	75.0%	68.0%	77.8%	68.0%	86.1%	66.0%

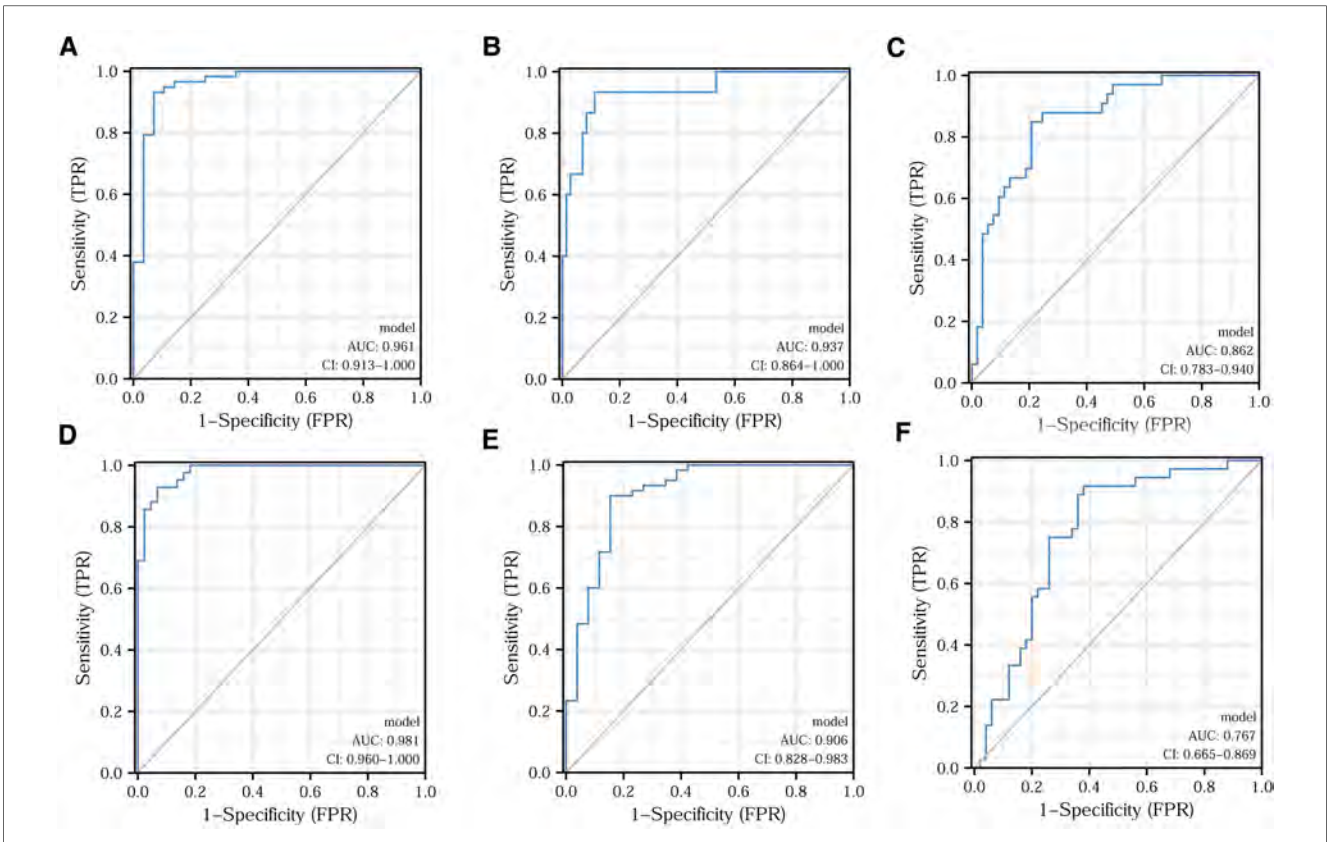

FIGURE 6
Model indicators predicting different clinical features. Efficacy of model indicators for predicting Ki67 expression (A), tumor differentiation (B), vascular infiltration (C), clinical pathological stage (D), T-stage (E), and nerve invasion (F).

TABLE 5 Predictive model indicators for each clinical characteristic.

Clinical Characteristics	Model Indicators	The Best Cut-off Value	Sensitivity	Specificity
Ki-67 expression	$-2.1488-0.1598\times CD4^{+}+0.4284\times CD8^{+}$	−0.608	93.1%	92.9%
Organization differentiation	$-5.7692+0.2147\times CD4^{+}-0.2488\times CD8^{+}$	−1.254	93.3%	88.7%
Vascular invasion	$-7.2618+0.0244\times CD4^{+}+0.2202\times CD8^{+}$	−0.749	84.8%	79.2%
Clinical stage	$-1.5199-0.3531\times CD4^{+}+0.5897\times CD8^{+}$	0.409	92.9%	93.2%
T stage	$2.1721-0.1509\times CD4^{+}+0.2161\times CD8^{+}$	0.121	90.0%	84.6%
Perineural invasion	$2.3227-0.1043\times CD4^{+}+0.0538\times CD8^{+}$	−0.588	91.7%	62.0%

As effective tumor markers should have both high sensitivity and specificity, we analyzed and compared the predictive power of the T-lymphocyte subsets for different clinical features. Through the ROC curve analysis, we clearly discerned that the $CD4^{+}$ and $CD8^{+}$ T-lymphocyte content and $CD4^{+}/CD8^{+}$ ratio have high sensitivity and specificity. Therefore, the above analysis of the relationship between T-lymphocyte subsets and major clinical features suggests that, as immune indicators, $CD4^{+}$ and $CD8^{+}$ T-lymphocyte content and $CD4^{+}/CD8^{+}$ ratio are significant predictors of the clinical features of CRC. The decrease in $CD4^{+}$ T-lymphocyte content and $CD4^{+}/CD8^{+}$ ratio and the increase in $CD8^{+}$ T-lymphocyte content reflect a tendency for immunity to decline, leading to the development of colorectal malignancies. The lower the body's immune defense, the more rapid the development of malignant tumors, the higher the degree of malignancy, and the more worrisome the clinicopathological features of the patients. In summary, the decrease in $CD4^{+}$ T-lymphocyte content and $CD4^{+}/CD8^{+}$ ratio and the increase in $CD8^{+}$ T-lymphocyte content are indicative of a worrying clinicopathological outcome and indirectly suggest an unpromising prognostic outcome for patients.

$CD4^{+}$ and $CD8^{+}$ T-lymphocyte content have their own advantages and disadvantages for predicting different clinical features. The predictive efficacy of the $CD4^{+}/CD8^{+}$ ratio for predicting major clinical features was superior to each of $CD4^{+}$ and $CD8^{+}$ T-lymphocyte content alone. After combining $CD4^{+}$ and $CD8^{+}$ T-lymphocyte content, we attempted to identify model indicators with higher sensitivity and specificity in predicting clinical features by applying logistic regression. Overall, the predictive efficacy of our constructed model indicators was superior to $CD4^{+}$ and $CD8^{+}$ T-lymphocyte content alone. Compared with the $CD4^{+}/CD8^{+}$ ratio, the model indicators had certain advantages. For example, model indicators appear to be more effective than the $CD4^{+}/CD8^{+}$ ratio for predicting Ki67 expression, tumor differentiation and vascular invasion. The model indicators and $CD4^{+}/CD8^{+}$ ratio were all suitable for predicting clinical pathological stage, T-stage, and nerve invasion. In the future, we will optimize and validate the model indicators using more eligible samples.

Collectively, T lymphocytes play an essential role in the fight against tumor cell invasion, metastasis, and recurrence (16). However, different T-lymphocyte subsets play different roles in the immune defense (17). $CD4^{+}$ T cells activate macrophages and $CD8^{+}$ T cells by secreting cytokines, such as interleukin (IL)-2, IL-12, and interferon-γ. We suggest that when malignancies weaken the body's immunity through different immunosuppressive pathways, the $CD4^{+}$ T-lymphocyte content may decrease as the body's immune function is weakened. Consequently, the immune-mediating role of $CD4^{+}$ T lymphocytes also decreases. Thus, a low $CD4^{+}$ T-lymphocyte content is associated with worrying clinical features in the course of tumor development. Thompson et al. demonstrates that both in gastrointestinal tumor tissue and in the peritumor stroma, the higher the density of $CD8^{+}$ T lymphocyte infiltration, the lower the progression-free survival and overall survival of patients (18). We believe that the anti-tumor effects of cytotoxic T cells that release granzyme and perforin (3) are substantially undermined as tumor malignancy increases. Immune dysfunction and immune rejection of $CD8^{+}$ T-lymphocyte was used to evaluate and assess prognosis of various malignant tumors (19). The more severe immune dysfunction and immune rejection of $CD8^{+}$ T-lymphocyte is, the more unpromising outcome of malignant tumor will be. It has been shown that a decrease in the level of immune-responsive $CD8^{+}$ T lymphocytes is a key factor in the progression of CRC (20). The $CD8^{+}$ T lymphocytes can be further divided into $CD8^{+}CD28^{+}$ T lymphocytes (CTL) and $CD8^{+}CD28^{-}$ T lymphocytes based on the expression of CD28 on the surface of $CD8^{+}$ T lymphocytes, of which $CD8^{+}CD28^{-}$ T lymphocytes are a class of regulatory T cells that do not have tumor-killing functions. Some researchers suggest that the chronic stimulation of cancer antigens leads to the cycle activation of the immune cells, which eventually causes $CD8^{+}CD28^{-}$ T lymphocytes to proliferate and exert negative regulatory functions, thus inhibiting the tumor-killing effect of CTL (21). At the same time, tumor cells produce large amounts of enzymes that degrade arginine and tryptophan to compete with immune cells for oxygen and nutrients, which ultimately leads to loss of immune function of $CD8^{+}$ T lymphocytes (22). Furthermore, some researchers have suggested that $CD8^{+}$ T cell inactivation originates from T cell exhaustion. In their study they found that naive $CD8^{+}$ T cells targeting tumor antigens are first initiated in peripheral lymphoid tissues to generate stem cell-like $PD\text{-}1^{lo}CD8^{+}$ T cells with self-renewal properties, which migrate toward TME and form immune-responsive $PD\text{-}1^{lo}CD8^{+}$ T cells in response to chemokines CCL5 and CXCL9. However, in TME, due to continuous antigenic stimulation, stem cell-like $PD\text{-}1^{lo}CD8^{+}$ T cells differentiate and proliferate into substantial $PD\text{-}1^{hi}CD8^{+}$ T cells without immune function (23). Based on those theories, we speculate that although $CD8^{+}$ T-lymphocyte content was higher in cases of CRC with advanced stage, poorer differentiation, and higher Ki67 expression, significantly fewer $CD8^{+}$ T lymphocytes

actually exerted anti-tumor effects because of the continuous cancer antigen stimulation, transformation of $CD8^+$ T-cell subtypes, serious immune dysfunction and rejection. As a result, $CD8^+$ T lymphocytes proliferate and infiltrate but lose their function in such tumor microenvironments. The majority of the remainder were compensated functional suppressed cytotoxic T cells. Overall, our results suggest that an increase in the $CD4^+/CD8^+$ ratio is associated with an increased immune response and may inhibit tumor progression. Conversely, a decrease in the $CD4^+/CD8^+$ ratio may be associated with a restricted immune response, allowing the tumor to proliferate.

Conclusions

In summary, $CD4^+$ T-lymphocyte content, $CD8^+$ T-lymphocyte content, and $CD4^+/CD8^+$ ratio are useful predictors of clinical features in CRC. Alterations in these indicators are closely associated with the clinical features and surgical treatment of CRC. A decreased $CD4^+$ T-lymphocyte content, a decreased $CD4^+/CD8^+$ ratio, and an increased $CD8^+$ T-lymphocyte content are associated with a poorer CRC prognosis. As a result, $CD4^+$ and $CD8^+$ T-lymphocyte content and $CD4^+/CD8^+$ ratio are expected to suitably reflect and predict major clinical characteristics of CRC. These results have potential clinical significance for reflecting and predicting the progression and outcome of CRC in the future.

Data availability statement

The original contributions presented in the study are included in the article, further inquiries can be directed to the corresponding authors.

Ethics statement

The Ethics Committee of China-Japan Union Hospital of Jilin University. The patients/participants provided their written informed consent to participate in this study.

Author contributions

All authors contributed to the study conception and design. Material preparation, data collection and analysis were performed by CY, RZ, and JZ. The first draft of the manuscript was written by CY and JH, and all authors commented on previous versions of the manuscript. All authors contributed to the article and approved the submitted version.

Conflict of interest

The authors declare that the research was conducted in the absence of any commercial or financial relationships that could be construed as a potential conflict of interest.

Publisher's note

All claims expressed in this article are solely those of the authors and do not necessarily represent those of their affiliated organizations, or those of the publisher, the editors and the reviewers. Any product that may be evaluated in this article, or claim that may be made by its manufacturer, is not guaranteed or endorsed by the publisher.

References

1. Sung H, Ferlay J, Siegel RL, Laversanne M, Soerjomataram I, Jemal A, et al. Global cancer statistics 2020: GLOBOCAN estimates of incidence and mortality worldwide for 36 cancers in 185 countries. *CA Cancer J Clin*. (2021) 71(3):209–49. doi: 10.3322/caac.21660

2. Li K, Baird M, Yang J, Jackson C, Ronchese F, Young S. Conditions for the generation of cytotoxic CD4(+) Th cells that enhance CD8(+) CTL-mediated tumor regression. *Clin Transl Immunology*. (2016) 5(8):e95. doi: 10.1038/cti.2016.46

3. Yu W, Wang Y, Guo P. Notch signaling pathway dampens tumor-infiltrating CD8 (+) T cells activity in patients with colorectal carcinoma. *Biomed Pharmacother*. (2018) 97:535–42. doi: 10.1016/j.biopha.2017.10.143

4. Lohneis P, Sinn M, Bischoff S, Jühling A, Pelzer U, Wislocka L, et al. Cytotoxic tumour-infiltrating T lymphocytes influence outcome in resected pancreatic ductal adenocarcinoma. *Eur J Cancer*. (2017) 83:290–301. doi: 10.1016/j.ejca.2017.06.016

5. Horn T, Laus J, Seitz AK, Maurer T, Schmid SC, Wolf P, et al. The prognostic effect of tumour-infiltrating lymphocytic subpopulations in bladder cancer. *World J Urol*. (2016) 34(2):181–7. doi: 10.1007/s00345-015-1615-3

6. Dushyanthen S, Teo ZL, Caramia F, Savas P, Mintoff CP, Virassamy B, et al. Agonist immunotherapy restores T cell function following MEK inhibition improving efficacy in breast cancer. *Nat Commun*. (2017) 8(1):606. doi: 10.1038/s41467-017-00728-9

7. Naito Y, Saito K, Shiiba K, Ohuchi A, Saigenji K, Nagura H, et al. CD8+ T cells infiltrated within cancer cell nests as a prognostic factor in human colorectal cancer. *Cancer Res*. (1998) 58(16):3491–4.

8. Kuwahara T, Hazama S, Suzuki N, Yoshida S, Tomochika S, Nakagami Y, et al. Correction: intratumoural-infiltrating CD4+and FOXP3+T cells as strong positive predictive markers for the prognosis of resectable colorectal cancer. *Br J Cancer*. (2019) 121(11):983–4. doi: 10.1038/s41416-019-0605-4

9. Koi M, Carethers JM. The colorectal cancer immune microenvironment and approach to immunotherapies. *Future Oncol*. (2017) 13(18):1633–47. doi: 10.2217/fon-2017-0145

10. Reeves E, James E. Antigen processing and immune regulation in the response to tumours. *Immunology*. (2017) 150(1):16–24. doi: 10.1111/imm.12675

11. Luo ZW, Zhu MG, Zhang ZQ, Ye FJ, Huang WH, Luo XZ. Increased expression of Ki-67 is a poor prognostic marker for colorectal cancer patients: a meta analysis. *BMC Cancer*. (2019) 19(1):123. doi: 10.1186/s12885-019-5324-y

12. Inoue A, Kagawa Y, Nishizawa Y, Hirano M, Song X, Nakai K, et al. Risk factors for recurrence in patients with pathological stage colorectal cancer. *Gan To Kagaku Ryoho*. (2021) 48(13):1938–40. doi: 10.7666/d.y2053693

13. Dimberg J, Andersson RE, Haglund S. Genomic profiling of stage II colorectal cancer identifies candidate genes associated with recurrence-free survival, tumor location, and differentiation grade. *Oncology*. (2020) 98(8):575–82. doi: 10.1159/000507118

14. Delattre JF, Selcen OEA, Cohen R, Shi Q, Emile JF, Taieb J, et al. A comprehensive overview of tumour deposits in colorectal cancer: towards a next TNM classification. *Cancer Treat Rev*. (2022) 103:102325. doi: 10.1016/j.ctrv.2021.102325

15. Shibutani M, Maeda K, Nagahara H, Ohtani H, Sakurai K, Toyokawa T, et al. Significance of CEA and CA19-9 combination as a prognostic indicator and for recurrence monitoring in patients with stage II colorectal cancer. *Anticancer Res.* (2014) 34(7):3753–8. doi: 10.7666/d.y1875864

16. Tran E, Robbins PF, Lu YC, Prickett TD, Gartner JJ, Jia L, et al. T-Cell transfer therapy targeting mutant KRAS in cancer. *N Engl J Med.* (2016) 375(23):2255–62. doi: 10.1056/NEJMoa1609279

17. Dong C. Helper T cells and cancer-associated inflammation: a new direction for immunotherapy? *J Interferon Cytokine Res.* (2017) 37(9):383–5. doi: 10.1089/jir.2017.0012

18. Thompson ED, Zahurak M, Murphy A, Cornish T, Cuka N, Abdelfatah E, et al. Patterns of PD-L1 expression and CD8 T cell infiltration in gastric adenocarcinomas and associated immune stroma. *GUT.* (2017) 66(5):794–801. doi: 10.1136/gutjnl-2015-310839

19. Jiang P, Gu S, Pan D, Fu J, Sahu A, Hu X, et al. Signatures of T cell dysfunction and exclusion predict cancer immunotherapy response. *Nat Med.* (2018) 24 (10):1550–8. doi: 10.1038/s41591-018-0136-1

20. Tanner SM, Daft JG, Hill SA, Martin CA, Lorenz RG. Altered T-cell balance in lymphoid organs of a mouse model of colorectal cancer. *J Histochem Cytochem.* (2016) 64(12):753–67. doi: 10.1369/0022155416672418

21. Strioga M, Pasukoniene V, Characiejus D. CD8+ CD28- and CD8+ CD57+ T cells and their role in health and disease. *Immunology.* (2011) 134(1):17–32. doi: 10.1111/j.1365-2567.2011.03470.x

22. Hadrup S, Donia M, Thor SP. Effector CD4 and CD8 T cells and their role in the tumor microenvironment. *Cancer Microenviron.* (2013) 6(2):123–33. doi: 10.1007/s12307-012-0127-6

23. Dolina JS, Van Braeckel-Budimir N, Thomas GD, Salek-Ardakani S. CD8(+) T cell exhaustion in cancer. *Front Immunol.* (2021) 12:715234. doi: 10.3389/fimmu.2021.715234

frontiers | Frontiers in Oncology

TYPE Original Research
PUBLISHED 08 May 2023
DOI 10.3389/fonc.2023.1090464

OPEN ACCESS

EDITED BY
Jorge Melendez-Zajgla,
National Institute of Genomic Medicine (INMEGEN), Mexico

REVIEWED BY
Shengyu Zhang,
Peking Union Medical College Hospital (CAMS), China
Francisco Miguel Sanchez Margallo,
Jesús Usón Minimally Invasive Surgery Center, Spain

*CORRESPONDENCE
Bin Deng
chinadbin@126.com

†These authors have contributed equally to this work

RECEIVED 16 November 2022
ACCEPTED 24 April 2023
PUBLISHED 08 May 2023

CITATION
Zhang K, Bile AM, Feng X, Xu Y, Li Y, She Q, Li G, Wu J, Xiao W, Ding Y and Deng B (2023) Image acquisition as novel colonoscopic quality indicator: a single-center retrospective study. *Front. Oncol.* 13:1090464. doi: 10.3389/fonc.2023.1090464

Image acquisition as novel colonoscopic quality indicator: a single-center retrospective study

Ke Zhang[1,2†], Abdiwahid Mohamed Bile[1,3†], Xinyi Feng[1,3], Yemin Xu[1,3], Yaoyao Li[1], Qiang She[1], Guiqing Li[1], Jian Wu[1], Weiming Xiao[1], Yanbing Ding[1] and Bin Deng[1*]

[1]Department of Gastroenterology, Affiliated Hospital of Yangzhou University, Yangzhou, China, [2]Graduate School, Dalian Medical University, Dalian, China, [3]Medical College, Yangzhou University, Yangzhou, China

Purpose: In order to reduce the incidence and mortality of colorectal cancer, improving the quality of colonoscopy is the top priority. At present, the adenoma detection rate is the most used index to evaluate the quality of colonoscopy. So, we further verified the relevant factors influencing the quality of colonoscopy and found out the novel quality indicators by studying the relationship between the influencing factors and the adenoma detection rate.

Materials/methods: The study included 3824 cases of colonoscopy from January to December 2020. We retrospectively recorded the age and sex of the subjects; the number, size, and histological features of lesions; withdrawal time and the number of images acquired during colonoscopy. We analyzed the associated factors affecting adenoma and polyp detection, and verified their effectiveness with both univariate and multivariate logistic regression analyses.

Results: Logistic regression analyses showed that gender, age, withdrawal time and the number of images acquired during colonoscopy could serve as independent predictors of adenoma/polyp detection rate. In addition, adenoma detection rate (25.36% vs. 14.29%) and polyp detection rate (53.99% vs. 34.42%) showed a marked increase when the number of images taken during colonoscopy was ≥29 (P<0.001).

Conclusions: Gender, age, withdrawal time and the number of images acquired during colonoscopy are influencing factors for the detection of colorectal adenomas and polyps. And we can gain higher adenoma/polyp detection rate when endoscopists capture more colonoscopic images.

KEYWORDS

colonoscopy, quality, adenoma detection rate, polyp detection rate, photodocumentation

Introduction

Colorectal cancer (CRC) has high incidence and accounts for roughly 10% of all cancer diagnoses and cancer-related deaths globally each year (1). Population-based screening is an important means of preventing CRC. The population-based screening and early detection program introduced in the United States in the 1990s had an impact on the incidence and mortality of CRC, which showed a decreasing trend (2).

Many CRC screening methods currently exist, but definitive diagnosis still depends on colonoscopy (3). Colonoscopy plays an increasingly important role in CRC prevention and has become a more common screening test for colorectal neoplasia (4, 5). It provides a direct visualization of the whole colon from the rectum to the cecum and even the anus and allows the histological evaluation of any abnormal endoscopic findings, as well as the complete removal of many precancerous lesion. According to the long-term follow-up of patients after colonoscopic polypectomy, early detection, early intervention, and long-term monitoring can remarkably reduce the incidence of CRC (6, 7). The wide application of colonoscopy has promoted the extensive research on the quality improvement of colonoscopy in recent years.

In fact, observational indicators are used to evaluate the quality of colonoscopy, especially in the early identification and intervention of tumors. These indicators including bowel preparation, cecal intubation rate (CIR), adenoma detection rate (ADR), polyp detection rate (PDR), rectal retroflection, withdrawal time, sedation practice and comfort level, annual procedure quantity. Among them, ADR is one of the most commonly used evaluation indicators. ADR, which is dependent on small adenomas, as they account for most of the adenomas detected during colonoscopy, has been the key point of most studies on CRC screening and has found remarkable differences between endoscopists (8–10). Improving ADR is believed to improve colonoscopy performance to reduce the morbidity and mortality of interval cancers (11, 12). Many methods have been developed to improve ADR (13). For example, Barclay found that a longer withdrawal time (>6 min) increases the detection rates of polyps and advanced tumors (14). Studies demonstrated that divided-dose bowel preparations increase ADR (15, 16). All of these parameters are artificially controllable factors during colonoscopy, but whether unknown factors may influence the ability of colonoscopy to detect lesions is unclear, such as pictures collection during colonoscopy. The images acquired during colonoscopy are the most intuitive evidence for the acquisition of colonoscopy results. Therefore, we hypothesized that the number of colonoscopy images acquired is also a factor that influences the quality of colonoscopy. We further verified the relevant factors influencing the quality of colonoscopy by studying the relationship between the influencing factors and the adenoma detection rate.

Patients and methods

Study population

Subjects who underwent colonoscopy at the Gastroscopy Center of the Affiliated Hospital of Yangzhou University from January to December 2020 were enrolled. The following inclusion criteria were applied: (1) subjects' age ≥18 years; (2) subjects underwent colonoscopy for the first time. The exclusion criteria listed below were applied: (1) subjects with a personal history of CRC or colorectal resection; (2) pregnant or lactating women; (3) subjects with severe systemic diseases, mental disorders, and other diseases that might interfere with the assessment of the examination; (4) colonoscopies that were discontinued because of poor bowel preparation or other reasons; and (5) colonoscopies performed by endoscopists with a minimal number of operations per year (annual number of colonoscopies performed <500) or those with insufficient experience in colonoscopy (number of years of activity as endoscopist <3) (Figure 1). The Yangzhou University Affiliated Hospital's Ethics Committee approved this study (No. 2021-YKL06-09-004). The need for informed consent was waived due to the retrospective nature of this study.

Study procedures

Sixteen endoscopists in this study had dedicated, hands-on instruction for colonoscopy. All colonoscopies were performed in a hospital outpatient endoscopy center under venous anesthesia. We recorded the subjects' age and sex, cecal intubation, withdrawal time and the number of images acquired during colonoscopy, as well as the number, size, location, and histological description of the lesions detected during colonoscopy. In the process of recording the number of colonoscopy pictures taken, when there are repeated pictures taken, i.e. the same pictures are taken two or more times, only one is recorded. When there were other errors, i.e. the pictures collected were blurred, in which case these pictures would be excluded from the study. The standard bowel preparation was a 3-liter oral lavage with polyethylene glycol electrolyte solution and dimeticone.

Statistical analysis

Intergroup differences were compared using Student's t-test. Chi-square test was used to analyze categorical data. Data were expressed as mean ± standard deviation. Multiple logistic regression

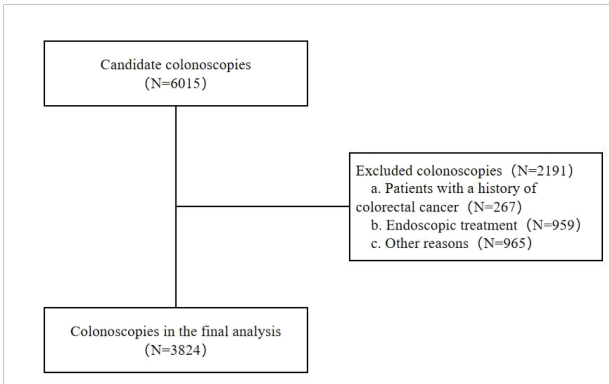

FIGURE 1
Study flow diagram and patients demographics.

analysis was used to determine the possible factors affecting lesion detection. Statistical Product and Service Solutions (SPSS) 22.0 software (SPSS Inc., Chicago, IL, USA) was used for statistical processing. Statistical significance was defined by $P \leq 0.05$. No guideline has been established for the number of images acquired during colonoscopy, thus, when we analyzed the number of images taken during colonoscopy, the median number of images acquired in all subjects was used, 29 as the basis for grouping.

Results

Study population

The baseline characteristics of subjects are illustrated in Table 1. Based on the inclusion and exclusion criteria, 3824 subjects were selected from 6015 subjects for inclusion in the study. The average age of the subjects included was 53.15 years, and 57.51% were male. Colorectal polyps were more frequently observed in participants who were older, male, with a longer withdrawal time and a higher number of images during colonoscopy (P<0.001).

Outcome measures

Relevant factors for lesion detection

The influence of various factors (age, sex, withdrawal time and the number of images taken during colonoscopy) on lesion detection rate was studied (Table 2). The subjects were divided into two groups depending on the presence or absence of colorectal adenomas and polyps. The ADR (23.40% vs. 9.08%) and PDR (52.93% vs. 33.35%) of subjects aged ≥45 years were significantly higher than those aged <45 years (P<0.001), and males were higher than females (P<0.001). The ADR (61.02% vs. 10.88%) and PDR (78.96% vs. 27.02%) are remarkably greater among endoscopists with a mean withdrawal time of ≥6 minutes and a higher number of images taken during colonoscopy (P<0.001).

Finally, in the univariate analyses, the odds of detecting an adenoma in women were 54.6% of those in men. People aged ≥45 years were more than three times as likely to develop adenomas as those aged <45 years. As the number of images collected during colonoscopy increased, ADR increased approximately 2-fold. Multivariate analyses showed that gender, age, withdrawal time and the number of images acquired during colonoscopy could serve as independent predictors of ADR (Table 3). Similar results were obtained in the analysis of polyp detection (Table 4).

Effect of the photodocumentation of colonoscopy on lesion detection

Based on the above results, we further specifically analyzed the impact of picture recording on the quality of colonoscopy. Table 5 describes the effect of the number of images acquired during colonoscopy on the detection of size, number, and pathology of lesions. According to the number of images, subjects were divided into two groups (1991 [≥29] vs. 1833 [<29]), and the difference in ADR (25.36% vs. 14.29%) and PDR (53.99% vs. 34.42%) between the two groups was significant (P<0.001). Excluding normal subjects, subjects in the lesion group were divided into two groups according to the number of images acquired during colonoscopy (1075 [≥29] vs. 631 [<29]). The difference in the detection rate of polyps with ≥6 mm diameter was significant between the two groups (P<0.05), and the difference in the detection rate of ≥3 polyps between the two groups was significant (P<0.001). The difference in the detection rates between nonneoplastic polyps and neoplastic polyps was also significant (P<0.05).

Detection of lesions in individual colonic segments

A strong correlation was found between the number of images acquired at each colorectal site and the detection rate of lesions (Table 6). Similarly, the median number of images acquired at different sites in the colon across all subjects was used as the cutoff. In the cecum and rectum, ADR and PDR were remarkably higher when the number of images acquired in each colonic segment was ≥3 compared with <3. In the ascending colon, transverse colon, descending colon, and sigmoid colon, ADR and PDR were remarkably higher when the number of images acquired in each colonic segment was ≥4. However, with the exception of the ascending and descending colons, no substantial differences were found between the two groups in the detection of large polyps (≥6 mm diameter). Moreover, no considerable difference was found between the two groups in terms of polyp number or polyp histopathology.

Discussion

Colonoscopy is the most common tool in CRC screening. It provides the chance to detect and remove benign lesions before the conditions deteriorate (14). ADR is the most commonly used marker for measuring colonoscopy quality and is used as an

TABLE 1 Clinical characteristics of the subjects.

Variables	Subjects without colorectal polyps (N=2090)	Subjects with colorectal polyps (N=1538)	$p^{\#}$ value
Male Sex (no. [%])	1022 (48.90)	1049 (68.21)	<0.001**
Age (years)	50.45 ± 11.99	56.26 ± 11.53	<0.001**
Withdrawal Time(mins)	3.83 ± 1.99	8.69 ± 7.64	<0.001**
Cecal Intubation (no. [%])	2012 (96.27)	1439 (93.56)	<0.001**
[a]No.	28.31 ± 10.14	33.90 ± 13.85	<0.001**

**p<0.001; #p value from χ^2 test (or Fisher's exact test, as appropriate) or t-test; a: number of images acquired during colonoscopy.

TABLE 2 Correlation between different factors and the detection of adenomas and polyps.

	ADR(%)	*p* value	PDR(%)	*p* value
Sex		<0.001**		<0.001**
Male	23.92	–	52.93	–
Female	14.83	–	33.35	–
Age (years)		<0.001**		<0.001**
≥ 45	23.40	–	49.97	–
< 45	9.08	–	27.02	–
Withdrawal Time(mins)		<0.001**		<0.001**
≥ 6	61.02	–	78.96	–
< 6	10.88	–	27.02	–
[a]No.		<0.001**		<0.001**
≥ 29	25.36	–	53.99	–
< 29	14.29	–	34.42	–

**p<0.001. a: number of images acquired during colonoscopy. ADR = adenoma detection rate, PDR = polyp detection rate.

TABLE 3 Logistic regression analysis of relevant risk factors that may influence adenoma detection.

Risk Factors	Univariate Analyses		Multivariate Analyses	
	OR (95%CI)	*p* value	OR (95%CI)	*p* value
Gender	0.546 (0.457–0.651)	<0.001**	0.613 (0.508–0.740)	<0.001**
Age	3.229 (2.489–4.190)	<0.001**	2.810 (2.145–3.680)	<0.001**
Withdrawal Time	4.996 (4.193–5.952)	<0.001**	4.406 (3.374–4.853)	<0.001**
[a]No.	2.037 (1.714–2.421)	<0.001**	1.542 (1.281–1.855)	<0.001**

**p<0.001; a: number of images acquired during colonoscopy.

TABLE 4 Logistic regression analysis of the relevant risk factors that may influence polyp detection.

Risk Factors	Univariate Analyses		Multivariate Analyses	
	OR (95%CI)	*p* value	OR (95%CI)	*p* value
Gender	0.446 (0.389–0.512)	<0.001**	0.451 (0.385–0.529)	<0.001**
Age	2.630 (2.219–3.118)	<0.001**	2.519 (2.074–3.060)	<0.001**
Withdrawal Time	10.136 (8.545–12.024)	<0.001**	8.712 (7.297–10.400)	<0.001**
[a]No.	2.114 (1.849–2.418)	<0.001**	1.575 (1.347–1.841)	<0.001**

*p<0.05, **p<0.001; [a]number of images acquired during colonoscopy.

observation indicator to evaluate whether a new technology or technique improves the quality of colonoscopy (17). Based on our study, gender, age, withdrawal time and the number of images acquired during colonoscopy could serve as independent predictors of ADR.

In the past few decades, CRC cases have increased dramatically in the United States and other high-income countries. The incidence rate of CRC is 30% higher in men than in women, which may be related to male androgen levels (18, 19). According to our study, compared with women, men have a higher ADR, which is also consistent with previous studies. Therefore, we believe that males should pay more attention to colorectal cancer screening activities.

The 2021 American College of Gastroenterology screening guidelines also recommend CRC screening in average-risk population among ages 45–49 to decrease the incidence of advanced adenomas and carcinoma (3). Previously, in 2018, the American Cancer Society also published guidelines with a

10.3389/fonc.2023.1090464

TABLE 5 Effect of the number of images acquired during colonoscopy on lesion detection.

	[a]No. ≥ 29	[a]No. < 29	*p* value
ADR (%)	505 (25.36%)	262 (14.29%)	<0.001**
PDR (%)	1075 (53.99%)	631 (34.42%)	<0.001**
Polyp size			0.011*
<6 mm	583	382	–
≥6 mm	492	249	–
Number of Polyps			<0.001**
≤2	633	446	–
>2	442	185	–
Histological Features of Polyps			0.029*
Nonneoplastic Polyps	570	369	–
Neoplastic Polyps	505	262	–

*p<0.05, **p<0.001; a: number of images acquired during colonoscopy. ADR = adenoma detection rate, PDR = polyp detection rate.

recommendation to reduce the initiation age for CRC screening in average-risk individuals from 50 years to 45 years and that starting screening at age 45 would result in a gain of approximately 25 additional life years per 1,000 individuals screened as compared with age 50 (20). Based on our findings, ADR and PDR substantially increased in subjects older than 45 years. Therefore, broadening the CRC screening population would be suitable.

According to a study involving 12 endoscopists, their analysis of screening colonoscopy in average-risk individuals found remarkable differences in the detection rates of lesions among endoscopists. Their results also showed that adequate withdrawal time can considerably improve colonoscopy quality (8). Shaukat et al. concluded that the incidence of interval cancer can be reduced by appropriately prolonging the withdrawal time during colonoscopy (21). Similarly, the increased withdrawal time also improved the ADR in our study. However, in normal subjects, their average withdrawal time was low and did not reach the guideline recommended time (3, 22), which requires further improvement later on.

In addition, we report for the first time in this study the effect of the number of images acquired taken during colonoscopy on colonoscopy quality in outpatients. Similar to withdrawal time, increasing the number of images acquired during colonoscopy suggests a more careful examination of the mucosa during colonoscopy and increases the chance of detecting lesions. The photodocumentation of cecal intubation had nominal effects on ADR and PDR. Acquiring more endoscopic images were more likely to demonstrate cecal intubation. Although their results did not reach statistical significance, the ADR and PDR of photographically confirmed colonoscopies were higher than those of deficiently photodocumented cases (23). Our results suggest that a difference in the number of images acquired during colonoscopy contributes to differences in the detection rates of lesions. In our study, ADR (25.36% vs. 14.29%) was significantly and markedly increased when the number of images taken during colonoscopy was ≥29. The resulting ADR was low, and the true ADR would be higher than our final ADR, because a large number of patients undergoing endoscopic treatment were initially excluded. In fact, the photodocumentation of abnormalities detected during colonoscopy has become universal. The habits of individual endoscopic operators in taking photos during colonoscopy vary, and the conception of images taken at normal sites, some prominent sites, and where abnormal lesions were present varies and may depend on the psychological state of the operator, which results in large differences in the number of drawings left. Our results suggest that the increased number of images acquired during colonoscopy increases the likelihood of detecting lesions and thus improves the quality of colonoscopy. However, whether this factor reduces the incidence and mortality of CRC is unclear, and future studies on photodocumentation during colonoscopy are warranted.

In our study, PDR paralleled ADR in trend, and the differences were significant. Most CRCs develop within adenomatous or serrated polyps, and the disruption of the polyp-to-cancer sequence prevents CRC progression. The increased detection and removal of colorectal polyps by colonoscopy is associated with a reduction in the incidence of advanced adenomas, carcinoma, and mortality from CRC (24). Briefly, our study results support the idea that the number of images acquired during colonoscopy correlates with the detection of polyps, and the results provide an opportunity for polypotomy, which may then reduce the incidence and mortality of CRC.

The ultimate aim of colonoscopy screening is to prevent CRC. Advanced adenomas in particular are more prone to develop into malignant diseases (25). According to the definition of the US Multi-Society Task Force on Colorectal Cancer, an advanced neoplasm is defined as an adenoma with a size of ≥10 mm, villous histology, or high-grade dysplasia. On follow-up after colonoscopy, patients found to have advanced adenomas are at increased risk of advanced neoplasia (26). However, the incidence of carcinoma is higher for lesions ≥6 mm than for lesions ≤5 mm (27). And it is difficult to differentiate benign and advanced adenomas by colonoscopy only (27–29). Therefore, the most recent clinical practice guidelines for the management of colorectal polyps strongly recommend endoscopic

TABLE 6 Effect of the number of images acquired in individual colonic segments during colonoscopy on lesion detection.

		ADR (%)	*p* value	PDR (%)	*p* value	Size of Polyps		*p* value	Number of Polyps		*p* value	Histological Features of Polyps		*p* value
						≥6 mm	<6 mm		≤2	>2		Nonneoplastic Polyps	Neoplastic Polyps	
Cecum			<0.001**		<0.001**			0.235			0.826			0.857
	[a]No. ≥ 3	2.22	–	4.81	–	36	68	–	82	22	–	56	48	–
	[a]No. < 3	0.42	–	0.96	–	8	8	–	13	3	–	9	7	–
Ascending Colon			<0.001**		<0.001**			0.001*			0.079			0.721
	[a]No. ≥ 4	5.81	–	11.86	–	146	95	–	197	44	–	123	118	–
	[a]No. < 4	1.90	–	4.07	–	28	45	–	66	7	–	39	34	–
Transverse Colon			<0.001**		<0.001**			0.234			0.419			0.670
	[a]No. ≥ 4	6.28	–	13.81	–	162	147	–	264	45	–	164	145	–
	[a]No. < 4	1.65	–	3.76	–	25	32	–	51	6	–	32	25	–
Descending Colon			<0.001**		<0.001**			0.016*			0.235			0.406
	[a]No. ≥ 4	5.22	–	12.72	–	146	132	–	237	41	–	146	114	–
	[a]No. < 4	1.22	–	3.48	–	20	37	–	45	12	–	37	20	–
Sigmoid Colon			<0.001**		<0.001**			0.978			0.595			0.235
	[a]No. ≥ 4	7.89	–	21.78	–	212	315	–	376	151	–	336	191	–
	[a]No. < 4	2.35	–	7.76	–	44	65	–	75	34	–	76	33	–
Rectum			<0.001**		<0.001**			0.583			0.977			0.302
	[a]No. ≥3	3.43	–	18.92	–	117	385	–	299	203	–	411	91	–
	[a]No.<	1.20	–	8.63	–	21	80	–	60	41	–	87	14	–

**p<0.001; a: number of images acquired during colonoscopy. ADR = adenoma detection rate, PDR = polyp detection rate.

10.3389/fonc.2023.1090464

resection for lesions ≥6 mm in size (30). Our results also showed that acquiring a greater number of images during colonoscopy is correlated with a higher detection rate of large lesions. This result has remarkable implications for CRC screening by colonoscopy.

Finally, our study has several limitations. On the one hand, the analysis was not adjusted for patient factors, such as sedation, family history of CRC, and smoking, which may have influenced the results. On the other hand, this study is a single-center study. Further multicenter studies are needed to further verify the impact of colonoscopy photodocumentation on colonoscopy quality.

In our study, it is the first to explore the effect of colonoscopy photodocumentation on ADR and PDR. Besides ADR, cecal intubation rate and withdrawal time, we think that the image recording of colonoscopy is a novel quality indicator of colonoscopy that has been neglected for a long time, which is worth considering in the future recommendations and guidelines for colonoscopy quality indicators and screening. We call on gastroenterologists to take more pictures during colonoscopy. Overall, no studies to date have demonstrated appropriate specifications for image capture during colonoscopies. We obtained a higher ADRs and PDRs when endoscopists acquired more colonoscopic images. But the effect of a different number of images acquired during colonoscopy on CRC prevention is unknown. Our study was a rudimentary investigation; therefore, benefit, universality and meanings for clinical practice must be determined by farther studies.

Data availability statement

The raw data supporting the conclusions of this article will be made available by the authors, without undue reservation.

Ethics statement

This article does not contain any studies with human or animal subjects. All procedures were carried out in compliance with the Helsinki Declaration (as revised in 2013). This study was approved by the Ethics Committee of the Affiliated Hospital of Yangzhou University (No. 2021-YKL06-09-004). The need for informed consent was waived due to the retrospective nature of this study.

Author contributions

All authors listed have made a substantial, direct, and intellectual contribution to the work. KZ, AB, and XF contributed to the study design. KZ, AB, YX, and GL contributed to data collection. JW, WX, YD, and BD were responsible for checking the data. YL and QS were responsible for revising critically of the article for important intellectual content. KZ, AB, and BD contributed to statistical analysis and preparation of the manuscript. All authors contributed to manuscript revision, read, and approved the submitted version.

Funding

This work was supported by the Key Project for Social Development of Yangzhou (No. YZ2020069).

Acknowledgments

This work was supported by the Department of Gastroenterology of the Affiliated Hospital of Yangzhou University.

Conflict of interest

The authors declare that the research was conducted in the absence of any commercial or financial relationships that could be construed as a potential conflict of interest.

Publisher's note

References

1. Bray F, Ferlay J, Soerjomataram I, Siegel RL, Torre LA, Jemal A. Global cancer statistics 2018: GLOBOCAN estimates of incidence and mortality worldwide for 36 cancers in 185 countries. *CA Cancer J Clin* (2018) 68(6):394–424. doi: 10.3322/caac.21492

2. Brenner H, Kloor M, Pox CP. Colorectal cancer. *Lancet* (9927) 2014:383. doi: 10.1016/S0140-6736(13)61649-9

3. Shaukat A, Kahi CJ, Burke CA, Rabeneck L, Sauer BG, Rex DK. ACG clinical guidelines: colorectal cancer screening 2021. *Am J Gastroenterol* (2021) 116(3):458–79. doi: 10.14309/ajg.0000000000001122

4. Prajapati DN, Saeian K, Binion DG, Staff DM, Kim JP, Massey BT, et al. Volume and yield of screening colonoscopy at a tertiary medical center after change in Medicare reimbursement. *Am J Gastroenterol* (2003) 98:194–9. doi: 10.1111/j.1572-0241.2003.07172.x

5. Harewood GC, Lieberman DA. Colonoscopy practice patterns since introduction of Medicare coverage for average-risk screening. *Clin Gastroenterol Hepatol* (2004) 2:72–7. doi: 10.1016/s1542-3565(03)00294-5

6. Citarda F, Tomaselli G, Capocaccia R, Barcherini S, Crespi MItalian Multicentre Study Group. Efficacy in standard clinical practice of colonoscopic polypectomy in reducing colorectal cancer incidence. *Gut* (2001) 48:812–5. doi: 10.1136/gut.48.6.812

7. Muller AD, Sonnenberg A. Prevention of colorectal cancer by flexible endoscopy and polypectomy: a case-control study of 32,702 veterans. *Ann Intern Med* (1995) 123:904–10. doi: 10.7326/0003-4819-123-12-199512150-00002

8. Barclay RL, Vicari JJ, Doughty AS, Johanson JF, Greenlaw RL. Colonoscopic withdrawal times and adenoma detection during screening colonoscopy. *N Engl J Med* (2006) 355:2533–41. doi: 10.1056/NEJMoa055498

9. Benson ME, Reichelderfer M, Said A, Gaumnitz EA, Pfau PR. Variation in colonoscopic technique and adenoma detection rates at an academic gastroenterology unit. *Dig Dis Sci* (2010) 55:166–71. doi: 10.1007/s10620-008-0703-2

10. Imperiale TF, Glowinski EA, Lin-Cooper C, Ransohoff DF. Tailoring colorectal cancer screening by considering risk of advanced proximal neoplasia. *Am J Med* (2012) 125:1181–7. doi: 10.1016/j.amjmed.2012.05.026

11. Rex DK, Petrini JL, Baron TH, Chak A, Cohen J, Deal SE, et al. Quality indicators for colonoscopy. *Am J Gastroenterol* (2006) 101:873–85. doi: 10.1111/j.1572-0241.2006.00673.x

12. Kaminski M, Regula J, Kraszewska E, Polkowski M, Wojciechowska U, Didkowska J, et al. Quality indicators for colonoscopy and the risk of interval cancer. *N Engl J Med* (2010) 362:1795–803. doi: 10.1056/NEJMoa0907667

13. Rees CJ, Bevan R, Zimmermann-Fraedrich K, Rutter MD, Rex D, Dekker E, et al. Expert opinions and scientific evidence for colonoscopy key performance indicators. *Gut* (2016) 65(12):2045–60. doi: 10.1136/gutjnl-2016-312043

14. Bresalier RS. Malignant neoplasms of the large intestine. In: Feldman M, Friedman LS, Sleisenger MH, editors. *Sleisenger & fordtran's gastrointestinal and liver disease: pathophysiology, diagnosis, management*, *7th ed*. Philadelphia: Saunders (2002). p. 2215–61.

15. Gurudu SR, Ramirez FC, Harrison ME, Leighton JA, Crowell MD. Increased adenoma detection rate with system-wide implementation of a split-dose preparation for colonoscopy. *Gastrointest Endosc* (2012) 76:603–8. doi: 10.1016/j.gie.2012.04.456

16. Radaelli F, Paggi S, Hassan C, Senore C, Fasoli R, Anderloni A, et al. Split-dose preparation for colonoscopy increases adenoma detection rate: a randomised controlled trial in an organised screening programme. *Gut* (2017) 66:270–7. doi: 10.1136/gutjnl-2015-310685

17. Wallace MB. Improving colorectal adenoma detection: technology or technique? *Gastroenterol* (2007) 132:1221–3. doi: 10.1053/j.gastro.2007.03.017

18. Sinicrope FA. Increasing incidence of early-onset colorectal cancer. *N Engl J Med* (2022) 386(16):1547–58. doi: 10.1056/NEJMra2200869

19. Yu X, Li S, Xu Y, Zhang Y, Ma W, Liang C, et al. Androgen maintains intestinal homeostasis by inhibiting BMP signaling *via* intestinal stromal cells. *Stem Cell Rep* (2020) 15:912–25. doi: 10.1016/j.stemcr.2020.08.001

20. Wolf AMD, Fontham ETH, Church TR, Flowers CR, Guerra CE, LaMonte SJ, et al. Colorectal cancer screening for average-risk adults: 2018 guideline update from the American cancer society. *CA Cancer J Clin* (2018) 68:250–81. doi: 10.3322/caac.21457

21. Shaukat A, Rector TS, Church TR, Lederle FA, Kim AS, Rank JM, et al. Longer withdrawal time is associated with a reduced incidence of interval cancer after screening colonoscopy. *Gastroenterology* (2015) 149:952–7. doi: 10.1053/j.gastro.2015.06.044

22. Keswani RN, Crockett SD, Calderwood AH. AGA clinical practice update on strategies to improve quality of screening and surveillance colonoscopy: expert review. *Gastroenterology* (2021) 161:701–11. doi: 10.1053/j.gastro.2021.05.041

23. Moran B, Sehgal R, O'Morain N, Slattery E, Collins C. Impact of photodocumentation of caecal intubation on colonoscopy outcomes. *Irish J Med Sci* (2021) 190(4):1397–402. doi: 10.1007/s11845-020-02469-z

24. Winawer SJ, Zauber AG, Ho MN, O'Brien MJ, Gottlieb LS, Sternberg SS, et al. Prevention of colorectal cancer by colonoscopic polypectomy. *Natl Polyp Study Workgroup. N Engl J Med* (1993) 329(27):1977–81. doi: 10.1056/NEJM199312303292701

25. O'Brien MJ, Winawer SJ, Zauber AG, Gottlieb LS, Sternberg SS, Diaz B, et al. The national polyp study: patient and polyp characteristics associated with high-grade dysplasia in colorectal adenomas. *Gastroenterology* (1990) 98:371–9. doi: 10.1016/0016-5085(90)90827-N

26. Lieberman DA, Rex DK, Winawer SJ, Giardiello FM, Johnson DA, Levin TR. Guidelines for colonoscopy surveillance after screening and polypectomy: a consensus update by the US Multi-Society Task Force on Colorectal Cancer. *Gastroenterology* (2012) 143(3):844–57. doi: 10.1053/j.gastro.2012.06.001

27. Aldridge AJ, Simson JN. Histological assessment of colorectal adenomas by size. *Are polyps less than 10 mm size clinically important? Eur J Surg* (2001) 167:777–81. doi: 10.1080/11024150152707770

28. Ahlawat SK, Gupta N, Benjamin SB, Al-Kawas FH. Large Colorectal polyps: endoscopic management and rate of malignancy: does size matter? *J Clin Gastroenterol* (2011) 45:347–54. doi: 10.1097/MCG.0b013e3181f3a2e0

29. Ponugoti PL, Cummings OW, Rex DK. Risk of cancer in small and diminutive colorectal polyps. *Dig Liver Dis* (2017) 49:34–7. doi: 10.1016/j.dld.2016.06.025

30. Tanaka S, Saitoh Y, Matsuda T, Igarashi M, Matsumoto T, Iwao Y, et al. Evidence-based clinical practice guidelines for management of colorectal polyps. *J Gastroenterol* (2021) 56(4):323–35. doi: 10.1007/s00535-014-1021-4

frontiers | Frontiers in Oncology

TYPE Original Research
PUBLISHED 10 May 2023
DOI 10.3389/fonc.2023.1123455

OPEN ACCESS

EDITED BY
Tadahiko Masaki,
Kyorin University, Japan

REVIEWED BY
Jorge Melendez-Zajgla,
National Institute of Genomic Medicine (INMEGEN), Mexico
Shahanavaj Khan,
Indian Institute of Health and Technology, India

*CORRESPONDENCE
Guiyu Wang
guiywang@hrbmu.edu.cn
Lei Yu
allengl0601@163.com

RECEIVED 14 December 2022
ACCEPTED 18 April 2023
PUBLISHED 10 May 2023

CITATION
Jun X, Gao S, Yu L and Wang G (2023) The clinical relevance and prediction efficacy from therapy of tumor microenvironment related signature score in colorectal cancer.
Front. Oncol. 13:1123455.
doi: 10.3389/fonc.2023.1123455

The clinical relevance and prediction efficacy from therapy of tumor microenvironment related signature score in colorectal cancer

Xiang Jun[1], Shengnan Gao[2], Lei Yu[1]* and Guiyu Wang[1]*

[1]Department of Colorectal Surgery, The Second Affiliated Hospital of Harbin Medical University, Harbin, China, [2]Department of Endocrinology and Metabolism, The Second Affiliated Hospital of Harbin Medical University, Harbin, China

Introduction: As the top 3 cancer in terms of incidence and mortality, the first-line treatment for CRC includes FOLFOX, FOLFIRI, Cetuximab or immunotherapy. However, the drug sensitivity of patients to regimens is different. There has been increasing evidence that immune components of TME can affect the sensitivity of patients to drugs. Therefore, it is necessary to define novo molecular subtypes of CRC based on TME immune components, and screen patients who are sensitive to the treatments, to make personalized therapy possible.

Methods: We analyzed the expression profiles and 197 TME-related signatures of 1775 patients using ssGSEA, univariate Cox proportional risk model and LASSO-Cox regression model, and defined a novo molecular subtype (TMERSS) of CRC. Simultaneously, we compared the clinicopathological factors, antitumor immune activity, immune cell abundance and differences of cell states in different TMERSS subtypes. In addition, patients sensitive to the therapy were screened out by correlation analysis between TMERSS subtypes and drug responses.

Results: Compared with low TMERSS subtype, high TMERSS subtype has a better outcome, which may be associated to higher abundance of antitumor immune cell in high TMERSS subtype. Our findings suggested that the high TMERSS subtype may have a higher proportion of respondents to Cetuximab agent and immunotherapy, while the low TMERSS subtype may be more suitable for treatment with FOLFOX and FOLFIRI regimens.

Discussion: In conclusion, the TMERSS model may provide a partial reference for the prognosis evaluation of patients, the prediction of drug sensitivity, and the implementation of clinical decision-making.

KEYWORDS

CRC, therapy, response, TMERSS, immune cell, prediction

Introduction

Colorectal cancer (CRC) represents the third most common malignancy and the second leading cause of cancer death worldwide (1, 2). In recent years, radical resection has been the mainstay of treatment for CRC. In order to avoid recurrence and prolong OS, neoadjuvant or adjuvant chemotherapy is often required for surgical patients. Fluorouracil-based combination chemotherapy is recommended for all patients with stage II or III (3). As first-line agents, fluorouracil-based combination chemotherapy includes FOLFOX, CapeOX, and FOLFIRI (4). However, the occurrence of resistance often makes patients benefit less in the course of treatment (5). Studies have shown that adjuvant chemotherapy improves survival rate by only 3% in patients with stage II CRC, and increases by 15% to 20% for stage III CRC (6). Therefore, it is necessary to screen out patients who have good response to fluorouracil-based combination chemotherapy, making personalized treatment possible.

Colorectal cancer has a complex pathogenesis, and many potential factors have an important impact on the occurrence and development of colorectal cancer. Currently, some studies have reported some factors that affect the occurrence and development of colorectal cancer. These include changes in the cellular microenvironment associated with growth and development (7), the microenvironment in which tumors occur, and the impact of gastrointestinal tumors and tumors outside the gastrointestinal tract, such as colon cancer (8), lung cancer (9), and prostate cancers (10, 11). Meanwhile, increasing evidence demonstrates that the tumor microenvironment (TME) plays a crucial role in tumorigenesis and tumor progression (12). The primary composition of TME includes infiltrating immune cells, mesenchymal cells, and extracellular matrix (13). The infiltrating immune cells are composed of multiple immune cell types, such as T cells, macrophages, and neutrophils (14). Various tumor-infiltrating immune cells make TME a double-edged sword, exhibiting an ability to either arrest or support malignancy (15). The complex role of TME makes it possible to classify cancer immunologically in terms of prognosis, chemotherapy, and immunotherapy response prediction. For example, microsatellite instability tumors show a high abundance of Th1 cells, and effector memory T cells, and have a favorable prognosis. Given that TME plays an indispensable role in chemotherapy and immunotherapy resistance (16), we used the gene expression profiles to define novo molecular classifications of CRC based on signatures of various immune components in order to distinguish between drug sensitivity and TME.

In order to define novel molecular classifications of CRC, gene expression profiles of 1775 patients were analyzed. In this study, our main work included: (1) Constructing a scoring model and redefining the molecular classifications of CRC; (2) Identifying TME differences between CRC and screening patients who respond to chemotherapy or immunotherapy, in order to provide the reference for individualized treatment of patients; (3) Evaluating the relationship between molecular classifications of CRC and clinicopathological factors.

Materials and methods

Data downloading and processing

The gene expression profile and clinical data of patients were obtained from GEO, TCGA, and cBioportal databases. The datasets obtained from GEO include GSE17538, GSE12945, GSE39582, and GSE103479. RNA-seq data were collected from the TCGA (https://portal.gdc.cancer.gov/) for 33 cancers. Meanwhile, RNA-seq data of CRC also were collected in cBioportal (https://www.cbioportal.org/).

We used datasets GSE17538, GSE12945, GSE39582, and GSE103479 as discovery cohorts, and used the ComBat function to remove potential multicenter batch effects between different experiments. CRC data from TCGA and cBioportal databases were used as testing cohorts 1 and 2, respectively. Simultaneously, all the data is integrated as the testing cohort 3.

In this research, we conducted systematic bioinformatics analysis on gene expression profile data of 1775 CRC specimens. In the discovery cohort, 1022 patients from four datasets were included in the study. The specific information of each dataset is as follows: The gene expression profile of tumor tissue samples from 62 patients in GSE12945 dataset; The GSE17538 dataset stores gene expression profiles of 244 specimens, of which 238 gene expression profiles from human CRC tissue samples were used for further analysis; The gene expression profiles of 156 patients in GSE103479 dataset were included in the study; The GSE39582 dataset collected the gene expression profile of 585 samples, including 566 colorectal tumor tissue samples and 19 colorectal normal tissue specimens, of which 566 tumor tissue samples were included in the study. The testing cohort 1 integrates the information of 521 colon cancer samples and 177 rectal cancer samples in TCGA database. After excluding 51 normal tissue samples, the gene expression profile of 647 patients was used for bioinformatics analysis. The testing cohort 2 is RNA-seq data from 106 CRC patients in the cBioportal database. The gene expression profile of all cohorts is integrated in cohort 3, including the gene expression profile of 1775 samples. Finally, we also collected the gene expression profiles of 33 cancers in TCGA database, and >1000,0 samples were used for pan-cancer related analysis.

We also collected gene expression profiles of patients with different treatment regimens, such as GSE104645, GSE72970, GSE78220, GSE91061, and IMvigor210 (17). In the dataset GSE104645, the chemotherapy scheme of 104 patients is FOLFOX, who was used for bioinformatics analysis; In the dataset GSE72970, the chemotherapy scheme of 87 patients is FOLFIRI, who was used for bioinformatics analysis; GSE78220 which includes 28 patients is a dataset on anti-PD1 inhibitor immunotherapy in melanoma; GSE91061 which includes 109 patients is a dataset on anti-PD1 and anti-CTLA4 inhibitor immunotherapy for melanoma; IMvigor210 which includes 348

patients is the dataset of anti-PDL1 inhibitor immunotherapy for patients with urothelial carcinoma.

Collection of TME related signatures

Through an extensive online literature search, we screened 197 representative TME-related signatures from diverse resources. Among them, 68 signatures come from the work of Wolf et al. (18), 25 signatures were from the work of Bindea et al. (19), 24 signatures were obtained from Miao et al.'s work results (20) and 17 signatures were obtained from the Import database (21). In addition, it also includes some marker genes of immune cells, such as marker genes of 22 immune cells in CIBERSORT (22), marker genes of 10 immune cells in MCP-Counter (23), marker genes of 10 immune cells in the Imsig database (24), and 20 signatures of immune cells recognized by TITR et al. (25). Finally, we also included the marker genes of exhausted $CD8^+$T cells (26). More detailed information is listed in the Supplementary Tables S1, S2.

Differential expression analysis and enrichment analysis

The differential expression analysis of the data is performed by the R package "limma". In this study, the threshold value is |log2FC| >1 and FDR<0.05.

We performed a single sample gene set enrichment analysis (ssGSEA) based on the gsva function to assess the infiltration level of signatures in each sample. The normalized enrichment scores (NESs) generated by ssGSEA are regarded as the infiltration level of signatures.

The enrichment analysis of GO and KEGG (27) is achieved by the R package "clusterProfiler". Meanwhile, we also used KEGG, gendoo, gene2pubmed and Reactome databases for gene set enrichment analysis (GSEA).

Construction of TME related signature score model

We used the discovery cohort for ssGSEA to calculate the NESs. Then, the NESs was used to construct a univariate Cox proportional hazard model for 197 signatures. And 129 signatures were determined significantly related to the OS (P<0.05).

To screen the most relevant signatures for CRC prognosis in the discovery cohort, the R package "glmnet" were used to construct the LASSO-Cox regression model for 129 signatures. 23 signatures with nonzero coefficients were included in the study, which is the best λ value generated by 10-fold cross validation.

Finally, the hazard ratio (HR) generated by the univariate Cox proportional hazard model was multiplied with the NESs of 23 signatures to construct the TME-related signature score (TMERSS). The calculation formula is as follows:

$$TMERSS = \sum_{i=1}^{n} log(HRi) * NESi$$

HR_i is the HR of the i^{th} TME related signature, and NES_i is the NES of the i^{th} TME related signature, n=23.

Calculating the proportion of immune cells and cell states

We quantified the proportion of immune cells in samples by CIBERSORT, MCP-Counter, xCell, and quanTIseq. In order to have a more comprehensive understanding of the state and functional patterns of different immune cells, we based on EcoTyper (https://ecotyper.stanford.edu/) calculating dominant cell states in each sample and the cell states abundance.

NTP analysis and filtering of signatures

The NTP classification tool (28) is used to calculate the classification of each sample in a specific signature. The signature list of CRC pathologic phenotypes and drug-related genes obtained from previous studies is as follows: intestinal stem cell signature (29), colon crypt signature (30), serrated CRC signature (31), EMT signature (32), FOLFIRI response signature (33), FOLFOX response signature (34) and VEFG/EGFRi signatures (35) described by Schutte et al., including Avastin, Cetuximab, Afatinib, Sapitinib, Gefitinib and Vandetanib.

Cell lines and qRT-PCR

Human CRC 5-FU sensitive/resistant cell line HCT8/HCT8-5FU and Cetuximab sensitive/resistant cell line Caco2/Caco2-CTX were purchased from Shanghai Meixuan Company (Shanghai, China) and cultured according to previous reports (36).

According to the manufacturer's instructions, total RNA was extracted and reverse transcribed using TRIzol reagents (Invitrogen, Carlsbad, CA, USA) and cDNA reverse transcription kits (Applied Biosystems, Foster City, CA). SYBR Green reagent (Thermo Fisher Scientific, Waltham, MA) was used for qRT-PCR experiments. With β-action is an internal parameter that is passed through $2^{-\Delta\Delta CT}$ method calculate the relative expression of the target gene. The primer sequence information is shown in Supplementary Table S3.

Western blot and CCK-8 assay

Western blot analysis was performed to determine the protein expression levels of LAMB1, APOC1, and AREG. The protein was extracted by SDS-PAGE and transferred to the PVDF membrane. They were incubated overnight with anti LAMB1 (1:1000, Cell Signaling Technology, 4723S), APOC1 (1:1000, Cell Signaling Technology, 3957S), AREG (1:1000, Cell Signaling Technology, 8751), and GAPDH (ZSGB-Bio, TA-8) primary antibodies at 4°C. After incubation with horseradish peroxidase linked secondary

antibodies for 2 hours, ECL (Beyotime, China) was used to visualize the signal.

Cells were implanted in 96 well microplates and administered 10 μg/ml of 5-FU, 200 μg/ml Cetuximab intervention for 24, 48, or 72 hours. Add 10 μl of CCK-8 solution (Dojindo) to each well, incubate at 37°C for 2 hours, and measure the OD value at 450 nm.

Statistical analysis

We used the R package "survminer" to calculate the optimal cut-off value. Meanwhile, Kaplan-Meier survival curves of patients with different subtypes were plotted based on R package "survminer" and "Survival". We divided patients into four consensus molecular subtypes (CMS) by using the R package "CMScaller".

In this study, all statistical analyses were conducted based on the R programming language. All statistical tests are two-sided, and P< 0.05 is considered statistically significant.

Results

Establishment of a scoring model based on TME related signatures

The design of this study is exhibited in Figure 1. Based on TME-related signatures, we conducted ssGSEA on all samples to calculate NESs. After initial screening, 192 signatures were obtained that were present in all cohorts. First, univariate Cox proportional hazard regression analysis was conducted on 192 signatures in the discovery cohort. We found that 129 signatures were significantly related to the OS of patients (P<0.05). Subsequently, LASSO-Cox regression models were used to screen for signatures highly associated with outcomes. In this model, lambda.1se=0.06028869 (Figures 2A, B), and the results show that the coefficients of 23 variables are nonzero. The relationship between infiltration level and survival of 23 signatures is shown in the forest (Figure 2C). By calculating the correlation coefficients among 23 signatures (Figure 2D), we found that there are mainly three types of relationships among signatures. Namely, negative correlation (Memory_B_cell, Proliferation_ImSig, LYMPHS_PCA and Translation_ImSig), positive correlation (IR7_score, Troester_WoundSig, Antigen_Processing_and_Presentation, Activated_dendertric_cell, DAP12_data, and Th1_cell) and weak correlation (MHC_I, ICR_INHIB_SCORE, STAT1, Monocyte, and Interleukins_Receptor). The results of the testing cohorts further confirmed the relationships among 23 signatures (Supplementary Figures 1A-C). Finally, based on the HRs of 23 signatures and their infiltration levels in each patient, we constructed the TMERSS model.

To analyze the transcriptome and immunology heterogeneity of patients, we calculated the optimal cut-off value based on TMERSS values, divided patients into high and low TMERSS subtypes, and compared the heterogeneity of 23 signatures of immune infiltration levels between the two subtypes. The results showed that there was no significant difference in immune infiltration levels between the two subtypes (Figure 2E; Supplementary Figure 1D–F).

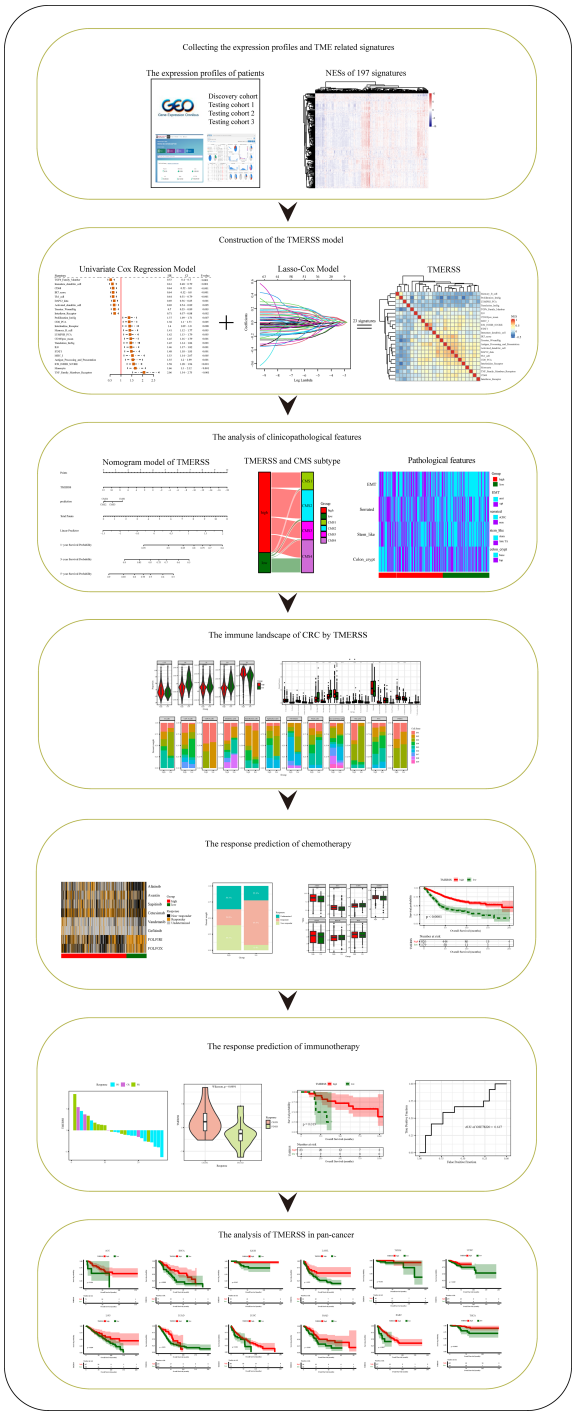

FIGURE 1
Schematic diagram of the study design. *p-value < 0.05, **p-value < 0.01, ***p-value < 0.001, ****p-value < 0.0001.

Furthermore, we conducted an enrichment analysis of 23 signature genes to determine their biological functions. As expected, the enrichment analysis results of these genes are closely related to TME (Figures 2F-H). For example, T–helper 17 type immune response and immune receiver activity. The KEGG

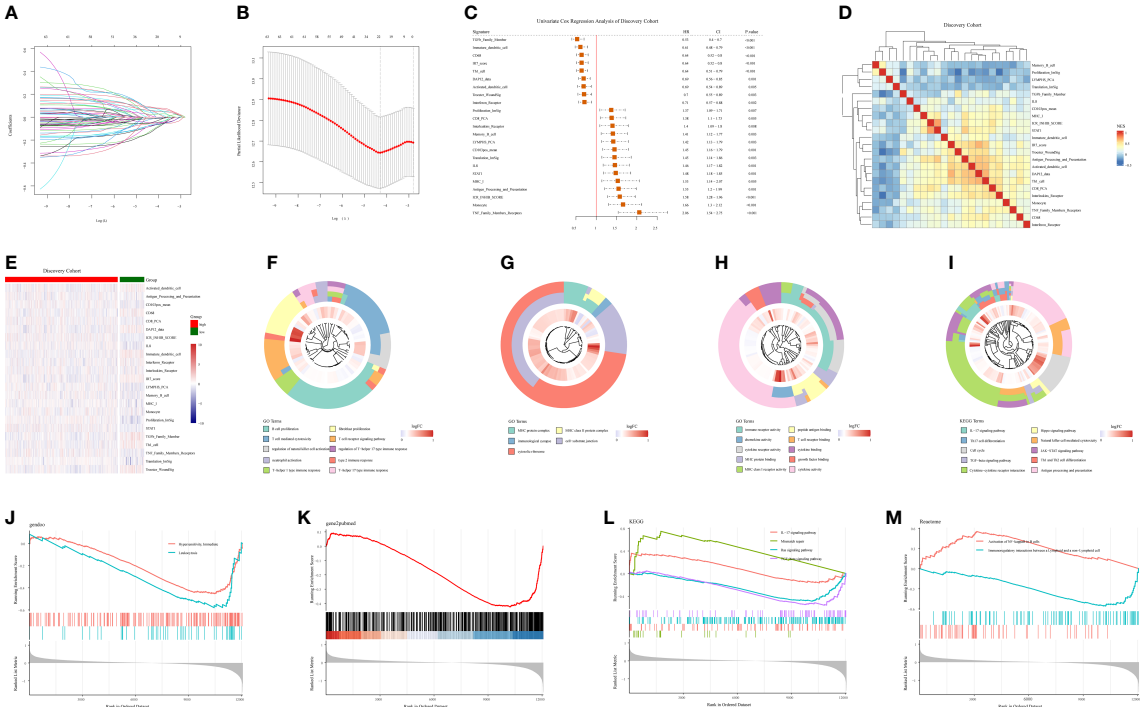

FIGURE 2
Building the TMERSS model by the discovery cohort. **(A)** LASSO coefficient distribution of 129 signatures; **(B)** LASSO regression model showed partial likelihood deviation in 10-fold across validation; **(C)** The forest of 23 signatures; **(D)** The heatmap of spearman's correlation between 23 signatures; **(E)** The heatmap according to NESs of 23 signatures; **(F–H)** Visualization of 10 terms in BP, CC and MF, respectively; **(I)** 10 KEGG pathways of differentially expressed genes in distinct TMERSS subtypes; **(J–M)** The databases gendoo, gene2pubmed, KEGG and Reactome were used for GSEA of TMERSS model related genes, and the terms associated with TMERSS was described.

pathway is enriched to immune and oncogenic related pathways, such as natural killer cell mediated cytotoxicity and JAK–STAT signaling pathway (Figure 2I). We also performed GSEA on the gene expression data of two subtypes of patients based on KEGG, gendoo, gene2pubmed, and Reactome databases (Figures 2J–M).

TMERSS is associated with clinicopathological features of colorectal cancer

We further analyzed the relationship between TMERSS and clinicopathological features in four cohorts. A nomogram model containing information about the TMERSS and CMS subtypes was constructed by the discovery cohort (Figure 3A). Compared with CMS subtypes, it was evident that TMERSS contributes most of the risk points. Based on nomogram calibration curves, we used TMERSS to predict the 1, 3, and 5-year survival probabilities of patients. The calibration curve of 1-year survival probability cannot perfectly fit the ideal curve (Figure 3B), while calibration curves of 3-year and 5-year survival probability can well predict the survival probability of patients (Figures 3C, D). Similarly, the decision curve analysis showed that the nomogram was poor at predicting 1-year survival probability because of its low clinical net benefit (Figure 3E); Because of the high clinical net benefit in the 3-year and 5-year decision curves, the nomogram can well predict the 3-year and 5-year survival probability (Figures 3F, G). Overall, these observations indicated that the nomogram of TMERSS proved well discrimination and calibration capabilities.

In 2015, Sabine et al. divided CRC into CMS1-CMS4 subtypes and analyzed the relationship between each subtype and the prognosis of patients (37). Here, by comparing the relationship between distinct TMERSS and CMS subtypes in the discovery cohort, we found that high TMERSS subtypes are mainly associated with CMS2, while low TMERSS subtypes are associated with CMS4 (Figures 3H, I). In testing cohort 1, the high TMERSS subtype was evenly distributed across CMS subtypes, while the low TMERSS subtype was strongly correlated with CMS4. Of course, the results of testing cohorts 2 and 3 were similar to the discovery cohort (Supplementary Figures 2A, B). It is well known that among CMS subtypes, CMS4 exhibits poorer OS, while CMS2 exhibits longer OS (37). The Kaplan-Meier survival curve of the study confirmed that the survival probability of the high TMERSS subtype was higher than that of the low TMERSS subtype (Figure 3H; Supplementary Figure 2C), which was consistent with the survival probability of patients among CMS subtypes.

We used the previously reported gene signatures to identify the cellular and precursor origins of TMERSS subtypes based on the NTP algorithm. Applying the intestinal stem cell signature and colon crypt signature to the expression data of four cohorts (Figure 3I; Supplementary Figure 2D), we found that low TMERSS subtype significantly enriched the stem-like and colon

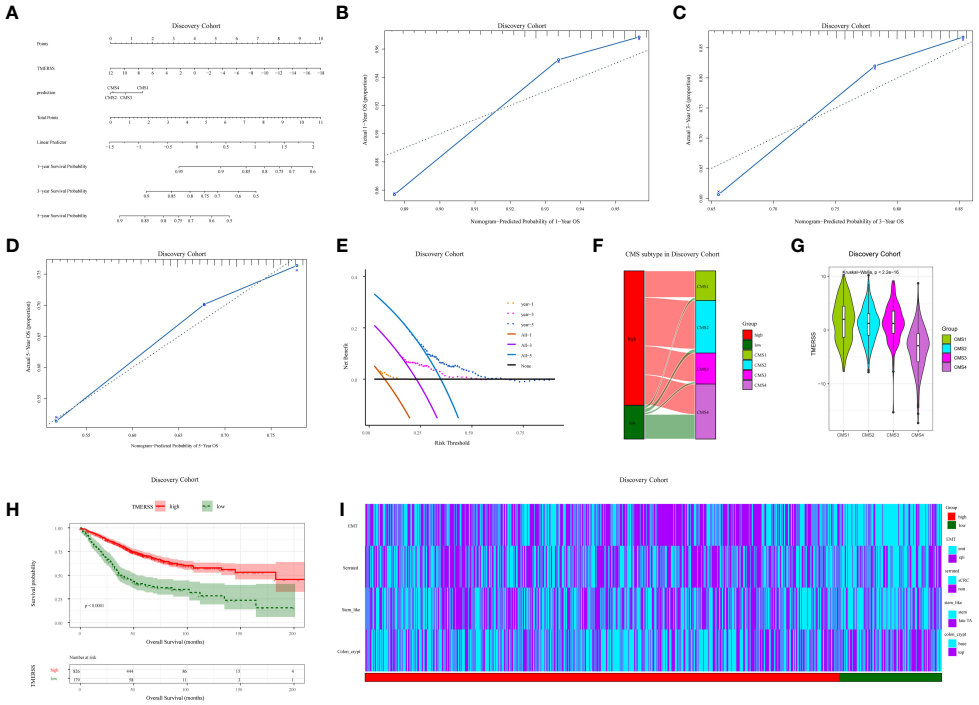

FIGURE 3
Correlation analysis of clinicopathological factors in the discovery cohort. **(A)** Nomogram, containing TMERSS and CMS; **(B-D)** Observing the consistency between the predicted 1, 3 and 5-year survival probability and the actual survival probability according to calibration curves. The predicted survival probability of nomogram is displayed on the x-axis, and the actual survival probability is displayed on the y-axis. The ideal curve of nomogram is represented by a dotted line along the 45-degree angle; **(E)** Analysis of decision curves for 1, 3, and 5-year, with black lines indicating assuming no patient dies within 1, 3, and 5-years; **(F)** Sankey of TMERSS and CMS subtypes; **(G)** The violin shows the distribution of TMERSS values of different CMS; **(H)** Kaplan-Meier survival curve according to the overall survival of TMERSS subtypes; **(I)** The heatmap of pathological factors of TMERSS subtypes based on published gene signatures.

top crypt phenotype. Considering that epithelial-mesenchymal transition (EMT) plays a crucial role in the development and progression of CRC (38), we used the EMT signature for analysis. The results showed that the low TMERSS subtype significantly enriched the "emt" phenotype, while the high TMERSS subtype more expressed the epi phenotype.

Heterogeneity of tumor immune response between TMERSS subtypes

We have constructed a TMERSS model based on 23 signatures. Although the infiltration level of 23 signatures has no apparent difference between TMERSS subtypes (Figure 2E; Supplementary Figures 1D–F), a more systematic characterization and comparison of the heterogeneity of immune responses in their classified samples was still needed. To this end, we summarized the characteristic divergence of TMERSS subtypes from the three aspects of antitumor immune activity, an abundance of tumor-infiltrating immune cells, and functional states of immune cells, and deepened the understanding of CRC classified based on the TMERSS model.

In combination with the characterization of the immune activity of CRC, we observed the differences between distinct TMERSS subtypes from the level of immune response activity. First, the variation in immune microenvironments of TMERSS subtypes is reflected in the overall level of immune infiltration. We calculated the immune score and stromal score for TME based on ESTIMATE. The results showed that the low TMERSS subtype had the higher immune score and stromal score, but tumor purity was lower than that of the high TMERSS subtype (Figure 4A, Supplementary Figure 3A). Simultaneously, there was significant variation in the antitumor immune activity of TMERSS subtypes, with high TMERSS subtype having a higher cytolytic activity (CYT).

Then, four deconvolution tools were used to analyze differences in the abundance of tumor-infiltrating immune cells. We observed that antitumor immune cells are highly expressed in high TMERSS subtypes, such as NK cells, cytotoxic T cells, $CD8^+$T cells, etc. (Figures 4B–E; Supplementary Figures 3B–E). Conversely, tumor-promoting immune cells are highly expressed in low TMERSS subtypes, such as cancer-associated fibroblasts, M2 macrophages, dendritic cells, and regulatory T cells.

To have a more comprehensive understanding of the state and functional pattern distinction of cells in different TMERSS subtypes, we determined the dominant cell states and cell state abundance in each sample based on the EcoTyper algorithm and carried out a comparative analysis. In the machine learning framework, EcoTyper, each immune cell is considered to have multiple cell states. Such as $CD8^+$T cells have 3 cell states (Naïve/central memory

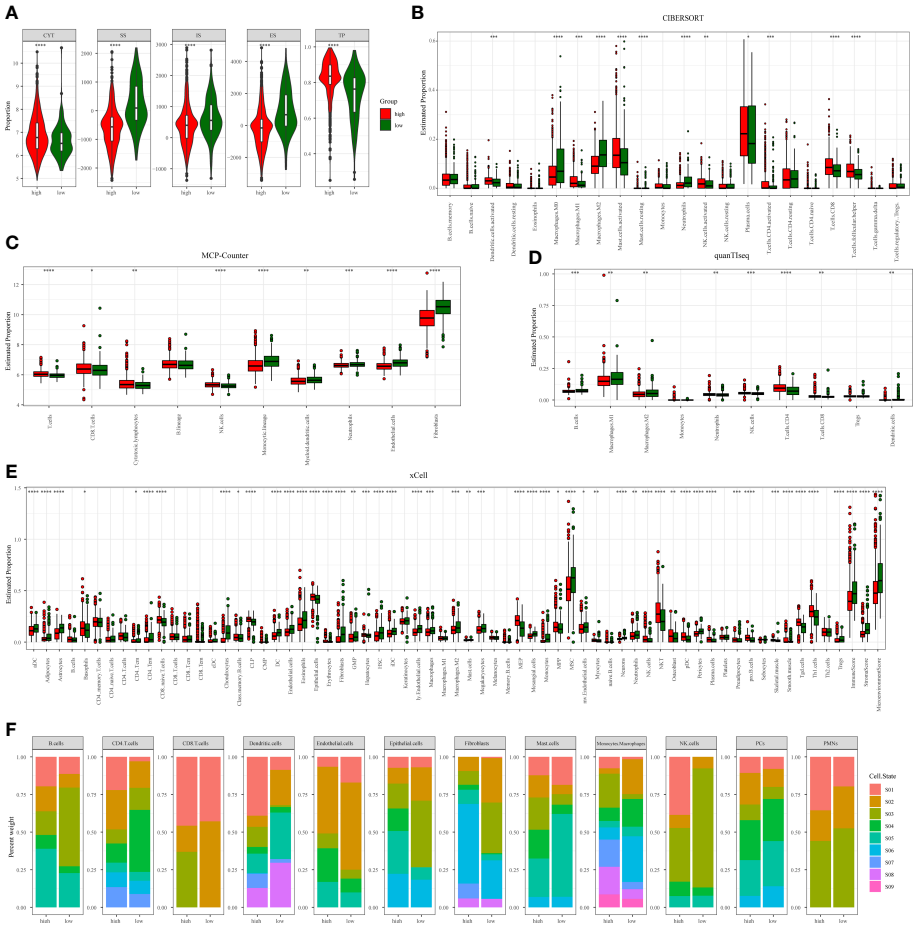

FIGURE 4
Immunological heterogeneity of TMERSS subtypes in the discovery cohort. **(A)** The differences of CYT, stromal score, immune score, ESTIMATE score and tumor purity among TMERSS subtypes; **(B-E)** Based on CIBERSORT, MCP-Counter, quanTIseq and xCell, the proportion of immune cells between high and low TMERSS subtypes was estimated. ns ≥ 0.05, *< 0.05, **< 0.01, ***< 0.001 and ****< 0.0001; **(F)** Distribution of immune cell states in different TMERSS subtypes.

(S01), Late-stage differentiated effector (S02), and Exhausted/effector memory (S03)), epithelial cells have 6 cell states (Basal-like (S01), Normal-enriched (S02), Pro-angiogenic (S03), Pro-inflammatory (S04), Unknown (S05), and Metabolic (S06)), mast cells have 6 cell states (Normal-enriched (S01), Normal-enriched (S02), Unknown (S03), Classical (S04), Unknown (S05), and Activated (S06)), dendritic cells have 8 cell states (Myeloid cDC1 (S01), Myeloid cDC2-B (Inflammatory) (S02), Mature immunogenic (S03), Unknown (S04), Mature (normal-enriched) (S05), Langerhans-like (S06), Migratory activated (S07), and Unknown (S08)) and NK cells have 5 cell states (Classical (S01), Normal-enriched (S02), Unknown (S03), Unknown (S04), and Unknown (S05)). The different cell states of more immune cells can be found in Supplementary Table S4. We observed significant differences in the proportional distribution of cell states between TMERSS subtypes (Figure 4F; Supplementary Figure 3F). Some cell states were dominant in the high TMERSS subtype with high immune activity (the proportion is significantly highest), while they are significantly reduced or almost absent in low TMERSS subtype (the proportion is almost 0). For example, the relative proportion of $CD8^+$T cells in the Exhausted/effector memory (S03) state, epithelial cells in the Pro-inflammatory (S04) state, Mast cells in the Classical (S04) state, dendritic cells in the Myeloid cDC1 (S01) state, and NK cells in the Classical (S01) state in low TMERSS subtype is almost 0.

These results indicated that there is heterogeneity of tumor immune response between TMERSS subtypes, and high TMERSS subtype show higher antitumor immune activity, abundances of antitumor immune cell, and antitumor immune cell states. This may explain the longer OS of high TMERSS subtype.

TMERSS model has a potential function to evaluate the chemotherapy response

Chemotherapy plays an indispensable role in the treatment of CRC. In order to make the TMERSS model applicable to the clinic, we analyzed differences in response to chemotherapy drugs in CRC between TMERSS subtypes. Based on the NTP algorithm, we applied drug-related signatures to the gene expression profile of four cohorts to predict the response of patients to eight chemotherapy regimens (Figure 5A; Supplementary Figures 4A–

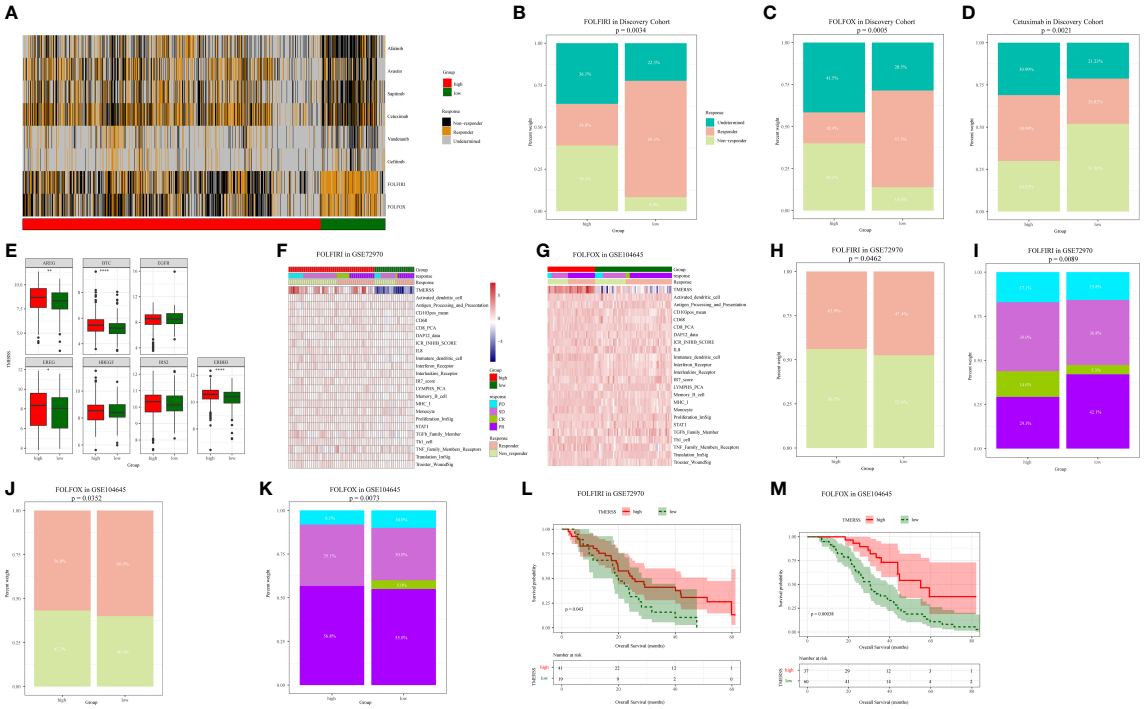

FIGURE 5
Correlation analysis between TMERSS subtypes and chemotherapy. **(A)** The heatmap of the correlation between the response of single CRC patient to FOLFIRI, FOLFOX and EGFR inhibitors, and the samples with FDR<0.2 were considered significant; **(B-D)** The histogram shows the number of clinical responses of high and low TMERSS subtypes to FOLFIRI, FOLFOX and Cetuximab. Chi-square test p-value differences are shown; **(E)** Boxplot showed differences in the expression of Cetuximab response-related genes in high and low TMERSS subtypes; **(F)** The heatmap of 23 signatures in GSE72970 cohort; **(G)** The heatmap of 23 signatures in GSE104645 cohort; **(H-I)** The histogram shows the number of clinical responses of high and low TMERSS subtypes to FOLFIRI in GSE72970 cohort. Chi-square test p-value differences are shown; **(J-K)** The histogram shows the number of clinical responses of high and low TMERSS subtypes to FOLFOX in GSE104645 cohort. Chi-square test p-value differences are shown; **(L-M)** Kaplan-Meier survival curve based on OS of TMERSS subtypes in GSE72970 and GSE104645 cohort. *p-value < 0.05, **p-value < 0.01, ***p-value < 0.001, ****p-value < 0.0001.

C). In the discovery cohort, the response rates of low TMERSS subtype to FOLFIRI, FOLFOX, and Cetuximab regimens were 69.3%, 57.5%, and 26.82% respectively (Figures 5B–D); Contemporary, the response rates of high TMERSS subtype to FOLFIRI, FOLFOX and Cetuximab regimens were 24.8%, 18.4%, and 38.98% respectively. It is obvious that the low TMERSS subtype has a higher response rate to FOLFIRI, and is more resistant to Cetuximab; However, the response rate of the high TMERSS subtype to FOLFIRI and FOLFOX regimen was low, and it was sensitive to Cetuximab. Except that the response rates of low TMERSS subtype in testing cohort 1 to the FOLFIRI were low (Supplementary Figure 4D), the analysis results in other testing cohorts are similar to those in the discovery cohort (Supplementary Figures 4D–F). To further analyze the reasons for the differences in the response of TMERSS subtypes to different chemotherapy regimens, we have collected FOLFIRI (33), FOLFOX (34), and Cetuximab (35) sensitive related genes in previous literature, and compared the expression of these genes in different TMERSS subtypes. Compared to the high TMERSS subtype, FOLFIRI, and FOLFOX sensitive related genes are highly expressed in the low TMERSS subtype (Supplementary Figures 5A, B). The Cetuximab sensitive related genes are highly expressed in the high TMERSS subtype (Figure 5E). In addition, we analyzed the expression of related genes in 5-FU sensitive/resistant cell lines HCT8/HCT8-5FU and Cetuximab sensitive/resistant cell lines Caco2/Caco2-CTX. Supplementary Figures 5C–E further confirmed our analysis results. After overexpression of LAMB1, APOC1, or AREG in HCT8-5FU and Caco2-CTX cells, we found that HCT8-5FU and Caco2-CTX cells restored their sensitivity to 5-FU and Cetuximab, respectively (Supplementary Figures 5F, G). Moreover, we found that overexpression of LAMB1 or APOC1 can reduce the resistance of HCT8-5FU; Overexpression of AREG can reduce the resistance of Caco2-CTX (Supplementary Figures 5H–I). Based on the above results, we speculate that the difference in the expression of chemotherapy-related genes in different TMERSS subtypes may explain to some extent the difference in response between TMERSS subtypes to distinct chemotherapy regimens.

In addition, we analyzed the responses of patients to FOLFIRI and FOLFOX based on datasets GSE72970 and GSE104645. We first analyzed the relationship between infiltration levels of 23 signatures and drug response in the TMERSS model. However, the infiltration level of 23 signatures was not significantly correlated with responses of FOLFOX or FOLFIRI (Figures 5F, G). Then, we explored whether the TMERSS model based on the datasets GSE72970 and GSE104645 was related to drug response. In GSE72970, the response rates of high and low TMERSS subtypes to FOLFIRI were 43.9% and 47.4%, respectively. Compared with the low TMERSS subtype, the high TMERSS subtype had a lower

proportion of drug resistance to FOLFIRI (Figures 5H, I). Similarly, in GSE104645, the response rates to FOLFIRI were 56.8% for the high TMERSS subtype and 60.0% for the low TMERSS subtype, and the low TMERSS subtype was more sensitive to FOLFOX (Figures 5J, K). Finally, the relationship between TMERSS subtypes and outcomes was clarified. As expected, the OS of the low TMERSS subtype is shorter (Figures 5L, M).

In general, these observations demonstrated that TMERSS model may be used as a potential tool to evaluate the response rate of CRC to chemotherapy. Concurrently, TMERSS subtypes can provide a reference for clinicians to use drugs. The low TMERSS subtype is more suitable for FOLFOX or FOLFIRI, while patients with high TMERSS are more sensitive to Cetuximab.

Immunotherapy benefits were positively correlated with TMERSS values

As a novel modality to remedy cancer, immunotherapy has been widely concerned because of the high response rates of cancer patients to immunotherapy. In this research, we wanted to investigate whether the TMERSS model can predict the benefit of immunotherapy in patients. However, after an extensive literature review and extensive literature search, we did not find suitable datasets for CRC immunotherapy, so we explored the relationship between immunotherapy responses and the TMERSS model in the melanoma and uroepithelial carcinoma immunotherapy datasets (GSE78220, GSE91061, and IMvigor210). Kaplan-Meier survival curves showed that the high TMERSS subtype had a better prognosis than the low TMERSS subtype (Figure 6A). Across the three immunotherapy datasets, we found that the high TMERSS subtype was more effective in responding to immunotherapy, with higher response rates (Figures 6B, C). Compared with progressive-disease (PD)/stable-disease (SD), the violin further confirmed that TMERSS values significantly increased the complete-response (CR)/partial-response (PR) of CRC (Figure 6D).

The TMERSS values in three datasets were also evaluated by ROC curves analysis to estimate their predictive potential for immunotherapy benefits. The areas under ROC curves of GSE78220, IMvigor210, and GSE91061 datasets were 0.62, 0.57, and 0.55, respectively (Figure 6E), suggesting that the TMERSS model has good predictive efficacy for immunotherapy benefit.

Analysis of TMERSS model in pan-cancer

We applied the TMERSS model to other cancers to determine whether it has universal applicability in pan-cancer. Firstly, TPM data of 33 cancers were downloaded from TCGA and TMERSS model was constructed. Then, optimal cut-off points were calculated based on the TMERSS values, and the patients were divided into high and low TMERSS subtypes. Finally, Kaplan-Meier survival curves showed that the prognosis of the high TMERSS subtype was better than that of the low TMERSS subtype in 12 cancers (Figure 7). The results confirmed that the TMERSS model may be universally applicable in these cancers.

Discussion

CRC, like other malignant tumors, is highly heterogeneous (39). The complex interaction between malignant tumor cells and TME contributes greatly to the development and progression of CRC (40). Effective recognition of the distinction of diver immune

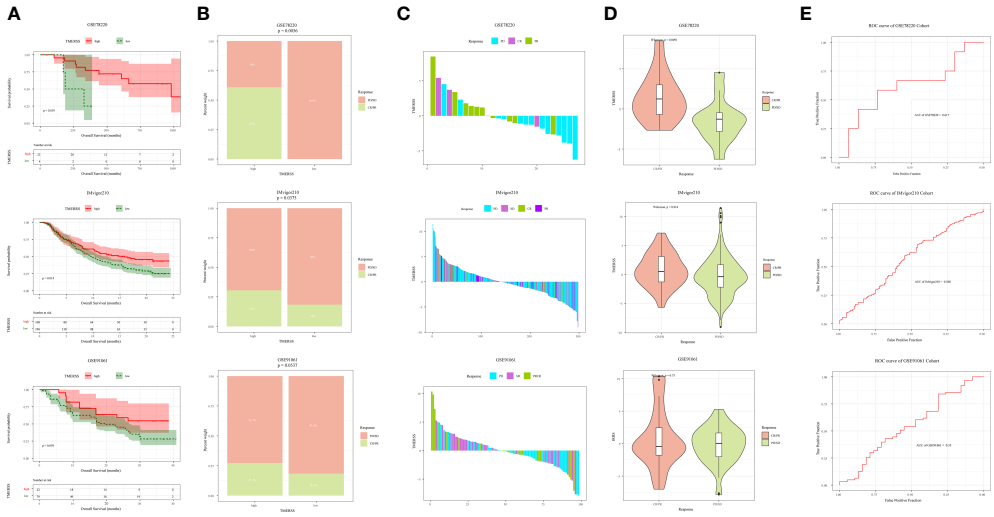

FIGURE 6
Correlation analysis between TMERSS subtypes and immunotherapy. **(A)** Kaplan-Meier curve according to the OS of TMERSS subtypes in immunotherapy cohort; **(B)** The histogram shows the number of immunotherapeutic responses in the high and low TMERSS subtypes of the immunotherapy cohort. Chi-square test p-value differences are shown. **(C)** The waterfall diagram shows the distribution of patients with different immunotherapeutic response in the immunotherapy cohort; **(D)** The boxplot of TMERSS distribution of patients with different immunotherapy response in immunotherapy cohort; **(E)** ROC curve for predicting response in immunotherapy cohort.

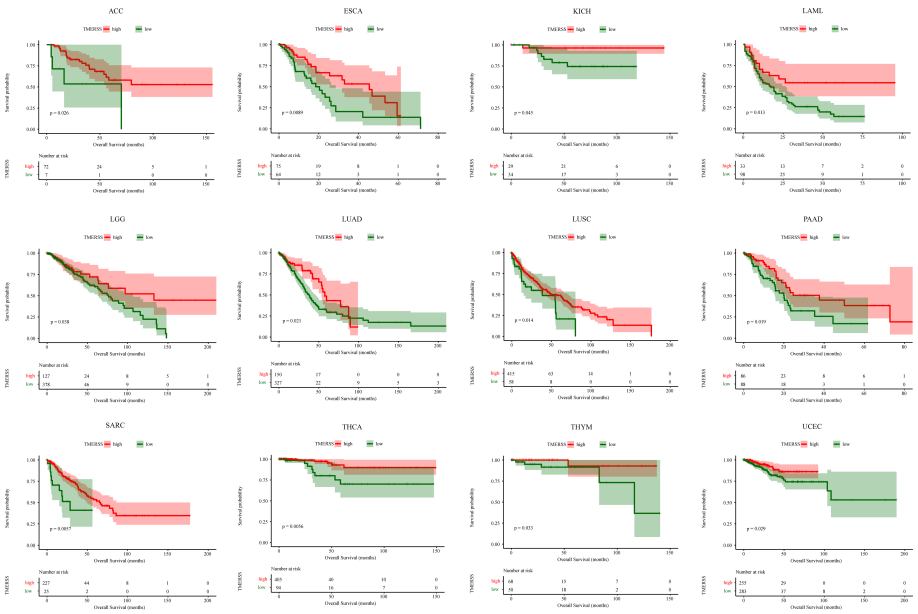

FIGURE 7
The application of the TMERSS model in pan-cancer. The Kaplan-Meier survival curves of TMERSS subtypes in 12 cancers, which includes ACC (Adrenocortical Carcinoma), ESCA (Esophageal Carcinoma), KICH (Kidney Chromophobe), LAML (Acute Myeloid Leukemia), LGG (Brain Lower Grade Glioma), LUAD (Lung Adenocarcinoma), LUSC (Lung Squamous Cell Carcinoma), PAAD (Pancreatic Adenocarcinoma), SARC (Sarcoma), THCA (Thyroid Carcinoma), THYM (Thymoma) and UCEC (Uterine Corpus Endometrial Carcinoma).

components in TME may help explain the heterogeneity of CRC. ESMO guideline recommends FOLFIRI and FOLFOX as first-line chemotherapies for metastatic CRC. Although FOLFIRI or FOLFOX can significantly prolong the median OS, nearly 50% of patients cannot benefit from it (41). Therefore, screening patients with potential responses to FOLFOX and FOLFIRI is an urgent priority.

We performed univariate Cox regression analysis on 197 signatures to identify those that are significant for prognosis. Then the optimal 23 variates were selected by the LASSO-Cox regression model, and the TMERSS model was constructed based on 23 signatures. Further analysis showed that the molecular subtype based on the optimal cut-off point could effectively distinguish TME and drug sensitivity.

Firstly, relationships between TMERSS subtypes and clinicopathological factors were analyzed. Of the two TMERSS subtypes, the high TMERSS subtype has a longer OS. The association analysis between TMERSS and CMS subtypes revealed that the majority of low TMERSS subtypes were included in CMS4, and the low TMERSS subtype had similar results with CMS4, that is, the OS was shorter (37); The high TMERSS subtype contains mainly CMS2, and the longer OS of high TMERSS subtype is consistent with the longer OS of CMS2 (37). In addition, the previously reported association analysis between gene signatures and TMERSS subtypes also revealed the potential biological characteristics behind TMERSS subtypes. For example, serrated precursor tumors were significantly associated with the low TMERSS subtype. In the low TMERSS subtype, the stem-like and emt phenotypes were significantly enriched.

The heterogeneity of tumor immune response determines differences in prognosis in different patients, and infiltrating immune cells play a vital role in tumor immune response. NK cells, $CD8^{+}$T cells, and cytotoxic T cells (42) are considered as main antitumor immune cells, while fibroblasts and regulatory T cells promote the occurrence and development of tumors. In our study, the high TMERSS subtype enriched antitumor immune cells, which is consistent with the improvement of prognosis of antitumor immune cells; In contrast, the low TMERSS subtype has a higher abundance of immunosuppressive cells. Our results show that the OS of the low TMERSS subtype is shorter than that of the high TMERSS subtype. Further cell states analysis also found that the immune cell states in the high TMERSS subtype mostly showed antitumor immune activity, while the low TMERSS subtype lacked such cells.

The high heterogeneity of CRC also affects the sensitivity of chemotherapy. Studies have shown that the stem-like phenotype of CRC has a high response rate to FOLFIRI (43), which is consistent with our results, low TMERSS subtypes enrich the stem-like phenotype and are sensitive to FOLFIRI. The response rates of FOLFOX were similar to that of FOLFIRI and were resistant to the high TMERSS subtype. The low TMERSS subtype has shorter OS but is more sensitive to FOLFOX or FOLFIRI, suggesting that the low TMERSS subtype is a potential response to FOLFOX or FOLFIRI and that FOLFOX or FOLFIRI has the potential to improve the prognosis of low TMERSS subtype. In our results, compared with the low TMERSS subtype, the high TMERSS subtype has a higher response rate to Cetuximab, which may be related to the higher expression of Cetuximab responsive-related genes in high TMERSS subtype.

In addition, there is growing evidence that patients with microsatellite instability are sensitive to immune checkpoint inhibitors, and CMS1 was rich in a higher proportion of microsatellite instability (37). In our analysis, CMS1 was mainly associated with a high TMERSS subtype. Based on datasets GSE78220, GSE91061, and IMvigor210, we analyzed the association of TMERSS subtypes with immune response and prognosis of patients. Unlike the low TMERSS subtype, which has high response rates to FOLFOX or FOLFIRI, TMERSS values significantly increased the sensitivity of patients to immune checkpoint inhibitors in immunotherapy cohorts. In short, high TMERSS subtypes are more sensitive to immunotherapy. We also observed that the OS of the high TMERSS subtype was longer than that of the low TMERSS subtype.

This study has several limitations worth acknowledging. First of all, the analysis is based on previously published data, which is a retrospective study, and more real data are needed for prospective analysis and verification; Secondly, due to the incomplete clinical information of data, more clinicopathological factors were not included in the study, such as TNM stage, age, sex, tumor pathological type, etc. Finally, we only divided patients into two subtypes according to the optimal cut-off value, and more classification algorithms need to be explored to further define and classify TMERSS subtypes.

Together, we constructed the TMERSS model by using public datasets and 197 signatures to define novo molecular subtypes. TMERSS subtypes have different effects on the prognosis of patients. Moreover, the TMERSS model reveals the efficiency of chemotherapy or immunotherapy to a certain extent and may be a potential tool for predicting the response of chemotherapy or immunotherapy. The high TMERSS subtype may be more suitable for Cetuximab treatment or immunotherapy, while the low TMERSS subtype may be more sensitive to FOLFIRI or FOLFOX regimens.

Data availability statement

The datasets presented in this study can be found in online repositories. The names of the repository/repositories and accession number(s) can be found in the article/Supplementary Material.

Ethics statement

All methods were carried out in accordance with relevant guidelines and regulations. Research involving human participants and human data, performed in accordance with the Declaration of Helsinki.

Author contributions

All authors contributed to the article and approved the submitted version. XJ and LY designed the project. XJ and SG performed administrative, technical, or material support. Jun Xiang performed statistical analysis. XJ wrote the manuscript. GW and LY revised the paper.

Funding

This work was supported by the National Nature Science Foundation of China (62276084), Central support for the reform and development of local colleges and universities (high-level talent project) (2020GSP05), and Heilongjiang Province Applied Technology Research and Development Plan Project (GA19C003).

Conflict of interest

The authors declare that the research was conducted in the absence of any commercial or financial relationships that could be construed as a potential conflict of interest.

Publisher's note

All claims expressed in this article are solely those of the authors and do not necessarily represent those of their affiliated organizations, or those of the publisher, the editors and the reviewers. Any product that may be evaluated in this article, or claim that may be made by its manufacturer, is not guaranteed or endorsed by the publisher.

Supplementary material

The Supplementary Material for this article can be found online at: https://www.frontiersin.org/articles/10.3389/fonc.2023.1123455/full#supplementary-material

References

1. Siegel RL, Miller KD, Fuchs HE, Jemal A. Cancer statistics, 2022. *CA Cancer J Clin* (2022) 72(1):7–33. doi: 10.3322/caac.21708

2. Sung H, Ferlay J, Siegel RL, Laversanne M, Soerjomataram I, Jemal A, et al. Global cancer statistics 2020: GLOBOCAN estimates of incidence and mortality worldwide for 36 cancers in 185 countries. *CA Cancer J Clin* (2021) 71(3):209–49. doi: 10.3322/caac.21660

3. Quasar Collaborative G, Gray R, Barnwell J, McConkey C, Hills RK, Williams NS, et al. Adjuvant chemotherapy versus observation in patients with colorectal cancer: a

randomised study. *Lancet* (2007) 370(9604):2020–9. doi: 10.1016/S0140-6736(07)61866-2

4. Van Cutsem E, Nordlinger B, Cervantes A, ESMO Guidelines Working Group. Advanced colorectal cancer: ESMO clinical practice guidelines for treatment. *Ann Oncol* (2010) 21 Suppl 5:v93–7. doi: 10.1093/annonc/mdq222

5. Vodenkova S, Buchler T, Cervena K, Veskrnova V, Vodicka P, Vymetalkova V, et al. 5-fluorouracil and other fluoropyrimidines in colorectal cancer: past, present and future. *Pharmacol Ther* (2020) 206:107447. doi: 10.1016/j.pharmthera.2019.107447

6. Benson A, Schrag D, Somerfield MR, Cohen AM, Figueredo AT, Flynn PJ, et al. American Society of clinical oncology recommendations on adjuvant chemotherapy for stage II colon cancer. *J Clin Oncol* (2004) 22(16):3408–19. doi: 10.1200/JCO.2004.05.063

7. Arthur JC, Perez-Chanona E, Mühlbauer M, Tomkovich S, Uronis JM, Fan TJ, et al. Intestinal inflammation targets cancer-inducing activity of the microbiota. *Science* (2012) 338(6103):120–3. doi: 10.1126/science.1224820

8. Khan S. Potential role of escherichia coli DNA mismatch repair proteins in colon cancer. *Crit Rev Oncol Hematol* (2015) 96(3):475–82. doi: 10.1016/j.critrevonc.2015.05.002

9. Khan S, Imran A, Khan AA, Abul Kalam M, Alshamsan A. Systems biology approaches for the prediction of possible role of chlamydia pneumoniae proteins in the etiology of lung cancer. *PloS One* (2016) 11(2):e0148530. doi: 10.1371/journal.pone.0148530

10. Khan S, Zakariah M, Rolfo C, Robrecht L, Palaniappan S. Prediction of mycoplasma hominis proteins targeting in mitochondria and cytoplasm of host cells and their implication in prostate cancer etiology. *Oncotarget* (2017) 8(19):30830–43. doi: 10.18632/oncotarget.8306

11. Khan S, Zakariah M, Palaniappan S. Computational prediction of mycoplasma hominis proteins targeting in nucleus of host cell and their implication in prostate cancer etiology. *Tumour Biol* (2016) 37(8):10805–13. doi: 10.1007/s13277-016-4970-9

12. Yue Y, Zhang Q, Sun Z. CX3CR1 acts as a protective biomarker in the tumor microenvironment of colorectal cancer. *Front Immunol* (2021) 12:758040. doi: 10.3389/fimmu.2021.758040

13. Hanahan D, Coussens LM. Accessories to the crime: functions of cells recruited to the tumor microenvironment. *Cancer Cell* (2012) 21(3):309–22. doi: 10.1016/j.ccr.2012.02.022

14. Chew V, Toh HC, Abastado JP. Immune microenvironment in tumor progression: characteristics and challenges for therapy. *J Oncol 2012* (2012) p:608406. doi: 10.1155/2012/608406

15. Pitt JM, Marabelle A, Eggermont A, Soria JC, Kroemer G, Zitvogel L, et al. Targeting the tumor microenvironment: removing obstruction to anticancer immune responses and immunotherapy. *Ann Oncol* (2016) 27(8):1482–92. doi: 10.1093/annonc/mdw168

16. Taube JM, Klein A, Brahmer JR, Xu H, Pan X, Kim JH, et al. Association of PD-1, PD-1 ligands, and other features of the tumor immune microenvironment with response to anti-PD-1 therapy. *Clin Cancer Res* (2014) 20(19):5064–74. doi: 10.1158/1078-0432.CCR-13-3271

17. Mariathasan S, Turley SJ, Nickles D, Castiglioni A, Yuen K, Wang Y, et al. TGFbeta attenuates tumour response to PD-L1 blockade by contributing to exclusion of T cells. *Nature* (2018) 554(7693):544–8. doi: 10.1038/nature25501

18. Wolf DM, Lenburg ME, Yau C, Boudreau A, van 't Veer LJ. Gene co-expression modules as clinically relevant hallmarks of breast cancer diversity. *PloS One* (2014) 9(2):e88309. doi: 10.1371/journal.pone.0088309

19. Bindea G, Mlecnik B, Tosolini M, Kirilovsky A, Waldner M, Obenauf AC, et al. Spatiotemporal dynamics of intratumoral immune cells reveal the immune landscape in human cancer. *Immunity* (2013) 39(4):782–95. doi: 10.1016/j.immuni.2013.10.003

20. Miao YR, Zhang Q, Lei Q, Luo M, Xie GY, Wang H, et al. ImmuCellAI: a unique method for comprehensive T-cell subsets abundance prediction and its application in cancer immunotherapy. *Adv Sci (Weinh)* (2020) 7(7):1902880. doi: 10.1002/advs.201902880

21. Bhattacharya S, Andorf S, Gomes L, Dunn P, Schaefer H, Pontius J, et al. ImmPort: disseminating data to the public for the future of immunology. *Immunol Res* (2014) 58(2-3):234–9. doi: 10.1007/s12026-014-8516-1

22. Newman AM, Liu CL, Green MR, Gentles AJ, Feng W, Xu Y, et al. Robust enumeration of cell subsets from tissue expression profiles. *Nat Methods* (2015) 12(5):453–7. doi: 10.1038/nmeth.3337

23. Becht E, Giraldo NA, Lacroix L, Buttard B, Elarouci N, Petitprez F, et al. Estimating the population abundance of tissue-infiltrating immune and stromal cell populations using gene expression. *Genome Biol* (2016) 17(1):218. doi: 10.1186/s13059-016-1070-5

24. Nirmal AJ, Regan T, Shih BB, Hume DA, Sims AH, Freeman TC, et al. Immune cell gene signatures for profiling the microenvironment of solid tumors. *Cancer Immunol Res* (2018) 6(11):1388–400. doi: 10.1158/2326-6066.CIR-18-0342

25. Magnuson AM, Kiner E, Ergun A, Park JS, Asinovski N, Ortiz-Lopez A, et al. Identification and validation of a tumor-infiltrating Treg transcriptional signature conserved across species and tumor types. *Proc Natl Acad Sci USA* (2018) 115(45):E10672–81. doi: 10.1073/pnas.1810580115

26. Zhao B, Wang Y, Wang Y, Dai C, Wang Y, Ma W, et al. Investigation of genetic determinants of glioma immune phenotype by integrative immunogenomic scale analysis. *Front Immunol* (2021) 12:557994. doi: 10.3389/fimmu.2021.557994

27. Kanehisa M, Sato Y. KEGG mapper for inferring cellular functions from protein sequences. *Protein Sci* (2020) 29(1):28–35. doi: 10.1002/pro.3711

28. Hoshida Y. Nearest template prediction: a single-sample-based flexible class prediction with confidence assessment. *PloS One* (2010) 5(11):e15543. doi: 10.1371/journal.pone.0015543

29. Merlos-Suarez A, Barriga FM, Jung P, Iglesias M, Céspedes MV, Rossell D, et al The intestinal stem cell signature identifies colorectal cancer stem cells and predicts disease relapse. *Cell Stem Cell* (2011) 8(5):511–24. doi: 10.1016/j.stem.2011.02.020

30. Kosinski C, Li VS, Chan AS, Zhang J, Ho C, Tsui WY, et al. Gene expression patterns of human colon tops and basal crypts and BMP antagonists as intestinal stem cell niche factors. *Proc Natl Acad Sci USA* (2007) 104(39):15418–23. doi: 10.1073/pnas.0707210104

31. Laiho P, Kokko A, Vanharanta S, Salovaara R, Sammalkorpi H, Järvinen H, et al. Serrated carcinomas form a subclass of colorectal cancer with distinct molecular basis. *Oncogene* (2007) 26(2):312–20. doi: 10.1038/sj.onc.1209778

32. Loboda A, Nebozhyn MV, Watters JW, Buser CA, Shaw PM, Huang PS, et al. EMT is the dominant program in human colon cancer. *BMC Med Genomics* (2011) 4:9. doi: 10.1186/1755-8794-4-9

33. Graudens E, Boulanger V, Mollard C, Mariage-Samson R, Barlet X, Grémy G, et al. Deciphering cellular states of innate tumor drug responses. *Genome Biol* (2006) 7(3):R19. doi: 10.1186/gb-2006-7-3-r19

34. Tong M, Risch T, Abdavi-Azar N, Boehnke K, Schumacher D, Keil M, et al. Identifying clinically relevant drug resistance genes in drug-induced resistant cancer cell lines and post-chemotherapy tissues. *Oncotarget* (2015) 6(38):41216–27. doi: 10.18632/oncotarget.5649

35. Schutte M, Risch T, Abdavi-Azar N, Boehnke K, Schumacher D, Keil M, et al. Molecular dissection of colorectal cancer in pre-clinical models identifies biomarkers predicting sensitivity to EGFR inhibitors. *Nat Commun* (2017) 8:14262. doi: 10.1038/ncomms14262

36. Hu H, Wang M, Guan X, Yuan Z, Liu Z, Zou C, et al. Loss of ABCB4 attenuates the caspase-dependent apoptosis regulating resistance to 5-fu in colorectal cancer. *Biosci Rep* (2018) 38(1):BSR20171428. doi: 10.1042/BSR20171428

37. Guinney J, Dienstmann R, Wang X, de Reyniès A, Schlicker A, Soneson C, et al. The consensus molecular subtypes of colorectal cancer. *Nat Med* (2015) 21(11):1350–6. doi: 10.1038/nm.3967

38. Heerboth S, Housman G, Leary M, Longacre M, Byler S, Lapinska K, et al. EMT and tumor metastasis. *Clin Transl Med* (2015) 4:6. doi: 10.1186/s40169-015-0048-3

39. Zhu X, Tian X, Ji L, Zhang X, Cao Y, Shen C, et al. A tumor microenvironment-specific gene expression signature predicts chemotherapy resistance in colorectal cancer patients. *NPJ Precis Oncol* (2021) 5(1):7. doi: 10.1038/s41698-021-00142-x

40. Zuo S, Wei M, Wang S, Dong J, Wei J, et al. Pan-cancer analysis of immune cell infiltration identifies a prognostic immune-cell characteristic score (ICCS) in lung adenocarcinoma. *Front Immunol* (2020) 11:1218. doi: 10.3389/fimmu.2020.01218

41. Goldberg RM. Therapy for metastatic colorectal cancer. *Oncologist* (2006) 11(9):981–7. doi: 10.1634/theoncologist.11-9-981

42. Denton AE, Roberts EW, Fearon DT. Stromal cells in the tumor microenvironment. *Adv Exp Med Biol 2018* (1060) p:99–114. doi: 10.1007/978-3-319-78127-3_6

43. Isella C, Terrasi A, Bellomo SE, Petti C, Galatola G, Muratore A, et al. Stromal contribution to the colorectal cancer transcriptome. *Nat Genet* (2015) 47(4):312–9. doi: 10.1038/ng.3224

frontiers | Frontiers in Immunology

TYPE Original Research
PUBLISHED 19 June 2023
DOI 10.3389/fimmu.2023.1160052

OPEN ACCESS

EDITED BY
Jorge Melendez-Zajgla,
National Institute of Genomic Medicine (INMEGEN), Mexico

REVIEWED BY
Robin Mjelle,
Norwegian University of Science and Technology, Norway
Lan Zhao,
Stanford University, United States

*CORRESPONDENCE
Feng Guo
guofeng27@gmail.com
Jiang Su
zhengmin1114@126.com

†These authors have contributed equally to this work and share first authorship

RECEIVED 06 February 2023
ACCEPTED 05 June 2023
PUBLISHED 19 June 2023

CITATION
Lu Y, Gu D, Zhao C, Sun Y, Li W, He L, Wang X, Kou Z, Su J and Guo F (2023) Genomic landscape and expression profile of consensus molecular subtype four of colorectal cancer.
Front. Immunol. 14:1160052.
doi: 10.3389/fimmu.2023.1160052

Genomic landscape and expression profile of consensus molecular subtype four of colorectal cancer

Yujie Lu[1†], Dingyi Gu[1†], Chenyi Zhao[1], Ying Sun[1], Wenjing Li[2], Lulu He[1], Xiaoyan Wang[1], Zhongyang Kou[3], Jiang Su[3*] and Feng Guo[1*]

[1]Department of Oncology, The Affiliated Suzhou Hospital of Nanjing Medical University, Suzhou Municipal Hospital, Gusu School, Nanjing Medical University, Suzhou, China, [2]Department of Clinical Laboratory, The Affiliated Suzhou Hospital of Nanjing Medical University, Suzhou Municipal Hospital, Gusu School, Nanjing Medical University, Suzhou, China, [3]Department of General Surgery, The Affiliated Suzhou Hospital of Nanjing Medical University, Suzhou Municipal Hospital, Gusu School, Nanjing Medical University, Suzhou, China

Background: Compared to other subtypes, the CMS4 subtype is associated with lacking of effective treatments and poorer survival rates.

Methods: A total of 24 patients with CRC were included in this study. DNA and RNA sequencing were performed to acquire somatic mutations and gene expression, respectively. MATH was used to quantify intratumoral heterogeneity. PPI and survival analyses were performed to identify hub DEGs. Reactome and KEGG analyses were performed to analyze the pathways of mutated or DEGs. Single-sample gene set enrichment analysis and Xcell were used to categorize the infiltration of immune cells.

Results: The CMS4 patients had a poorer PFS than CMS2/3. *CTNNB1* and *CCNE1* were common mutated genes in the CMS4 subtype, which were enriched in Wnt and cell cycle signaling pathways, respectively. The MATH score of CMS4 subtype was lower. *SLC17A6* was a hub DEG. M2 macrophages were more infiltrated in the tumor microenvironment of CMS4 subtype. The CMS4 subtype tended to have an immunosuppressive microenvironment.

Conclusion: This study suggested new perspectives for exploring therapeutic strategies for the CMS4 subtype CRC.

KEYWORDS

colorectal cancer, consensus molecular subtype, genomic mutations, gene expression, tumor immune microenvironment

Abbreviations: CMS, consensus molecular subtype; CRC, colorectal cancer; MATH, Mutant-allele tumor heterogeneity; PPI, Protein and protein network; KEGG, Kyoto Encyclopedia of Genes and Genomes; DEGs, differentially expressed genes; PFS, progression-free survival.

1 Introduction

According to the National Cancer Center of China, colorectal cancer (CRC) has the second highest incidence among all malignant tumors and is the fourth leading cause of cancer-associated mortality (1). CRC can be divided into different subtypes based on different standards. Tumor node metastasis (TNM) classification and Duke's classification are traditional classification models for CRC, according to infiltration depth of tumor and metastasis (2). TNM classification is applied predominantly to predict the prognosis of CRC patients (3), as well as to guide the choice of therapeutic schedule.

With the development of medical technology, it has entered into the stage of precise diagnosis and treatment. Genetic variation of different molecular, such as *KRAS*, *NRAS*, *BRAF*, *Her2* and MSI-H, has been applied to guide clinical treatment and prognosis. It has been proved that *KRAS*/*NRAS*/*BRAF* wild-type patients have a better prognosis than *KRAS*/*NRAS*/*BRAF* mutated ones. Bazan et al. compared 74 *KRAS* mutated patients with 86 *KRAS* wild-type and found that patients with codon 13 *KRAS* mutation were related to risk of relapse or death independently (4). Schirripa et al. found that compared to all wild-type patients, *RAS* mutation were related to shorter overall survival (5). *KRAS*/*NRAS*/*BRAF* wild-type patients had a better prognosis when treated with monoclonal antibodies to the epithelial growth factor receptor (*EGFR*) and chemotherapy than treated with chemotherapy only. While addition of Cetuximab to standard chemotherapy couldn't benefit *RAS* mutated patients (6, 7). What's more, part of patients with *BRAF V600E* mutation can benefit from combination therapy including *EGFR* and *BRAF* inhibitors (8).

The consensus molecular subtype (CMS) is a developed classification model defined by Guinney et al. in 2015 and is determined by transcriptomic analyses (9). Although the CMS system was originally developed to classify early-stage non-metastatic CRC, it was used to classify metastasis CRC (mCRC) patients in recent several clinical trials (10, 11). CMS can be classified into four subtypes according to the transcriptomics of CRC. Immunohistochemistry of five markers, including *ZEB1*, *FRMD6*, *KER*, *CDX2* and *HTR2B*, can also be used to identify CMS1-4 subtypes (12). Expression of *CDX2* is higher in epithelial-like tumor (CMS2/3), while expression of *HTR2B* and *FRMD6* is higher in mesenchymal-like tumor (CMS4). These five markers can be applied to differentiate mesenchymal from epithelial tumor (12). Suggested by the GALGB/SWOG 80405 trial, CMS2 is the most common subtype both in total and left-sided mCRC, while CMS1 is most common in right-sided mCRC (13).

Compared to the other three subtypes, the CMS4 subtype is revealed to possess high somatic copy number alterations, upregulation of genes related to epithelial mesenchymal transformation (EMT), activation of angiogenesis, transforming growth factor β (TGF-β) signaling and matrix remodeling pathways, notable stromal infiltration. In addition, the CMS4 subtype is also reported to show upregulation of integrin-β3, wound-like responses upregulation and a platelet activation signature (14). Importantly, the CMS4 subtype is confirmed to have poorer OS and relapse-free survival, and is associated with a higher risk of recurrence (15).

There are currently no effective therapies for the majority of mCRC patients, especially CMS4 patients. In the AGITG MAX trial, there is no significance in PFS can be found for the addition of bevacizumab to chemotherapy in CMS4 (16). Most mCRC patients with peritoneal metastases belong to the CMS4 subtype and show resistance to oxaliplatin (17). Compared to CMS2/3 patients treated with first-line chemotherapy, CMS4 patients can't benefit from the combination of bevacizumab with chemotherapy (18). Thus, the CMS4 subtype is generally considered to be related to therapy resistance (19). Few studies have investigated the genetic landscape and its association with CMS4 and few potential mechanism for the phenomena has been reported.

In this study, we investigated the molecular landscape and profiled gene expression in mCRC with CMS4 subtype. *FBXW7* and *CARD11* mutation only occurred in the CMS2/3 subtypes, while *CTNNB1*, *CDH1* and *CCNE1* mutation merely occurred in CMS4. Mutated genes in CMS4 subtypes were enriched in Wnt signalosome, cellular localization, androgen receptor binding and signaling by FGFR1 pathway, etc. Notch pathway was enriched in the CMS2/3 subtype, while Wnt and cell cycle pathway was enriched in the CMS4 subtype. MATH was found significantly lower in the CMS4 subtype than in CMS2/3. We also first identified a PFS-related gene, several immune-related genes and immunologic signature gene in the CMS4 subtype. It was indicated that the CMS4 group had an immunosuppressive microenvironment. The discovery of our study may guide the select of treatment for CMS4 patients and allow more patients benefit from it in the future.

2 Methods

2.1 Immunohistochemical staining of tumor specimens

Paraffin-embedded specimens were cut into 4 μm thick sections, baked at 65°C for 60 min, and deparaffinized using leicaBondMax (Leica Biosystems, Wetzlar, Germany). Antigen retrieval was performed in BOND Epitope Retrieval Solution 2 (Cat. No. AR9640, pH9.0, Leica) by heating at 100°C for 20 min. Sections were incubated in 3% hydrogen peroxide for 5 min and rinsed with phosphate buffered saline (PBS). Sections were incubated with anti-FRMD6/Willin antibody (ab218209, dilution 1:150, Abcam, Shanghai, China), Anti-5-HT-2B antibody (HPA012867, dilution 1:2000, Merck, Beijing, China), Anti-CDX2 antibody [EPR2764Y] (ab76541, dilution 1:2000, Abcam, Shanghai, China), Anti-ZEB1 antibody [EPR17375] (ab203829, dilution 1:150, Abcam, Shanghai, China), Anti-pan Cytokeratin antibody [AE1/AE3] (ab27988, dilution 1:100, Abcam, Shanghai, China) for 20 min, respectively. Sections were washed by PBS, followed by incubation with primary antibody at 25°C for 10 min, washing by PBS, and incubation with secondary antibody at 25°C for 10 min. Finally, 3,3'-diaminobenzidine tetrahydrochloride (DAB) staining was performed at 25°C for 10 min and incubated by Hematoxylin for 5 min before sealing the sections.

2.2 Patients

Clinicopathological data of 24 patients with mCRC were obtained from the Department of Oncology, the Affiliated Suzhou Hospital of

Nanjing Medical University. The patients were divided into two groups (G1 (CMS2/3) and G2 (CMS4)) according to an online IHC mini classifier tool (20) after acquiring IHC staining of *FRMD6*, *ZEB1*, *HTR2B*, *CDX2* and *KER* in tumor specimens (Figure S1). Meanwhile, the CMS classification was also separately verified by the CMScaller R package (21) based on transcriptome data. The inclusion criteria were as follows: 1) aged between 18 and 80 years, 2) CRC as the only tumor, 3) confirmed by histopathological diagnosis, 4) treated with standard regimens, 5) CMS1 excluded, and 6) detailed clinical pathology information. All specimens were performed for DNA and RNA analyses, and DNA data of 13 specimens was further analyzed. Written informed consent to participate in the study was obtained from the patients. This study was approved by the ethics board of the Affiliated Suzhou Hospital of Nanjing Medical University (approval number: KL901250).

2.3 Targeted DNA sequencing and data analysis

Genomic DNA was acquired from formalin-fixed, paraffin-embedded (FFPE) specimens using the Tianquick FFPE DNA Kit (Beijing, China) following the manual guide. The DNA was quantified using a Qubit dsDNA HS assay kit (ThermoFisher Scientific, Waltham, MA, USA). After shearing the genomic DNA into 150-200 bp fragments using a Covaris M220 Focused-ultrasonicator (Covaris, Woburn, MA, USA), the fragmented DNA was used for library generation per the KAPA HTP Library Preparation Kit (KAPA Biosystems, Wilmington, MA, USA). The DNA library was hybridized using a 579-gene panel (Genecast, Wuxi, China) and sequenced I Illumina Novaseq platform (Illumina, San Diego, CA, USA). For somatic mutation calling, raw data were de-multiplexed. After removing low-quality reads, reads were aligned to the hg19 reference genome using BWA MEM and the aligned sequence was indexed using Samtools. Tumor tissues were analyzed using matched blood samples as controls. Somatic mutations analyzed by Varscan2 were defined as follows: 1) in exonic regions; 2) with a depth of ≥ 100× and an allele frequency of ≥ 5%; and 3) with an allele frequency of ≥ 0.2% in the Exome Aggregation Consortium and the Genome Aggregation Database. The calculation of MATH scores was referenced to Rocco et al. (22). Tumor mutation burden (TMB) (mutations/Mb) was calculated using algorithm as reported by Chalmers et al. (23). Nonsynonymous somatic mutations (variant frequencies no less than 5%) at the exonic and splicing regions were quantified. The total number of mutations counted was divided based on the size of the coding region of the targeted panel to calculate the TMB per megabase.

2.4 RNA sequencing and data analysis

RNA was acquired from FFPE samples using Rneasy FFPE Kit (Qiagen, Germantown, MA, USA). The RNA quality was assessed on a 2100 Bioanalyzer (Agilent Technologies, Santa Clara, CA, USA). Samples with high quality of RNA (with DV200 ≥ 25%) were used for subsequent experiments. The mRNA libraries were prepared using the NEBNext® Ultra™ RNA Library Prep Kit and they were sequenced on the Illumina NovaSeq platform. Raw reads were processed to remove low quality sequences (de-junction contamination, rRNA removal, etc). For gene expression analysis, clean reads were aligned to the reference human genome (hg19) using HISAT2 25751142 (http://ccb.jhu.edu/software/hisat2/index.shtml). Transcript assembly was performed using StringTie51 (v1.2.3). FeatureCounts (24) was used to estimate the expression level of each gene. Gene expression was determined by HTSeq. The quantification of gene expression was determined by fragments per kilobase per million mapped reads. We used the DESseq2 package (25) in the R software to screen differentially expressed genes between comparisons. Data were normalized by a negative binomial distribution statistical method. The resulting P values were subjected to multiple test corrections according to the Benjamini and Hochberg methods to exclude false positives. Genes, with $|\log2(\text{fold change})| > 1$ and $P < 0.05$, were defined as differentially expressed genes (DEGs) by DESseq.

2.5 Protein network analysis

For protein network analysis, protein-protein interaction (PPI) network data were obtained to retrieve the Interacting Genes (STRING; https://string-db.org/). An interaction score of > 0.4 was set as the threshold. The PPI network was envisioned by Cytoscape, and hub genes were identified by CytoHubba (26).

2.6 Tumor immune microenvironment analysis

For tumor immune composition analysis, gene set enrichment analysis (GSEA) was performed using GSEA tools (http://www.broadinstitute.org/gsea). Innate anti-PD-1 resistance (IPRES) data were downloaded from http://software.broadinstitute.org/gsea/msigdb (27). Single-sample gene set enrichment analysis (ssGSEA) and Xcell were used to quantify the infiltration of different types of immune cells.

2.7 Statistical analysis

Statistics was conducted by R package (version 4.0, https://cran.r-project.org/), and different groups were analyzed using Fisher's exact test. Student's *t*-test and chi-square test were used to analyze clinical characteristics and categorical variables, respectively. Kaplan–Meier curves were used to predict PFS and compared statistically using log-rank test (28, 29). Statistical significance was set at $P < 0.05$.

3 Results

3.1 Clinicopathological characteristics

Patients are classified into two groups according to the IHC expression and the transcriptome-based CMS classification, G1 and

G2, represents CMS2/3 and CMS4 subtypes, respectively. The clinicopathological characteristics of CRC patients in the G1 and G2 groups are shown in Table 1. The median age is 56 years in both groups (P=0.70). 11 males and 4 females are in the G1 group, while 4 males and 5 females in G2. Most patients are adenocarcinomas (87.5%, 21/24) and others are signet ring cell carcinoma (2/24) and cancerization (1/24). All the G2 patients are adenocarcinomas. Ninety percent of the lesions are located on the left side of colon (21/24). The Eastern Cooperative Oncology Group (ECOG) performance status (PS) score of most patients are lower than 2 (87.5%, 21/24). Mutations in the *KRAS*, *NARS* and *BRAF* genes are more common in the G2 group than those in the G1 group (88.9% vs. 40.0%, P=0.02). The median values of tumor mutational burden (TMB) of the G1 group are 5.3, while those of the G2 group are 3.9 (P=0.31). Among all clinicopathological characteristics, only mutation type is statistically different between the two groups.

As shown in Figure 1A, the PFS of the G2 group (7.0 months) is significantly shorter than that of the G1 group (14.0 months, P=0.041). Compared to patients with *KRAS*, *NRAS* and *BRAF* wild-types (15.0 months), those carrying the *RAS* (8.0 months) or *BRAF* (7.5 months) mutations have shorter PFS (P=0.008, Figure 1B). Patients treated with cetuximab and chemotherapy have a significantly longer PFS than those treated with bevacizumab and chemotherapy (P=0.047, Figure 1C).

3.2 Somatic mutations analyses

The landscape of somatic mutations is investigated and the top 50 mutated genes in the G1 and G2 groups are listed in Figure 2A. *TP53* (92%), *APC* (69%) and *KRAS* (31%) are the most frequently mutated genes in the whole cohort. Missense mutations, nonsense mutations and frame-shift insertion/deletions are the major types in both G1 and G2 groups (Figures 2A-C). Interestingly, with regard to each specific mutated gene, the mutation types are completely different between the two groups. Such as the *APC* gene, nonsense mutation is the major type in the G1 group, while frame-shift deletion is predominant in the G2 group (Figures 2A-C). In the G1 group, the top 10 mutated genes are *TP53*, *APC*, *FBXW7*, *CARD11*, *NRAS*, *BRAF*, *BMPR1A*, *B2M*, *ARID1B* and *AR* (Figure 2B); while *APC*, *TP53*, *KRAS*, *CTNNB1*, *CDH1*, *CCNE1*, *BRAF*, *BLM*, *AXL* and *ALK* in G2 (Figure 2C). Of note, the *FBXW7* and *CARD11*

TABLE 1 Clinicopathological characteristics of the G1 and G2 patients.

Characteristics	G1, CMS2/3 (N=15)	G2, CMS4 (N=9)	*P* value
Age (median, years)	56	56	0.70
Gender			0.16
Male	11	4	
Female	4	5	
Pathology			0.15
Adenocarcinoma	12	9	
Other Signetring cell carcinoma Cancerization	3 2 1	0 0 0	
Primary site			0.15
Right	3	0	
Left	12	9	
ECOG PS			0.54
0	1	2	
1	12	6	
2	2	1	
Mutations			0.02*
KNB mt[#]	6	8	
RAS	4	8	
BRAF	2	0	
KNB wt[##]	9	1	
TMB (median)	5.3	3.9	0.31

[#]KNB mt represents Ras or Braf mutation. [##]KNB wt represents Ras and Braf wild-types. *P value < 0.05.

10.3389/fimmu.2023.1160052

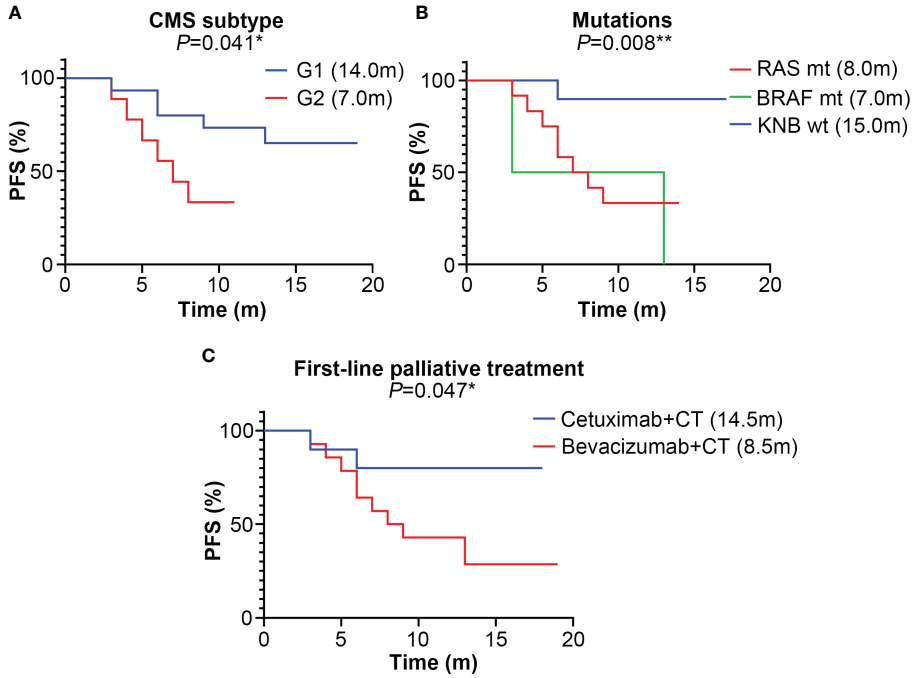

FIGURE 1
The median progression-free survival (PFS) (month) of different subtype groups of colorectal cancer patients. **(A)** The median PFS of the G1 (CMS2/3) and G2 (CMS4) groups; **(B)** The median PFS of KRAS, NRAS and BRAF mutation subtypes; mt represents mutant-type, wt represents wild-type; **(C)** The median PFS of different first-line palliative treatment subtypes; CT represents chemotherapy. * represents $P<0.05$; ** represents $P<0.01$; *** represents $P<0.001$.

mutations only occur in the G1 group (Figures 2A, B), whereas *CTNNB1*, *CDH1* and *CCNE1* mutations predominantly occur in the G2 group (Figures 2A, C).

3.3 Enrichment analysis of mutated genes in the G1 and G2 groups

Gene ontology (GO) enrichment analysis shows that in the cellular component-associated category, the mutated genes in the G1 group are enriched in HFE-transferrin receptor complex, plasma membrane receptor complex and so on (Figure S2A), and the mutated genes in the G2 group are enriched in Wnt signalosome and catenin complex, etc (Figure S2B). For biologic process category, the mutated genes in the G1 group are enriched in signal transduction by protein phosphorylation (Figure S2C), and those in the G2 group are cellular localization, positive regulation of macromolecule metabolic process and regulation of transferase activity, etc (Figure S2D). For molecular function, the mutated genes in the G1 group are enriched in transcription factor activity (Figure S2E), and those in the G2 group are androgen receptor binding and kinase binding (Figure S2F).

KEGG pathway analysis reveals that the Notch pathway, in which the *FBXW7* mutation located, is enriched in the G1 group. The cell cycle pathway that *CCNE1* and *RB1* mutations located in is enriched in the G2 group. Similarly, the Wnt pathway that the *CTNNB1* mutation located in is enriched in the G2 group (Figure 3A). Reactome pathway analysis reveals the mutated genes in the G1 group are enriched in transcriptional regulation by RUNX2 pathway (Figure 3B), and those in G2 are enriched in signaling by FGFR1 and signaling by FGFR2 pathways (Figure 3C).

3.4 MATH in the G1 and G2 groups

MATH score is used to quantify intratumor heterogeneity and is predictive for drug resistance and tumor recurrence. Although the TMB value between G1 and G2 groups is insignificant, the MATH score in the G2 group is significantly lower than that in G2 (P=0.027, Figure 4), indicating that the level of intratumor genetic heterogeneity of CMS4 patients is lower than that of CMS2/3.

3.5 Gene expression profiling in the G1 and G2 groups

A total of 3,510 DEGs are identified, and the majority of which are downregulated in the G2 group. The volcano plot of differentially expressed genes is shown in Figure 5A. PPI network downloaded from the STRING database is displayed in Figure S3. The top 20 hub genes with the highest nodes, including *SLC17A6*, *ALB*, *AQP4*, *PGK2*, *PASD1*, *NANOG*, *FRMPD2*, *SCL7A3*, *BRDT*, *CRISP2*, *FTHL17*, *CA10*, *IL4*, *MAGEC2*, *TDRD12*, *SERPINA7*, *PLCZ1*, *RAD21L1*, *SPACA1* and *ACTRT1*, are shown in Figure 5B. Survival analysis of these hub genes shows only *SLC17A6* is associated with the prognosis of CMS4 patients, and

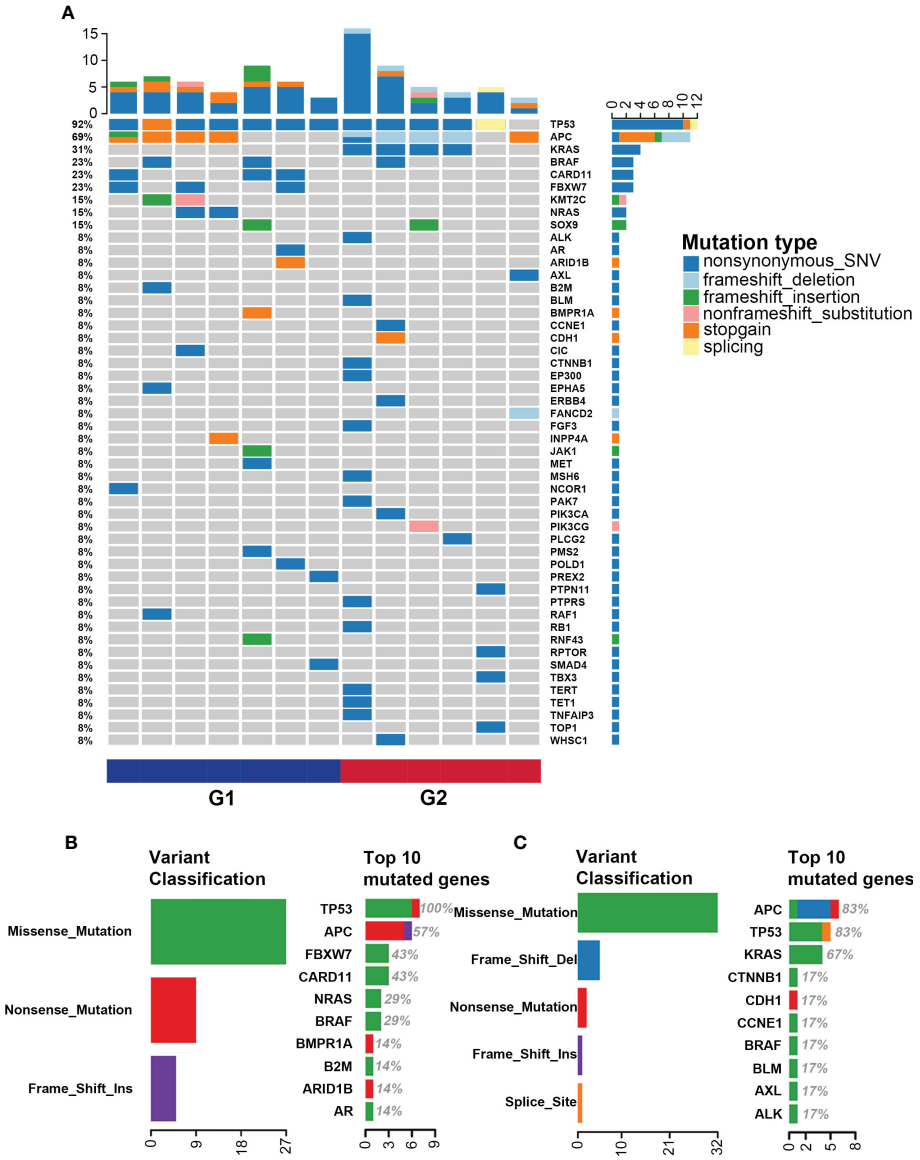

FIGURE 2
Single nucleotide variation landscape of both groups. **(A)** Landscape of somatic mutations in the G1 (CMS2/3) and G2 (CMS4) groups; **(B)** Detailed information of gene mutations in the G1 group; **(C)** Detailed information of gene mutations in the G2 group.

higher mRNA expression of *SLC17A6* is associated with worse PFS (P=0.04, Figure S4).

Among the differentially expressed genes, at least ten immune-related genes (*CD1C, IDO2, IL4, IL17F, IL1A, CCL3, MAGEC2, KRT5, CEACAM8 and VTCN1*) are found. The expression of these genes is higher in the G2 group than that in G1 except of *CDIC* and *CEACAM8* (Figure S5). Of which, *IDO2*, *IL4* and *VTCN1* negatively regulate checkpoint and immune response; *KRT5* is an oncogene that regulate tumorigenesis. *CD1C* stimulates immune response and *CEACAM8* functions as lymphocyte markers (30, 31). Two immunologic signature gene sets, GSE29615 and GSE16395 are identified with high confidence in GSEA (P<0.05, Figure 5C). Reactome analysis shows the top ten enrichment pathways, including SLC-mediated transmembrane transport and formation of the cornified envelope (Figure 5D).

Thus, through analyzing gene expression profiling in both groups, a PFS-related gene, several immune-related genes and immunologic signature gene sets are first identified in the CMS4 subtype.

3.6 Immune-related genes and pathways associated with G2 group

IPRES contains 26 gene signatures that proven to be associated with PD-1 immunotherapy resistance. The IPRES analysis indicates that the immunotherapy resistance of MAPK inhibitor-induced EMT in the G2 group is significantly higher than that in G1 (G1=0.66 vs. G2=0.72, P<0.05). However, other gene sets, such as TGF-β signaling, tumor angiogenesis and VEGFA targets, are not significantly different between the two groups (Figure S6).

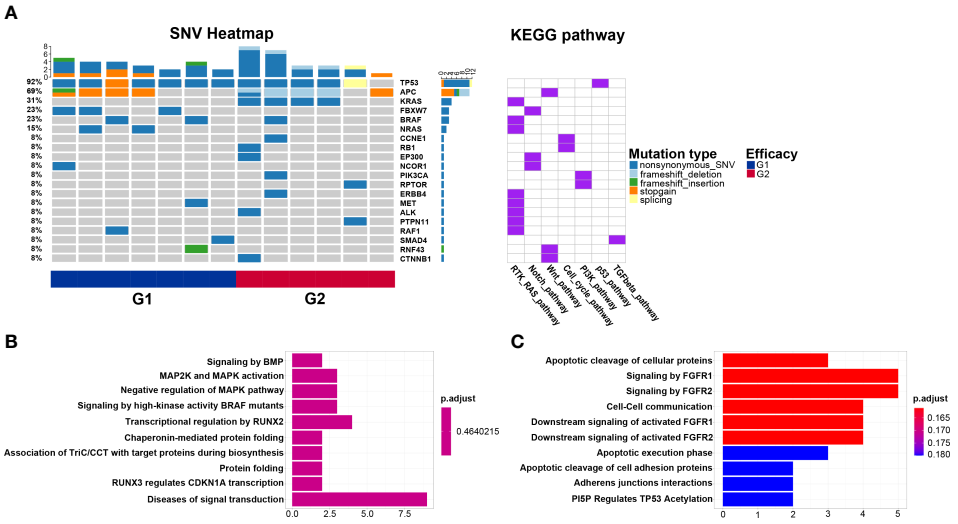

FIGURE 3
Biological pathways enriched from mutated genes. **(A)** Kyoto Encyclopedia of Genes and Genomes pathways of mutated genes in the G1 (CMS2/3) and G2 (CMS4) groups; **(B)** Reactome pathways of mutated genes in the G1 group; **(C)** Reactome pathways of mutated genes in the G2 group.

According to ssGSEA analysis, the G2 group is significantly associated with lower infiltration of effector memory CD4+ T cells (P<0.05), immature B cells (P<0.05), and myeloid-derived suppressor cells (MDSC, P<0.05, Figure 6A). Xcell analysis shows that some immune cells, including CD4+ T cells, CD8+ T cells, natural killer (NK) cells and macrophages, have no difference in infiltration levels (Figure 6B). The infiltration levels of CD4+ naïve T cells (P<0.05), CD4+ central memory T cells (Tcm) (P<0.01) and class-switched memory B cells (P<0.05) are lower in the G2 group, while the level of hepatocytes (P<0.05) is higher in the G2 group. The immune, stroma and microenvironment scores in the G2 group are all lower than those in the G1 group, although there are no statistical differences. Thus, immune-related analyses indicate the CMS4 group has an immunosuppressive microenvironment.

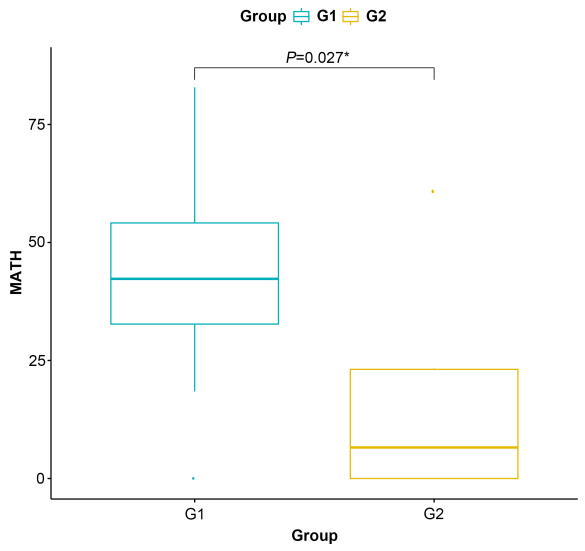

FIGURE 4
Mutant-allele tumor heterogeneity score of the G1 (CMS2/3) and G2 (CMS4) groups. * represents *P*<0.05.

4 Discussion

In this study, CMS2/3 or CMS4 subtype was differentiated based on IHC staining with *FRMD6*, *ZEB1*, *HTR2B*, *CDX2* and *KER* markers, which was in line with the transcriptome-based classification system (12, 20). We found that the cell cycle and Wnt pathways were enriched in the CMS4 group. Immunologic signature gene sets and enrichment pathways as well as a novel predictor for CMS4 CRC patients were identified through gene expression analysis. Tumor microenvironment analysis implied a lower immune, stroma, and microenvironment scores in the CMS4 group, which indicated immunotherapy may not be beneficial to these patients. Our results provide a potential mechanism for the poor outcome of mCRC patients with CMS4 subtype and imply different treatment strategies based on the CMS subtype.

In our study, *FBXW7* mutation, the most frequently mutated gene after *TP53* and *APC* in the CMS2/3 group, was not found in the CMS4 group. FBXW7, as a ubiquitin ligase, can combine with lots of cancer-related factors, including c-Myc, cyclin E and mTOR (32–34). *FBXW7* mutation in CRC leads to tumor cell proliferation, increases resistance to paclitaxel, 5-fluorouracil and oxaliplatin, as well as becomes sensitive to mTOR inhibitors (35–37). No correlation between *FBXW7* mutation and CMS4 CRC has been reported in previous studies. *FBXW7* mutation, enriched in the Notch pathway, was not been found in the CMS4 mCRC patients in our study, suggesting that the FBXW7-Notch axis might not be involved in the tumorigenesis of CMS4 CRC. Therefore, treatment targeting Notch or mTOR signaling might not be beneficial to the CMS4 CRC patients.

10.3389/fimmu.2023.1160052

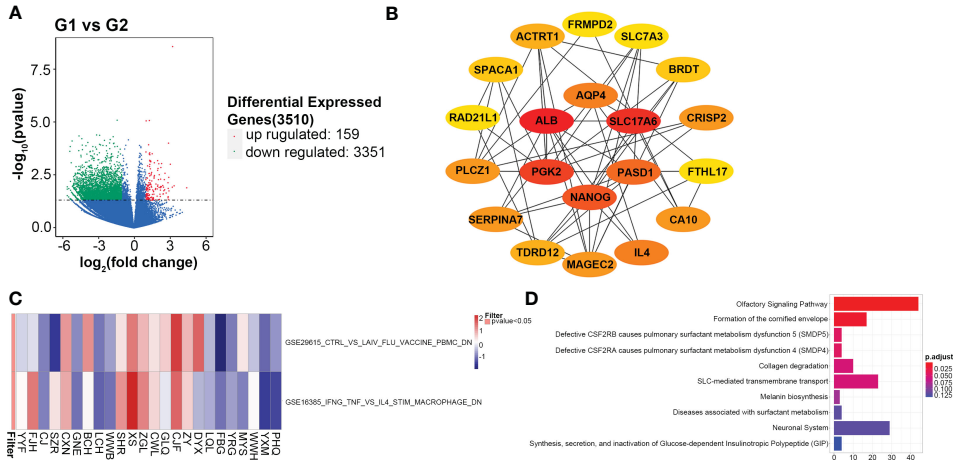

FIGURE 5
Gene expression profiling analyses. **(A)** Differential expressed genes between the G1 (CMS2/3) and G2 (CMS4) groups; **(B)** Top 20 hub genes in the protein and protein interaction network; **(C)** The enrichment analysis for immunologic signature gene sets; **(D)** Reactome pathways of differential expressed genes.

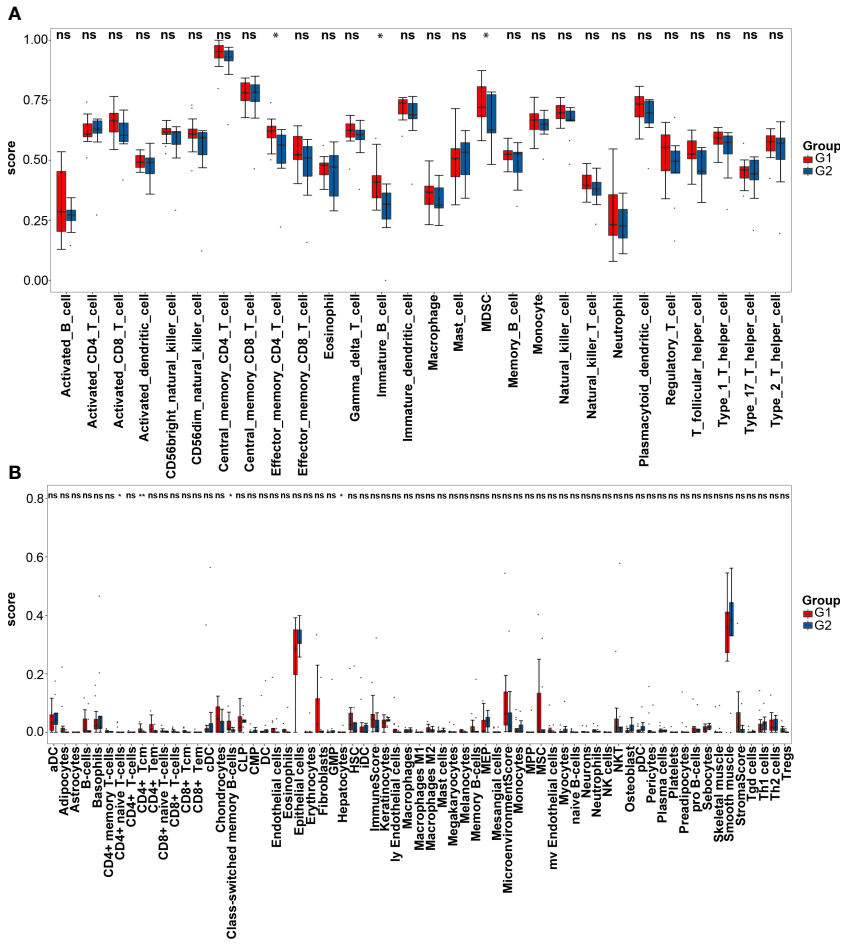

FIGURE 6
Immune infiltration analyses. **(A)** Single sample gene set enrichment analysis of the G1 (CMS2/3) and G2 (CMS4) groups; **(B)** Xcell analysis of the two groups. * represents P*P*<0.05; ** represents *P*<0.01; ns represents *P*>0.05.

CTNNB1 and *CCNE1* were the most frequently mutated genes found in the CMS4 group in our study. *CTNNB1* mutation occurred in about half of CRC patients (38), while the mutation frequency of *CCNE1* in CRC had not been explored. The mutation of these two genes in the CMS4 mCRC had not been reported previously. *CTNNB1* is a significant Wnt signaling regulator that interacts with E-cadherin to mediate cell adhesion (39). The Wnt signaling pathway that *CTNNB1* lies is a critical pathway in EMT, an important feature of CMS4 subtype (20, 40). In our study, *CTNNB1* mutation was enriched in the Wnt pathway, suggesting that *CTNNB1*-Wnt axis might function importantly in the CMS4 mCRC. Further, therapeutic drugs targeting the Wnt pathway, including small molecules, biological agents and natural compounds (41), might be effective treatment of CMS4 subtype mCRC.

CCNE1 acts as a positive regulator of cell cycle and promotes the transition from G1 to S (42). Abnormal expression of *CCNE1* activates cyclin-dependent kinase 2 to phosphorylate its substrate, resulting in tumor cell proliferation (43). In our study, *CCNE1* mutation was enriched in the cell cycle pathway, suggesting that CCNE1-cell cycle axis might be involved in the tumorigenesis of CMS4 CRC. KEGG pathway analysis also showed that the cell cycle pathway was a unique pathway in the CMS4 type rather than CMS2/3. The arrest of the cell cycle in the G1 phase can be caused by TGF-β, which can induce the cell cycle pathway and effectively inhibit cell proliferation (44). Several studies show that combining ICIs and selective TGF-β inhibitors might be helpful for immunotherapy in CMS4 type mCRC patients (45, 46).

In our study, *SLC17A6*, one member of solute carrier family, was identified as a hub DEG between the two groups, and most hub DEGs were significantly enriched in the SLC-mediated transmembrane transport pathway. Tumor survival, migration, proliferation, and sensitivity to radiotherapy are regulated by *SLC3A2*, and its high expression is associated with poor prognosis (47–49). In a xenograft model, antitumor activity against human colon cancer was mediated by anti-*SLC7A5* monoclonal antibodies (50). The exact roles of *SLC17A6* in CMS4 subtype colon cancer warrant further investigation.

In our study, the mutated genes of the CMS4 subtype were enriched in signaling by *FGFR1* and *FGFR2* pathways according to Reactome pathway analysis. The FGFR tyrosine kinase family regulates migration, differentiation, apoptosis and angiogenesis after ligands (51). A combination of FGFR inhibitors and immune checkpoint blockers is reported to be a promising treatment strategy for malignant tumors (52). However, its application in CMS4 CRC patients requires further research.

According to the GSEA and tumor immune microenvironment analyses, the CMS4 CRC patients tended to have an immunosuppressive microenvironment. MDSCs are a heterogeneous group of cells derived from both myeloid progenitors and immature myeloid cells, which are precursors of dendritic cells, macrophages, and/or granulocytes (53). In our study, fewer MDSCs infiltrated in the CMS4 subtype than in CMS2/43, suggesting that CMS4 CRC cells tended to promote tumor growth (54). GSE16385 is a GEO dataset containing expression data from human macrophages, obtained by comparing macrophages activated by interleukin-4 (M2) and those activated by interferon-gamma and tumor necrosis factor (M1) (55). Macrophages in the immune environment of most cancer cells act as M2 phenotype and express various anti-inflammatory molecules, leading to an immunosuppressive microenvironment (56). Our study found that M2 macrophages infiltrated the tumor microenvironment in most CMS4 samples. Regorafenib transforms tumor-associated macrophage from M2 type to M1 type with anti-tumor function by inhibiting the colony-stimulating factor 1 receptor (57). Meanwhile, regorafenib can inhibit tumor angiogenesis by TIE2 pathway, and reduce proliferation of CMS4 subtype tumor cells in a patient-derived xenograft trail (58, 59). When combined with ICIs, it may have synergistic anti-tumor effect in CRC. One patient with CMS4 in our study, who failed first-line cetuximab and chemotherapy second-line bevacizumab and chemotherapy, was beneficial markedly from the treatment of regorafenib (data not shown). This might change the current clinical practice for mCRC patients with CMS4 subtype, overcome the lack of effective treatment options, and prolong their overall survival. The combination of modalities deserves further studies *in vitro* and *in vivo*. Besides MDSCs and macrophages, there were several other immune cell types infiltrating differently between the two CMS subtypes. Tcm is a long-term T cell derived from naive T cells activated by antigens and can home to lymph nodes to receive antigen re-stimulation. Activated Tcm cells can produce a large number of cloned effective memory T cells carrying the same antigen under the re-stimulation of antigen (60). In our study, the CMS4 subtype tended to have a malignant inflammatory environment that potentially blocked the antitumor effect of active T/immune cells, resulting in a poor immune response.

Additionally, several immune-related genes with significantly different expression levels between CMS4 and CMS2/3 subtypes were identified in our study. IL17F is a member of the IL−17 family of proteins. The investigation by Quan et al. showed that the upregulation of IL17F in mCRC promotes tumor invasion by inducing EMT transition (61) and elevated levels of Th17-associated cytokines in advanced-stage mCRC are associated with poorer overall survival and possible resistance to chemotherapy (62). The high expression of CEACAM8 was reported by Peng et al. (30) to be an independent factor of poor disease-free survival and inversely correlated with CD8+ T lymphocyte cells, predicting distant metastasis and inefficiency of chemotherapy. VTCN1 is an immunoregulatory protein that negatively regulates T cell-mediated immune response in the tumor microenvironment (63). Overexpression of VTCN1 was reported to play an oncogenic role, induce EMT, proliferation, and migration of CRC cells through the Wnt signaling pathway (64) and promote CRC stemness (65). VTCN1 can inhibit T cell activation and proliferation, negatively regulate T cell immune response, and its overexpression promotes tumor tolerance and might contribute to Treg development in a CRC tolerogenic milieu (66). Serving as a negative regulator of T-cell-mediated antitumor immunity, VTCN1 can inhibit T cell activation and cytokine secretion, and regulate cytotoxic T lymphocytes (CTLs) during tumor progression (67).

Our study provides new insights into the molecular characteristic of the CMS4 subtype. The CTNNB1-Wnt and CCNE1-cell cycle axes are likely involved in the tumorigenesis of CMS4 CRC and could be functioned as therapeutic targets. In contrast, the FBXW7-Notch pathway is unlikely involved in the tumorigenesis of CMS4 CRC. The CMS4 CRC patients have been found having an immunosuppressive microenvironment and transforming tumor-associated macrophages from M2 type to M1 type in CMS4 CRC cells might be a therapeutic direction. Through analyzing gene expression profiling in both groups, a PFS-related gene, several immune-related genes and immunologic signature gene sets were first identified in the CMS4 subtype. *SLC17A6*, as a novel predictor for PFS of CMS4 CRC patients, needs further exploration. The study requires more patient recruitment and data collections. Further verification in clinics is warrant.

Data availability statement

The data presented in the study are deposited in the GSA for Human repository, accession number PRJCA011830.

Ethics statement

The studies involving human participants were reviewed and approved by The ethics board of the Affiliated Suzhou Hospital of Nanjing Medical University (approval number: KL901250). The ethics committee waived the requirement of written informed consent for participation.

Author contributions

Contributions: (I) Conception and design: YL, JS, FG. (II) Administrative support: JS, FG. (III) Provision of study materials or patients: YL, DG. (IV) Collection and assembly of data: DG, YS, CZ, WL, LH, XW, ZK. (V) Data analysis and interpretation: YL, DG. (VI) Manuscript writing: All authors. All authors contributed to the article and approved the submitted version.

Funding

This study was funded by grants from Suzhou Municipal Science and Technology Bureau (Grant Number SKY2022006, SLJ202011 and SLT201959), Jiangsu Commission of Health (Grant Number M2020043) and China Digestive Tumor Clinical Research Public Welfare Project (Grant Number P014-038).

Conflict of interest

The authors declare that the research was conducted in the absence of any commercial or financial relationships that could be construed as a potential conflict of interest.

Publisher's note

All claims expressed in this article are solely those of the authors and do not necessarily represent those of their affiliated organizations, or those of the publisher, the editors and the reviewers. Any product that may be evaluated in this article, or claim that may be made by its manufacturer, is not guaranteed or endorsed by the publisher.

Supplementary material

The Supplementary Material for this article can be found online at: https://www.frontiersin.org/articles/10.3389/fimmu.2023.1160052/full#supplementary-material

SUPPLEMENTARY FIGURE 1
Immunohistochemical staining of CMS2/3 and CMS4 subtypes metastasis colorectal cancer.

SUPPLEMENTARY FIGURE 2
Gene ontology (GO) analysis of mutated genes in the G1 (CMS2/3) and G2 (CMS4) groups. **(A)** Cellular component analysis of mutated genes in the G1 group; **(B)** Cellular component analysis of mutated genes in the G2 group; **(C)** Biological process analysis of mutated genes in the G1 group; **(D)** Biological process analysis of mutated genes in the G2 group; **(E)** Molecular Function analysis of mutated genes in the G1 group; **(F)** Molecular Function analysis of mutated genes in the G2 group.

SUPPLEMENTARY FIGURE 3
Protein and protein interaction network of the differential expressed genes.

SUPPLEMENTARY FIGURE 4
Survival curves of patients with different SLC17A6 expression.

SUPPLEMENTARY FIGURE 5
Average expression of different immune-related genes in the G1 (CMS2/3) and G2 (CMS4) groups.

SUPPLEMENTARY FIGURE 6
The innate anti–PD-1 resistance analysis of immune-related genes/pathways in the G1 (CMS2/3) and G2 (CMS4) groups.

References

1. Chen W, Zheng R, Baade PD, Zhang S, Zeng H, Bray F, et al. Cancer statistics in China, 2015. *CA Cancer J Clin* (2016) 66:115–32. doi: 10.3322/caac.21338
2. Greene FL. Current TNM staging of colorectal cancer. *Lancet Oncol* (2007) 8:572–3. doi: 10.1016/S1470-2045(07)70185-7
3. Zhou K, Shi H, Chen R, Cochuyt JJ, Hodge DO, Manochakian R, et al. Association of race, socioeconomic factors, and treatment characteristics with overall survival in patients with limited-stage small cell lung cancer. *JAMA Netw Open* (2021) 4:e2032276. doi: 10.1001/jamanetworkopen.2020.32276

4. Bazan V, Migliavacca M Fau - Zanna I, Zanna I Fau - Tubiolo C, Tubiolo C Fau - Grassi N, Grassi N Fau - Latteri MA, Latteri Ma Fau - La Farina M, et al. Specific codon 13 K-ras mutations are predictive of clinical outcome in colorectal cancer patients, whereas codon 12 K-ras mutations are associated with mucinous histotype. *Ann Oncol* (2002) 13(9):1438–46.doi: 10.1093/annonc/mdf226

5. Schirripa M, Cremolini C Fau - Loupakis F, Loupakis F Fau - Morvillo M, Morvillo M Fau - Bergamo F, Bergamo F Fau - Zoratto F, Zoratto F Fau - Salvatore L, et al. Role of NRAS mutations as prognostic and predictive markers in metastatic colorectal cancer. *Int J Cancer* (2015) 136(1):83–90. doi: 10.1002/ijc.28955

6. Pentheroudakis G, Kotoula V Fau - De Roock W, De Roock W Fau - Kouvatseas G, Kouvatseas G Fau - Papakostas P, Papakostas P Fau - Makatsoris T, Makatsoris T Fau - Papamichael D, et al. Biomarkers of benefit from cetuximab-based therapy in metastatic colorectal cancer: interaction of EGFR ligand expression with RAS/RAF, PIK3CA genotypes. *BMC Cancer* (2013) 13:49. doi: 10.1186/1471-2407-13-49

7. Mao C, Yang Zy Fau - Hu XF, Hu Xf Fau - Chen Q, Chen Q Fau - Tang JL, Tang JL. PIK3CA exon 20 mutations as a potential biomarker for resistance to anti-EGFR monoclonal antibodies in KRAS wild-type metastatic colorectal cancer: a systematic review and meta-analysis. *Ann Oncol* (2012) 23(6):1518–25. doi: 10.1093/annonc/mdr464

8. Biller LH, Schrag D. Diagnosis and treatment of metastatic colorectal cancer: a review. *JAMA* (2021) 325:669–85. doi: 10.1001/jama.2021.0106

9. Guinney J, Dienstmann R, Wang X, de Reynies A, Schlicker A, Soneson C, et al. The consensus molecular subtypes of colorectal cancer. *Nat Med* (2015) 21:1350–6. doi: 10.1038/nm.3967

10. Stahler A, Hoppe B, Na IK, Keilholz L, Muller L, Karthaus M, et al. Consensus molecular subtypes as biomarkers of fluorouracil and folinic acid maintenance therapy with or without panitumumab in RAS wild-type metastatic colorectal cancer (PanaMa, AIO KRK 0212). *J Clin Oncol* (2023) 41(16):2975–87. JCO2202582. doi: 10.1200/JCO.22.02582

11. Stahler A, Heinemann V, Schuster V, Heinrich K, Kurreck A, Giessen-Jung C, et al. Consensus molecular subtypes in metastatic colorectal cancer treated with sequential versus combined fluoropyrimidine, bevacizumab and irinotecan (XELAVIRI trial). *Eur J Cancer* (2021) 157:71–80. doi: 10.1016/j.ejca.2021.08.017

12. Trinh A, Trumpi K, De Sousa EMF, Wang X, de Jong JH, Fessler E, et al. Practical and robust identification of molecular subtypes in colorectal cancer by immunohistochemistry. *Clin Cancer Res* (2017) 23:387–98. doi: 10.1158/1078-0432.CCR-16-0680

13. Lenz HJ, Ou FS, Venook AP, Hochster HS, Niedzwiecki D, Goldberg RM, et al. Impact of consensus molecular subtype on survival in patients with metastatic colorectal cancer: results from CALGB/SWOG 80405 (Alliance). *J Clin Oncol* (2019) 37:1876–85. doi: 10.1200/JCO.18.02258

14. Lam M, Roszik J, Kanikarla-Marie P, Davis JS, Morris J, Kopetz S, et al. The potential role of platelets in the consensus molecular subtypes of colorectal cancer. *Cancer Metastasis Rev* (2017) 36:273–88. doi: 10.1007/s10555-017-9678-9

15. Trinh A, Lädrach C, Dawson HE, Ten Hoorn S, Kuppen PJK, Reimers MS, et al. Tumour budding is associated with the mesenchymal colon cancer subtype and RAS/RAF mutations: a study of 1320 colorectal cancers with consensus molecular subgroup (CMS) data. *Br J Cancer* (2018) 119:1244–51. doi: 10.1038/s41416-018-0230-7

16. Mooi JK, Wirapati P, Asher R, Lee CK, Savas P, Price TJ, et al. The prognostic impact of consensus molecular subtypes (CMS) and its predictive effects for bevacizumab benefit in metastatic colorectal cancer: molecular analysis of the AGITG MAX clinical trial. *Ann Oncol* (2018) 29:2240–6. doi: 10.1093/annonc/mdy410

17. Laoukili J, Constantinides A, Wassenaar ECE, Elias SG, Raats DAE, van Schelven SJ, et al. Peritoneal metastases from colorectal cancer belong to consensus molecular subtype 4 and are sensitised to oxaliplatin by inhibiting reducing capacity. *Br J Cancer* (2022) 126:1824–33. doi: 10.1038/s41416-022-01742-5

18. Sawayama H, Miyamoto Y, Ogawa K, Yoshida N, Baba H. Investigation of colorectal cancer in accordance with consensus molecular subtype classification. *Ann Gastroenterol Surg* (2020) 4:528–39. doi: 10.1002/ags3.12362

19. Peters NA, Constantinides A, Ubink I, van Kuik J, Bloemendal HJ, van Dodewaard JM, et al. Consensus molecular subtype 4 (CMS4)-targeted therapy in primary colon cancer: a proof-of-concept study. *Front Oncol* (2022) 12:969855. doi: 10.3389/fonc.2022.969855

20. Ten Hoorn S, Trinh A, de Jong J, Koens L, Vermeulen L. Classification of colorectal cancer in molecular subtypes by immunohistochemistry. *Methods Mol Biol* (2018) 1765:179–91. doi: 10.1007/978-1-4939-7765-9_11

21. Eide PW, Bruun J, Lothe RA, Sveen A. CMScaller: an r package for consensus molecular subtyping of colorectal cancer pre-clinical models. *Sci Rep* (2017) 7:16618. doi: 10.1038/s41598-017-16747-x

22. Mroz EA, Tward AD, Hammon RJ, Ren Y, Rocco JW. Intra-tumor genetic heterogeneity and mortality in head and neck cancer: analysis of data from the cancer genome atlas. *PloS Med* (2015) 12:e1001786. doi: 10.1371/journal.pmed.1001786

23. Chalmers ZR, Connelly CF, Fabrizio D, Gay L, Ali SM, Ennis R, et al. Analysis of 100,000 human cancer genomes reveals the landscape of tumor mutational burden. *Genome Med* (2017) 9:34. doi: 10.1186/s13073-017-0424-2

24. Liao Y, Smyth GK, Shi W. featureCounts: an efficient general purpose program for assigning sequence reads to genomic features. *Bioinformatics* (2014) 30:923–30. doi: 10.1093/bioinformatics/btt656

25. Love MI, Huber W, Anders S. Moderated estimation of fold change and dispersion for RNA-seq data with DESeq2. *Genome Biol* (2014) 15:550. doi: 10.1186/s13059-014-0550-8

26. Chin CH, Chen SH, Wu HH, Ho CW, Ko MT, Lin CY. cytoHubba: identifying hub objects and sub-networks from complex interactome. *BMC Syst Biol* (2014) 8 Suppl 4:S11. doi: 10.1186/1752-0509-8-S4-S11

27. Bin Lim S, Chua MLK, Yeong JPS, Tan SJ, Lim WT, Lim CT. Pan-cancer analysis connects tumor matrisome to immune response. *NPJ Precis Oncol* (2019) 3:15. doi: 10.1038/s41698-019-0087-0

28. Rich JT, Neely JG, Paniello RC, Voelker CC, Nussenbaum B, Wang EW. A practical guide to understanding Kaplan-Meier curves. *Otolaryngol Head Neck Surg* (2010) 143:331–6. doi: 10.1016/j.otohns.2010.05.007

29. Rai S, Mishra P, Ghoshal UC. Survival analysis: a primer for the clinician scientists. *Indian J Gastroenterol* (2021) 40:541–9. doi: 10.1007/s12664-021-01232-1

30. Hu X, Li YQ, Ma XJ, Zhang L, Cai SJ, Peng JJ, et al. And T immune cells infiltration in colorectal cancer predicting distant metastases and efficiency of chemotherapy. *Front Oncol* (2019) 9:704. doi: 10.3389/fonc.2019.00704

31. Adams EJ. Diverse antigen presentation by the group 1 CD1 molecule, CD1c. *Mol Immunol* (2013) 55:182–5. doi: 10.1016/j.molimm.2012.10.019

32. Inuzuka H, Shaik S, Onoyama I, Gao D, Tseng A, Maser RS, et al. SCF(FBW7) regulates cellular apoptosis by targeting MCL1 for ubiquitylation and destruction. *Nature* (2011) 471:104–9. doi: 10.1038/nature09732

33. Cao J, Ge MH, Ling ZQ. Fbxw7 tumor suppressor: a vital regulator contributes to human tumorigenesis. *Med (Baltimore)* (2016) 95:e2496. doi: 10.1097/MD.0000000000002496

34. Fan J, Bellon M, Ju M, Zhao L, Wei M, Fu L, et al. Clinical significance of FBXW7 loss of function in human cancers. *Mol Cancer* (2022) 21:87. doi: 10.1186/s12943-022-01548-2

35. Yumimoto K, Nakayama KI. Recent insight into the role of FBXW7 as a tumor suppressor. *Semin Cancer Biol* (2020) 67:1–15. doi: 10.1016/j.semcancer.2020.02.017

36. Wang Y, Liu Y, Lu J, Zhang P, Wang Y, Xu Y, et al. Rapamycin inhibits FBXW7 loss-induced epithelial-mesenchymal transition and cancer stem cell-like characteristics in colorectal cancer cells. *Biochem Biophys Res Commun* (2013) 434:352–6. doi: 10.1016/j.bbrc.2013.03.077

37. Chan SM, Weng AP, Tibshirani R, Aster JC, Utz PJ. Notch signals positively regulate activity of the mTOR pathway in T-cell acute lymphoblastic leukemia. *Blood* (2007) 110:278–86. doi: 10.1182/blood-2006-08-039883

38. Sparks AB, Morin PJ, Vogelstein B, Kinzler KW. Mutational analysis of the APC/beta-catenin/Tcf pathway in colorectal cancer. *Cancer Res* (1998) 58:1130–4.

39. Willert K, Jones KA. Wnt signaling: is the party in the nucleus? *Genes Dev* (2006) 20:1394–404. doi: 10.1101/gad.1424006

40. Krishnamurthy N, Kurzrock R. Targeting the wnt/beta-catenin pathway in cancer: update on effectors and inhibitors. *Cancer Treat Rev* (2018) 62:50–60. doi: 10.1016/j.ctrv.2017.11.002

41. Zhao H, Ming T, Tang S, Ren S, Yang H, Liu M, et al. Wnt signaling in colorectal cancer: pathogenic role and therapeutic target. *Mol Cancer* (2022) 21:144. doi: 10.1186/s12943-022-01616-7

42. Zhang C, Zhu Q, Gu J, Chen S, Li Q, Ying L. Down-regulation of CCNE1 expression suppresses cell proliferation and sensitizes gastric carcinoma cells to cisplatin. *Biosci Rep* (2019) 39(6):BSR20190381. doi: 10.1042/BSR20190381

43. Möröy T, Geisen C. Cyclin E. *Int J Biochem Cell Biol.* (2004) 36:1424–39. doi: 10.1016/j.biocel.2003.12.005

44. Liu F. Smad3 phosphorylation by cyclin-dependent kinases. *Cytokine Growth Factor Rev* (2006) 17:9–17. doi: 10.1016/j.cytogfr.2005.09.010

45. Jackstadt R, van Hooff SR, Leach JD, Cortes-Lavaud X, Lohuis JO, Ridgway RA, et al. Epithelial NOTCH signaling rewires the tumor microenvironment of colorectal cancer to drive poor-prognosis subtypes and metastasis. *Cancer Cell* (2019) 36:319–336.e7. doi: 10.1016/j.ccell.2019.08.003

46. Mishra S, Bernal C, Silvano M, Anand S, Ruiz IAA. The protein secretion modulator TMED9 drives CNIH4/TGFα/GLI signaling opposing TMED3-WNT-TCF to promote colon cancer metastases. *Oncogene* (2019) 38:5817–37. doi: 10.1038/s41388-019-0845-z

47. Bajaj J, Konuma T, Lytle NK, Kwon HY, Ablack JN, Cantor JM, et al. CD98-mediated adhesive signaling enables the establishment and propagation of acute myelogenous leukemia. *Cancer Cell* (2016) 30:792–805. doi: 10.1016/j.ccell.2016.10.003

48. Cantor JM, Ginsberg MH. CD98 at the crossroads of adaptive immunity and cancer. *J Cell Sci* (2012) 125:1373–82. doi: 10.1242/jcs.096040

49. Fenczik CA, Sethi T, Ramos JW, Hughes PE, Ginsberg MH. Complementation of dominant suppression implicates CD98 in integrin activation. *Nature* (1997) 390:81–5. doi: 10.1038/36349

50. Ueda S, Hayashi H, Miyamoto T, Abe S, Hirai K, Matsukura K, et al. Anti-tumor effects of mAb against l-type amino acid transporter 1 (LAT1) bound to human and monkey LAT1 with dual avidity modes. *Cancer Sci* (2019) 110:674–85. doi: 10.1111/cas.13908

51. Turner N, Grose R. Fibroblast growth factor signalling: from development to cancer. *Nat Rev Cancer* (2010) 10:116–29. doi: 10.1038/nrc2780

52. Katoh M. FGFR inhibitors: effects on cancer cells, tumor microenvironment and whole-body homeostasis (Review). *Int J Mol Med* (2016) 38:3–15. doi: 10.3892/ijmm.2016.2620

53. Nakamura T, Ushigome H. Myeloid-derived suppressor cells as a regulator of immunity in organ transplantation. *Int J Mol Sci* (2018) 19. doi: 10.3390/ijms19082357

54. Veglia F, Perego M, Gabrilovich D. Myeloid-derived suppressor cells coming of age. *Nat Immunol* (2018) 19(8):2357. doi: 10.1038/s41590-017-0022-x

55. Szanto A, Balint BL, Nagy ZS, Barta E, Dezso B, Pap A, et al. STAT6 transcription factor is a facilitator of the nuclear receptor PPARγ-regulated gene expression in macrophages and dendritic cells. *Immunity* (2010) 33:699–712. doi: 10.1016/j.immuni.2010.11.009

56. Hao NB, Lü MH, Fan YH, Cao YL, Zhang ZR, Yang SM. Macrophages in tumor microenvironments and the progression of tumors. *Clin Dev Immunol* (2012) 2012:948098. doi: 10.1155/2012/948098

57. Arai H, Battaglin F, Wang J, Lo JH, Soni S, Zhang W, et al. Molecular insight of regorafenib treatment for colorectal cancer. *Cancer Treat Rev* (2019) 81:101912. doi: 10.1016/j.ctrv.2019.101912

58. Wilhelm SM, Dumas J, Adnane L, Lynch M, Carter CA, Schutz G, et al. Regorafenib (BAY 73-4506): a new oral multikinase inhibitor of angiogenic, stromal and oncogenic receptor tyrosine kinases with potent preclinical antitumor activity. *Int J Cancer* (2011) 129:245–55. doi: 10.1002/ijc.25864

59. Lafferty A, O'Farrell AC, Migliardi G, Khemka N, Lindner AU, Sassi F, et al. Molecular subtyping combined with biological pathway analyses to study regorafenib response in clinically relevant mouse models of colorectal cancer. *Clin Cancer Res* (2021) 27:5979–92. doi: 10.1158/1078-0432.CCR-21-0818

60. Mahnke YD, Brodie TM, Sallusto F, Roederer M, Lugli E. The who's who of T-cell differentiation: human memory T-cell subsets. *Eur J Immunol* (2013) 43:2797–809. doi: 10.1002/eji.201343751

61. Chen Y, Yang Z, Wu D, Min Z, Quan Y. Upregulation of interleukin17F in colorectal cancer promotes tumor invasion by inducing epithelialmesenchymal transition. *Oncol Rep* (2019) 42:1141–8. doi: 10.3892/or.2019.7220

62. Sharp SP, Avram D, Stain SC, Lee EC. Local and systemic Th17 immune response associated with advanced stage colon cancer. *J Surg Res* (2017) 208:180–6. doi: 10.1016/j.jss.2016.09.038

63. Podojil JR, Miller SD. Potential targeting of B7-H4 for the treatment of cancer. *Immunol Rev* (2017) 276:40–51. doi: 10.1111/imr.12530

64. Yin Y, Shi L, Yang J, Wang H, Yang H, Wang Q. B7 family member H4 induces epithelial-mesenchymal transition and promotes the proliferation, migration and invasion of colorectal cancer cells. *Bioengineered* (2022) 13:107–18. doi: 10.1080/21655979.2021.2009411

65. Feng Y, Yang Z, Zhang C, Che N, Liu X, Xuan Y. B7-H4 induces epithelial-mesenchymal transition and promotes colorectal cancer stemness. *Pathol Res Pract* (2021) 218:153323. doi: 10.1016/j.prp.2020.153323

66. Zhao LW, Li C, Zhang RL, Xue HG, Zhang FX, Zhang F, et al. B7-H1 and B7-H4 expression in colorectal carcinoma: correlation with tumor FOXP3(+) regulatory T-cell infiltration. *Acta Histochem* (2014) 116:1163–8. doi: 10.1016/j.acthis.2014.06.003

67. Ni L, Dong C. New B7 family checkpoints in human cancers. *Mol Cancer Ther* (2017) 16:1203–11. doi: 10.1158/1535-7163.MCT-16-0761

frontiers | Frontiers in Oncology

TYPE Review
PUBLISHED 20 June 2023
DOI 10.3389/fonc.2023.1176950

OPEN ACCESS

EDITED BY
Jorge Melendez-Zajgla,
National Institute of Genomic Medicine (INMEGEN), Mexico

REVIEWED BY
Antonella Argentiero,
National Cancer Institute Foundation (IRCCS), Italy
Eleonora Lai,
University Hospital and University of Cagliari, Italy

*CORRESPONDENCE
Christopher G. Cann
christopher.g.cann@vumc.org

RECEIVED 01 March 2023
ACCEPTED 30 May 2023
PUBLISHED 20 June 2023

CITATION
Cann CG, LaPelusa MB, Cimino SK and Eng C (2023) Molecular and genetic targets within metastatic colorectal cancer and associated novel treatment advancements. *Front. Oncol.* 13:1176950.
doi: 10.3389/fonc.2023.1176950

Molecular and genetic targets within metastatic colorectal cancer and associated novel treatment advancements

Christopher G. Cann[1*], Michael B. LaPelusa[1], Sarah K. Cimino[2] and Cathy Eng[1]

[1]Department of Medicine: Hematology/Oncology, Vanderbilt University Medical Center, Nashville, TN, United States, [2]Department of Pharmacy, Vanderbilt University Medical Center, Nashville, TN, United States

Colorectal cancer results in the deaths of hundreds of thousands of patients worldwide each year, with incidence expected to rise over the next two decades. In the metastatic setting, cytotoxic therapy options remain limited, which is reflected in the meager improvement of patient survival rates. Therefore, focus has turned to the identification of the mutational composition inherent to colorectal cancers and development of therapeutic targeted agents. Herein, we review the most up to date systemic treatment strategies for metastatic colorectal cancer based on the actionable molecular alterations and genetic profiles of colorectal malignancies.

KEYWORDS

EGFR inhibitor, KRAS, metastatic colorectal cancer, HER2, mismatch repair

Introduction

Within the United States, colorectal cancer (CRC) continues to be a substantial source of morbidity and mortality, with an estimated 153,000 new cases diagnosed and over 52,000 deaths projected in 2023 alone (1). Nearly a quarter of patients are afflicted with metastatic disease (mCRC) at disease presentation, while another 20% of patient initially diagnosed with localized disease, progressing to stage IV disease (2, 3). Stage IV disease portends a very poor prognosis, with an estimated 5-year survival rate of only 14%. While survival rates have improved within the United States and globally over the past several decades for CRC of all stages, mCRC survival rates have remained stable without significant progress (3–5). Therefore, extensive comprehension of the varying molecular and genetic profiles within mCRC and development of associated anti-neoplastic targets is pivotal to treatment advancement and improving patient outcomes. We present a review of the most current, trial-based evidence of the treatment of mCRC based on unique molecular and genetic profiles that allow for refinement and strengthening of therapeutic options for patients limited cytotoxic therapy options.

EGFR inhibitors

The role of EGFR in cellular signaling and its inhibition

The propagation of many known human neoplasms are driven by activation of epidermal growth factor receptor (EGFR) and its subsequential signaling pathways (6). Binding of an activating ligand to EGFR results in phosphorylation of EGFR tyrosine kinase, triggering downstream signaling pathways involved in cellular proliferation and metabolism. EGFR is involved in several pathways, including the phosphatidylinositol 3-kinase (PI3K)/Akt/mammalian target of rapamycin (mTOR) pathway as well as the RAS/RAF/mitogen-activated protein kinase (MAPK) pathway (7). Activation or dysregulation of the of these pathways or imbalance of the sensitive feedback loops results in transcription of genes promoting cell survival, anti-apoptosis, proliferation, angiogenesis and metastatic potential (6, 8).

Cetuximab and panitumumab are monoclonal antibodies used in the treatment of metastatic colon cancer, directed against EGFR. Cetuximab is a chimeric IgG-1 monoclonal antibody while panitumumab is a recombinant humanized IgG-2 kappa monoclonal antibody, both working to competitively inhibit the extracellular ligand of EGFR, limiting the aforementioned abnormal cellular signaling that result in tumorigenesis (9). Although considered equivalent in their efficacy, cetuximab has been shown to have a higher incidence of hypersensitivity reactions, with an estimated risk ratio of 5.47. This hypersensitivity was shown likely to be secondary to previously developed IgE antibodies against galactose-alpha-1,3-galactose present on the Fab portion of the cetuximab heavy chain. The prevalence of this pre-existing IgE antibody is higher in the Southeastern United states, thought related to regional exposure (10).

EGFR inhibitors and efficacy based on *RAS* mutational status

Mutations in genes (notably *KRAS*, *NRAS*, and *BRAF*) that encode proteins involved in EGFR-mediated cellular signaling pathways are associated with a lack of response to anti-EGFR therapy in mCRC (11–17). Mutations in the *RAS* family of genes result in protein expression that lead to inappropriate constitutive activation of the RAS/RAF/MAPK signaling that is less likely to be affected by inhibition of the upstream interaction of EGFR with an activating ligand. Thus, testing for these mutations is essential to ensure patients whose tumors harbor these mutations are not subjected to ineffective therapy with potentially severe toxicity and expense.

The first study to evaluate the use of EGFR inhibition in mCRC was in 2008, comparing the cetuximab use of cetuximab versus best supportive care (Table 1). The authors found that patients with wild

TABLE 1 Pivotal Clinical Trials in Metastatic Colorectal Cancer categorized by tumor characteristics.

Trial Name	Target Tumor Characteristics	Therapy Line	Arms	Primary Outcomes	Secondary Outcomes
Open-Label Phase III Trial (NCT00113763)	*KRAS*	Second and beyond	Investigational Arm: Panitumumab as an intravenous (IV) infusion at a dose of 6 mg/kg once every 2 weeks until participants develop progressive disease or are unable to tolerate study drug. Participants will also receive best supportive care as judged appropriate by the investigator and according to institutional guidelines Comparison Arm: Best supportive care	Median Progression Free Survival (mPFS): 8.0 v 7.3 weeks; Hazard Ratio (HR): 0.54 (95% CI, 0.44 to 0.66; p < 0.0001)	Overall Survival (OS): 30 vs 31 weeks (HR: 1.00; 95% CI, 0.82 to 1.22)
CAN-NCIC-CO17 (NCT00079066)	*KRAS*	Refractory or ineligible for fluoropyrmidine, irinotecan and oxaliplatin	Arm A: Patients receive an initial loading dose of cetuximab IV over 120 minutes on day 1. Patients continue to receive maintenance infusions of cetuximab IV over 60 minutes weekly. Patients also receive best supportive care, defined as measures designed to provide palliation of symptoms and improve quality of life as much as possible. Arm B: Patients receive best supportive care as in Arm A. In both arms, treatment continues in the absence of disease progression or unacceptable toxicity.	*KRAS wt* Median Overall Survival (mOS): 9.5 vs 4.8, HR: 0.55 (95% CI, 0.41 to 0.74; p<0.001); no significant difference in *mutated KRAS* tumors OS reported	*KRAS wt* mPFS: 3.7 vs 1.9, HR:0.40 (95% CI, 0.03 to 0.54; p<0.001); no significant difference in *mutated KRAS* tumors PFS reported
PRIME (NCT00364013)	*KRAS Wild-type (wt)*	First	Investigational Arm: panitumumab IV infusion at a dose of 6 mg/kg on Day 1 and FOLFOX chemotherapy regimen on Days 1 and 2 of each 14-day cycle until disease progression or unacceptable toxicity Comparison Arm: FOLFOX chemotherapy regimen on Days 1 and	mPFS: 9.6 v 8.0 months; HR: 0.80 (95% CI, 0.66	mOS: 23.9 v 19.7 months; HR: 0.83 (95% CI, 0.67 to

(Continued)

TABLE 1 Continued

Trial Name	Target Tumor Characteristics	Therapy Line	Arms	Primary Outcomes	Secondary Outcomes
			2 of each 14-day cycle until disease progression or until unacceptable toxicity	to 0.97; p = 0.02)	1.02; p = 0.072)
FIRE-3 (NCT00433927)	*KRAS wt*	First	Arm A: standard standard FOLFIRI regimen consisting of 5-fluorouracil (5-FU), leucovorin and irinotecan plus cetuximab as an IV infusion of 400 mg/m2 at inittal infusion then 250 mg/m2 on day 1 and 8 of each cycle Arm B: standard FOLFIRI regimen plus bevacizumab as an IV infusion at a dose of 5mg/kg on day 1	Objective Response Rate (ORR): 62.0% v 58.0%; HR 1.18 (95% CI, 0.85 to 1.64; p = 0.18)	mPFS: 10.0 v 10.3 months, HR 1.06 (95% CI, 0.88 to 1.26; p = 0.55); mOS: 28.7 vs 25.0 months, HR 0.77 (95% CI, 0.62 to 0.96; p = 0.017)
CALGB/SWOG 80405 (NCT00265850)	*KRAS wt*	First	Investigational Arm: Patients receive cetuximab 400mg/m^2 IV over 2 hours on the first day of treatment, then 250 mg/m^2 IV over 1 hour weekly thereafter. Patients also receive either FOLFOX or FOLFIRI every two weeks as described in the intervention section. One cycle is defined as 8 weeks of treatment. Comparison Arm: bevacizumab 5 mg/kg IV every two weeks and then receive either FOLFOX or FOLFIRI every two weeks as described in the intervention section. One cycle is defined as 8 weeks of treatment.	mOS: 30.0 vs 29.0 months; HR 0.88 (95% CI, 0.77 to 1.01; p = 0.08)	mPFS: 10.5 v 10.6 months; HR 0.95 (95% CI, 0.84 to 1.08; p = 0.45)
PARADIGM (NCT02394795)	*KRAS wt*	First	Investigational Arm: 6mg/kg FOLFOX plus panitumumab Comparison Arm: 5mg/kg FOLFOX plus bevacizumab	mOS: 36.2 v 31.3; HR 0.84 (95% ci, 0.72 to 0.98; P = 0.030); *KRAS wt* left-sided tumors only mOS: 37.9 v 34.3 months; HR 0.82 (95.798% CI, 0.68 to 0.99; p = 0.031)	
20050181 (NCT00339183)	*KRAS wt*	Second	Investigational Arm: panitumumab as an IV infusion at a dose of 6 mg/kg plus a standard FOLFIRI regimen consisting of 5-fluorouracil (5-FU), leucovorin and irinotecan. Treatment was administered in cycles every two weeks Comparison Arm: standard chemotherapy regimen (FOLFIRI) consisting of 5-FU, leucovorin and irinotecan. Treatment is administered in cycles every two weeks	mPFS: 6.7 v 4.9 months; HR: 0.82 (95% CI, 0.69 to 0.97; p = 0.023);	mOS: 14.5 v 12.5 months; HR 0.92 (95% CI, 0.78 to 1.10; p = 0.37)
KRYSTAL-1 (NCT03785249)	*KRAS G12C mutated*	Chemotherapy-refractory	Phase dose exploration and tolerability of Adagrasib; combination dosing with Pembrolizumab, Cetuximab, or Afatinib	ORR: 46% (95% CI, 28 to 66) v 19% (95% CI, 8 to 33) ; mPFS: 6.9 (95% CI, 5.4 to 9.1) v 5.6 months (95% CI, 4.1 to 8.3)	mDOR: 7.6 (95% CI, 5.7 to not yet reached) v 4.3 months (95% CI, 2.3 to 8.3)
CodeBreaK 100 (NCT03600883)	*KRAS G12C mutated*	Chemotherapy-refractory	Phase dose exploration and tolerability of Sotorasib	ORR: 9.7% (95% CI, 3.6 to 19.9)	
MOUNTAINEER (NCT03043313)	*HER2+, RAS wt*	Chemotherapy-refractory	Cohort A (non-randomized): tucatinib twice per day orally on Days 1-21 and trastuzumab IV on Day 1. Cycles repeat every 21 days. Cohort B (randomized): tucatinib twice per day orally on Days 1-21 and trastuzumab intravenously (into the vein; IV) on Day 1. Cycles repeat every 21 days. Cohort C (randomized): tucatinib twice per orally every day.	ORR: 38% (95% CI: 28, 49)	mDoR: 12.4 months; 95% CI, 8.5 to 20.5 ; mPFS: 8.2 month (95% CI, 4.2 to

(Continued)

TABLE 1 Continued

Trial Name	Target Tumor Characteristics	Therapy Line	Arms	Primary Outcomes	Secondary Outcomes
			Participants who do not respond to therapy may have the option to receive tucatinib and trastuzumab.		10.3); mOS: 24.1 months (95% CI 20.3 to 36.8)
HERACLES (NCT03225937)	*HER2 +, RAS wt*	Refractory or ineligble for fluoropyrmidine, irinotecan, oxaliplatin, EGFR inhibtors	Arm A: lapatinib 1000 mg daily per os + trastuzumab 4 mg/kg IV load, followed by 2 mg/kg IV weekly. Arm B: pertuzumab 840 mg iv load, followed by 420 mg iv Q3weeks + trastuzumab-emtansine 3.6 mg/kg iv on day 1 of each subsequent 3 week cycle.	Arm A: ORR: 28%.; Arm B: ORR: 9.7% (95% CI: 0 to 28)	Arm A: mPFS: 4.7 months (95% CI, 3.7–6.1). mOS: 10.0 months (95% CI, 7.9–15.8); Arm B: mPFS: 4.1 months (95% CI: 3.6 to 5.9) Stable Disease (SD): 67.7% (95% CI: 50 to 85)
BEACON (NCT02928224)	*BRAF V600E mutated*	Second and beyond	Investigational Triplet Arm:Encorafenib, (orally once daily) plus binimetinib (orally twice daily) plus cetuximab (standard of care regimen) Investigational Doublet Arm: Encorafenib (orally once daily) plus cetuximab (standard of care regimen) Comparison Arm: Cetuximab plus either FOLFIRI or irinotecan	Arm A: mOS: 9.0 v 5.4 months; HR 0.52; 95% CI, 0.39 to 0.70; p< 0.001 ; Arm B: mOS: 8.4 v 5.4 months; HR 0.60; 95% CI, 0.45 to 0.79; P < 0.001	
CheckMate 142 (NCT02060188)	MSI-H/dMMR	First-line	Cohort A: Nivolumab Monotherapy Cohort B: Nivolumab + Ipilimumab Cohort C: Nivolumab + Ipilimumab Cohort D: Nivolumab + Ipilimumab + Cobimetinib Cohort E: Nivolumab + BMS-986016 Cohort F: Nivolumab + Daratumumab	ORR: 69% (95% CI, 53 to 82)	DCR: 84% (95% CI, 70.5 to 93.6)
KEYNOTE-177 (NCT02563002)	MSI-H/dMMR	First-line	Investigational Arm: pembrolizumab 200 mg IV on Day 1 of each 21-day cycle for up to 35 treatments (approximately 2 years). Participants that have stopped the initial course of pembrolizumab and have stable disease but progress after discontinuation can initiate a second course of pembrolizumab for up to 17 cycles (approximately 1 year additional). Comparative Arm: Participants receive 1 of 6 possible standard chemotherapy regimens. Participants with documented disease progression following chemotherapy can crossover to receive pembrolizumab for up to 35 cycles (approximately 2 years). Participants that have stopped pembrolizumab and have stable disease but progress after discontinuation can initiate a second course of pembrolizumab for up to 17 cycles (approximately 1 year additional).	mOS: not reached v 36.7 months; HR 0.74 (95% CI, 0.53 to 10.3; p = 0.036); mPFS: 16.5 vs 8.2 months; HR 0.59 (95% CI, 0.45 to 0.79)	
CORRECT (NCT01103323)	No specified criteria	Chemotherapy-refractory	Investigational Arm: Regorafenib 160 mg per oral once daily for 3 weeks on 1 week off of every 4 week cycle plus Best Supportive Care Comparison Arm: placebo tablets per oral once daily for 3 weeks on 1 week off of every 4 week cycle plus Best Supportive Care	mOS: 6.4 v 5.0 months; HR 0.77 (95% CI, 0.64 to 0.96; p = 0.0005)	
FRESCO-2 (NCT04322539)	No specified criteria	Chemotherapy-refractory	Investigational Arm: Fruquintinib plus best supportive care Comparison Arm: Best supportive care	mOS: 7.4 v 4.8 months; HR 0.66 (95% CI, 0.55 to 0.80; p < 0.001)	mPFS: 3.7 v 1.8 months; HR 0.32 (95% CI, 0.27 to 0.39; p = 0.002)

type KRAS tumors had a significantly improved OS (9.5 *vs* 4.8 months HR0.55; 95% CI 0.41-0.74) with the use of cetuximab, versus no difference in survival or PFS for those with KRAS mutated tumors (Table 1). This was followed by studies investigating EGFR inhibition in combination with cytotoxic chemotherapy (14).

A retrospective analysis of three randomized controlled trials compared the outcomes of patients with mCRC who received chemotherapy or best supportive care with or without panitumumab in various lines of therapy, concluding patients with *KRAS* mutated mCRC were unlikely to benefit from EGFR inhibitors (Table 1) (18). Similarly, a subset analysis of patients enrolled in the CRYSTAL trial, which randomized untreated patients with mCRC to receive FOLFIRI either with or without cetuximab, found that patients with *KRAS* wild-type exon 2 tumors who received FOLFIRI and cetuximab experienced a longer median PFS compared to those who received FOLFIRI alone (9.9 *vs* 8.7 months; HR 0.68; 95% CI 0.50–0.94; p = 0.02) (12). An updated analysis of data from the CRYSTAL trial showed longer overall survival (OS) in patients who received cetuximab (23.5 *vs* 20.0 months; p = 0.009), a benefit largely derived by patients with *RAS* wild-type tumors (HR 0.69; 95% CI 0.54–0.88). Those with *RAS*-mutated tumors did not derive a survival benefit (1.05; 95% CI 0.86–1.28) (19, 20). This effect was also observed in the phase III PRIME trial, which compared groups of patients with untreated mCRC who received FOLFOX with or without panitumumab (Table 1). Among patients with wild-type *KRAS* and *NRAS* mCRC, improvements in PFS (HR 0.72; 95% CI 0.58–0.90; p = 0.004) and OS (HR 0.77; 95% CI 0.64–0.94; p = 0.009) were seen in patients who received FOLFOX plus panitumumab. Importantly, PFS was found to be worse in patients whose tumor harbored a *KRAS/NRAS* mutation (11, 21). The results reflect the current clinical practice of ensuring patients with *RAS* wild type tumors are provided anti-EGFR therapy, and that these therapies are avoided in those with a *RAS* mutated tumors due to lack efficacy or potentiation of worse outcomes. Please reference Figure 1 for the suggested treatment algorithm based on mutational status.

EGFR inhibition and primary tumor sidedness

The impact of EGFR inhibitors and the side of primary colon tumor is associated with treatment response, or lack thereof. This is believed to be a result of tumor sidedness being a surrogate for differing cumulative molecular subtypes (22).

In a multicenter analysis of 75 patients with *RAS* and *BRAF* wild-type mCRC who received cetuximab alone, panitumumab alone, or irinotecan plus cetuximab (in any line of therapy), no responses were observed in patients who had right-sided primary tumors while a response rate of 41% was seen in patients with left-sided primary tumors (p = 0.003). Progression free survival (PFS) (2.3 *vs* 6.6 months) was also longer in patients with left-sided tumors (HR 3.97; 95% CI 2.09–7.53; p < 0.0001) (23).

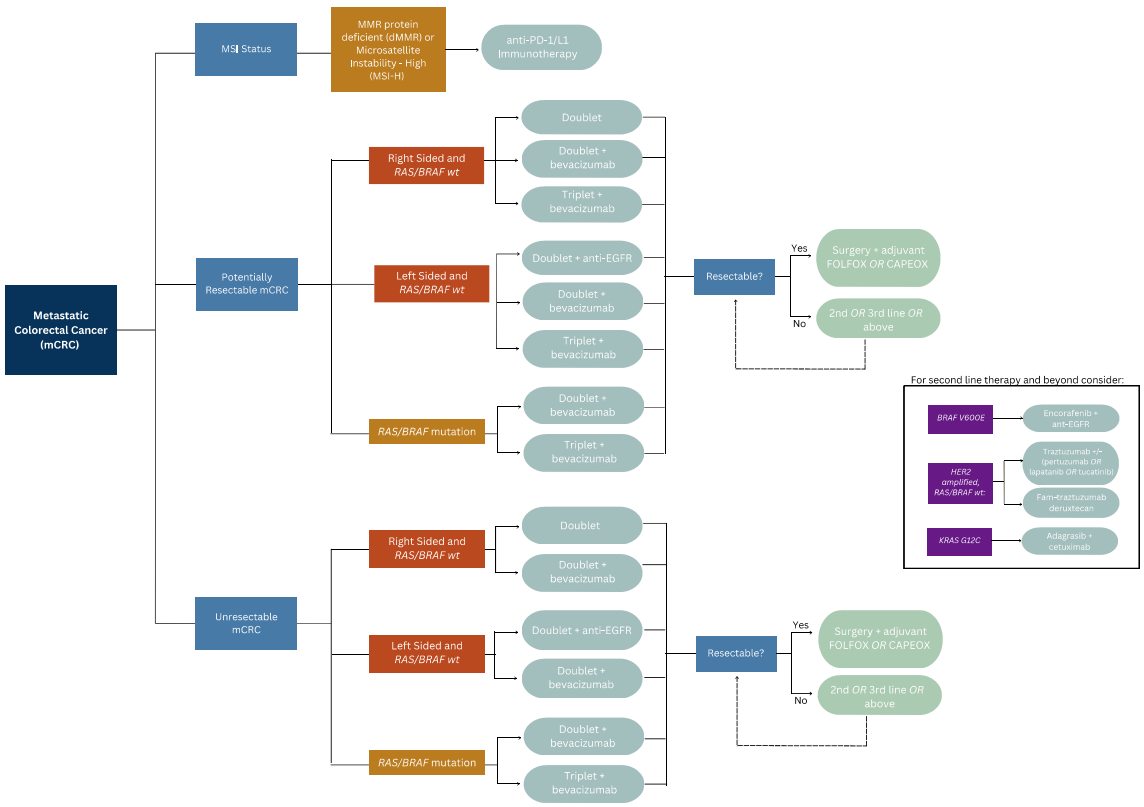

FIGURE 1
Flowchart depicting treatment options for mCRC based on tumor mutational status.

This phenomenon was demonstrated in retrospective evaluations of landmark CRC trials. First, in the CRYSTAL trial, referenced above, which randomized patients to FOLFIRI plus cetuximab versus FOLFIRI alone, and the FIRE-3 trial comparing FOLFIRI plus cetuximab versus FOLFIRI plus bevacizumab, patients with *RAS* wild type left sided tumors had had superior objective response rate (ORR), PFS and OS with the addition of cetuximab, in contrast to minimal efficacy seen in right sided wild type tumors (Table 1) (12, 24, 25). The CALGB/SWOG 80405 not only demonstrated poorer prognosis associated with right sided CRC, but *KRAS* wild type right sided tumors had significantly worse median OS relative to left sided *KRAS* wild type tumors when treated with cetuximab and chemotherapy (16.7 months (95% CI 13.1-19.4) *vs* 36 months (95% CI 32.6-40.3) (Table 1) (26). Most recently, the phase III, open-label multicenter PARADIGM trial was designed to determine the superiority of anti-EGFR therapy or anti-vascular endothelial growth factor (anti-VEGF) therapy when added to modified FOLFOX6 in *RAS* wild type mCRC (Table 1). This showed an improvement in overall survival by 3.6 months in patients with left sided tumors that were treated with panitumumab compared to bevacizumab (27).

EGFR inhibitors and conversion to resectable disease

EGFR inhibitors, when combined with chemotherapy, have also shown an ability to increase the possibility of liver metastases resection in patients with *RAS* wild-type mCRC. In a randomized trial from China, the addition of cetuximab to chemotherapy resulted in 20 of 70 (29%) of patients becoming eligible for hepatic resection compared to 9 of 58 (13%) of patients who did not receive cetuximab. R0 resection rates were 25.7% in cetuximab arm compared to 7.4% in those who didn't receive cetuximab ($p < 0.01$). Additionally, surgery improved median survival compared to those who did not receive surgery in the cetuximab arm (46.6 *vs* 25.7 months; $p = 0.007$) and the control arm (36.0 *vs* 19.6 months; $p = 0.016$) (28). In the VOLFI phase II trial, 75% of patients with *RAS* wild-type mCRC and liver metastases deemed potentially resectable were successfully converted to resectable disease upon receiving FOLFOXIRI with panitumumab compared to 36.4% in group of patients who received FOLFOXIRI alone. ORR was higher in the panitumumab arm, while PFS and OS were similar between both arms, with OS trend in favor of the arm that received panitumumab (29).

EGFR inhibitors in patients with refractory disease

For patients with wild-type *KRAS/NRAS/BRAF* mCRC whose disease progressed on a therapeutic regimen that contained an EGFR inhibitor, the use of an EGFR inhibitor as part of therapy in the next line is generally not recommended. However, if these patients' first-line regimen did not include an EGFR inhibitor, there is evidence that use of an EGFR inhibitor in the subsequent line of therapy is beneficial. For example, in a phase III trial analyzing wild-type *KRAS* exon 2 tumors that exhibited disease progression on oxaliplatin-based and irinotecan-based chemotherapy, panitumumab monotherapy was compared to best supportive care. This trial demonstrated an overall survival benefit of nearly 3 months with the use of panitumumab (10.0 *vs* 7.4 months; HR 0.73; 95% CI 0.57–0.93; $p < 0.01$) (30). Not all studies evaluating EGFR inhibitors in this setting have improved overall survival, however. In Study 20050181, the addition of panitumumab to FOLFIRI compared to FOLFIRI alone in patients with mCRC who had wild-type *KRAS* exon 2 tumors resulted in an improvement in median PFS (6.7 *vs* 4.9 months; HR 0.82; 95% CI 0.69–1.10; $p = 0.023$) but no difference in OS (median 14.5 *vs*. 12.5 months; HR 0.92; 95% CI 0.78–1.10; $p = 0.37$) (Table 1) (31, 32). In the EPIC trial, which compared irinotecan plus cetuximab to irinotecan alone as second line treatment in patients with mCRC who progressed on first-line fluoropyrimidine and oxaliplatin based therapy, both ORR and median PFS, were significantly improved in the combination group (PFS 5.4 *vs* 2.6 months (95% CI 0.46-0.69), ORR 29.4% *vs* 5.0% (95% CI 4.04-17.40) respectively). There was no statically significant difference in median OS between arms, however, a post study treatment analysis indicated improvement in OS in those who received post-study cetuximab relative to those who received subsequent therapy without cetuximab or no therapy at all. Importantly, quality of life was found to be improved in the combination arm, including improvement in physical functioning, nausea, vomiting, appetite loss and pain (33, 34).

Chemotherapy choice when used in conjunction with EGFR inhibitors

There is conflicting data to suggest that oxaliplatin-based chemotherapy regimens reduce the efficacy of cetuximab in patients with untreated *RAS* wild-type mCRC. In the phase II OPUS trial, patients with mCRC and *KRAS* wild-type exon 2 tumors who received FOLFOX plus cetuximab in the first-line setting did not derive a statistically significant benefit with regard to OS compared to patients who received FOLFOX alone (22.8 *vs* 18.5 months; HR 0.85; $p = 0.39$) (16, 35). The lack of survival benefit when cetuximab is added to oxaliplatin-based regimens was also observed in the phase III MRC COIN trial, in which patients with *KRAS* wild-type mCRC or locally advanced disease who received cetuximab and either FOLFOX or CAPEOX did not have longer OS relative to patients who received chemotherapy alone (17.9 *vs* 17.0 months; HR 1.04; 95% CI 0.87–1.23; $p = 0.67$). However, a subgroup analysis of this trial indicated that those who received FOLFOX, rather than CAPEOX, might have experienced a benefit (36).

In contrast to the above findings, the results found by the phase III TAILOR trial, showed prolonged PFS (9.2 *vs* 7.4 months; $p = 0.004$) and OS (20.7 *vs* 17.8 months $p = 0.02$), and ORR (61.1% *vs* 39.5%; $p < 0.001$) among patients with untreated *RAS* wild-type mCRC who received cetuximab with FOLFOX compared to those who received FOLFOX alone (37). The results of the PARADIGM trial discussed above also demonstrated opposing results, with

significantly improved OS in *RAS* wild type, left sided tumors with the use of oxaliplatin based therapy with the addition of panitumumab. Given these mixed results, suggested clinical practice is such that in the treatment of left sided *RAS* wild type tumors, the use of anti-EGFR therapy in conjunction with irinotecan or oxaliplatin based chemotherapy backbone is standard, with backbone choice based on individual patient co-morbidities and side effect profile.

Efficacy of EGFR inhibition in patients with *BRAF* mutations

BRAF encodes a protein that functions downstream of *RAS* in the EGFR-mediated signaling pathway and, when mutated, is constitutively active (3, 27). Therefore, upstream EGFR inhibition alone is not thought to prevent abnormal signaling mediated by *BRAF* mutations.

Specifically, *BRAF V600E* mutations result in the inappropriate activation of MAPK independently of RAS (38). Abnormal regulation of these pathways is invariably linked to carcinogenesis (4). Given this downstream effect, inhibition of EGFR presents little utility in the setting of concurrent RAS wild type and BRAF mutated CRC.

Approximately five to nine percent of patients with mCRC have *BRAF* V600E mutations, which do not typically occur in co-existence with *RAS* mutations (39). In subset analyses of patients in the aforementioned PRIME trial, as well as the COIN trial, *BRAF* mutations were not found to be predictive of response to the combination of chemotherapy and an EGFR inhibitor in patients with untreated mCRC (24). One meta-analysis that included 463 patients with *BRAF* mutant mCRC including nine phase III trials and one phase II trial with mCRC concluded that the addition of an EGFR inhibitor did not improve PFS (HR 0.88; 95% CI 0.67–1.14; p = 0.33) or OS (HR 0.91; 95% CI 0.62–1.34; p = 0.63) (29). Another meta-analysis of seven randomized control trials (RCT) found EGFR inhibitors did not improve PFS (HR 0.86; 95% CI 0.61–1.21) or OS (HR 0.97; 95% CI 0.67–1.41) in patients with *BRAF* mutations (30). Therefore, the use of ant-EGFR therapy in the setting of BRAF mutations is of little to no efficacy.

VEGF inhibitors

The role of VEGF in cellular signaling

Vascular endothelial growth factor (VEGF) is a protein that, upon binding to VEGF receptors 1 and 2 on the surface of endothelial cells, promotes tumor angiogenesis by promoting permeability, survival, and proliferation of endothelial cells. VEGF is expressed in the majority of human malignancies, while having little role in normal physiological angiogenesis. The activity of VEGF is inhibited by bevacizumab, a humanized monoclonal antibody against circulating VEGF-A, that has become a mainstay adjunctive therapy in the treatment of mCRC (40, 41).

Bevacizumab as part of first-line therapy

Several trials have investigated the efficacy of adding bevacizumab to chemotherapy in patients with untreated mCRC and have displayed varying results. Pooled results from several phase II trials of patients with untreated mCRC have indicated that OS was prolonged by the addition of bevacizumab to 5-flurouracil (5-FU)/leucovorin with or without irinotecan (42–44). A combined analysis of the results of these trials showed that adding bevacizumab to 5-FU/leucovorin improved median survival compared to 5-FU/leucovorin or irinotecan without bevacizumab (17.9 *vs* 14.6 months; p = 0.008) (45). In patients 70 years and older with untreated mCRC, the addition of bevacizumab to capecitabine prolonged PFS compared to capecitabine alone (9.1 *vs* 5.1 months; HR 0.53; 95% CI 0.41–0.69; p < 0.0001) in the AVEX trial (46).

Chemotherapy choice when used in conjunction with bevacizumab

A meta-analysis of six RCTs encompassing a total of 3,060 patients showed that the addition of bevacizumab to chemotherapy in the first line setting prolonged PFS (HR 0.72; 95% CI 0.66–0.78; p < 0.00001) and OS (HR 0.84; 95% CI 0.77–0.91; p < 0.00001) relative to chemotherapy alone (47). Subgroup analyses, however, indicated that this addition was largely limited to patients who received irinotecan-based regimens. This result was also reflected in a SEER analysis which showed the addition of bevacizumab to oxaliplatin-based chemotherapy did not improve OS but did improve OS for patients who received irinotecan (48). Additionally, in a large phase III trial, PFS, but not OS, was prolonged by 1.4 months by addition of bevacizumab to oxaliplatin-based chemotherapy (HR 0.83; 97.5% CI 0.72–0.95; p = 0.0023) in patients with untreated mCRC, yet a subset analysis suggested that those who received CAPEOX (rather than FOLFOX) were most likely to experience that benefit (49). To date, no trials have compared FOLFIRI to FOLFIRI plus bevacizumab or FOLFOXIRI to FOLFOXIRI plus bevacizumab. Despite the results discussed above, clinical practice prioritizes the use of bevacizumab in those with RAS mutant or right sided RAS wild type metastatic colon cancers in patients without contraindications to its use.

Bevacizumab and conversion to resectable disease

Few trials have been conducted to investigate the utility of bevacizumab in the peri-operative setting. The BECOME trial specifically evaluated the role of bevacizumab, in conjunction with FOLFOX, in the conversion of unresectable mCRC to resectable disease in patients with unresectable liver-limited mCRC. This trial found that the addition of bevacizumab to FOLFOX improved the rate at which patients underwent R0 hepatic resection (22.3% *vs* 5.8%; p < 0.01) (50). The multinational phase II OLIVIA trial sought to evaluate if the role of bevacizumab to either FOLFOX or FOLFOXIRI to facilitate

oligometastatic resection in patients initially determined to have unresectable liver metastasis. The combination of FOLFOXIRI with bevacizumab resulted in higher ORR (81% (95% CI 65-91) *vs* 62% (95% CI 45-77), rate of resection (61% (95% CI 45-76) *vs* 49% (95% CI 32-65)), R0 resection rate (49% *vs* 23%) and median PFS (18.6 (95% CI 12.9-22.3) *vs* 11.5 months (95% CI 9.6-13.6)) relative to bevacizumab plus FOLFOX. These response rates were at the expense of higher grade ≥3 adverse events, including neutropenia (50% *vs* 35%), febrile neutropenia (13% *vs* 8%), and diarrhea (30% *vs* 14%) (51).

In the post-operative setting, the HEPATICA trial was designed to evaluate DFS in patents with mCRC who received CAPEOX with or without bevacizumab after resection of liver metastases. Unfortunately, due to low accrual and subsequent study closure no statistically significant conclusion was able to be drawn. However, the group who received CAPEOX and bevacizumab demonstrated higher scores related to quality of life than patients who received CAPEOX alone (52).

Bevacizumab as maintenance therapy

The utility of administering bevacizumab after disease stability has been achieved with chemotherapy-based regimens has been studied in several large trials with conflicting results. The CAIRO3 trial, analyzing patients with mCRC deemed to have at least stable disease after first-line treatment with CAPEOX and bevacizumab, were assigned to receive either maintenance capecitabine plus bevacizumab or observation. At time of progression, patients in both groups subsequently received CAPEOX plus bevacizumab until their disease progressed further. The study found that time to second progression was improved in patients who received maintenance capecitabine plus bevacizumab compared to those who were randomized to observation (8.5 *vs* 11.7 months; HR 0.67; 95% CI 0.56–0.81; $p < 0.0001$). No significant difference in OS was observed, although a trend towards improved OS was seen in patients who received maintenance capecitabine plus bevacizumab (53, 54). AIO 0207 trial showed bevacizumab alone was non-inferior to fluorouracil plus bevacizumab in time to first progression (HR 1.08; 95% CI 0.85–1.37; $p = 0.53$). Additionally, this study indicated that no treatment in the maintenance setting was not non-inferior to either bevacizumab alone or fluorouracil plus bevacizumab in patients who previously received induction therapy with oxaliplatin-based chemotherapy plus bevacizumab (55).

The previously mentioned data supporting maintenance bevacizumab conflicts with the outcome of PRODIGE9, which found that bevacizumab did not improve tumor control duration (15.08 *vs* 14.98 months HR 1.09; 95% CI 0.87–1.37), PFS (9.20 *vs* 8.90 months; HR 0.92; 95% CI 0.76–1.10), or OS (21.65 *vs* 21.98 months; HR 1.05; 95% CI 0.86–1.28) relative to no maintenance treatment among patients initially treated with FOLFIRI and bevacizumab (56). Similarly, the SAKK 41/06 trial found that non-inferiority in time to progression was not reached when comparing maintenance bevacizumab to no maintenance treatment in patient previously receiving previous chemotherapy plus bevacizumab (4.1 *vs* 2.9 months; HR 0.74; 95% CI 0.58–0.96) (57).

Maintenance bevacizumab was compared to maintenance bevacizumab plus erlotinib, an EGFR inhibitor, in the GERCOR DREAM; OPTIMOX3 trial. Median PFS from maintenance was not significantly different but trended towards use of both drugs (5.4 *vs* 4.9 months; stratified HR 0.81; 95% CI 0.66–1.01; $p = 0.059$) while median OS from maintenance was longer in patients that received both bevacizumab and erlotinib (24.9 *vs* 22.1 months; stratified HR 0.79; 95% CI 0.63–0.99; $p = 0.036$). However, Grade 3-4 adverse effects occurred in 21% of patients who received bevacizumab plus erlotinib compared to 0% of patients who received bevacizumab alone (58). Due to these significantly higher adverse effects of this combination in the setting of non-curative disease, the erlotinib is not routinely used in the maintenance setting. In clinical practice, largely based on the CAIRO3 study, de-escalated chemotherapy plus bevacizumab is safely and effectively used in the maintenance setting.

Bevacizumab in patients with refractory disease

Single agent bevacizumab is not recommended after progression on chemotherapy is generally not recommended due to inferior efficacy compared to chemotherapy alone or chemotherapy plus bevacizumab. Several trials have evaluated the efficacy of bevacizumab, in conjunction with chemotherapy, in patients with mCRC who experienced progression on first-line chemotherapy. In the ML18147 trial, patients with mCRC who progressed on first-line chemotherapy and bevacizumab were subsequently randomized to a different chemotherapy backbone with or without bevacizumab. Patients who were provided bevacizumab saw a statistically significant OS benefit (11.2 *vs* 9.8 months; HR 0.81; 95% CI 0.69–0.94; $p = 0.0062$) (59). The benefit of continuing bevacizumab, with a different chemotherapeutic regimen, in the second-line setting after progression on a regimen containing bevacizumab was also observed in the BEBYP trial, noting a longer PFS in patients who were continued on a regimen that contained bevacizumab (6.8 *vs* 5.0 months; HR 0.70; 95% CI 0.52–0.95; $p = 0.001$) (60). Further, adding bevacizumab to second-line FOLFOX for patients with mCRC who progressed on first-line irinotecan-based therapy that did not include bevacizumab was the focus of Study E3200. An improvement in median duration of survival was seen in the patients treated with second line FOLFOX plus bevacizumab compared to FOLFOX alone (12.9 *vs* 10.8 months; HR 0.75; $p = 0.0011$) (61). Retrospective and observational analyses also concur that continuation of bevacizumab after progression first-line chemotherapy containing bevacizumab provides a survival benefit (62, 63).

Ziv-aflibercept

Ziv-aflibercept is a recombinant protein designed to inhibit angiogenesis by preventing VEGF -A, B and placental growth factor from activating VEGF receptors. This novel drug evaluated in the phase III VELOUR trial studying its use in conjunction with FOLFIRI in patients with mCRC who had prior disease

progression on oxaliplatin-based chemotherapy. OS was longer in patients who received FOLFIRI and ziv-aflibercept compared to FOLFIRI alone (13.5 *vs* 12.1 months; HR 0.82; 95% CI 0.71–0.94; p = 0.003) (64). Overall, clinical practice favors bevacizumab use in this setting due to its superior toxicity profile and lower cost.

Ramucirumab

Ramucirumab, a human IgG-1 monoclonal antibody against the extracellular portion of the VEGF receptor 2, has been studied in the chemotherapy refractory setting combined with cytotoxic regimens. In the phase III RAISE trial, patients with mCRC who had disease progression on FOLFOX and bevacizumab were randomized to FOLFIRI with or without ramucirumab. Patients in the ramucirumab arm experienced longer OS (13.3 *vs* 11.7 months; HR 0.84; 95% CI 0.73–0.98; p = 0.02) although therapy was discontinued more frequently in the group that received ramucirumab (11.5% *vs* 4.5%), most frequently secondary to neutropenia, thrombocytopenia, stomatitis and diarrhea (65). As a result of this study, the addition of ramucirumab to irinotecan or FOLFIRI for patients with refractory mCRC not previously exposed to irinotecan-based therapy is considered an acceptable regimen. However, bevacizumab remains most utilized clinically.

Regorafenib

Regorafenib is a multi-targeted tyrosine kinase inhibitor (TKI) that blocks interactions of ligands with VEGF, PDGF, BRAF, KIT, and RET and has been studied primarily in patients with refractory mCRC. Its broad receptor influence modulates downstream pathways involved in angiogenesis, cell growth, differentiation, and survival. The CORRECT trial evaluated the administration of regorafenib or placebo to patients with refractory mCRC whose disease had progressed on several lines of chemotherapy (Table 1). The study indicated prolonged OS in patients who received regorafenib (6.4 *vs* 5.0 months; HR 0.77; 95% CI 0.64–0.94); p = 0.005) (66). The CONCUR trial conducted in Asia observed this similar outcome, with prolonged OS with use of regorafenib compared to placebo in the refractory setting (8.8 *vs* 6.3 months; HR 0.55; 95% CI 0.40–0.77; p < 0.001) (67). Hand-foot skin reaction was the most frequent grade 3 (or higher) adverse effect and occurred in 17% of patients who received regorafenib in this trial. Other, but less common grade 3 (or higher) adverse effects included fatigue, hypertension, diarrhea, rash/desquamation. The ReDos trial utilized a dose-escalation of regorafenib to mitigate toxicity, while maintaining efficacy, however, adverse events remained significant (68). Due to the findings in these two trials, regorafenib is considered an accepted treatment regimen for patients with mCRC whose disease has progressed on chemotherapy, but its side effect profile warrants careful monitoring while on therapy.

Fruquintinib

Fruquintinib is a highly selective TKI that blocks VEGFR-1, VEGFR-2, and VEGFR-3 which was recently evaluated in the phase III FRESCO 2 trial, which randomized patients with refractory, previously treated mCRC (Table 1). Patients were allowed to have received prior trifluridine/tipiracil and/or regorafenib (median lines of therapy 5) to receive either best supportive care with or without fruquintinib. Patients who received fruquintinib experienced prolonged OS (7.4 *vs* 4.8 months; HR 0.66; 95% CI 0.55–0.80; p < 0.001 and PFS (3.7 *vs* 1.8 months; HR 0.32; 95% CI 0.27–0.39; p < 0.001). Grade 3 or higher adverse effects were seen in 62.7% of patients who received fruquintinib compared to 50.4% in patients who received placebo. Specific side effects seen in over 5% of patients were hand-foot syndrome, asthenia, and hypertension (69). Importantly, 97% of enrolled patients had received prior bevacizimab. Fruquitinib can be used after progression on other VEGF inhibitors including bevacizumab and regorafenib.

EGFR inhibitors versus bevacizumab

RAS mutational status and tumor sidedness impact the efficacy of bevacizumab and EGFR inhibitors in the first-line setting. As previously mentioned, in the CALGB/SWOG 80405 trial, no statistically significant OS benefit (30.0 *vs* 29.0 months; HR 0.88; 95% CI 0.77–1.01; p = 0.08) was seen among patients with wild-type *KRAS* exon 2 mCRC who received first-line chemotherapy (either FOLFOX or FOLFIRI) with cetuximab versus bevacizumab (70). However, patients with *RAS* wild-type, right-sided mCRC who received bevacizumab in the first-line setting showed a trend toward longer OS than those who received cetuximab (HR 1.36; 95% CI 0.93–1.99; p = 0.10). Conversely, patients with *RAS* wild-type, left-sided primary tumors who received cetuximab had significantly longer overall survival than those who received bevacizumab (HR 0.77; 95% CI 0.59–0.99; p = 0.04) (71).

In contrast, the FIRE-3 trial found an improvement in OS among patients who received first line FOLFIRI plus cetuximab compared to FOLFIRI plus bevacizumab (28.7 *vs* 25.0 months; HR 0.77; 95% CI 0.62–0.96; p = 0.017) in patients with *KRAS* exon 2 wild type mCRC (24, 72). However, trial has been criticized for its lack of third-party review and low rate of administration of second-line therapy (70). Improved efficacy with an EGFR inhibitor was also seen in the phase II PEAK trial, in which patients with wild-type *RAS* who received FOLFOX with panitumumab had longer PFS (12.8 *vs* 10.1 months; HR 0.68; 95% CI 0.48–0.96; p = 0.029) than patients who received FOLFOX and bevacizumab, although some have argued the small sample size limit its generalizability (73, 74). The more recent PARADIGM trial, discussed above, which compared FOLFOX plus panitumumab to FOLFOX plus bevacizumab in the first line for patients with *RAS* wild-type mCRC, showed longer OS for patients with left sided tumors using panitumumab (37.9 *vs* 34.3 months; HR 0.82; 95% CI 0.68–0.99; p =. 0.031) (27).

In the second-line setting, there is a paucity of data comparing bevacizumab and EGFR inhibitors. In the phase II SPIRITT trial, treatment with FOLFIRI plus panitumumab did not yield longer PFS survival compared to FOLFIRI plus bevacizumab in patients with *KRAS* wild type mCRC whose disease progressed on first-line oxaliplatin-based chemotherapy and bevacizumab (7.7 months *vs* 9.2 months; HR 1.01; 95% CI 0.68–1.50; p = 0.97) (75).

Combination EGFR and VEGF inhibition

The combination of EGFR and VEGF inhibition has shown efficacy in preclinical setting, finding improved survival and tumor inhibition in mouse models (76, 77). Given these findings and the proven benefit of the addition of EGFR or VEGF to cytotoxic therapy, investigators sought to determine the utility of VEGF in conjunction EGFR therapies in the metastatic setting.

The addition of bevacizumab and panitumumab to chemotherapy in first-line treatment of patients with mCRC (of all *KRAS* mutational subtypes) was studied in the phase III PACCE trial. Patients received chemotherapy and bevacizumab with or without panitumumab. The addition of panitumumab resulted in higher toxicity and shorter PFS (10.0 *vs* 11.4 months; HR 1.27; 95% CI 1.06–1.52), regardless of *KRAS* mutational status (78). The CAIRO2 trial came to a similar conclusion, with the addition of cetuximab to CAPEOX plus bevacizumab yielded a higher incidence of grade 3-4 toxicity (81% *vs* 72%; p = 0.03) and shorter PFS (9.4 *vs* 10.7 months; HR 1.22; 95% CI 1.04–1.43) (79). No difference in PFS between groups was observed among patients with wild-type KRAS tumors.

Conversely, the phase II randomized BOND-2 study investigated the use of cetuximab and bevacizumab in irinotecan-refractory mCRC. This study indicated that the addition of cetuximab and bevacizumab to irinotecan in this patient population resulted in improved time to progression (7.3 *vs* 4.9 months), improved response rate (37% *vs* 20%) and an overall survival benefit (14.5 *vs* 11.4 months) relative to cetuximab and bevacizumab alone, and without unexpected or higher rates of toxicity (80).

Due to the incidence of adverse effects experienced by patients in the PACCE and CAIRO2 trials, as well as the lack of efficacy, it is not recommended to combine these two drug classes within the same line of therapy.

BRAF inhibitors

Treatment for *BRAF* V600E mutation positive disease in non-first line setting

Inhibition of BRAF has been primarily studied in second line or greater setting. For patients with mCRC whose tumors contain *BRAF* V600E mutations with progression on first or second-line therapy, a triplet of therapy comprising encorafenib, a BRAF inhibitor, plus binimetinib, a MEK inhibitor, and cetuximab was compared to the doublet of encorafenib and cetuximab as well as to cetuximab plus either irinotecan or FOLFIRI in the BEACON trial (Table 1). Treatment with the triplet or doublet led to an OS benefit relative to treatment with cetuximab plus either irinotecan or FOLFIRI (9.3 *vs* 9.3 *vs* 5.9 months, respectively). Grade 3 adverse effects occurred more commonly in patients who received the triplet than those who received the doublet (58% *vs* 50%). Therefore, to limit toxicity while maintaining efficacy, doublet therapy (encorafenib plus either cetuximab or panitumumab) is recommended (81).

Irinotecan plus cetuximab and vemurafenib, a BRAF inhibitor, was evaluated in the treatment refractory setting, indicating improvement in PFS and disease control rate compared to irinotecan plus cetuximab alone in this population (82). To mitigate EGFR-mediated adaptive feedback reactivation of MAPK signaling, different combinations of dabrafenib, a BRAF inhibitor, panitumumab, and trametinib, a MEK inhibitor, were studied in patients with *BRAF* V600E mutation positive mCRC, with variable response rates. The triplet combination of these therapies was found to have the highest response rate (21%), but has not been adopted as a standard of care (83).

BRAF inhibitors in the first-line setting

Due to the significantly worse OS and limited response to standard first line therapy of BRAF mutated mCRC, BRAF inhibitors are also being studied in the first-line systemic therapy for patients with *BRAF* V600E mutated mCRC. The BREAKWATER trial (NCT040607421) is a phase 3 trial investigating the efficacy and safety of encorafenib, cetuximab, and either FOLFIRI or FOLFOX in patients with untreated *BRAF* V600E mutated mCRC. Additionally, the SEAMARK trial (NCT05217446) is a phase 2 trial comparing the combination of encorafenib, cetuximab, and pembrolizumab, an inhibitor of programmed death-1 receptor, to pembrolizumab alone in patients with untreated deficient mismatch repair (dMMR) and *BRAF* V600E mutated mCRC. Results are still pending for both trials.

Anti-HER2 therapy

HER2 in colorectal cancer

Human epidermal growth factor receptor 2 (HER2), which is encoded by the proto-oncogene *ErbB2* (also known as *HER2*), is a member of the same family of signaling kinase receptors as EGFR. Dimerization of HER2 with other members of the EGFR family results in activation of several downstream signaling pathways, including RAS/RAF/ERK, PI3K/AKT/mTOR, and JAK/STAT3 (84, 85). *HER2* is not commonly amplified or overexpressed in CRC with a prevalence estimated at 3 to 5%, however, is more frequently amplified or overexpressed in *RAS*/*BRAF* wild type tumors (86). HER2 has become one of the latest areas of study in targeted medicine within colorectal cancer. HER2 amplification or overexpression may predispose to the development of resistance upon treatment with an EGFR inhibitor for patients with *RAS*/*BRAF* wild type mCRC (83, 87). The prognostic value of HER2 expression or amplification is not well defined, however attempts to understand its impact have been performed. Specifically, In a cohort of patients with *RAS*/*BRAF* wild type mCRC whose treatment regimen included an EGFR inhibitor, median PFS was shorter among those with HER2 amplification compared to those without HER2 amplification (2.8 *vs* 8.1 months; HR 7.05; 95% CI 3.4–14.9; p < 0.001) (88). At this time, HER2-directed therapy is generally

recommended in patients with *HER2*-amplified mCRC whose disease has progressed on systemic cytotoxic therapy, only to be considered first-line for patients who are not appropriate for cytotoxic therapy.

Trastuzumab-based therapy

The combination of two HER2-directed monoclonal antibodies, trastuzumab and pertuzumab, has been studied in two basket studies of patients with HER2-amplified cancers. In refractory HER2-amplified mCRC, an ORR of 23.1% (95% CI 18.1%–28.7%) and DCR of 44.2% (95% CI 38.1%–50.5%) was observed among 57 patients in the MyPathway study while an ORR of 14% (90% CI 4%–33%) and disease control rate of 50% (90% CI 36%–60%) was seen in 28 patients in the TAPUR study. Grade 3 or 4 AEs were limited, noted in up to 37% of patients in the MyPathway study while two patients in the TAPUR study developed grade 3 AEs (86, 89).

Trastuzumab has also been studied in combination with several other agents in this setting. The phase II HERACLES trial studied 27 patients with refractory HER2-positive, KRAS wild type mCRC who received trastuzumab plus the oral tyrosine kinase inhibitor lapatinib targeting EGFR1 and HER2 (Table 1). Nearly one third of patients had an object response (30% 95% CI 14%–50%), with 22% of patients experiencing grade 3 AEs, without any grade 4 events (90–92). Additionally, the efficacy of fam-trastuzumab deruxtecan, an antibody drug conjugate containing anti-HER2 antibody and a cytotoxic topoisomerase I inhibitor linked by a cleavable tetrapeptide linker, was the focus of the phase II DESTINY-CRC01 trial. 78 patients with refractory HER2-expressing, *BRAFV600E* and *RAS* wild type mCRC were stratified into three groups based on HER2 expression. Responses were only seen in patients with high tumoral HER2 expression (IHC3+ or IHC2+/ISH+), with an ORR of 45.3% (95% CI 31.6%–59.6%) and PFS 6.9 months (95% CI 4.1–8.7 months). Importantly, these responses were seen regardless of previous exposure to HER2 directed therapy. Unfortunately, 65.1% of the studied patients experienced grade 3 or higher AEs. Specifically, 9% of patients developed life threatening interstitial lung disease, with 3 fatalities (93).

More recently, The MOUNTAINEER trial evaluated the combination of trastuzumab and the HER2 selective tyrosine kinase inhibitor tucatinib (Table 1). Over 100 patients with refractory HER2-positive, *RAS* wild type mCRC were stratified to receive trastuzumab plus tucatinib or tucatinib monotherapy, with cross over permitted to the combination arm upon progression. 84 patients received trastuzumab and tucatinib, with an ORR of 38.1%, median duration of response of 12.4 months, median PFS of 8.2 months, and median OS of 24.1 months. Tucatinib monotherapy had a limited objective response of 3%, with no PFS or OS reported due to extensive cross over into the combination arm. This regimen had a superior side effect profile relative to other HER2 directed strategies, noting minimal grade 3 events, only 5 patients discontinuing therapy due to adverse effects, and no treatment related deaths (94). The results led to expedited FDA approval for this combination in refractory mCRC, and the phase III MOUNTAINEER-03 trial (NCT05253651), is ongoing, comparing trastuzumab plus FOLFOX to either FOLFOX, FOLFOX plus bevacizumab, or FOLFOX plus cetuximab for patients with untreated HER2-positive mCRC.

KRAS G12C

With the recognition of inferior outcomes utilizing EGFR inhibition in *KRAS* mutated CRC, it has become standard of care to test for RAS mutations *via* next generation sequencing prior to initiation of systemic therapy if possible. It is estimated that half of CRC harbor a KRAS mutation, varying in frequency amongst ethnicities KRAS mutation, with multiple studies suggesting associated worse prognosis (95–99).

A specific mutation within this family, *KRASG12C*, found in an estimated 3% of metastatic CRC, has shown to have poorer OS relative to other KRAS mutated CRC by up 10 months (99). However, this mutation has recently been found to be a valuable target for systemic therapy across various histologies and within CRC. CodeBreaK100, a phase II single arm trial published in 2021, used the irreversible *KRASG12C* protein inhibitor sotorasib in solid tumors harboring the KRASG12C mutation, including 62 CRC patients previously treated with 5-FU, oxaliplatin and irinotecan. In the CRC cohort, a modest 9.7% of patients had an objective response, not reaching primary endpoint of an 20% objective response rate (100).

This lack of response in the CRC relative to other histologies such as non-small lung cancer, is related to several factors including upstream basal receptor tyrosine kinase activation interfering with *KRASG12C* inhibitors and feedback suppression of the MAPK signaling with KRAS inhibition. Most clinically relevant, however, is the downstream activation of *KRASG12C* from high levels of EGFR signaling. Therefore, it was postulated, and shown in KRAS CRC cell line analysis, that concomitant EGFR and *KRAS G12C* blockade overcomes secondary resistance to anti-EGFR antibodies, increasing cell death rate (101). This concept led to the KRYSTAL-1 trial, a phase 1-2 open label non-randomized trial of patients with pre-treated *KRAS G12C* mutated CRC in which patients were provided adagrasib, an oral small molecule inhibitor of *KRAS G12C* protein in combination with cetuximab or adagrasib monotherapy (Table 1). The combination therapy had a statistically significant higher response rate (46% *vs* 19%), median duration of response (7.6 *vs* 4.3 months), and median PFS (6.9 *vs* 5.6 months), with a lower percentage of grade 3 or 4 treatment related adverse events (102). Additionally, the currently ongoing phase II clinical trial CodeBreaK 101, subprotocol H is attempting to combine sotorasib with panitumumab (Table 1) (100). Targeted therapy of KRASG12C in combination with ant-EGFR therapy appears to be a promising late-line therapy in patients harboring this mutation, improving response rates and PFS in patients that otherwise would be very limited in remaining effective treatment options.

DNA mismatch repair and microsatellite unstable tumors

The advent of immune checkpoint and its application in tumors deficient in mismatch repair (dMMR) has resulted in significant

improvement not only in the treatment efficacy but quality of life of the estimated 15% of colorectal cancer patients with this alteration. Mismatch repair genes including MLH1 (human mutL homolog 1), MSH2 (human mutS homolog 2), MSH6 (humab mutS homolog 6) and PMS2 (human postmeiotic segregation 2) are committed to mending errors during DNA replication such as incorrect base pairing, deletions or insertions (103–105). Up to eighty percent of cases are sporadic in etiology, secondary to epigenetic influences *via* the lack of methylation or excess methylation of DNA or DNA promotor regions respectively (106–110). This is in contrast to germline mutations within MMR genes, seen in hereditary forms of dMMR, leading to lack gene expression as seen in Lynch syndrome (111, 112). MMR deficiency lends tumor cells to amass large amounts of errors within DNA, developing microsatellites of repeated nucleotide bases that can result in significant abnormalities in DNA promoters responsible for cell proliferation, hence the term high microsatellite instability or MSI-H (108, 113).

The use of immunotherapy, specifically, anti-programmed cell death 1 monoclonal antibodies (anti-PD-1) in mCRC was first demonstrated in the treatment refractory setting. Specifically, in the 2015 phase II study of pembrolizumab monotherapy at 10mg/kg every 2 weeks in patients with treatment refractory dMMR mCRC, dMMR metastatic noncolorectal and MMR proficient (pMMR) mCRC, those with dMMR mCRC demonstrated an 89% DCR, and 50% ORR, relative to pMMR patients who had 16% DCR and 0% ORR. At a nearly 6-month treatment duration, PFS and OS were not reached in the dMMR group *vs* a PFS and OS of 2.3 months and 7.6 months respectively in the pMMR group (114). Based on these results, the authors opened the phase II open label, multicenter KEYNOTE 164 trial (Tables 1, 2). In this study, patients with treatment refractory dMMR mCRC were provided pembrolizumab at 200mg every 3 weeks. OR was 33% in patients with ≥2 lines of therapy (cohort A) or ≥ 1 line of therapy (cohort B), with median OS of 31.4 months (95% CI 21.4 to 8.1months) in cohort A and not reached (95% CI 19.2 to not reached) in cohort B at a median follow up of 31.3 months (115). These results significantly contributed to the FDA approval of pembrolizumab for patients with dMMR or MSI-H disease that progressed on prior cytotoxic chemotherapy.

Similarly, the PD-1 inhibitor, nivolumab, received expedited approval the same year for treatment refractory dMMR or MSI-H mCRC based on the CheckMate 142 trial, in addition to its combination with ipilimumab (cytotoxic T-lymphocyte associated antigen-4 inhibitor) the following year (Tables 1, 2). In this phase II, non-randomized multicohort study, patients with progressive dMMR mCRC were provided 3mg/kg nivolumab every 3 weeks

TABLE 2 Treatment of Metastatic MSI-H or dMMR.

Trial	KEYNOTE 177	CheckMate 142
Phase	Randomized; III	Non-randomized; II
Eligibility	Untreated MSI-H or dMMR Metastatic disease	MSI-H or dMMR Untreated *in the metastatic setting**
Line of Therapy	1st	1+ (1st treatment in metastatic disease)
Intervention vs Control	Pembrolizumab 200mg q3weeks vs mFOLFOX6 or FOLFIRI q2weeks +/- cetuximab q1week or +/-bevacizumab q2weeks	Nivolumab 3 mg/kg q2weeks and Ipilimumab 1 mg/kg q6weeks
Enrollment	307 patients -Pembrolizumab: 153 -Chemotherapy: 154	45 patients
Crossover Allowed	Yes	N/A
Objective Response Rate	Pembrolizumab: 44% Chemotherapy: 33%	Investigator assessment: 69% Blinded central review: 62%
Progression Free Survival	Pembrolizumab: 16.5 months (95% CI 5.4-38.1) Chemotherapy: 8.2 months (95% CI 6.1-10.2)	Not reached 24 month PFS rate: 73.6%
Median Overall Survival*	Pembrolizumab: Not Reached(95% CI 49.2–NR) Chemotherapy: 36.7 months (95% CI 27.6–NR)	Not reached 24-month OS rate: 79.4%
Grade ≥ 3 AE	Pembrolizumab: 22% No treatment related deaths Chemotherapy: 66% Treatment related deaths: 1	22% No treatment related deaths

-KEYNOTE 177: Median follow up of 44.5 months.
-CheckMate 142: Median follow up 29 months.
*40% of patients had prior adjuvant or neoadjuvant therapies.
N/A means not applicable.

and ipilimumab (CTLA-4 inhibitor) 1mg/kg every 3 weeks for 4 doses followed by nivolumab 3mg/kg every 2 weeks until disease progression, death or unacceptable toxicity, or nivolumab monotherapy 3mg/kg every 2 weeks. First analyzed and reported were the results from the nivolumab monotherapy arm, indicating that at a median follow up of 12 months, 69% (95% CI 57-79) of the 74 patients had disease control for 12 weeks or longer and 31.1% (CI 20.8-42.9) had objective response (116). In the cohorts that received both nivolumab and ipilimumab, a 4 year follow up has been reported. At a median follow up of 50.9 months, OR was seen in 65% of patients (95% CI 55%-73%), and a disease control of greater than or equal to 12 weeks was seen in 81% of patients (95% CI 72%-87%). Although median PFS and OS were not reached, 48-month PFS and OS percentage were 53% (95% CI 43-62) and 71% (95% CO 61-78) respectively (117). Notably, responses mentioned in both CheckMate 142 analyses responses were seen regardless of PD-L1 status, *BRAF* or *KRAS* status. Although no direct comparison has been made between dual checkpoint inhibitors versus immunotherapy monotherapy, risks and benefits must be weighed in this treatment refractory setting given the higher frequency of immune related toxicity with combination therapy (118).

Importantly, however, it has been concluded that early identification of MSI-H/dMMR tumors and subsequent first line treatment with immunotherapy in mCRC has improved responses relative to first line cytotoxic chemotherapy. First, the use of pembrolizumab monotherapy was analyzed in the phase III open label, randomized trial, assigning untreated patients with dMMR/MSI-H mCRC to pembrolizumab 200mg every 3 weeks or standard of care chemotherapy with 5-FU based therapy with oxaliplatin or irinotecan. Of note, cross over to pembrolizumab was allowed after disease progression. At a median follow up of 32.4 months, OR was seen in 43.8% in the pembrolizumab cohort *vs* 33.1% in those treated with chemotherapy. PFS was significantly longer in the pembrolizumab cohort versus chemotherapy at 16.5 months *vs* 8.2 months respectively (HR 0.6, 95% CI 0.95 0.45 to 0.80). Those patients that had complete or partial response to therapy, 83% of patients in the pembrolizumab arm had continued response at 24 months relative to 35% of patients in the

TABLE 3 Early Phase and Developing Studies of Immunotherapy in MSI-Stable Disease.

Trial	NCT 04126733	NCT 04362839	NCT 03860272**
Phase	Open Label; II	Non-randomized; I	Expanded phase Ia/Ib
Eligibility	Previously treated MSS/pMMR Metastatic disease	Previously treated MSS/pMMR Metastatic disease	Previously treated MSS/pMMR Metastatic disease
Line of Therapy	>2 for RAS mutant >3 RAS wild type	1+	1+
Intervention vs Control	Regorafenib 80 mg/day 3 weeks on, 1 week off *increase to 120mg daily on C2 if well tolerated and Nivolumab 480mg q4 weeks	Regorafenib 80mg/day (Recommended phase II dosing determination) 3 weeks on, 1 week off and Nivolumab 240mg q2weeks and Ipilimumab 1 mg/kg q6weeks	Botensilimab 1 mg or 2 mg (or 150mg) q6 weeks and Balstilimab 3mg/kg (or 450mg) q2 weeks
Enrollment	94 patients 70 treated	39 patients	59 patients
Crossover Allowed	N/A	N/A	From monotherapy to combination
Objective Response Rate	7% (p = 0.27)	27.6% (all patients) 36.4% (without liver metastasis)	22% (all patients) (95% CI 12-35) -1 mg/kg: 38% -2 mg/kg: 20%
Progression Free Survival	1.8 months (95% CI 1.8-2.4)	4 months (all patients) (IQR 2-9 months) 5 months (without liver metastasis) (IQR 2-11 months)	Not available
Median Overall Survival	11.9 months (95% CI 7.0-not evaluable)	20 months (IQR 7 months – not estimable) >22 months	12 month OS: 61% (95% CI 42-75)
Grade ≥ 3 AE	Grade 3: 40% Grade 4: 3% Grade 5: 3%	N/A *No dose de-escalation needed at 80mg	Grade 3: 32% Grade 4: 2% Grade 5: 0%

IQR, Interquartile range.
**Open label Phase II multicenter study is currently active and enrolling.
N/A means not applicable.

chemotherapy arm. Importantly, pembrolizumab resulted in less grade 3-5 adverse events relative to standard chemotherapy (22% *vs* 66%), and improved health related quality of life (119, 120). There was a trend toward overall survival benefit with the use of pembrolizumab, but this result was skewed due to 60% of patients treated with chemotherapy crossing over to pembrolizumab (121). Due to these results, the American Society of Clinical Oncology 2022 guidelines recommended that patients with dMMR mCRC should be offered pembrolizumab monotherapy as first line therapy if eligible (122).

A subset of CheckMate 142 analyzed 45 patients with MSI-H/dMMR mCRC that were treatment naive. These patients were treated with nivolumab 3mg/kg every 2 weeks plus ipilimumab 1mg/kg every 6 weeks, with both drugs continued until disease progression. At a median follow up of 29 months, disease control rate was 84% (95 CI 70.5 vs 93.5), and ORR was 69% (95% CI 53-82), with 13% of patients having a complete response. Median PFS and OS was not reached (123). With these results, nivolumab with or without ipilimumab are considered first line therapy options in patients with dMMR/MSI-H mCRC, however, pembrolizumab remains the preferred regimen.

Under active study is the use of immunotherapy for patients with metastatic, chemo-refractory, microsatellite stable (MSS) disease. Early phase studies suggest that combination of the multikinase inhibitor regorafenib with immunotherapy provide objective response and improvement in PFS and OS. Table 3 compares completed phase I and II studies of this combination along with a phase Ia/Ib study of the novel therapy botensilimab, an antibody directed against T-cell receptor cytotoxic T-lymphocyte-associated antigen 4 in combination with the novel monoclonal PD-1 antibody balstilimab (124–127).

Discussion

The utilization of molecular and genetic tumor analysis of patients with mCRC has become increasingly paramount to optimize first line treatment, allow for thoughtful pursuit of subsequent line therapy, and improve overall survival for patients with mCRC. It has become evident that proper use of adjunctive therapies added to established cytotoxic chemotherapy, particularly monoclonal antibodies, can provide meaningful impact on the survival to patients with mCRC. Continued investigation of novel mutational targets is necessary to further the quality of life and survival benefits already demonstrated by harnessing the inhibition of HER2, KRAS G12C, BRAF, VEGF and EGFR. As additional therapeutic molecular and genetic targets are discovered, easily accessible and rapidly resulting testing modalities, such as next generation sequencing, need to be made available for all oncology centers to provide optimal and equitable oncology care to all patients.

Author contributions

All authors contributed to the article and approved the submitted version.

Conflict of interest

The authors declare that the research was conducted in the absence of any commercial or financial relationships that could be construed as a potential conflict of interest.

Publisher's note

References

1. Siegel RL, Miller KD, Wagle NS, Jemal A. Cancer statistics, 2023. *CA Cancer J Clin* (2023) 73(1):17–48. doi: 10.3322/caac.21763

2. Riihimaki M, Hemminki A, Sundquist J, Hemminki K. Patterns of metastasis in colon and rectal cancer. *Sci Rep* (2016) 6:29765. doi: 10.1038/srep29765

3. National Cancer Institute. *SEER cancer stat facts: colorectal cancer* (2022). Available at: https://seer.cancer.gov/statfacts/html/colorect.html.

4. Jiang Y, Yuan H, Li Z, Ji X, Shen Q, Tuo J, et al. Global pattern and trends of colorectal cancer survival: a systematic review of population-based registration data. *Cancer Biol Med* (2021) 19(2):175–86. doi: 10.20892/j.issn.2095-3941.2020.0634

5. Crooke H, Kobayashi M, Mitchell B, Nwokeji E, Laurie M, Kamble S, et al. Estimating 1- and 5-year relative survival trends in colorectal cancer (CRC) in the united states: 2004 to 2014. *J Clin Oncol* (2018) 36(4_suppl):587–. doi: 10.1200/JCO.2018.36.4_suppl.587

6. Krasinskas AM. EGFR signaling in colorectal carcinoma. *Patholog Res Int* (2011) 2011:932932. doi: 10.4061/2011/932932

7. Li QH, Wang YZ, Tu J, Liu CW, Yuan YJ, Lin R, et al. Anti-EGFR therapy in metastatic colorectal cancer: mechanisms and potential regimens of drug resistance. *Gastroenterol Rep* (2020) 8(3):179–91. doi: 10.1093/gastro/goaa026

8. Samatar AAP, Poulikos I. Targeting RAS-ERK signalling in cancer: promises and challenges. *Nat Rev Drug Discovery* (2014) 13(12):928–42. doi: 10.1038/nrd4281

9. Li S, Schmitz KR, Jeffrey PD, Wiltzius JJW, Kussie P, Ferguson KM. Structural basis for inhibition of the epidermal growth factor receptor by cetuximab. *Cancer Cell* (2005) 7(4):301–11. doi: 10.1016/j.ccr.2005.03.003

10. Chung CH, Mirakhur B, Chan E, Le QT, Berlin J, Morse M, et al. Cetuximab-induced anaphylaxis and IgE specific for galactose-alpha-1,3-galactose. *N Engl J Med* (2008) 358(11):1109–17. doi: 10.1056/NEJMoa074943

11. Douillard J-Y, Oliner KS, Siena S, Tabernero J, Burkes R, Barugel M, et al. Panitumumab–FOLFOX4 treatment and RAS mutations in colorectal cancer. *New Engl J Med* (2013) 369(11). doi: 10.1056/NEJMoa1305275

12. Van Cutsem E, Kohne CH, Hitre E, Zaluski J, Chang Chien CR, Makhson A, et al. Cetuximab and chemotherapy as initial treatment for metastatic colorectal cancer. *N Engl J Med* (2009) 360(14):1408–17. doi: 10.1056/NEJMoa0805019

13. Tejpar S, Celik I, Schlichting M, Sartorius U, Bokemeyer C, Van Cutsem E. Association of KRAS G13D tumor mutations with outcome in patients with metastatic colorectal cancer treated with first-line chemotherapy with or without cetuximab. *J Clin Oncol* (2012) 30(29):3570–7. doi: 10.1200/JCO.2012.42.2592

14. Karapetis CS, Khambata-Ford S, Jonker DJ, O'Callaghan CJ, Tu D, Tebbutt NC, et al. K-Ras mutations and benefit from cetuximab in advanced colorectal cancer. *N Engl J Med* (2008) 359(17):1757–65. doi: 10.1056/NEJMoa0804385

15. De Roock W, Piessevaux H, De Schutter J, Janssens M, De Hertogh G, Personeni N, et al. KRAS wild-type state predicts survival and is associated to early radiological

response in metastatic colorectal cancer treated with cetuximab. *Ann Oncol* (2008) 19 (3):508–15. doi: 10.1093/annonc/mdm496

16. Bokemeyer C, Bondarenko I, Makhson A, Hartmann JT, Aparicio J, de Braud F, et al. Fluorouracil, leucovorin, and oxaliplatin with and without cetuximab in the first-line treatment of metastatic colorectal cancer. *J Clin Oncol* (2009) 27(5):663–71. doi: 10.1200/JCO.2008.20.8397

17. Lièvre A, Bachet JB, Boige V, Cayre A, Le Corre D, Buc E, et al. KRAS mutations as an independent prognostic factor in patients with advanced colorectal cancer treated with cetuximab. *J Clin Oncol* (2008) 26(3):374–9. doi: 10.1200/JCO.2007.12.5906

18. Peeters M, Douillard JY, Van Cutsem E, Siena S, Zhang K, Williams R, et al. Mutant KRAS codon 12 and 13 alleles in patients with metastatic colorectal cancer: assessment as prognostic and predictive biomarkers of response to panitumumab. *J Clin Oncol* (2013) 31(6):759–65. doi: 10.1200/JCO.2012.45.1492

19. Láng I, Köhne CH, Folprecht G, Rougier P, Curran D, Hitre E, et al. Quality of life analysis in patients with KRAS wild-type metastatic colorectal cancer treated first-line with cetuximab plus irinotecan, fluorouracil and leucovorin. *Eur J Cancer* (2013) 49 (2):439–48. doi: 10.1016/j.ejca.2012.08.023

20. Van Cutsem E, Köhne CH, Láng I, Folprecht G, Nowacki MP, Cascinu S, et al. Cetuximab plus irinotecan, fluorouracil, and leucovorin as first-line treatment for metastatic colorectal cancer: updated analysis of overall survival according to tumor KRAS and BRAF mutation status. *J Clin Oncol* (2011) 29(15):2011–19. doi: 10.1200/JCO.2010.33.5091

21. Douillard JY, Siena S, Cassidy J, Tabernero J, Burkes R, Barugel M, et al. Randomized, phase III trial of panitumumab with infusional fluorouracil, leucovorin, and oxaliplatin (FOLFOX4) versus FOLFOX4 alone as first-line treatment in patients with previously untreated metastatic colorectal cancer: the PRIME study. *J Clin Oncol* (2010) 28(31):4697–705. doi: 10.1200/JCO.2009.27.4860

22. Yaeger R, Chatila WK, Lipsyc MD, Hechtman JF, Cercek A, Sanchez-Vega F, et al. Clinical sequencing defines genomic landscape metastatic colorectal cancer. *Cancer Cell* (2018) 33(1):125–36.e3. doi: 10.1016/j.ccell.2017.12.004

23. Moretto R, Cremolini C, Rossini D, Pietrantonio F, Battaglin F, Mennitto A, et al. Location of primary tumor and benefit from anti-epidermal growth factor receptor monoclonal antibodies in patients with RAS and BRAF wild-type metastatic colorectal cancer. *Oncologist*. (2016) 21(8):988–94. doi: 10.1634/theoncologist.2016-0084

24. Heinemann V, von Weikersthal LF, Decker T, Kiani A, Vehling-Kaiser U, Al-Batran SE, et al. FOLFIRI plus cetuximab versus FOLFIRI plus bevacizumab as first-line treatment for patients with metastatic colorectal cancer (FIRE-3): a randomised, open-label, phase 3 trial. *Lancet Oncol* (2014) 15(10):1065–75. doi: 10.1016/S1470-2045(14)70330-4

25. Tejpar S, Stintzing S, Ciardiello F, Tabernero J, Van Cutsem E, Beier F, et al. Prognostic and predictive relevance of primary tumor location in patients with RAS wild-type metastatic colorectal cancer: retrospective analyses of the CRYSTAL and FIRE-3 trials. *JAMA Oncol* (2017) 3(2):194–201. doi: 10.1001/jamaoncol.2016.3797

26. Venook AP, Niedzwiecki D, Lenz HJ, Innocenti F, Fruth B, Meyerhardt JA, et al. Effect of first-line chemotherapy combined with cetuximab or bevacizumab on overall survival in patients with KRAS wild-type advanced or metastatic colorectal cancer: a randomized clinical trial. *JAMA* (2017) 317(23):2392–401. doi: 10.1001/jama.2017.7105

27. Yoshino T, Uetake H, Tsuchihara K, Shitara K, Yamazaki K, Watanabe J, et al. PARADIGM study: a multicenter, randomized, phase III study of mFOLFOX6 plus panitumumab or bevacizumab as first-line treatment in patients with RAS (KRAS/NRAS) wild-type metastatic colorectal cancer. *J Clin Oncol* (2021) 39(3_suppl):85–. doi: 10.1200/JCO.2021.39.3_suppl.85

28. Ye LC, Liu TS, Ren L, Wei Y, Zhu DX, Zai SY, et al. Randomized controlled trial of cetuximab plus chemotherapy for patients with KRAS wild-type unresectable colorectal liver-limited metastases. *J Clin Oncol* (2013) 31(16):1931–8. doi: 10.1200/JCO.2012.44.8308

29. Modest DP, Martens UM, Riera-Knorrenschild J, Greeve J, Florschutz A, Wessendorf S, et al. FOLFOXIRI plus panitumumab as first-line treatment of RAS wild-type metastatic colorectal cancer: the randomized, open-label, phase II VOLFI study (AIO KRK0109). *J Clin Oncol* (2019) 37(35):3401–11. doi: 10.1200/JCO.19.01340

30. Kim TW, Elme A, Kusic Z, Park JO, Udrea AA, Kim SY, et al. A phase 3 trial evaluating panitumumab plus best supportive care vs best supportive care in chemorefractory wild-type KRAS or RAS metastatic colorectal cancer. *Br J Cancer* (2016) 115(10):1206–14. doi: 10.1038/bjc.2016.309

31. Peeters M, Price TJ, Cervantes A, Sobrero AF, Ducreux M, Hotko Y, et al. Randomized phase III study of panitumumab with fluorouracil, leucovorin, and irinotecan (FOLFIRI) compared with FOLFIRI alone as second-line treatment in patients with metastatic colorectal cancer. *J Clin Oncol* (2010) 28(31):4706–13. doi: 10.1200/JCO.2009.27.6055

32. Peeters M, Price TJ, Cervantes A, Sobrero AF, Ducreux M, Hotko Y, et al. Final results from a randomized phase 3 study of FOLFIRI +/- panitumumab for second-line treatment of metastatic colorectal cancer. *Ann Oncol* (2014) 25(1):107–16. doi: 10.1093/annonc/mdt523

33. Sobrero AF, Maurel J, Fehrenbacher L, Scheithauer W, Abubakr YA, Lutz MP, et al. EPIC: phase III trial of cetuximab plus irinotecan after fluoropyrimidine and oxaliplatin failure in patients with metastatic colorectal cancer. *J Clin Oncol* (2008) 26 (14):2311–9. doi: 10.1200/JCO.2007.13.1193

34. Sobrero A, Lenz HJ, Eng C, Scheithauer W, Middleton G, Chen W, et al. Extended RAS analysis of the phase III EPIC trial: irinotecan + cetuximab versus irinotecan as second-line treatment for patients with metastatic colorectal cancer. *Oncologist* (2021) 26(2):e261–e9. doi: 10.1002/onco.13591

35. Bokemeyer C, Bondarenko I, Hartmann JT, de Braud F, Schuch G, Zubel A, et al. Efficacy according to biomarker status of cetuximab plus FOLFOX-4 as first-line treatment for metastatic colorectal cancer: the OPUS study. *Ann Oncol* (2011) 22 (7):1535–46. doi: 10.1093/annonc/mdq632

36. Maughan TS, Adams RA, Smith CG, Meade AM, Seymour MT, Wilson RH, et al. Addition of cetuximab to oxaliplatin-based first-line combination chemotherapy for treatment of advanced colorectal cancer: results of the randomised phase 3 MRC COIN trial. *Lancet* (2011) 377(9783):2103–14. doi: 10.1016/S0140-6736(11)60613-2

37. Qin S, Li J, Wang L, Xu J, Cheng Y, Bai Y, et al. Efficacy and tolerability of first-line cetuximab plus leucovorin, fluorouracil, and oxaliplatin (FOLFOX-4) versus FOLFOX-4 in patients with RAS wild-type metastatic colorectal cancer: the open-label, randomized, phase III TAILOR trial. *J Clin Oncol* (2018) 36(30):3031–9. doi: 10.1200/JCO.2018.78.3183

38. Davies H, Bignell GR, Cox C, Stephens P, Edkins S, Clegg S, et al. Mutations of the BRAF gene in human cancer. *Nature* (2002) 417(6892):949–54. doi: 10.1038/nature00766

39. Wan PT, Garnett MJ, Roe SM, Lee S, Niculescu-Duvaz D, Good VM, et al. Mechanism of activation of the RAF-ERK signaling pathway by oncogenic mutations of b-RAF. *Cell.* (2004) 116(6):855–67. doi: 10.1016/S0092-8674(04)00215-6

40. Diaz-Rubio E. Vascular endothelial growth factor inhibitors in colon cancer. *Adv Exp Med Biol* (2006) 587:251–75. doi: 10.1007/978-1-4020-5133-3_20

41. Ferrara N, Hillan KJ, Gerber HP, Novotny W. Discovery and development of bevacizumab, an anti-VEGF antibody for treating cancer. *Nat Rev Drug Discovery* (2004) 3(5):391–400. doi: 10.1038/nrd1381

42. Hurwitz H, Fehrenbacher L, Novotny W, Cartwright T, Hainsworth J, Heim W, et al. Bevacizumab plus irinotecan, fluorouracil, and leucovorin for metastatic colorectal cancer. *N Engl J Med* (2004) 350(23):2335–42. doi: 10.1056/NEJMoa032691

43. Kabbinavar FF, Schulz J, McCleod M, Patel T, Hamm JT, Hecht JR, et al. Addition of bevacizumab to bolus fluorouracil and leucovorin in first-line metastatic colorectal cancer: results of a randomized phase II trial. *J Clin Oncol* (2005) 23 (16):3697–705. doi: 10.1200/JCO.2005.05.112

44. Kabbinavar FF, Schulz J, McCleod M, Patel T, Hamm JT, Hecht JR, et al. Phase II, randomized trial comparing bevacizumab plus fluorouracil (FU)/leucovorin (LV) with FU/LV alone in patients with metastatic colorectal cancer. *J Clin Oncol* (2005) 23 (16):3697–705. doi: 10.1200/JCO.2005.05.112

45. Kabbinavar FF, Hambleton J, Mass RD, Hurwitz HI, Bergsland E, Sarkar S. Combined analysis of efficacy: the addition of bevacizumab to fluorouracil/leucovorin improves survival for patients with metastatic colorectal cancer. *J Clin Oncol* (2005) 23 (16):3706–12. doi: 10.1200/JCO.2005.00.232

46. Cunningham D, Lang I, Marcuello E, Lorusso V, Ocvirk J, Shin DB, et al. Bevacizumab plus capecitabine versus capecitabine alone in elderly patients with previously untreated metastatic colorectal cancer (AVEX): an open-label, randomised phase 3 trial. *Lancet Oncol* (2013) 14(11):1077–85. doi: 10.1016/S1470-2045(13)70154-2

47. Macedo LT, da Costa Lima AB, Sasse AD. Addition of bevacizumab to first-line chemotherapy in advanced colorectal cancer: a systematic review and meta-analysis, with emphasis on chemotherapy subgroups. *BMC Cancer* (2012) 12:89. doi: 10.1186/1471-2407-12-89

48. Meyerhardt JA, Li L, Sanoff HK, Wt C, Schrag D. Effectiveness of bevacizumab with first-line combination chemotherapy for Medicare patients with stage IV colorectal cancer. *J Clin Oncol* (2012) 30(6):608–15. doi: 10.1200/JCO.2011.38.9650

49. Saltz LB, Clarke S, Diaz-Rubio E, Scheithauer W, Figer A, Wong R, et al. Bevacizumab in combination with oxaliplatin-based chemotherapy as first-line therapy in metastatic colorectal cancer: a randomized phase III study. *J Clin Oncol* (2008) 26 (12):2013–9. doi: 10.1200/JCO.2007.14.9930

50. Tang W, Ren L, Liu T, Ye Q, Wei Y, He G, et al. Bevacizumab plus mFOLFOX6 versus mFOLFOX6 alone as first-line treatment for RAS mutant unresectable colorectal liver-limited metastases: the BECOME randomized controlled trial. *J Clin Oncol* (2020) 38(27):3175–84. doi: 10.1200/JCO.20.00174

51. Gruenberger T, Bridgewater J, Chau I, García Alfonso P, Rivoire M, Mudan S, et al. Bevacizumab plus mFOLFOX-6 or FOLFOXIRI in patients with initially unresectable liver metastases from colorectal cancer: the OLIVIA multinational randomised phase II trial. *Ann Oncol* (2015) 26(4):702–8. doi: 10.1093/annonc/mdu580

52. Snoeren N, van Hillegersberg R, Schouten SB, Bergman AM, van Werkhoven E, Dalesio O, et al. Randomized phase III study to assess efficacy and safety of adjuvant CAPOX with or without bevacizumab in patients after resection of colorectal liver metastases: HEPATICA study. *Neoplasia* (2017) 19(2):93–9. doi: 10.1016/j.neo.2016.08.010

53. Goey KKH, Elias SG, van Tinteren H, Lacle MM, Willems SM, Offerhaus GJA, et al. Maintenance treatment with capecitabine and bevacizumab versus observation in metastatic colorectal cancer: updated results and molecular subgroup analyses of the phase 3 CAIRO3 study. *Ann Oncol* (2017) 28(9):2128–34. doi: 10.1093/annonc/mdx322

54. Simkens LH, van Tinteren H, May A, ten Tije AJ, Creemers GJ, Loosveld OJ, et al. Maintenance treatment with capecitabine and bevacizumab in metastatic

colorectal cancer (CAIRO3): a phase 3 randomised controlled trial of the Dutch colorectal cancer group. *Lancet* (2015) 385(9980):1843–52. doi: 10.1016/S0140-6736(14)62004-3

55. Hegewisch-Becker S, Graeven U, Lerchenmuller CA, Killing B, Depenbusch R, Steffens CC, et al. Maintenance strategies after first-line oxaliplatin plus fluoropyrimidine plus bevacizumab for patients with metastatic colorectal cancer (AIO 0207): a randomised, non-inferiority, open-label, phase 3 trial. *Lancet Oncol* (2015) 16(13):1355–69. doi: 10.1016/S1470-2045(15)00042-X

56. A T, B J, LM K, G F, B V, T J, et al. Final results of PRODIGE 9, a randomized phase III comparing no treatment to bevacizumab maintenance during chemotherapy-free intervals in metastatic colorectal cancer. *J Clin Oncol* (2016) 34(15_supplemental):3531–31. doi: 10.1200/JCO.2016.34.15_suppl.3531

57. Koeberle D, Betticher DC, von Moos R, Dietrich D, Brauchli P, Baertschi D, et al. Bevacizumab continuation versus no continuation after first-line chemotherapy plus bevacizumab in patients with metastatic colorectal cancer: a randomized phase III non-inferiority trial (SAKK 41/06). *Ann Oncol* (2015) 26(4):709–14. doi: 10.1093/annonc/mdv011

58. Tournigand C, Chibaudel B, Samson B, Scheithauer W, Vernerey D, Mesange P, et al. Bevacizumab with or without erlotinib as maintenance therapy in patients with metastatic colorectal cancer (GERCOR DREAM; OPTIMOX3): a randomised, open-label, phase 3 trial. *Lancet Oncol* (2015) 16(15):1493–505. doi: 10.1016/S1470-2045(15)00216-8

59. Bennouna J, Sastre J, Arnold D, Osterlund P, Greil R, Van Cutsem E, et al. Continuation of bevacizumab after first progression in metastatic colorectal cancer (ML18147): a randomised phase 3 trial. *Lancet Oncol* (2013) 14(1):29–37. doi: 10.1016/S1470-2045(12)70477-1

60. Masi G, Salvatore L, Boni L, Loupakis F, Cremolini C, Fornaro L, et al. Continuation or reintroduction of bevacizumab beyond progression to first-line therapy in metastatic colorectal cancer: final results of the randomized BEBYP trial. *Ann Oncol* (2015) 26(4):724–30. doi: 10.1093/annonc/mdv012

61. Giantonio BJ, Catalano PJ, Meropol NJ, O'Dwyer PJ, Mitchell EP, Alberts SR, et al. Bevacizumab in combination with oxaliplatin, fluorouracil, and leucovorin (FOLFOX4) for previously treated metastatic colorectal cancer: results from the Eastern cooperative oncology group study E3200. *J Clin Oncol* (2007) 25(12):1539–44. doi: 10.1200/JCO.2006.09.6305

62. Grothey A, Flick ED, Cohn AL, Bekaii-Saab TS, Bendell JC, Kozloff M, et al. Bevacizumab exposure beyond first disease progression in patients with metastatic colorectal cancer: analyses of the ARIES observational cohort study. *Pharmacoepidemiol Drug Saf* (2014) 23(7):726–34. doi: 10.1002/pds.3633

63. Cartwright TH, Yim YM, Yu E, Chung H, Halm M, Forsyth M. Survival outcomes of bevacizumab beyond progression in metastatic colorectal cancer patients treated in US community oncology. *Clin Colorectal Cancer* (2012) 11(4):238–46. doi: 10.1016/j.clcc.2012.05.005

64. Van Cutsem E, Tabernero J, Lakomy R, Prenen H, Prausova J, Macarulla T, et al. Addition of aflibercept to fluorouracil, leucovorin, and irinotecan improves survival in a phase III randomized trial in patients with metastatic colorectal cancer previously treated with an oxaliplatin-based regimen. *J Clin Oncol* (2012) 30(28):3499–506. doi: 10.1200/JCO.2012.42.8201

65. Tabernero J, Yoshino T, Cohn AL, Obermannova R, Bodoky G, Garcia-Carbonero R, et al. Ramucirumab versus placebo in combination with second-line FOLFIRI in patients with metastatic colorectal carcinoma that progressed during or after first-line therapy with bevacizumab, oxaliplatin, and a fluoropyrimidine (RAISE): a randomised, double-blind, multicentre, phase 3 study. *Lancet Oncol* (2015) 16(5):499–508. doi: 10.1016/S1470-2045(15)70127-0

66. Grothey A, Van Cutsem E, Sobrero A, Siena S, Falcone A, Ychou M, et al. Regorafenib monotherapy for previously treated metastatic colorectal cancer (CORRECT): an international, multicentre, randomised, placebo-controlled, phase 3 trial. *Lancet* (2013) 381(9863):303–12. doi: 10.1016/S0140-6736(12)61900-X

67. Li J, Qin S, Xu R, Yau TC, Ma B, Pan H, et al. Regorafenib plus best supportive care versus placebo plus best supportive care in Asian patients with previously treated metastatic colorectal cancer (CONCUR): a randomised, double-blind, placebo-controlled, phase 3 trial. *Lancet Oncol* (2015) 16(6):619–29. doi: 10.1016/S1470-2045(15)70156-7

68. Bekaii-Saab TS, Ou FS, Ahn DH, Boland PM, Ciombor KK, Heying EN, et al. Regorafenib dose-optimisation in patients with refractory metastatic colorectal cancer (ReDOS): a randomised, multicentre, open-label, phase 2 study. *Lancet Oncol* (2019) 20(8):1070–82. doi: 10.1016/S1470-2045(19)30272-4

69. Dasari A, Sobrero A, Yao J, Yoshino T, Schelman W, Yang Z, et al. FRESCO-2: a global phase III study investigating the efficacy and safety of fruquintinib in metastatic colorectal cancer. *Future Oncol* (2021) 17(24):3151–62. doi: 10.2217/fon-2021-0202

70. Modest DP, Stintzing S, von Weikersthal LF, Decker T, Kiani A, Vehling-Kaiser U, et al. Impact of subsequent therapies on outcome of the FIRE-3/AIO KRK0306 trial: first-line therapy with FOLFIRI plus cetuximab or bevacizumab in patients with KRAS wild-type tumors in metastatic colorectal cancer. *J Clin Oncol* (2015) 33(32):3718–26. doi: 10.1200/JCO.2015.61.2887

71. Venook AP, Ou F-S, Lenz H-J, Kabbarah O, Qu X, Niedzwiecki D, et al. Primary (1°) tumor location as an independent prognostic marker from molecular features for overall survival (OS) in patients (pts) with metastatic colorectal cancer (mCRC): analysis of CALGB / SWOG 80405 (Alliance). *J Clin Oncol* (2017) 35(15_suppl):3503–. doi: 10.1200/JCO.2017.35.15_suppl.3503

72. Heinemann V, von Weikersthal LF, Decker T, Kiani A, Kaiser F, Al-Batran SE, et al. FOLFIRI plus cetuximab or bevacizumab for advanced colorectal cancer: final survival and per-protocol analysis of FIRE-3, a randomised clinical trial. *Br J Cancer* (2021) 124(3):587–94. doi: 10.1038/s41416-020-01140-9

73. Wolpin BM, Bass AJ. Managing advanced colorectal cancer: have we reached the PEAK with current therapies? *J Clin Oncol* (2014) 32(21):2200–2. doi: 10.1200/JCO.2014.55.6316

74. Rivera F, Karthaus M, Hecht JR, Sevilla I, Forget F, Fasola G, et al. Final analysis of the randomised PEAK trial: overall survival and tumour responses during first-line treatment with mFOLFOX6 plus either panitumumab or bevacizumab in patients with metastatic colorectal carcinoma. *Int J Colorectal Dis* (2017) 32(8):1179–90. doi: 10.1007/s00384-017-2800-1

75. Hecht JR, Cohn A, Dakhil S, Saleh M, Piperdi B, Cline-Burkhardt M, et al. SPIRITT: a randomized, multicenter, phase II study of panitumumab with FOLFIRI and bevacizumab with FOLFIRI as second-line treatment in patients with unresectable wild type KRAS metastatic colorectal cancer. *Clin Colorectal Cancer* (2015) 14(2):72–80. doi: 10.1016/j.clcc.2014.12.009

76. Ciardiello F, Bianco R, Damiano V, Fontanini G, Caputo R, Pomatico G, et al. Antiangiogenic and antitumor activity of anti-epidermal growth factor receptor C225 monoclonal antibody in combination with vascular endothelial growth factor antisense oligonucleotide in human GEO colon cancer cells. *Clin Cancer Res* (2000) 6(9):3739–47.

77. Shaheen RM, Ahmad SA, Liu W, Reinmuth N, Jung YD, Tseng WW, et al. Inhibited growth of colon cancer carcinomatosis by antibodies to vascular endothelial and epidermal growth factor receptors. *Br J Cancer* (2001) 85(4):584–9. doi: 10.1054/bjoc.2001.1936

78. Hecht JR, Mitchell E, Chidiac T, Scroggin C, Hagenstad C, Spigel D, et al. A randomized phase IIIB trial of chemotherapy, bevacizumab, and panitumumab compared with chemotherapy and bevacizumab alone for metastatic colorectal cancer. *J Clin Oncol* (2009) 27(5):672–80. doi: 10.1200/JCO.2008.19.8135

79. Tol J, Koopman M, Cats A, Rodenburg CJ, Creemers GJ, Schrama JG, et al. Chemotherapy, bevacizumab, and cetuximab in metastatic colorectal cancer. *N Engl J Med* (2009) 360(6):563–72. doi: 10.1056/NEJMoa0808268

80. Saltz LB, Lenz HJ, Kindler HL, Hochster HS, Wadler S, Hoff PM, et al. Randomized phase II trial of cetuximab, bevacizumab, and irinotecan compared with cetuximab and bevacizumab alone in irinotecan-refractory colorectal cancer: the BOND-2 study. *J Clin Oncol* (2007) 25(29):4557–61. doi: 10.1200/JCO.2007.12.0949

81. Kopetz S, Grothey A, Yaeger R, Van Cutsem E, Desai J, Yoshino T, et al. Encorafenib, binimetinib, and cetuximab in BRAF V600E-mutated colorectal cancer. *N Engl J Med* (2019) 381(17):1632–43. doi: 10.1056/NEJMoa1908075

82. Kopetz S, Guthrie KA, Morris VK, Lenz HJ, Magliocco AM, Maru D, et al. Randomized trial of irinotecan and cetuximab with or without vemurafenib in BRAF-mutant metastatic colorectal cancer (SWOG S1406). *J Clin Oncol* (2021) 39(4):285–94. doi: 10.1200/JCO.20.01994

83. Sartore-Bianchi A, Amatu A, Porcu L, Ghezzi S, Lonardi S, Leone F, et al. HER2 positivity predicts unresponsiveness to EGFR-targeted treatment in metastatic colorectal cancer. *Oncologist*. (2019) 24(10):1395–402. doi: 10.1634/theoncologist.2018-0785

84. Yarden Y, Sliwkowski MX. Untangling the ErbB signalling network. *Nat Rev Mol Cell Biol* (2001) 2(2):127–37. doi: 10.1038/35052073

85. Neve RM, Lane HA, Hynes NE. The role of overexpressed HER2 in transformation. *Ann Oncol* (2001) 12 Suppl 1:S9–13. doi: 10.1093/annonc/12.suppl_1.S9

86. Gupta R, Garrett-Mayer E, Halabi S, Mangat PK, D'Andre SD, Meiri E, et al. Pertuzumab plus trastuzumab (P+T) in patients (Pts) with colorectal cancer (CRC) with ERBB2 amplification or overexpression: results from the TAPUR study. *J Clin Oncol* (2020) 38(4_suppl):132. doi: 10.1200/JCO.2020.38.4_suppl.132

87. Martin V, Landi L, Molinari F, Fountzilas G, Geva R, Riva A, et al. HER2 gene copy number status may influence clinical efficacy to anti-EGFR monoclonal antibodies in metastatic colorectal cancer patients. *Br J Cancer* (2013) 108(3):668–75. doi: 10.1038/bjc.2013.4

88. Raghav K, Loree JM, Morris JS, Overman MJ, Yu R, Meric-Bernstam F, et al. Validation of HER2 amplification as a predictive biomarker for anti-epidermal growth factor receptor antibody therapy in metastatic colorectal cancer. *JCO Precis Oncol* (2019) 3:1–13. doi: 10.1200/PO.18.00226

89. Meric-Bernstam F, Hainsworth J, Bose R, Burris Iii HA, Friedman CF, Kurzrock R, et al. MyPathway HER2 basket study: pertuzumab (P) + trastuzumab (H) treatment of a large, tissue-agnostic cohort of patients with HER2-positive advanced solid tumors. *J Clin Oncol* (2021) 39(15_suppl):3004–. doi: 10.1200/JCO.2021.39.15_suppl.3004

90. Sartore-Bianchi A, Trusolino L, Martino C, Bencardino K, Lonardi S, Bergamo F, et al. Dual-targeted therapy with trastuzumab and lapatinib in treatment-refractory, KRAS codon 12/13 wild-type, HER2-positive metastatic colorectal cancer (HERACLES): a proof-of-concept, multicentre, open-label, phase 2 trial. *Lancet Oncol* (2016) 17(6):738–46. doi: 10.1016/S1470-2045(16)00150-9

91. Sartore-Bianchi A, Lonardi S, Martino C, Fenocchio E, Tosi F, Ghezzi S, et al. Pertuzumab and trastuzumab emtansine in patients with HER2-amplified metastatic colorectal cancer: the phase II HERACLES-b trial. *ESMO Open* (2020) 5(5):e000911. doi: 10.1136/esmoopen-2020-000911

92. Federica T, Sartore-Bianchi A, Lonardi S, Amatu A, Leone F, Ghezzi S, et al. Long-term clinical outcome of trastuzumab and lapatinib for HER2-positive metastatic

colorectal cancer. *Clin Colorectal Cancer* (2020) 19(4):256–62. doi: 10.1016/j.clcc.2020.06.009

93. Yoshino T, Di Bartolomeo M, Raghav KPS, Masuishi T, Loupakis F, Kawakami H, et al. Trastuzumab deruxtecan (T-DXd; DS-8201) in patients (pts) with HER2-expressing metastatic colorectal cancer (mCRC): final results from a phase 2, multicenter, open-label study (DESTINY-CRC01). *J Clin Oncol* (2021) 39 (15_suppl):3505–. doi: 10.1200/JCO.2021.39.15_suppl.3505

94. Strickler JH, Ng K, Cercek A, Fountzilas C, Sanchez FA, Hubbard JM, et al. MOUNTAINEER:open-label, phase II study of tucatinib combined with trastuzumab for HER2-positive metastatic colorectal cancer (SGNTUC-017, trial in progress). *J Clin Oncol* (2021) 39(3_suppl):TPS153–TPS. doi: 10.1200/JCO.2021.39.3_suppl.TPS153

95. Andreyev HJ, Norman AR, Cunningham D, Oates JR, Clarke PA. Kirsten ras mutations in patients with colorectal cancer: the multicenter "RASCAL" study. *J Natl Cancer Inst* (1998) 90(9):675–84. doi: 10.1093/jnci/90.9.675

96. Yoon HH, Tougeron D, Shi Q, Alberts SR, Mahoney MR, Nelson GD, et al. KRAS codon 12 and 13 mutations in relation to disease-free survival in BRAF-wild-type stage III colon cancers from an adjuvant chemotherapy trial (N0147 alliance). *Clin Cancer Res* (2014) 20(11):3033–43. doi: 10.1158/1078-0432.CCR-13-3140

97. Modest DP, Ricard I, Heinemann V, Hegewisch-Becker S, Schmiegel W, Porschen R, et al. Outcome according to KRAS-, NRAS- and BRAF-mutation as well as KRAS mutation variants: pooled analysis of five randomized trials in metastatic colorectal cancer by the AIO colorectal cancer study group. *Ann Oncol* (2016) 27 (9):1746–53. doi: 10.1093/annonc/mdw261

98. Taieb J, Le Malicot K, Shi Q, Penault-Llorca F, Bouche O, Tabernero J, et al. Prognostic value of BRAF and KRAS mutations in MSI and MSS stage III colon cancer. *J Natl Cancer Inst* (2017) 109(5):djw272. doi: 10.1093/jnci/djw272

99. Henry JT, Coker O, Chowdhury S, Shen JP, Morris VK, Dasari A, et al. Comprehensive clinical and molecular characterization of KRAS (G12C)-mutant colorectal cancer. *JCO Precis Oncol* (2021) 5:613–21. doi: 10.1200/PO.20.00256

100. Fakih MG, Kopetz S, Kuboki Y, Kim TW, Munster PN, Krauss JC, et al. Sotorasib for previously treated colorectal cancers with KRAS(G12C) mutation (CodeBreaK100): a prespecified analysis of a single-arm, phase 2 trial. *Lancet Oncol* (2022) 23(1):115–24. doi: 10.1016/S1470-2045(21)00605-7

101. Amodio V, Yaeger R, Arcella P, Cancelliere C, Lamba S, Lorenzato A, et al. EGFR blockade reverts resistance to KRAS(G12C) inhibition in colorectal cancer. *Cancer Discovery* (2020) 10(8):1129–39. doi: 10.1158/2159-8290.CD-20-0187

102. Yaeger R, Weiss J, Pelster MS, Spira AI, Barve M, Ou SI, et al. Adagrasib with or without cetuximab in colorectal cancer with mutated KRAS G12C. *N Engl J Med* (2023) 388(1):44–54. doi: 10.1056/NEJMoa2212419

103. Papadopoulos N, Nicolaides NC, Wei YF, Ruben SM, Carter KC, Rosen CA, et al. Mutation of a mutL homolog in hereditary colon cancer. *Science.* (1994) 263 (5153):1625–9. doi: 10.1126/science.8128251

104. Baker SM, Bronner CE, Zhang L, Plug AW, Robatzek M, Warren G, et al. Male Mice defective in the DNA mismatch repair gene PMS2 exhibit abnormal chromosome synapsis in meiosis. *Cell.* (1995) 82(2):309–19. doi: 10.1016/0092-8674(95)90318-6

105. Chung DC, Rustgi AK. DNA Mismatch repair and cancer. *Gastroenterology.* (1995) 109(5):1685–99. doi: 10.1016/0016-5085(95)90660-6

106. Koopman M, Kortman GA, Mekenkamp L, Ligtenberg MJ, Hoogerbrugge N, Antonini NF, et al. Deficient mismatch repair system in patients with sporadic advanced colorectal cancer. *Br J Cancer* (2009) 100(2):266–73. doi: 10.1038/sj.bjc.6604867

107. Arnold CN, Goel A, Compton C, Marcus V, Niedzwiecki D, Dowell JM, et al. Evaluation of microsatellite instability, hMLH1 expression and hMLH1 promoter hypermethylation in defining the MSI phenotype of colorectal cancer. *Cancer Biol Ther* (2004) 3(1):73–8. doi: 10.4161/cbt.3.1.590

108. Goel A, Boland CR. Epigenetics of colorectal cancer. *Gastroenterology.* (2012) 143(6):1442–60.e1. doi: 10.1053/j.gastro.2012.09.032

109. Veigl ML, Kasturi L, Olechnowicz J, Ma AH, Lutterbaugh JD, Periyasamy S, et al. Biallelic inactivation of hMLH1 by epigenetic gene silencing, a novel mechanism causing human MSI cancers. *Proc Natl Acad Sci U S A* (1998) 95(15):8698–702. doi: 10.1073/pnas.95.15.8698

110. Cui H, Horon IL, Ohlsson R, Hamilton SR, Feinberg AP. Loss of imprinting in normal tissue of colorectal cancer patients with microsatellite instability. *Nat Med* (1998) 4(11):1276–80. doi: 10.1038/3260

111. Boland CR, Thibodeau SN, Hamilton SR, Sidransky D, Eshleman JR, Burt RW, et al. A national cancer institute workshop on microsatellite instability for cancer detection and familial predisposition: development of international criteria for the determination of microsatellite instability in colorectal cancer. *Cancer Res* (1998) 58(22):5248–57.

112. Latham A, Srinivasan P, Kemel Y, Shia J, Bandlamudi C, Mandelker D, et al. Microsatellite instability is associated with the presence of lynch syndrome pan-cancer. *J Clin Oncol* (2019) 37(4):286–95. doi: 10.1200/JCO.18.00283

113. Ionov Y, Peinado MA, Malkhosyan S, Shibata D, Perucho M. Ubiquitous somatic mutations in simple repeated sequences reveal a new mechanism for colonic carcinogenesis. *Nature.* (1993) 363(6429):558–61. doi: 10.1038/363558a0

114. Le DT, Uram JN, Wang H, Bartlett BR, Kemberling H, Eyring AD, et al. PD-1 blockade in tumors with mismatch-repair deficiency. *N Engl J Med* (2015) 372 (26):2509–20. doi: 10.1056/NEJMoa1500596

115. Le DT, Kim TW, Van Cutsem E, Geva R, Jager D, Hara H, et al. Phase II open-label study of pembrolizumab in treatment-refractory, microsatellite instability-High/Mismatch repair-deficient metastatic colorectal cancer: KEYNOTE-164. *J Clin Oncol* (2020) 38(1):11–9. doi: 10.1200/JCO.19.02107

116. Overman MJ, McDermott R, Leach JL, Lonardi S, Lenz HJ, Morse MA, et al. Nivolumab in patients with metastatic DNA mismatch repair-deficient or microsatellite instability-high colorectal cancer (CheckMate 142): an open-label, multicentre, phase 2 study. *Lancet Oncol* (2017) 18(9):1182–91. doi: 10.1016/S1470-2045(17)30422-9

117. Andre T, Lonardi S, Wong KYM, Lenz HJ, Gelsomino F, Aglietta M, et al. Nivolumab plus low-dose ipilimumab in previously treated patients with microsatellite instability-high/mismatch repair-deficient metastatic colorectal cancer: 4-year follow-up from CheckMate 142. *Ann Oncol* (2022) 33(10):1052–60. doi: 10.1016/j.annonc.2022.06.008

118. Zhou S, Khanal S, Zhang H. Risk of immune-related adverse events associated with ipilimumab-plus-nivolumab and nivolumab therapy in cancer patients. *Ther Clin Risk Manage* (2019) 15:211–21. doi: 10.2147/TCRM.S193338

119. Andre T, Shiu KK, Kim TW, Jensen BV, Jensen LH, Punt C, et al. Pembrolizumab in microsatellite-Instability-High advanced colorectal cancer. *N Engl J Med* (2020) 383(23):2207–18. doi: 10.1056/NEJMoa2017699

120. Andre T, Amonkar M, Norquist JM, Shiu KK, Kim TW, Jensen BV, et al. Health-related quality of life in patients with microsatellite instability-high or mismatch repair deficient metastatic colorectal cancer treated with first-line pembrolizumab versus chemotherapy (KEYNOTE-177): an open-label, randomised, phase 3 trial. *Lancet Oncol* (2021) 22(5):665–77. doi: 10.1016/S1470-2045(21)00064-4

121. Diaz LAJr., Shiu KK, Kim TW, Jensen BV, Jensen LH, Punt C, et al. Pembrolizumab versus chemotherapy for microsatellite instability-high or mismatch repair-deficient metastatic colorectal cancer (KEYNOTE-177): final analysis of a randomised, open-label, phase 3 study. *Lancet Oncol* (2022) 23(5):659–70. doi: 10.1016/S1470-2045(22)00197-8

122. Morris VK, Kennedy EB, Baxter NN, Benson AB3rd, Cercek A, Cho M, et al. Treatment of metastatic colorectal cancer: ASCO guideline. *J Clin Oncol* (2023) 41 (3):678–700. doi: 10.1200/JCO.22.01690

123. Lenz HJ, Van Cutsem E, Luisa Limon M, Wong KYM, Hendlisz A, Aglietta M, et al. First-line nivolumab plus low-dose ipilimumab for microsatellite instability-High/Mismatch repair-deficient metastatic colorectal cancer: the phase II CheckMate 142 study. *J Clin Oncol* (2022) 40(2):161–70. doi: 10.1200/JCO.21.01015

124. El-Khoueiry AB, Fakih M, Gordon MS, Tsimberidou AM, Bullock AJ, Wilky BA, et al. Results from a phase 1a/1b study of botensilimab (BOT), a novel innate/adaptive immune activator, plus balstilimab (BAL; anti-PD-1 antibody) in metastatic heavily pretreated microsatellite stable colorectal cancer (MSS CRC). *J Clin Oncol* (2023) 41(4_suppl):LBA8–8. doi: 10.1200/JCO.2023.41.4_suppl.LBA8

125. Fakih M, Sandhu J, Lim D, Li X, Li S, Wang C. Regorafenib, ipilimumab, and nivolumab for patients with microsatellite stable colorectal cancer and disease progression with prior chemotherapy; a phase 1 nonrandomized clinical trial. *JAMA Oncol* (2023) 9(5):627–34. doi: 10.1001/jamaoncol.2022.7845

126. Fakih M, Raghav KPS, Chang DZ, Larson T, Cohn AL, Huyck TK, et al. Regorafenib plus nivolumab in patients with mismatch repair-proficient/microsatellite stable metastatic colorectal cancer: a single-arm, open-label, multicenter phase 2 study. *eClinicalMedicine* (2023) 58(101917):2589–5370. doi: 10.1016/j.eclinm.2023.101917

127. Agenus Inc. *A study of botensilimab and balstilimab for the treatment of colorectal cancer*. ClinicalTrials (2022). Available at: https://clinicaltrials.gov/ct2/show/NCT05608044.

frontiers | Frontiers in Oncology

TYPE Original Research
PUBLISHED 23 June 2023
DOI 10.3389/fonc.2023.1145753

OPEN ACCESS

EDITED BY
Jorge Melendez-Zajgla,
National Institute of Genomic Medicine (INMEGEN), Mexico

REVIEWED BY
Bo Feng,
Shanghai Jiao Tong University, China
Xuelei Ma,
Sichuan University, China

*CORRESPONDENCE
Bin Ma
mabin0326cmu@163.com

†These authors have contributed equally to this work

RECEIVED 25 January 2023
ACCEPTED 12 June 2023
PUBLISHED 23 June 2023

CITATION
Ma B, Bao S and Li Y (2023) Identification and validation of m6A-GPI signatures as a novel prognostic model for colorectal cancer.
Front. Oncol. 13:1145753.
doi: 10.3389/fonc.2023.1145753

Identification and validation of m6A-GPI signatures as a novel prognostic model for colorectal cancer

Bin Ma[1,2*†], Simeng Bao[3†] and Yongmin Li[1]

[1]Department of Colorectal Surgery, Cancer Hospital of China Medical University, Cancer Hospital of Dalian University of Technology, Liaoning Cancer Hospital and Institute, Shenyang, China, [2]The Liaoning Provincial Key Laboratory of Interdisciplinary Research on Gastrointestinal Tumor Combining Medicine with Engineering, Shenyang, China, [3]Central Laboratory, Cancer Hospital of China Medical University, Cancer Hospital of Dalian University of Technology, Liaoning Cancer Hospital and Institute, Shenyang, China

In order to develop an N6-methyladenosine-related gene prognostic index (m6A-GPI) that can predict the prognosis in colorectal cancer (CRC), we obtained m6A-related differentially expressed genes (DEGs) based on The Cancer Genome Atlas (TCGA) and m6Avar database, seven genes were screened by weighted gene co-expression network analysis (WGCNA) and least absolute shrinkage and selection operator (LASSO) analysis. Then, m6A-GPI was constructed based on the risk score. Survival analysis indicated that patients in the lower m6A-GPI group have more prolonged disease-free survival (DFS), and different clinical characteristic groups (tumor site and stage) also showed differential risk scores. In the analysis of the molecular characteristics, the risk score is positively associated with homologous recombination defects (HRD), copy number alterations (CNA), and the mRNA expression-based stemness index (mRNAsi). In addition, m6A-GPI also plays an essential role in tumor immune cell infiltration. The immune cell infiltration in the low m6A-GPI group is significantly higher in CRC. Moreover, we found that CIITA, one of the genes in m6A-GPI was up-regulated in CRC tissues based on real-time RT-PCR and Western blot. m6A-GPI is a promising prognostic biomarker that can be used to distinguish the prognosis of CRC patients in CRC.

KEYWORDS

colorectal cancer, N6-methyladenosine, prognostic signature, immune infiltration, CIITA

1 Introduction

Colorectal cancer (CRC) has risen rapidly in recent years (1–3), and the treatment of CRC is mainly based on surgery, targeted therapy, neoadjuvant chemoradiotherapy, neoadjuvant radiotherapy and adjuvant chemotherapy. Unfortunately, current treatments for CRC remain limited (4–6). Precision oncology enables the administration of therapies to specific subsets of

patients who exhibit the most favorable responses based on their characteristics. Prognostic models based on prognostic biomarkers have been employed for clinical decision-making and prognostication of therapeutic response (7). Moreover, some studies also have proposed the utilization of intelligent technologies and prognostic biomarkers to provide essential guidance of precision therapy (8, 9). Therefore, we need to identify those high-risk CRC patients with poor prognosis, and further clarify the relevant mechanisms, so that individualized treatment can be implemented as soon as possible.

The tumor immune microenvironment (TIME) has an important impact on tumor prognosis and therapeutic effect (10, 11). As the most abundant internal modification of eukaryotic mRNA and non-coding RNA, N6-methyladenosine (m6A) modification is not only associated with tumor growth, proliferation, and metastasis but also affects the process of immune cell recruitment and metabolic regulation of the TIME (12, 13), which will seriously affect the prognosis in CRC. The modification of m6A is performed by m6A writers, erasers and reader. Among these, METTL3 and METTL14 make up the majority of m6A methyltransferases (m6A writers). YTHDF1 is a m6A reader protein that promotes the translation of m6A-modified mRNA (14, 15). Some studies have shown that blocking METTL3 can enhance the chemotherapeutic response and reduce stem cell frequency and tumor size both in vitro and in vivo (16). Han et al. found that mice with blockade of YTHDF1 show an elevated antigen-specific $CD8^+$ T cell antitumor response compared with wild-type mice, and the therapeutic efficacy of programmed cell death-ligand 1 (PD-L1) checkpoint blockade is enhanced in $YTHDF1^{-/-}$ mice, which implies that YTHDF1 can serve as a potential therapeutic target in tumors (17). In another study, the consumption of METTL3 or METTL14 in CT26 tumor mice with anti-PD-1 therapy significantly slowed tumor proliferation and prolonged the survival rate (18). These results suggest that m6A modification may serve as a target affecting immune infiltration and survival time in CRC patients.

Despite this, there is no reliable tool for predicting the prognosis in CRC, and effective indicators are urgently needed. In this study, we developed a prognostic biomarker that can predict the prognosis and the immune infiltration in CRC patients. We focused on m6A-related genes, and seven genes were screened. Then, we established an m6A-related gene prognostic index (m6A-GPI) based on the risk score. We conducted a series of stratification analysis and revealed the molecular and immune cell infiltration characteristics in the m6A-GPI subgroups. In addition, m6A-GPI was an independent predictor for CRC, and we constructed a nomogram including m6A-GPI to help clinicians accurately predict the prognosis of CRC patients. Moreover, we found that CIITA, one of the genes in m6A-GPI was up-regulated in CRC tissues based on real-time RT-PCR and Western blotting. These results showed that m6A-GPI is a reliable biomarker for predicting the prognosis of CRC.

2 Methods

2.1 Datasets acquisition

We downloaded the RNA-seq data and clinical features of CRC from The Cancer Genome Atlas (TCGA) (https://portal.gdc.cancer.gov) database, which contained 616 tumor tissue samples and 51 paracancerous tissue samples. Mutation data were downloaded using the "TCGAbiolinks" packages in R language, and the independent validation datasets (GSE17538, 200 samples) were obtained from Gene Expression Omnibus (GEO) (https://www.ncbi.nlm.nih.gov/geo/).

2.2 Identification of m6A-related genes

Then, pertinent references were searched and 21 m6A-related genes were screened, we identified 6,797 m6A-related genes in colorectal cancer from the m6Avar database (http://rmvar.renlab.org/). The differential expression analysis was performed in the "limma" R package, and differentially expressed genes (DEGs) were obtained in this process (adj. $P< 0.05$, log2FC > 0.585 or< 0.67). Consensus clustering, Gene Ontology (GO) and Kyoto Encyclopedia of Genes and Genomes (KEGG) analysis were then performed in Metascape (https://metascape.org/) after consideration in the context of the m6A-related genes obtained from TCGA and m6Avar.

2.3 WGCNA analysis

We conducted WGCNA analysis to identify hub genes. First, the similarity matrix was transformed into an adjacency matrix and then into a topological overlap matrix (TOM); TOM distances were used to cluster genes into WGCNA modules, and modules were determined by the dynamic pruning tree with a minimum of 30 genes per module.

2.4 Construction and validation of m6A-GPI

In order to identify prognostic genes, using the R package "survival" to perform univariate Cox regression analysis. Next, we implemented LASSO Cox regression to construct m6A-GPI that can predict the disease-free survival (DFS) of CRC patients, m6A-GPI was calculated based on the coefficient of genes, and the formula is:

$$risk\ \ score = \sum_{i=1}^{n} Coef_i * x_i$$

where $Coef_i$ is the coefficient, and the x_i is the FPKM value of the m6A-related genes. We constructed Kaplan–Meier (K-M) survival curves of two subgroups and analyzed the 1-, 3-, and 5-year DFS rates of the cases. Validation datasets were downloaded from the GEO database, and we combined TCGA clinical information and explored the stability of m6A-GPI with different clinical characteristics.

2.5 Comprehensive analysis of molecular and immune characteristics in different m6A-GPI subgroups

DNA changes are the basic factor in the development of cancer and play an important role in promoting the progress of cancer

(19), and tumor immune escape mechanisms indicate that malignant tumors are capable of evading the immune response. To explore the immunogenicity of CRC, we analyzed the effect of m6A-GPI on mutation load, homologous recombination defects (HRD), neoantigen loads, copy number alterations (CNA) and the mRNA expression-based stemness index (mRNAsi). We obtained immune characteristics from the Genomic Data Commons (GDC) data portal (https://gdc.cancer.gov/about-data/publications/panimmune), and the HRD score comes from PMID: 29617664. Furthermore, we analyzed the somatic mutation difference between the low- and high-risk groups by the R package "maftools."

The CIBERSORT (https://cibersort.stanford.edu/) is a novel algorithm and it can evaluate gene expression data from RNA sequences and assess the immune cell compositions of complex tissues (20, 21). CIBERSORT can be used to calculate the content of 22 kinds of human immune cell phenotypes and the sum of all estimates of immune cell type fractions yields one. We compared the relative proportions of 22 immune cells between the two subgroups and presented the results in a landscape map.

In the tumor microenvironment, non-tumor components are divided into two types that are valuable for tumor diagnosis and prognostic evaluation, immune cells and stromal cells (22). To determine the impact of immune cell infiltration (such as T cells, Tregs, NK cells and macrophages) on the treatment of ICIs, we calculated the immune score, matrix score, and tumor purity in each CRC sample based on the ESTIMATE algorithm.

2.6 Independent prognostic factor and nomogram

To verify whether m6A-GPI can serve as an independent prognostic factor in CRC, we conducted univariate and multivariate Cox regression analysis. In order to provide doctors with a quantitative method for predicting the prognosis of patients with CRC, we constructed a nomogram using the risk status, age, cancer type, sex, cancer stage, and cancer site, then established calibration plots of DFS at 1-, 3-, and 5-year in the TCGA cohorts.

2.7 CRC tissue samples

Colorectal samples and their adjacent normal tissues were collected from Liaoning Cancer Hospital and Institute (Shenyang, China), and the colorectal samples showed a confirmed histological diagnosis of CRC. The study was approved by the institutional ethics committee, and individual consent forms were signed by each patient.

2.8 Quantitative real-time RT-PCR

Total RNA was extracted from colorectal tumors and their adjacent normal tissues of 16 patients by using Trizol reagent (Life Technologies, Carlsbad, CA) following the manufacturer recommendations. Concentration of RNA was quantified by Nanodrop 2000 (Thermo, Wilmington, DE). Reverse-transcription to cDNA (50 ng per sample) was using with iScript cDNA Supermix (TaKaRa, Dalian, China). Quantitative RT-PCR was performed using a reaction mixture containing SYBR mix (TaKaRa, Dalian, China), and real-time fluorescence was detected by Quant Studio 6 Flex (ABI, Foster City, CA). The primers were designed and synthesized by Life Technologies. The sequences of the primer pairs were as follows, *GBP2*: forward 5′-CTATCTGCAATTACGCAGCCT-3′, reverse 5′-TGTTCTGGCTTCTTGGGATGA-3′, *CXCL10*: forward 5′-GTGGCATTCAAGGAGTACCTC-3′, reverse 5′-TGATGGCCTTCGATTCTGGATT-3′, *CXCL13*: forward 5′-GCTTGAGGTGTAGATGTGTCC-3′, reverse 5′-CCCACGGGGCAAGATTTGAA-3′, *FASLG*: forward 5′- TGCCTTGGTAGGATTGGGC-3′, reverse 5′-GCTGGTAGACTCTCGGAGTTC-3′, *CIITA*: forward 5′-CCTGGAGCTTCTTAACAGCGA-3′, reverse 5′-TGTGTCGGGTTCTGAGTAGAG-3′, *IL12RB1*: forward 5′-TAGGGACCTGAGATGCTATCG-3′, reverse 5′-CCCGGAGCTAAGGCAACAC-3′, *CXCR6*: forward 5′-GACTATGGGTTCAGCAGTTTCA-3′, reverse 5′-GGCTCTGCAACTTATGGTAGAAG-3′, *GAPGH*: forward 5′-TCCCATCACCATCTTCCA-3′, reverse 5′-ACTCACGCCACAGTTTCC-3′.

2.9 Western blot analysis

CRC samples and their adjacent normal tissues of 7 patients were lysed according to the kit (PC101-PC104, Epizyme Biomedical Technology, Shanghai, China). Total protein concentration was quantified using a BCA protein assay kit (DQ111-01, TransGen Biotech Co., Ltd., Beijing, China). 50 μg of protein was separated by SDS–PAGE and was electrophoretically transferred to polyvinylidene difluoride (PVDF) membranes. The membranes were blocked with 3% BSA in Tris-buffered saline (TBS) containing 0.05% Tween-20 for 1 h. After blocking, the membranes were incubated with corresponding primary antibodies overnight at 4°C. The primary antibody for CIITA (#55099-1-AP; 1:1000) was purchased from Proteintech Group, Inc. (Wuhan, China). Membranes were washed by 1× TBST, followed by incubation with anti-Rabbit IgG-HRP (ZB-2301, Zhong Shan-Golden Bridge Biological Technology Co., Beijing, China) for 1 h. Immunoreactive bands were visualized by using Tanon 5500 (Tanon, Shanghai, China). Equal loading of proteins was verified by GAPDH (#60004-1-Ig; 1:3000, Proteintech Group, Inc., Wuhan, China).

2.10 Statistical analysis

SPSS 24.0 (IBM Corporation, Armonk, United States) and R programming language (version 4.0.2) were used to perform the statistical analysis. Kaplan–Meier curves and the log-rank test were used to compare the DFS between various subgroups. The prognostic ability of the predictors for 1-, 3-, and 5-year DFS was evaluated by receiver operating characteristic (ROC) curves and the area under the curve (AUC) values. Univariate and multivariate Cox regression analysis were utilized to evaluate the independent

prognostic value of the model. A two-sided $P< 0.05$ was considered significant.

3 Results

3.1 Identification of m6A-related genes

Based on our workflow (Supplementary Figure 1), we obtained 6,803 m6A-related and referred to as GeneSet 1. These genes intersected with 5,220 DEGs from the TCGA database, and 1,291 differentially expressed m6A-related genes were screened for GO and KEGG analysis. In the KEGG and GO analysis, we extracted a total of 5,642 genes from the significantly enriched pathways, which were referred to as GeneSet 2. In addition, we also clustered 1,291 differentially expressed m6A-related genes, and finally obtained two sets of samples, and screened out 644 DEGs between them, which were referred to as GeneSet 3. The three gene sets contained a total of 10,893 genes (Figure 1A). The screening process is shown in Supplementary Figure 2.

3.2 33 key genes were identified by WGCNA analysis

To obtain key genes related to m6A modification, we performed WGCNA on 10,893 genes and finally obtained 18 modules (Figures 1B, C). Then, the Gene Significance (GS) value of each module was calculated, with a larger GS indicating that the module was more related to the phenotypic characteristics of the sample (Figure 1D). We calculated the Pearson correlation coefficient between each module and the phenotypic characteristics of the sample (Figure 1E).

According to the results, we identified two key modules, green-yellow and brown, and selected the genes in these two modules for subsequent analysis. We constructed a protein-protein interaction (PPI) network based on two modules, and 105 hub genes were screened in the network (Supplementary Figure 3A). At the same time, 185 hub genes were screened in these two modules according to the thresholds of MM > 0.6 and GS > 0.2 (Supplementary Figure 3B, C). The intersection contains 33 genes, which are considered to be the key genes related to m6A (Figure 1F).

3.3 Construction of the m6A-GPI in the TCGA dataset

Univariate Cox analysis was performed on 33 key genes, and the results showed that 10 genes (IL12RB1, IL2RB, IFNG, FASLG, CXCL9, CXCL13, GBP2, CXCL10, CXCR6, and CIITA) had a significant relationship with the prognosis of CRC ($P< 0.05$). The forest plot is presented (Figure 2A). To further determine the genes used to construct m6A-GPI, LASSO analysis was performed to identify the 7 most important genes and their coefficients (IL12RB1, FASLG, CXCL13, GBP2, CXCL10, CXCR6, and CIITA) (Figure 2B, C), we utilized m6A-GPI to determine the patient's risk score and divided all patients into a high-risk group and a low-risk group based on the median risk score (Figure 2D).

Compared with patients with high-risk scores, lower risk scores represent better DFS and a relatively longer survival time in the K-M curves ($P< 0.05$) (Figure 2E). At the same time, a ROC curve was used to test the accuracy of m6A-GPI in predicting patient survival. The AUC of the 1-, 3-, and 5-year DFS rates reach 0.66, 0.67 and 0.65, respectively (Figure 2F), which indicated that m6A-GPI has the potential to predict the DFS of patients in the TCGA cohort.

3.4 Validation of the m6A-GPI

Generally, the pathological stage is of great significance to the prognosis of CRC (23), but other factors such as age and gender can also affect the prognosis. Therefore, we tested the stability of m6A-GPI in different clinical characteristics. In the stratified samples based on GEO dataset, the results showed that the high- and low-risk groups still had significant survival differences after distinguishing age, sex, and stage ($P< 0.05$) (Figure 3A–F), which indicates that the m6A-GPI has good stability in stratified samples.

The external dataset was obtained from the GSE17538 cohort, and we used the same formula to calculate the risk score of the patients in this cohort. Similarly, patients were divided into high- and low-risk groups (Figure 3G). Patients with higher risk scores had poor DFS in the GEO cohort ($P<0.05$), which is consistent with the previous analysis of the TCGA cohort (Figure 3H).

Furthermore, we compared the risk score in the clinical characteristics of the TCGA cohort (age, cancer type, sex, stage and cancer site), and the results showed that the risk score was significantly different in stages and cancer sites ($P< 0.05$) (Supplementary Figure 4A–E). As the stage increases, the risk score has an upward trend, and the risk score of left colon cancer is higher than that of right colon cancer.

3.5 The molecular and mutation characteristics of different m6A-GPI groups

We compared some potential factors that determine tumor immunogenicity in two subgroups, and the results indicated that the risk score was positively correlated with HRD, CNA, and mRNAsi (Supplementary Figure 5). HRD mainly include loss of heterozygosity (LOH), telomere allele imbalance (TAI), and large-scale transition (LST). These three indicators can be used to determine the genomic instability score (GIS) and then evaluate the HRD status. CNA, LOH, TAI, and LST represent the level of chromosome instability (24). The mRNAsi is an index that can assess the similarity between tumor cells and stem cells and is related to the active biological processes in stem cells and the high degree of tumor dedifferentiation (25).

In addition, we used the "maftools" R package to analyze the distribution of somatic mutations between two subgroups in the

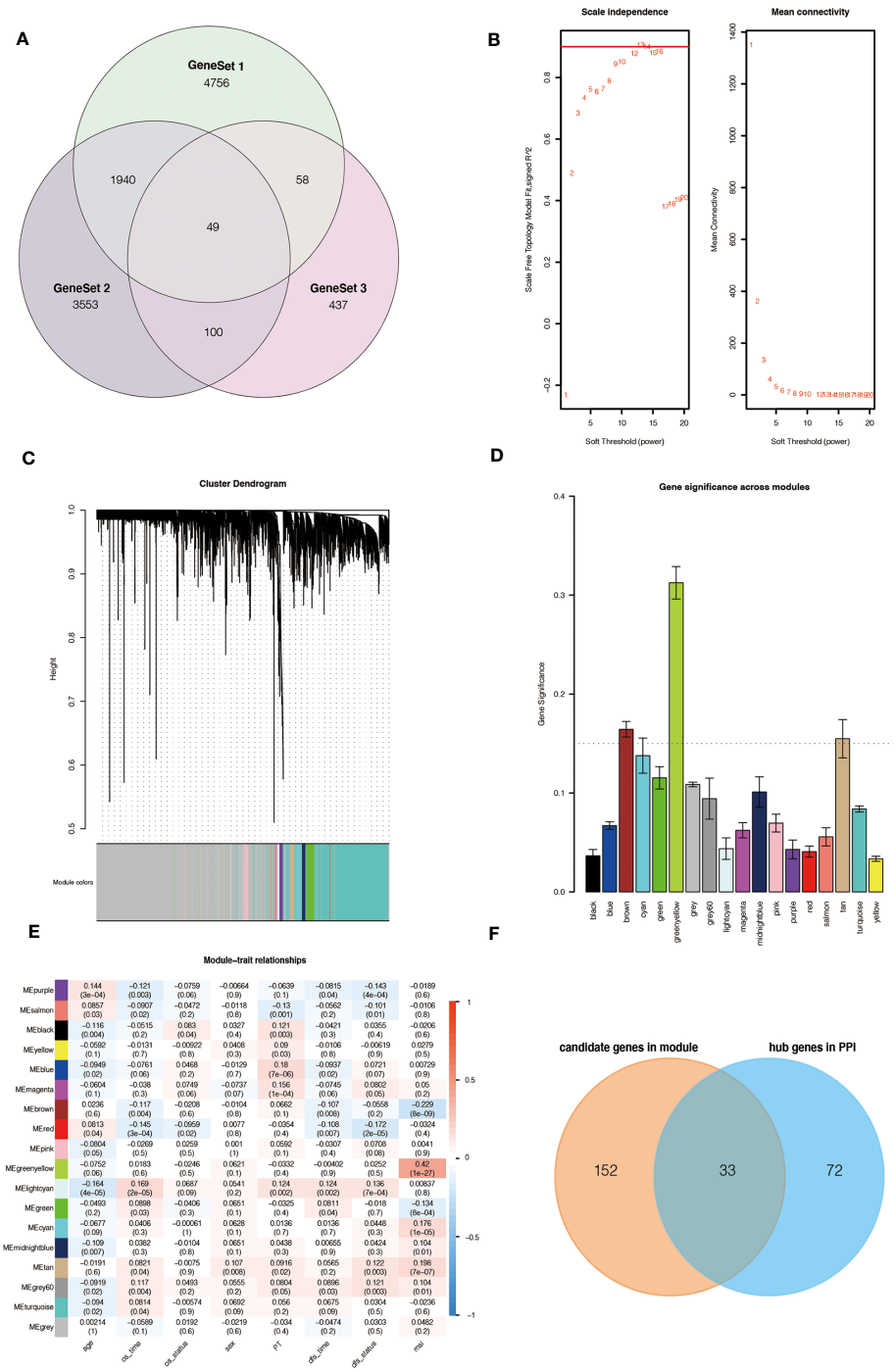

FIGURE 1
Source of m6A-related genes and weighted correlation network analysis. **(A)** Venn diagram of the three gene sets. **(B)** Identification of soft-thresholding power for the scale-free network. **(C)** Clustering dendrogram and merging of co-expression modules. **(D)** Gene significance of each module. **(E)** The correlation heatmap of mRNA modules and clinical traits is related to color changes. Red represents positive correlation, and blue represents negative correlation. **(F)** Venn diagram of the candidate genes in the green-yellow and brown modules and the hub genes in the PPI network.

TCGA cohort. Then we sorted the genes according to the mutation rate and identified the genes with the highest mutation rate in two groups. The mutation rates of APC, TP53, KRAS, TTN, MUC16, PIK3CA, SYNE1, FAT4, OBSCN, and MUC4 were higher than 20% in both groups (Figures 4A, B). After we grouped samples according to the risk score, the high-risk samples showed significant amplifications on chromosomes 8, 11, 12, 17, and 20, while deletions were found on chromosomes 1, 3 to 6, 8, 10, 12, 16 to 20. However, the low-risk samples showed significant amplifications on chromosomes 5, 6, 8, 10, 12, 13, 16, 17, 19, and 20, while deletions were found on chromosomes 1, 3 to 8, 10, 15 to 22 (Figures 4C, D).

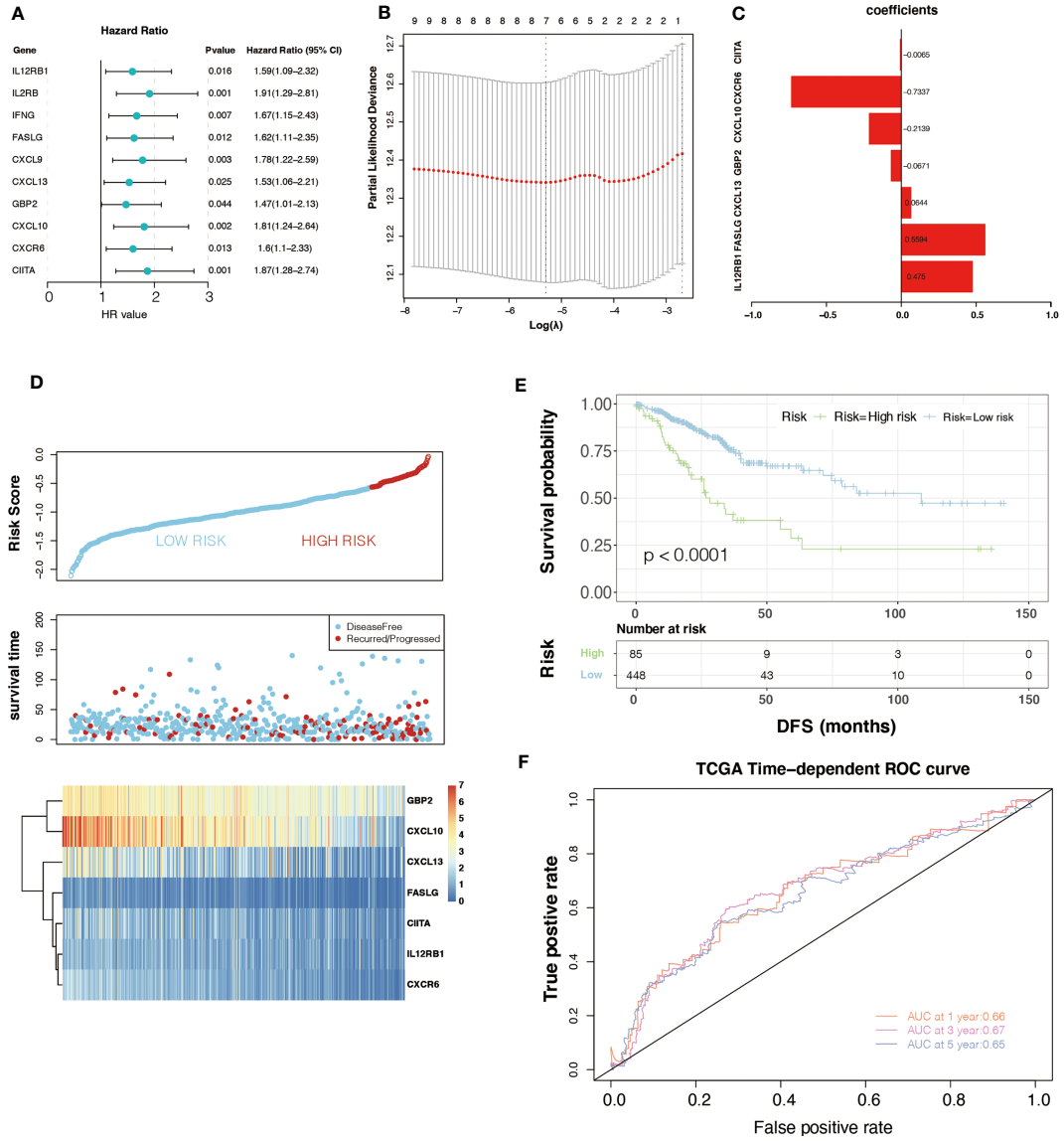

FIGURE 2
Univariate Cox regression analysis and the prognostic model. **(A)** Univariate Cox regression analysis indicated that ten genes play a critical role in the prognosis of colorectal cancer. **(B, C)** The calculation of minimum criteria and the coefficients. **(D)** The distribution of risk score and the status of colorectal cancer patients and the heatmap of hub genes. **(E)** Kaplan–Meier curves showed that the patients in the high-risk group had worse DFS in the TCGA dataset. **(F)** ROC curves of m6A-GPI for predicting the 1-, 3-, and 5-year survival in the TCGA dataset.

3.6 Immune characteristics of different m6A-GPI groups

The effect of tumor treatment depends not only on the tumor immunogenicity of the tumor but also on the TIME. TIME is formed by various cells, including immune cells (such as T cells, Tregs, NK cells, and macrophages), endothelial cells, and inflammatory mediators (26). The role of immune cells is particularly important, and it may affect the patient's response to treatment. To compare the distribution of immune cells in m6A-GPI subgroups, we analyzed the relative proportions of immune cells between the two m6A-GPI subgroups. Compared with low-risk patients, high-risk patients showed more infiltration of NK cells, M0 macrophages, and mast cells. However, in this group, there were fewer CD4+ T cells, CD8+ T cells, M1 macrophages, and M2 macrophages (Figure 5A).

Then we explored the level of the stromal score, immune score and tumor purity among the two groups, and the results showed that the high-risk group had higher tumor purity and that the low-risk group had a higher stromal score and immune score (Figures 5B–D). It suggests that the high-risk patients had a higher proportion of cancer cells in the tissue, and the TIME of the low-risk group contains contained abundant immune or matrix components.

3.7 Independent prognostic factor and nomogram

By using univariate Cox regression analysis and multivariate Cox regression analysis, we sought to determine whether m6A-GPI was an independent prognostic factor for patients with CRC. Univariate Cox

10.3389/fonc.2023.1145753

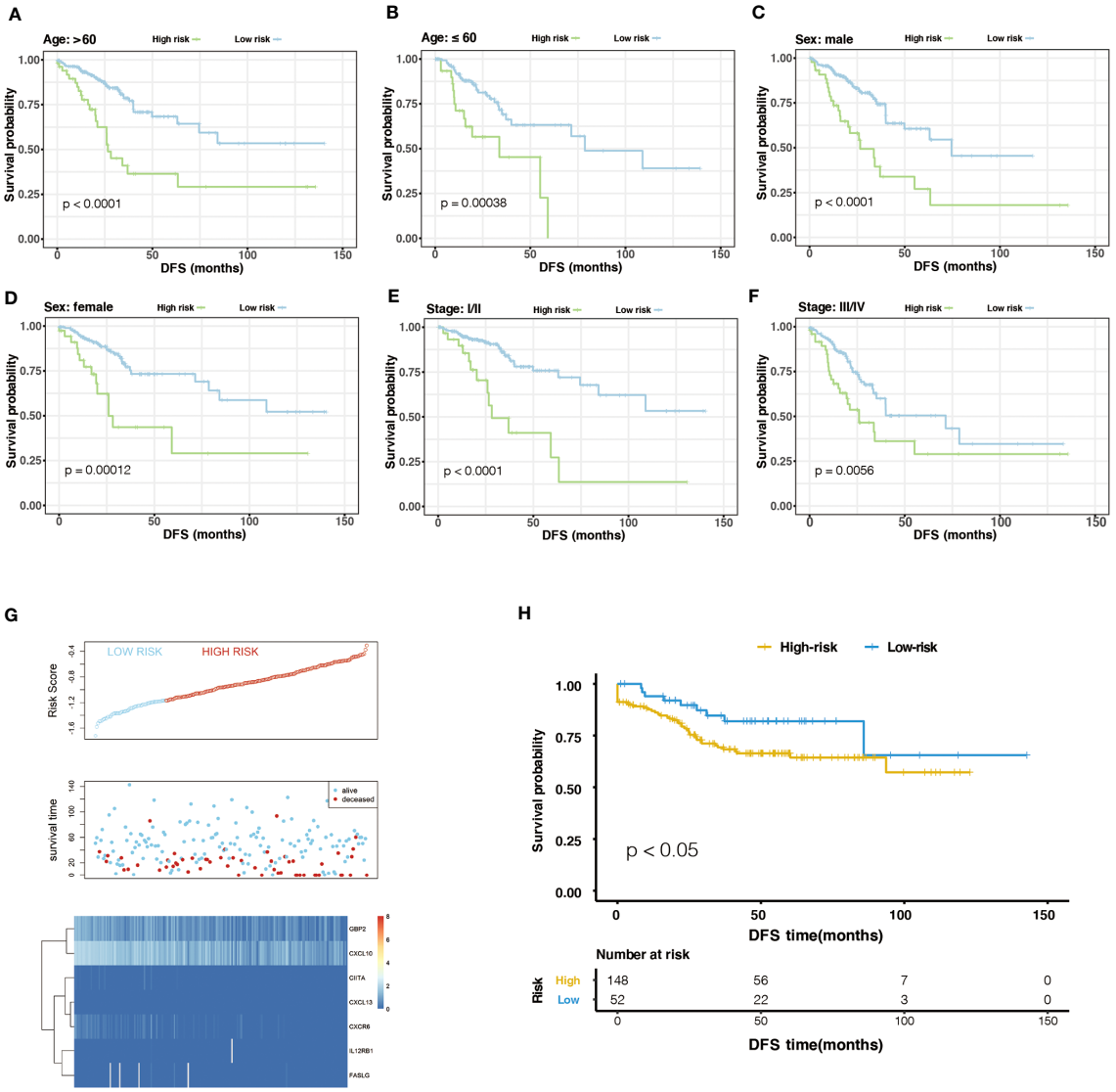

FIGURE 3
The stratification analysis and validation of the GEO dataset. **(A-F)** The stability of m6A-GPI in stratified samples (divided by age, sex, and stage). **(G)** The distribution of risk score and the status of colorectal cancer patients and the heatmap of hub genes in the GEO dataset. **(H)** Kaplan–Meier curves showed that the patients of the high-risk group had worse DFS in the GEO dataset.

analysis showed that m6A-GPI was closely related to the prognosis of CRC [hazard ratio (HR) = 3.041, 90% CI: 2.06–4.5, *P*< 0.001]. Multivariate Cox analysis further showed that m6A-GPI can be used as an independent predictor in CRC [hazard ratio (HR) = 2.4, 90% CI: 1.6–3.59, *P*< 0.001] (Figure 6A). At the same time, we constructed a nomogram and calibration plots of DFS at 1-, 3-, and 5-year in the TCGA dataset (Figures 6B–E), which provides doctors with a method to quantitatively predict the prognosis of CRC. The accuracy of prediction at 3 years can be increased to 0.75 after combining the risk score and clinical characteristics (Figure 6F).

3.8 Validation of m6A-related genes expression levels in CRC tissues

To further investigate the expression levels of m6A-related genes in CRC clinical tissues. We first detected the mRNA expression of m6A-related genes (*IL12RB1*, *FASLG*, *CXCL13*, *GBP2*, *CXCL10*, *CXCR6*, and *CIITA*). Notably, the expression of *CIITA* was substantially increased in CRC tissues (Figure 7A). However, there was no significant difference of others genes between CRC and adjacent normal tissues (Figure 7A). Subsequently, protein level of CIITA was detected in CRC and adjacent normal tissues. Consistent with mRNA levels, the protein level of CIITA was also obviously increased in CRC tissues (Figure 7B).

4 Discussion

Several lines of evidence indicate that m6A modification has become an important target in tumor immunity (27, 28). We believe that a novel prognostic marker based on m6A-related genes will

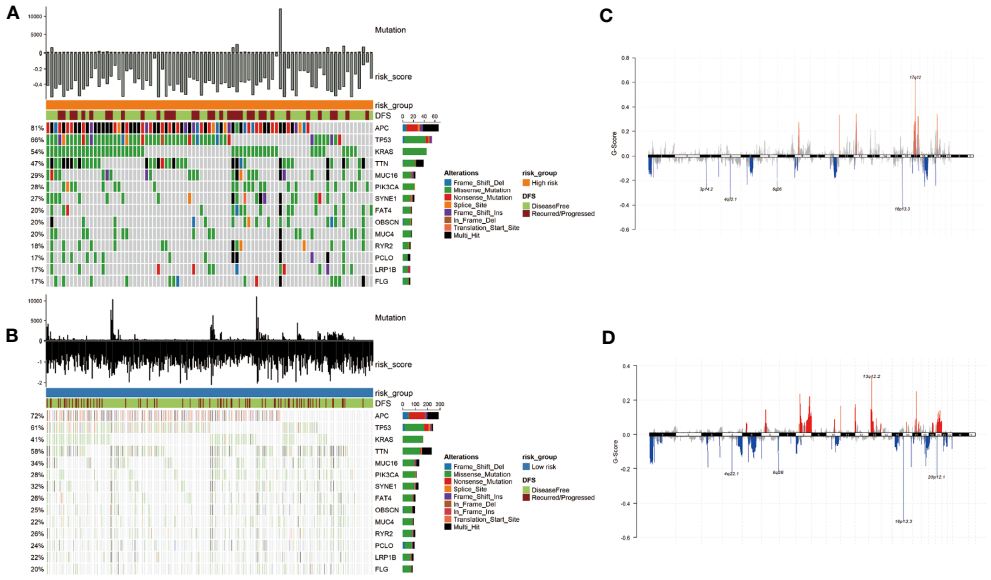

FIGURE 4
Mutational landscape and CNV of two groups in the TCGA-COAD. **(A, B)** Genes with high frequency mutation in the COAD samples of high-risk subgroup **(A)** and low-risk subgroup **(B)**. **(C, D)** CNV of the high- and low-risk groups. The markedly amplified part is displayed above the x-axis and marked with red; the markedly deleted part is displayed below the x-axis and marked with blue.

help predict the prognosis and immune infiltration of colorectal cancer. For this reason, we screened 7 m6A-related genes (IL12RB1, FASLG, CXCL13, GBP2, CXCL10, CXCR6, and CIITA) through WGCNA and LASSO regression in this study and established an m6A-GPI in colorectal cancer. Survival analysis based on m6A-GPI showed that a lower risk score means longer DFS for patients. At the same time, we found that groups with different clinical characteristics (such as tumor site and stage) also showed differences in risk scores. We explored the molecular factors that affect tumor immunogenicity. The risk score was positively correlated with the HRD, CNA, and mRNAsi, and people with higher risk scores may have chromosomal instability. It is worth noting that m6A-GPI not only has good prognostic predictive ability but is also related to tumor immunogenicity, immune cell infiltration in CRC patients, which indicates that m6A-GPI may become a predictive indicator of tumor treatment. We also confirmed that m6A-GPI is an independent prognostic factor for CRC patients, which will provide useful guidance for clinical treatment strategies. Finally, we verified the expression levels of m6A-related genes (IL12RB1, FASLG, CXCL13, GBP2, CXCL10, CXCR6, and CIITA) in CRC tissues. Our results indicated that CIITA might play a crucial role in the prognosis of colorectal cancer.

At present, many studies have shown that m6A-related genes play an indispensable role in cancer progression and metastasis (29). Abnormal expression of genes associated with m6A has a significant impact on the prognosis of colorectal cancer. Overexpression of METTL3, a m6A writer, facilitates tumorigenesis of CRC by regulating the expression of genes related to cell cycle, noncoding RNA metabolism and glycolysis pathway (<xr rid="r36">30</xr>; 31, 32). The dysregulation of long non-coding RNA XIST, mediated by the loss of METTL14, has been found to be significantly associated with an unfavorable prognosis in patients with CRC (33). The m6A reader, YTHDC2, has been found to facilitate the metastasis of CRC by stimulating the translation of HIF-1α (34). However, the mechanisms by which m6A-related genes regulate immune cell infiltration in CRC remain elusive. In our study, the tumor immune microenvironment of patients with higher risk scores had increased infiltration of immune cells, such as resting NK cells, and M0 macrophages. Previous studies have shown that macrophages can be recruited to tumor tissues and contribute to tumor angiogenesis (35), which may cause poor DFS in high-risk groups. In addition, a significantly higher proportion of $CD4^+$ T cells, $CD8^+$ T cells, memory B cells, and M1 macrophages were found in patients in the low-risk group, indicating that there is a greater proportion of T cells and B cells in low-risk CRC tumors. $CD8^+$ T cells play a major role in tumor immunity. $CD8^+$ T cells differentiate into cytotoxic T cells in the body, and cytotoxic T cells can enter the tumor microenvironment and inhibit the growth of the tumor (36). In the TIME, there is a tendency for $CD8^+$ T cells to increase in METTL3- or METTL14-null tumors, accompanied by increased secretion of IFN-γ, CXCL9 and CXCL10 (18). Meanwhile, studies have confirmed that the expression of ALKBH5 is specifically upregulated when T cells are activated, and ALKBH5 increases m6A modification on IFN-

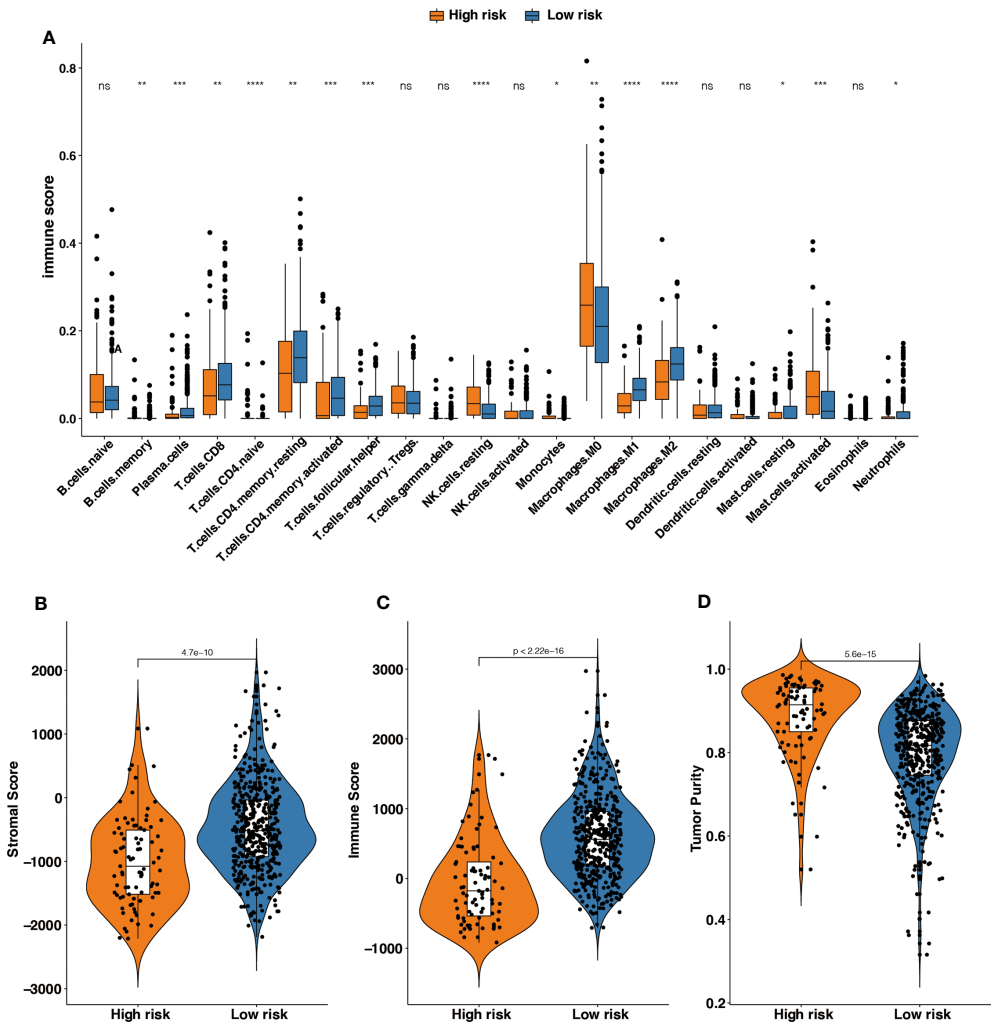

FIGURE 5
The different tumor-infiltrating immune cells between high- and low-risk groups based on m6A-GPI. **(A)** Profiles of 22 types of tumor-infiltrating immune cells in two groups. **(B–D)** Patients with a different stromal score, immune score, and tumor purity had different levels of risk scores. *p < 0.05; **p < 0.01; ***p < 0.001; ****p < 0.0001; ns, no significance.

γ and CXCL2 in $CD4^+$ T cells, thereby affecting mRNA stability and protein expression. These modifications lead to changes in the response of $CD4^+$ T cells (37). The infiltration of M1 macrophages can promote inflammation and inhibit tumor cells in the TIME, M1 cells can be activated by IFN-γ and destroy tumors by producing nitric oxide, type 1 cytokines, and chemokines (38), which is consistent with the trend we observed in the low-risk group. Finally, this study found that compared with the high-risk group, CRC patients in the low-risk group had higher immune scores and stromal scores, and had lower tumor purity.

m6A modification changes the TIME, which largely affects the therapeutic response to antitumor immunotherapy. Approximately 85% of CRC patients have mismatch-repair-proficient or microsatellite instability-low (pMMR-MSI-L) tumors. This type of patient failed to benefit from any single immunotherapy, but microsatellite instability-high (pMMR-MSI-H) CRC responds well to immunotherapy because it can recruit a large number of immune cells such as $CD8^+/CD4^+$ T cells and macrophages into the microenvironment (39–42). Wang et al. proposed that the destruction of m6A methyltransferase enhances the immunotherapy response of pMMR-MSI-L colorectal cancer by regulating the tumor microenvironment and tumor-infiltrating cells (18). In fact, the loss of METTL3 or METTL14 enhances the interaction between the tumor and the immune system through the IFN-γ-STAT1-IRF1. In another study on "eraser" ALKBH5, researchers found that the knockout of ALKBH5 in mice with CT26 colorectal cancer or B16 melanoma significantly reduced tumor growth and prolonged the survival rate of mice during immunotherapy. This may be related to ALKBH5 inhibiting immune cells in the tumor microenvironment and regulating lactic acid. These processes increase the response to anti-PD-L1 therapy and the loss of ALKBH5 changes the composition of

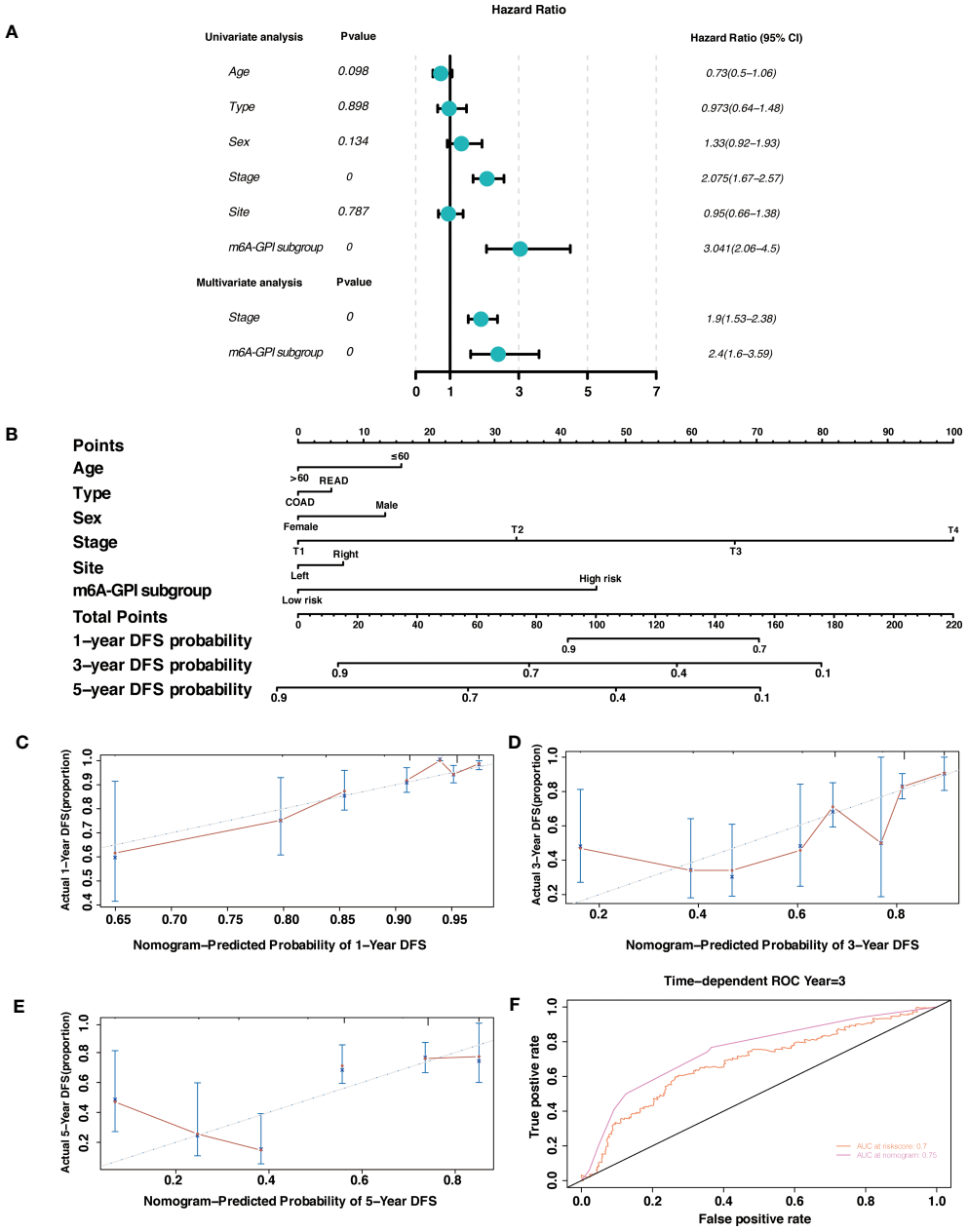

FIGURE 6
Independent prognostic factor and nomogram. **(A)** Univariate and multivariate analysis revealed that risk score based on m6A-GPI was an independent prognostic predictor. **(B)** Nomogram based on age, type, sex, stage, site, and risk group. **(C-E)** Calibration plots of the nomogram for predicting the probability of OS at 1-, 3-, and 5-year in the TCGA dataset. **(F)** The ROC curves of risk score and nomogram.

immune cells and metabolite tumor microenvironment (13). In the subgroups based on m6A-GPI, the TIME and immune cells have changed. We found that tumors in the low-risk group recruited more $CD4^+/CD8^+$ T cells, our research provides important guidance for predicting the proportion of immune cells in CRC.

Our research provides ideal predictors for the prognosis and immune cell infiltration, but it is undeniable that there are several limitations in this study. First, we used retrospective data from public databases to construct and verify the m6A-GPI, and it would be more rigorous to use a larger-scale prospective data to evaluate its reliability. Second, the population in our study was mainly Americans, and different countries may have deviations in the results due to ethnic differences. In fact, this manuscript is the first part of our research, and our next research project will stem from these results.

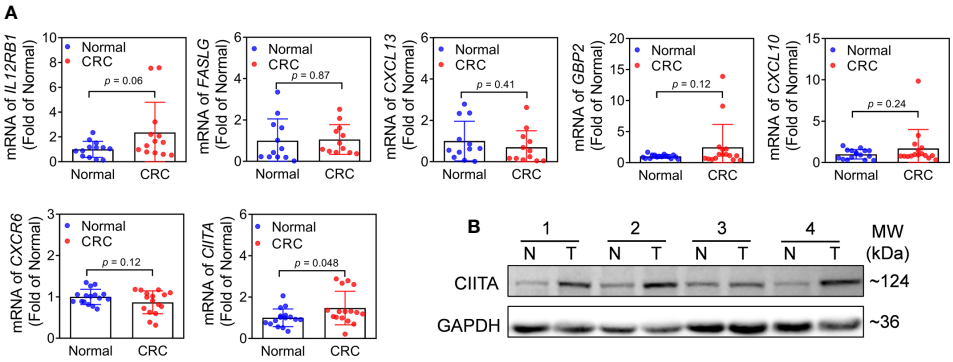

FIGURE 7
Expression of m6A-related genes in CRC and adjacent normal tissues. **(A)** mRNA expression levels of *IL12RB1*, *FASLG*, *CXCL13*, *GBP2*, *CXCL10*, *CXCR6*, and *CIITA* in CRC and adjacent normal tissues. n = 16, *p< 0.05 vs adjacent normal tissues. **(B)** Protein level of CIITA. Representative images were shown. n = 7, T: CRC tissues, N: adjacent normal tissues. Full-length blots of immunoblotting were presented in Supplementary Figure 6.

In conclusion, m6A-GPI is a promising m6A-related prognostic biomarker. Our study divides patients into different risk subgroups based on m6A-GPI, which will help doctors identify the molecular and immune characteristics and predict the progression, prognosis of CRC. Moreover, m6A-GPI may be a potential indicator in the adjustment of tumor treatment strategies.

Data availability statement

The datasets presented in this study can be found in online repositories. The names of the repository/repositories and accession number(s) can be found in the article/Supplementary Material.

Ethics statement

The studies involving human participants were reviewed and approved by The Ethics Committee of the Liaoning Cancer Hospital, Shenyang, China. The patients/participants provided their written informed consent to participate in this study.

Author contributions

BM conceived and designed this study. BM performed the bioinformatic analysis and visualization. SB performed the experimental validation. YL collected data and performed the statistical analysis. BM and SB wrote the original draft and BM revised the manuscripts. All authors revised and approved the final manuscript. All authors contributed to the article and approved the submitted version.

Funding

Cultivation Program of National Science Foundation of Liaoning Cancer Hospital (2021-ZLLH-03); Beijing Xisike Clinical Oncology Research Foundation (Y-QL202101-0039).

Acknowledgments

We obtained data from and we sincerely thank The Cancer Genome Atlas (TCGA) database for the establishment and management of the database.

Conflict of interest

The authors declare that the research was conducted in the absence of any commercial or financial relationships that could be construed as a potential conflict of interest.

Publisher's note

All claims expressed in this article are solely those of the authors and do not necessarily represent those of their affiliated organizations, or those of the publisher, the editors and the reviewers. Any product that may be evaluated in this article, or claim that may be made by its manufacturer, is not guaranteed or endorsed by the publisher.

Supplementary material

The Supplementary Material for this article can be found online at: https://www.frontiersin.org/articles/10.3389/fonc.2023.1145753/full#supplementary-material

References

1. Thrumurthy SG, Thrumurthy SS, Gilbert CE, Ross P, Haji A. Colorectal adenocarcinoma: risks, prevention and diagnosis. *Bmj* (2016) 354:i3590. doi: 10.1136/bmj.i3590

2. Arnold M, Sierra MS, Laversanne M, Soerjomataram I, Jemal A, Bray F. Global patterns and trends in colorectal cancer incidence and mortality. *Gut* (2017) 66(4):683–91. doi: 10.1136/gutjnl-2015-310912

3. Mauri G, Sartore-Bianchi A, Russo AG, Marsoni S, Bardelli A, Siena S. Early-onset colorectal cancer in young individuals. *Mol Oncol* (2019) 13(2):109–31. doi: 10.1002/1878-0261.12417

4. Van der Jeught K, Xu HC, Li YJ, Lu XB, Ji G. Drug resistance and new therapies in colorectal cancer. *World J Gastroenterol* (2018) 24(34):3834–48. doi: 10.3748/wjg.v24.i34.3834

5. Lefèvre JH, Mineur L, Cachanado M, Denost Q, Rouanet P, de Chaisemartin C, et al. Does a longer waiting period after neoadjuvant radio-chemotherapy improve the oncological prognosis of rectal cancer?: three years' follow-up results of the greccar-6 randomized multicenter trial. *Ann Surg* (2019) 270(5):747–54. doi: 10.1097/sla.0000000000003530

6. Mao R, Yang F, Wang Z, Xu C, Liu Q, Liu Y, et al. Clinical significance of a novel tumor progression-associated immune signature in colorectal adenocarcinoma. *Front Cell Dev Biol* (2021) 9:625212. doi: 10.3389/fcell.2021.625212

7. Al-Tashi Q, Saad MB, Muneer A, Qureshi R, Mirjalili S, Sheshadri A, et al. Machine learning models for the identification of prognostic and predictive cancer biomarkers: a systematic review. *Int J Mol Sci* (2023) 24(9). doi: 10.3390/ijms24097781

8. Shao J, Ma J, Zhang Q, Li W, Wang C. Predicting gene mutation status *via* artificial intelligence technologies based on multimodal integration (MMI) to advance precision oncology. *Semin Cancer Biol* (2023) 91:1–15. doi: 10.1016/j.semcancer.2023.02.006

9. Zhang Z, Wei X. Artificial intelligence-assisted selection and efficacy prediction of antineoplastic strategies for precision cancer therapy. *Semin Cancer Biol* (2023) 90:57–72. doi: 10.1016/j.semcancer.2023.02.005

10. Lim H, He D, Qiu Y, Krawczuk P, Sun X, Xie L. Rational discovery of dual-indication multi-target PDE/Kinase inhibitor for precision anti-cancer therapy using structural systems pharmacology. *PloS Comput Biol* (2019) 15(6):e1006619. doi: 10.1371/journal.pcbi.1006619

11. Li X, Warren S, Pelekanou V, Wali V, Cesano A, Liu M, et al. Immune profiling of pre- and post-treatment breast cancer tissues from the SWOG S0800 neoadjuvant trial. *J Immunother Cancer* (2019) 7(1):88. doi: 10.1186/s40425-019-0563-7

12. Vassilakopoulou M, Avgeris M, Velcheti V, Kotoula V, Rampias T, Chatzopoulos K, et al. Evaluation of PD-L1 expression and associated tumor-infiltrating lymphocytes in laryngeal squamous cell carcinoma. *Clin Cancer Res* (2016) 22(3):704–13. doi: 10.1158/1078-0432.Ccr-15-1543

13. Li N, Kang Y, Wang L, Huff S, Tang R, Hui H, et al. ALKBH5 regulates anti-PD-1 therapy response by modulating lactate and suppressive immune cell accumulation in tumor microenvironment. *Proc Natl Acad Sci U.S.A.* (2020) 117(33):20159–70. doi: 10.1073/pnas.1918986117

14. Ren W, Yuan Y, Li Y, Mutti L, Peng J, Jiang X. The function and clinical implication of YTHDF1 in the human system development and cancer. *biomark Res* (2023) 11(1):5. doi: 10.1186/s40364-023-00452-1

15. Sendinc E, Shi Y. RNA m6A methylation across the transcriptome. *Mol Cell* (2023) 83(3):428–41. doi: 10.1016/j.molcel.2023.01.006

16. Li T, Hu PS, Zuo Z, Lin JF, Li X, Wu QN, et al. METTL3 facilitates tumor progression *via* an m(6)A-IGF2BP2-dependent mechanism in colorectal carcinoma. *Mol Cancer* (2019) 18(1):112. doi: 10.1186/s12943-019-1038-7

17. Han D, Liu J, Chen C, Dong L, Liu Y, Chang R, et al. Anti-tumour immunity controlled through mRNA m(6)A methylation and YTHDF1 in dendritic cells. *Nature* (2019) 566(7743):270–4. doi: 10.1038/s41586-019-0916-x

18. Wang L, Hui H, Agrawal K, Kang Y, Li N, Tang R, et al. m(6) a RNA methyltransferases METTL3/14 regulate immune responses to anti-PD-1 therapy. *EMBO J* (2020) 39(20):e104514. doi: 10.15252/embj.2020104514

19. Huang D, Zhang F, Tao H, Zhang S, Ma J, Wang J, et al. Tumor mutation burden as a potential biomarker for PD-1/PD-L1 inhibition in advanced non-small cell lung cancer. *Target Oncol* (2020) 15(1):93–100. doi: 10.1007/s11523-020-00703-3

20. Newman AM, Liu CL, Green MR, Gentles AJ, Feng W, Xu Y, et al. Robust enumeration of cell subsets from tissue expression profiles. *Nat Methods* (2015) 12 (5):453–7. doi: 10.1038/nmeth.3337

21. Jiang YZ, Ma D, Suo C, Shi J, Xue M, Hu X, et al. Genomic and transcriptomic landscape of triple-negative breast cancers: subtypes and treatment strategies. *Cancer Cell* (2019) 35(3):428–440.e425. doi: 10.1016/j.ccell.2019.02.001

22. Duan J, Pan Y, Yang X, Zhong L, Jin Y, Xu J, et al. Screening of T cell-related long noncoding RNA-MicroRNA-mRNA regulatory networks in non-Small-Cell lung cancer. *BioMed Res Int* (2020) 2020:5816763. doi: 10.1155/2020/5816763

23. Qiang JK, Sutradhar R, Giannakeas V, Bhatia D, Singh S, Lipscombe LL. Impact of diabetes on colorectal cancer stage and mortality risk: a population-based cohort study. *Diabetologia* (2020) 63(5):944–53. doi: 10.1007/s00125-020-05094-8

24. Chao A, Lai CH, Wang TH, Jung SM, Lee YS, Chang WY, et al. Genomic scar signatures associated with homologous recombination deficiency predict adverse clinical outcomes in patients with ovarian clear cell carcinoma. *J Mol Med (Berl)* (2018) 96(6):527–36. doi: 10.1007/s00109-018-1643-8

25. Zhang Y, Tseng JT, Lien IC, Li F, Wu W, Li H. mRNAsi index: machine learning in mining lung adenocarcinoma stem cell biomarkers. *Genes (Basel)* (2020) 11(3). doi: 10.3390/genes11030257

26. Wang M, Zhao J, Zhang L, Wei F, Lian Y, Wu Y, et al. Role of tumor microenvironment in tumorigenesis. *J Cancer* (2017) 8(5):761–73. doi: 10.7150/jca.17648

27. Gu Y, Wu X, Zhang J, Fang Y, Pan Y, Shu Y, et al. The evolving landscape of N (6)-methyladenosine modification in the tumor microenvironment. *Mol Ther* (2021) 29(5):1703–15. doi: 10.1016/j.ymthe.2021.04.009

28. Li M, Zha X, Wang S. The role of N6-methyladenosine mRNA in the tumor microenvironment. *Biochim Biophys Acta Rev Cancer* (2021) 1875(2):188522. doi: 10.1016/j.bbcan.2021.188522

29. He L, Li H, Wu A, Peng Y, Shu G, Yin G. Functions of N6-methyladenosine and its role in cancer. *Mol Cancer* (2019) 18(1):176. doi: 10.1186/s12943-019-1109-9

30. Wu Y, Yang X, Chen Z, Tian L, Jiang G, Chen F, et al. m(6)A-induced lncRNA RP11 triggers the dissemination of colorectal cancer cells *via* upregulation of Zeb1. *Mol Cancer* (2019) 18(1):87. doi: 10.1186/s12943-019-1014-2

31. Shen C, Xuan B, Yan T, Ma Y, Xu P, Tian X, et al. m(6)A-dependent glycolysis enhances colorectal cancer progression. *Mol Cancer* (2020) 19(1):72. doi: 10.1186/s12943-020-01190-w

32. Zhu W, Si Y, Xu J, Lin Y, Wang JZ, Cao M, et al. Methyltransferase like 3 promotes colorectal cancer proliferation by stabilizing CCNE1 mRNA in an m6A-dependent manner. *J Cell Mol Med* (2020) 24(6):3521–33. doi: 10.1111/jcmm.15042

33. Yang X, Zhang S, He C, Xue P, Zhang L, He Z, et al. METTL14 suppresses proliferation and metastasis of colorectal cancer by down-regulating oncogenic long non-coding RNA XIST. *Mol Cancer* (2020) 19(1):46. doi: 10.1186/s12943-020-1146-4

34. Tanabe A, Tanikawa K, Tsunetomi M, Takai K, Ikeda H, Konno J, et al. RNA Helicase YTHDC2 promotes cancer metastasis *via* the enhancement of the efficiency by which HIF-1α mRNA is translated. *Cancer Lett* (2016) 376(1):34–42. doi: 10.1016/j.canlet.2016.02.022

35. Fu LQ, Du WL, Cai MH, Yao JY, Zhao YY, Mou XZ. The roles of tumor-associated macrophages in tumor angiogenesis and metastasis. *Cell Immunol* (2020) 353:104119. doi: 10.1016/j.cellimm.2020.104119

36. Iwahori K. Cytotoxic CD8(+) lymphocytes in the tumor microenvironment. *Adv Exp Med Biol* (2020) 1224:53–62. doi: 10.1007/978-3-030-35723-8_4

37. Zhou J, Zhang X, Hu J, Qu R, Yu Z, Xu H, et al. m(6)A demethylase ALKBH5 controls CD4(+) T cell pathogenicity and promotes autoimmunity. *Sci Adv* (2021) 7 (25). doi: 10.1126/sciadv.abg0470

38. Gui T, Shimokado A, Sun Y, Akasaka T, Muragaki Y. Diverse roles of macrophages in atherosclerosis: from inflammatory biology to biomarker discovery. *Mediators Inflammation* (2012) 2012:693083. doi: 10.1155/2012/693083

39. Deschoolmeester V, Baay M, Lardon F, Pauwels P, Peeters M. Immune cells in colorectal cancer: prognostic relevance and role of MSI. *Cancer Microenviron* (2011) 4 (3):377–92. doi: 10.1007/s12307-011-0068-5

40. Le DT, Uram JN, Wang H, Bartlett BR, Kemberling H, Eyring AD, et al. PD-1 blockade in tumors with mismatch-repair deficiency. *N Engl J Med* (2015) 372 (26):2509–20. doi: 10.1056/NEJMoa1500596

41. Llosa NJ, Cruise M, Tam A, Wicks EC, Hechenbleikner EM, Taube JM, et al. The vigorous immune microenvironment of microsatellite instable colon cancer is balanced by multiple counter-inhibitory checkpoints. *Cancer Discovery* (2015) 5(1):43–51. doi: 10.1158/2159-8290.Cd-14-0863

42. Ganesh K, Stadler ZK, Cercek A, Mendelsohn RB, Shia J, Segal NH, et al. Immunotherapy in colorectal cancer: rationale, challenges and potential. *Nat Rev Gastroenterol Hepatol* (2019) 16(6):361–75. doi: 10.1038/s41575-019-0126-x

frontiers | Frontiers in Oncology

TYPE Original Research
PUBLISHED 31 July 2023
DOI 10.3389/fonc.2023.1192378

OPEN ACCESS

EDITED BY
Jorge Melendez-Zajgla,
National Institute of Genomic Medicine (INMEGEN), Mexico

REVIEWED BY
Mansoor-Ali Vaali-Mohammed,
King Saud University, Saudi Arabia
Tianbo Jin,
Northwest University, China
Antonella Argentiero,
National Cancer Institute Foundation (IRCCS), Italy
Mónica Alejandra Rosales-Reynoso,
Centro de Investigación Biomédica de Occidente (CIBO), Mexico

*CORRESPONDENCE
Shuyong Yu
yushuyong2022@163.com

†These authors share first authorship

RECEIVED 23 March 2023
ACCEPTED 28 June 2023
PUBLISHED 31 July 2023

CITATION
Song J, Wang K, Chen Z, Zhong D, Li L, Guo L and Yu S (2023) Association study between *C10orf90* gene polymorphisms and colorectal cancer.
Front. Oncol. 13:1192378.
doi: 10.3389/fonc.2023.1192378

Association study between *C10orf90* gene polymorphisms and colorectal cancer

Jian Song[1†], Kaixuan Wang[2†], Zhaowei Chen[3†], Dunjing Zhong[3], Li Li[4], Liangliang Guo[3] and Shuyong Yu[4*]

[1]Department of Gastroenterology, Southern University of Science and Technology Hospital, Shenzhen, Guangdong, China, [2]Department of Gastroenterology, The First Affiliated Hospital of Naval Medical University, Shanghai, China, [3]Department of Gastroenterology, Hainan Cancer Hospital, Haikou, Hainan, China, [4]Department of Gastrointestinal Surgery, Hainan Cancer Hospital, Haikou, Hainan, China

Background: Colorectal cancer (CRC) is the third most common malignant tumor in the world. The morbidity and mortality rates in Western countries have decreased, but they are still on the rise in China. *C10orf90* is associated with a variety of cancers, but the correlation between *C10orf90* and CRC is not yet known.

Methods: A total of 1,339 subjects were randomly enrolled in our study. After extracting their DNA, three single-nucleotide polymorphisms (SNPs) of *C10orf90* were genotyped to analyze the potential relationship between these variants and CRC risk. PLINK software packages (version 1.07) were used to evaluate multiple genetic models by calculating the odds ratio (OR) and 95% confidence interval (95% CI). The best SNP–SNP interaction model was defined by the multifactor dimensionality reduction (MDR) analysis.

Results: *C10orf90* rs12412320 was significantly associated with CRC risk (p = 0.006) and might be associated with the lower CRC risk (OR: 0.78; 95% CI: 0.65–0.93). The relationship of rs12412320 with lower CRC risk was found in people aged >60 years and ≤60 years, women, non-smokers, or non-drinkers. Rs11245008 in people aged ≤60 years and rs11245007 among men had a higher CRC susceptibility. Rs12412320 was related to the lower risk of advanced stages (III/IV stage), while rs11245007 might be associated with the higher risk of advanced stages (III/IV stage). Moreover, rs12412320 had the most significant relationship with the susceptibility to rectal cancer.

Conclusion: This study is the first to report between *C10orf90* gene polymorphisms and CRC risk in Chinese people, which suggests that *C10orf90* rs12412320 might play a crucial role in preventing CRC occurrence.

KEYWORDS

colorectal cancer, *C10orf90*, gene polymorphisms, demographic characteristics, clinical features

Introduction

Colorectal cancer (CRC) is the third (3.11%) most common malignant tumor in the world and the second (3.5%) leading cause of cancer death (1). Globally, there are approximately 1 million new CRC patients every year, and more than 915,880 patients die each year (1). The CRC incidence and mortality rates in China, Europe, and North America account for more than half of the world's CRC incidence and mortality, respectively (2). Most recently, the incidence rate of CRC has been increasing and has become the second most common malignant tumor in China, which seriously threatens the life and health of residents (3). In China, the survival rate of CRC in the recent 5 years is significantly lower than that of many developed countries (4, 5). Despite the high incidence and low survival rate of CRC in China, the pathogenesis of CRC remains unclear. Genetics and environment are the major factors in the development of CRC (6, 7). Previously, hyperlipidemia, obesity, alcohol consumption, and smoking were suggested to be risk factors, and other potential risk factors included hypertension, metabolic syndrome, dietary factors, sedentary behavior, and occupational exposure (8). Furthermore, genetic predisposition is one of the key risk factors in the development of CRC (9).

C10orf90 (Chromosome 10 Open Reading Frame 90) is a protein coding gene and is known as the fragile-site associated tumor suppressor (FATS), which is also a regulator of the p53-p21 pathway (10). Studies have shown that in conjunctival melanoma, the deletion of the tumor suppressor gene *C10orf90* is related to the significantly reduced metastasis-free survival of tumor patients (11). In addition, *C10orf90* is a target gene of p53, and its overexpression can inhibit tumorigenicity *in vivo*, which is related to anti-tumor activity (12). FATS is an E2- and E3-independent ubiquitin ligase for promoting p53 stability and activation in response to DNA damage (13). The expression of *C10orf90* gene is downregulated or silenced in many cancers, and it is related to non-small cell lung cancer, breast cancer, and others (14, 15). Furthermore, *C10orf90* variants have been reported to be associated with the risk of various cancers, including breast cancer (16) and conjunctival melanomas (11). However, whether the genetic variants in *C10orf90* may modulate CRC susceptibility remain unknown.

Single-nucleotide polymorphism (SNP) in the coding regions of genes may affect protein function. Here, three polymorphisms in the exon region of *C10orf90* were genotyped to explore the relationship with CRC susceptibility in the Chinese Han population and to correlate these with demographic characteristics and clinical features.

Methods

Subjects

In this study, a total of 666 CRC patients at Hainan Province Cancer Hospital from August 2020 to December 2022 were randomly enrolled in the case group. A total of 673 healthy adults form the control group; they were from the same hospital during the same period without a history of cancer and chronic or severe diseases. The selection criteria of patients complied with the "Guidelines for diagnosis and treatment of colorectal cancer (2021 CSCO)" (17), and all patients were independent of each other. Patients suffering from inflammation, renal dysfunction, digestive system disease, and other chronic or endocrine disease, and who have been receiving any anti-cancer drugs or treatments were excluded. Demographic and clinical information of all subjects were gathered through standardized questionnaires and medical records, which include age, sex, smoking status, drinking status, body mass index (BMI), cancer stage, lymph node metastasis status, cancer style, carcinoembryonic antigen (CEA), alpha-fetoprotein (AFP), and cancer antigen-199 (CA199). The study was approved by the ethical committee of Hainan Province Cancer Hospital, and informed consent forms were signed by all subjects before the study, according to the Helsinki Declaration.

DNA extraction and SNP genotyping

Three SNPs (rs12412320, rs11245007, and rs11245008) in *C10orf90* were selected for the study of their potential role in the risk of CRC based on a minor allele frequency (MAF) > 0.05 through the 1000 Genome Project. The potential biological functions of these loci were predicted through bioinformatics databases, including dbSNP, RegulomeDB, VannoPortal, and HaploReg v4.2.

Genomic DNA was extracted from peripheral blood samples (5 mL) of each subject using the Whole Blood Genomic DNA Isolation Kit (Xi'an Gold Mag Biotechnology, Xi'an, China). DNA was stored together with EDTA in a tube at −80°C. DNA concentrations were measured using NanoDrop 2000 (Ultra-fine ultraviolet spectrophotometer, Thermo, Waltham, MA, USA). SNP genotyping with a standard protocol was carried out using Agena MassARRAY RS1000. Agena Typer Software version 4.0 was used for data management.

Data analysis

Independent samples *t*-test and Chi-square test were used to assess the differences in demographic characteristics of the study participants. We used Fisher's test to evaluate the Hardy–Weinberg equilibrium (HWE) of each SNP in the subjects. Odds ratio (OR) and 95% confidence interval (95% CI) were assessed to estimate the correlations of SNPs and CRC risk using logistic regression analysis. PLINK software packages (version 1.07) were used to evaluate multiple genetic models (allele model, genotype model, dominant model, recessive model, and additive model). Statistical analysis was performed using Microsoft Excel and SPSS 17.0 statistical packages (SPSS, Chicago, IL). A two-tailed $p < 0.05$ was considered statistically significant, and a Bonferroni-corrected $p < 0.05/3$ was considered significant. In addition, we used the multifactor

dimensionality reduction (MDR) analysis to identify the best SNP–SNP interaction model.

Results

Characteristics of subjects

There were 1,339 subjects in this study, namely, 666 CRC patients (age: 60.02 ± 11.28 years) and 673 healthy controls (age: 59.53 ± 9.63 years). Table 1 shows the relevant characteristics of all subjects including the case group and the control group. It can be seen that there are no statistical differences between CRC patients and healthy controls in these indexes such as age ($p = 0.391$), sex ($p = 0.698$), smoking ($p = 0.372$), and drinking ($p = 0.438$). There was a significant difference in BMI between CRC patients and healthy controls ($p < 0.001$).

Relationship between *C10orf90* SNPs and CRC risk

The relationship between SNPs of *C10orf90* and CRC risk is listed in Table 2. All SNPs were missense variants. All SNPs of *C10orf90* complied with the Hardy–Weinberg equilibrium ($p > 0.05$). The MAF of each SNP was above 5% in the Chinese Han population. *C10orf90* rs12412320 was significantly associated with CRC risk ($p = 0.006$) and might be

TABLE 1 Characteristics of colorectal cancer patients and healthy controls.

variable	Patients (n=666)	Controls (n=673)	*p*
Age (years)	60.017 ± 11.275	59.525 ± 9.634	
> 60	350 (52.6%)	377 (56.0%)	0.391
≤ 60	316 (47.4%)	296 (44.0%)	
Sex			
male	383 (57.5%)	395 (58.7%)	0.698
female	283 (42.5%)	278 (41.3%)	
Smoking Status			
Yes	257 (38.6%)	276 (41.0%)	0.372
No	409 (61.4%)	397 (59.0%)	
Drinking Status			
Yes	270 (40.5%)	287 (42.6%)	0.438
No	396 (59.5%)	386 (57.4%)	
BMI (kg/m^2)	22.441 ± 3.355	24.215 ± 3.364	
> 24	155 (23.3%)	214 (31.8%)	**$p < 0.001$**
≤ 24	305 (45.8%)	200 (29.7%)	
Missing	252 (37.8%)	213 (31.6%)	
Stage			
I/II	94 (14.1%)		
III/IV	212 (31.8%)		
Missing	360 (54.1%)		
Lymph node metastasis			
Yes	233 (35.0%)		
No	133 (20.0%)		
Missing	300 (45.0%)		
Cancer Style			
Colon cancer	293 (44%)		
Rectal cancer	351 (52.7%)		
Missing	22 (3.3%)		

BMI, body mass index.
p values were calculated using Chi-square test or T test, two sided.
Bold indicates statistical significance at P < 0.05.

TABLE 2 The based information of selected SNPs in *C10orf90* and the association with the risk of colorectal cancer in the allele model.

SNP	Chromosome	Alleles A / B	dbSNP func annot	MAF		p HWE	OR (95% CI)	p *	RegulomeDB	HaploReg v4.2
				Case	Control					
rs12412320	10:126461527	T/G	Missense D (Asp) > E (Glu)	0.205	0.249	0.758	0.78 (0.65 - 0.93)	**0.006***	TF binding or DNase peak	Enhancer histone marks, Motifs changed
rs11245007	10:126504416	T/C	Missense D (Asp) > N (Asn)	0.480	0.452	0.436	1.12 (0.96 - 1.31)	0.134	TF binding + any motif + DNase peak	Promoter histone marks, Enhancer histone marks, DNAse, Proteins bound, Motifs changed
rs11245008	10:126504799	T/C	Missense R (Arg) > L (Leu)	0.137	0.121	0.145	1.16 (0.92 - 1.45)	0.209	TF binding + any motif + DNase peak	Enhancer histone marks, DNAse, Motifs changed

SNP, Single nucleotide polymorphism; MAF, Minor allele frequency; HWE, Hardy-Weinberg equilibrium; OR, Odds ratio; 95% CI, 95% confidence interval.
p values of Hardy-Weinberg equilibrium were calculated using Chi-square test.
p values were calculated by two sided Chi-square test, and * $p < 0.05$ was considered statistical significance.
Bold p means that the data is statistically significant after Bonferroni correction ($p < 0.05/3$).
dbSNP (https://www.ncbi.nlm.nih.gov/snp/), RegulomeDB (https://regulome.stanford.edu/regulome-search/) and HaploReg v4.2 (https://pubs.broadinstitute.org/mammals/haploreg/haploreg.php).

associated with the lower CRC risk (OR: 0.78; 95% CI: 0.65–0.93). Bioinformatics analysis found that these SNPs may be involved in promoter/enhancer histone marks, and protein-bound motifs changed the binding of transcription factors (TFs) and the action of DNase. Figure 1 shows the most significant Hi–C interactions between the variant locus and the target regions.

Table 3 shows the relationship between CRC risk and the different genetic models of *C10orf90* polymorphisms in the overall analysis. Logistic regression analysis showed that, whether corrected or not, there were significant differences in the correlation between SNPs of *C10orf90* rs12412320 and the risk of CRC. Among them, three allele models of rs12412320 (Heterozygous: $p = 0.003$, OR: 0.70, 95% CI: 0.56, 0.89; Dominant: $p = 0.002$, OR:0.71, 95% CI: 0.57, 0.88; Additive: $p = 0.005$, OR: 0.77, 95% CI: 0.64, 0.93, adjusted) were significantly correlated with the risk of CRC. The protective significance of rs12412320 for CRC occurrence still existed after Bonferroni multiple correction ($p < 0.05/3$).

C10orf90 SNPs associated with CRC risk in the stratified analysis

To explore the relationship of three SNPs with CRC, we performed the subgroup stratification analysis by demographic characteristics (age, sex, smoking, drinking, and BMI), as shown in Supplementary Table S1 and Figure 2. After Bonferroni multiple correction, the relationship of rs12412320 in people aged >60 years ($p = 0.008$, OR: 0.65) and ≤60 years ($p = 0.013$, OR: 0.35, and $p = 0.013$, OR: 0.70) and that of rs11245008 in people aged ≤60 years ($p = 0.011$, OR: 1.57) were also remarkable. In the sex-stratified analysis, rs12412320 ($p = 0.001$, OR: 0.56; and $p = 0.005$, OR: 0.61) had a lower CRC risk in women, whereas rs11245007 ($p = 0.011$, OR: 1.30; $p = 0.008$, OR: 1.52; and $p = 0.011$, OR: 1.29) had a higher CRC susceptibility among men after Bonferroni multiple correction. After Bonferroni multiple correction, *C10orf90* rs12412320 was also significantly associated with CRC in non-smokers ($p = 0.001$, OR: 0.58; $p = 0.001$, OR: 0.60; and $p = 0.004$, OR: 0.71) and non-drinkers ($p = 0.003$, OR: 0.70; $p < 0.001$, OR: 0.57; $p < 0.001$, OR: 0.58; and $p = 0.002$, OR: 0.69).

Stratified analysis by clinical features (stage, lymph node metastasis, and cancer style) for the association between *C10orf90* variants and the risk of CRC is displayed in Supplementary Table S2 and Figure 3. After Bonferroni multiple correction, rs12412320 ($p = 0.002$, OR: 0.52; $p = 0.008$, OR: 0.23; $p = 0.010$, OR: 0.51; and $p = 0.003$, OR: 0.53) was related to the lower risk of advanced stages (III/IV stage), while rs11245007 ($p = 0.001$, OR: 1.80; $p = 0.002$, OR: 3.06; $p = 0.003$,

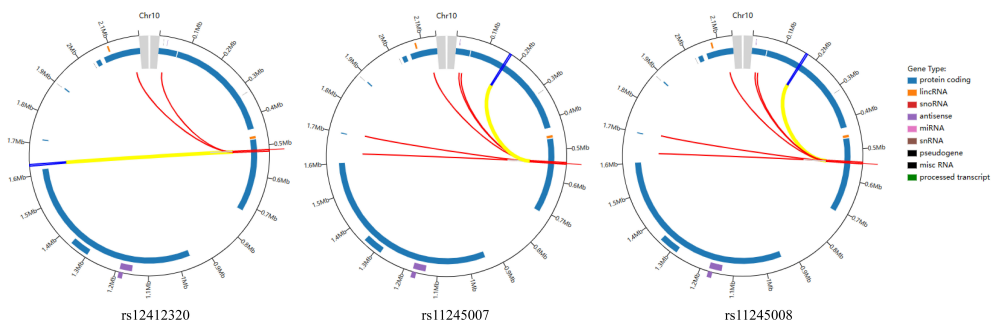

FIGURE 1
Virtual 4C circular plot for the most significant Hi–C interactions between the variant locus and the target regions.

OR: 2.53; and $p = 0.002$, OR: 1.71) might be associated with the higher risk of advanced stages (III/IV stage). Rs12412320 ($p = 0.009$, OR: 0.69; and $p = 0.016$, OR: 0.72) had the most significant relationship with the susceptibility of rectal cancer after Bonferroni multiple correction. Moreover, rs12412320 was associated with the risk of colon cancer, but no significance was found after Bonferroni multiple correction.

MDR analysis for *C10orf90* variants

Then, the relationship between the interaction of *C10orf90* SNPs and CRC risk was analyzed by the MDR method. The results of the MDR model analysis of the SNP–SNP interactions are demonstrated in Table 4 and Figure 4. The dendrogram (Figure 4A) shows that loci with strong interactions were located very close to each other on the branches, while loci with weak interactions were far apart from each other. The most significant single-locus model was rs12412320 [testing accuracy: 0.5338, $p = 0.0077$, cross-validation consistency (CVC): 10/10] with an information gain of 0.50% (Figure 4B); the best two-locus models were rs12412320 and rs11245008 (testing accuracy: 0.5308, $p = 0.0041$, CVC: 6/10); and the best three-locus models were rs12412320, rs11245007, and rs11245008 (testing accuracy: 0.5300, $p = 0.0007$, CVC: 10/10), which is the best SNP–SNP interaction model. Therefore, the impact of the three candidate SNPs on the risk of CRC may be interdependent.

TABLE 3 Selected variants in C10orf90 associated with the risk of colorectal cancer.

SNP	Model	Genotype	Control	Case	Without adjusted		With adjusted	
					OR (95% CI)	p	OR (95% CI)	p
rs12412320	Genotype	G/G	377 (56.1%)	427 (64.1%)	1			
		G/T	255 (38.0%)	205 (30.8%)	0.71 (0.56, 0.89)	**0.004***	0.70 (0.56, 0.89)	**0.003***
		T/T	40 (6.0%)	34 (5.1%)	0.75 (0.46, 1.21)	0.239	0.74 (0.46, 1.19)	0.211
	Dominant	G/G	377 (56.1%)	427 (64.1%)	1			
		G/T-T/T	295 (43.9%)	239 (35.9%)	0.72 (0.57, 0.89)	**0.003***	0.71 (0.57, 0.88)	**0.002***
	Recessive	G/G-G/T	632 (94.0%)	632 (94.9%)	1			
		T/T	40 (6.0%)	34 (5.1%)	0.85 (0.53, 1.36)	0.498	0.84 (0.52, 1.34)	0.463
	Additive	—	—	—	0.78 (0.65, 0.93)	**0.007***	0.77 (0.64, 0.93)	**0.005***
rs11245007	Genotype	C/C	207 (30.9%)	192 (28.8%)	1			
		C/T	322 (48.0%)	308 (46.2%)	1.03 (0.80, 1.33)	0.810	1.04 (0.81, 1.34)	0.747
		T/T	142 (21.2%)	166 (24.9%)	1.26 (0.94, 1.70)	0.128	1.27 (0.94, 1.72)	0.113
	Dominant	C/C	207 (30.9%)	192 (28.8%)	1			
		C/T-T/T	464 (69.2%)	474 (71.2%)	1.10 (0.87, 1.39)	0.420	1.13 (0.88, 1.41)	0.375
	Recessive	C/C-C/T	529 (78.8%)	500 (75.1%)	1			
		T/T	142 (21.2%)	166 (24.9%)	1.24 (0.96, 1.60)	0.103	1.24 (0.96, 1.61)	0.098
	Additive	—	—	—	1.12 (0.96, 1.30)	0.144	1.12 (0.97, 1.30)	0.127
rs11245008	Genotype	C/C	524 (77.9%)	497 (74.6%)	1			
		C/T	135 (20.1%)	155 (23.3%)	1.21 (0.93, 1.57)	0.152	1.21 (0.93, 1.58)	0.148
		T/T	14 (2.1%)	14 (2.1%)	1.05 (0.50, 2.23)	0.890	1.03 (0.49, 2.20)	0.931
	Dominant	C/C	524 (77.9%)	497 (74.6%)	1			
		C/T-T/T	149 (22.1%)	169 (25.4%)	1.20 (0.93, 1.54)	0.164	1.20 (0.93, 1.54)	0.164
	Recessive	C/C-C/T	659 (97.9%)	652 (97.9%)	1			
		T/T	14 (2.1%)	14 (2.1%)	1.01 (0.48, 2.14)	0.978	0.99 (0.47, 2.11)	0.987
	Additive	—	—	—	1.15 (0.92, 1.44)	0.218	1.15 (0.92, 1.44)	0.223

SNP, Single nucleotide polymorphis; OR, Odds ratio; 95% CI, 95% confidence interval.
p values were calculated by logistic regression analysis without and with adjusted by sex, age, smoking, and drinking
*$p < 0.05$ was considered statistical significance.
Bold p means that the data is statistically significant after Bonferroni correction ($p < 0.05/3$).

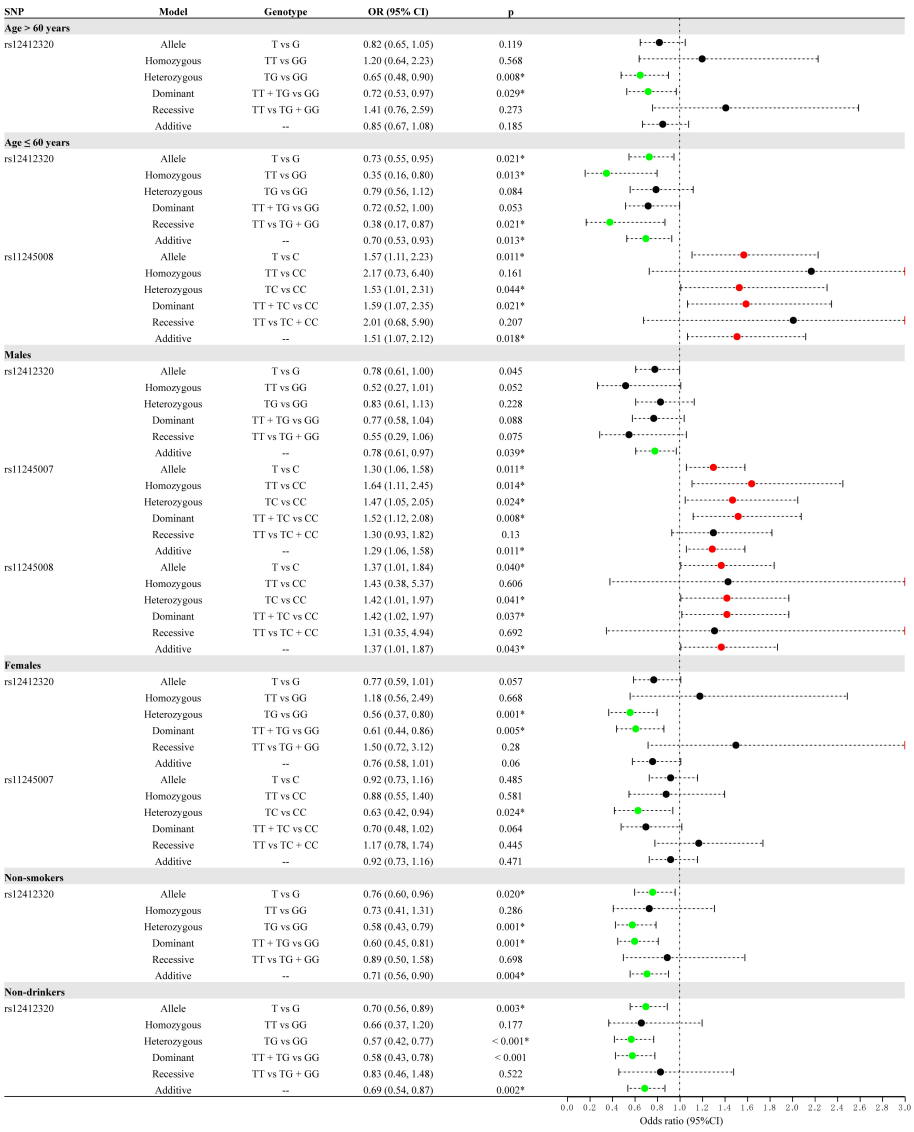

FIGURE 2
Forest map for the stratification analysis by demographic characteristics (age, sex, smoking, and drinking) for the association between *C10orf90* variants and colorectal cancer (CRC) risk.

Discussion

The multi-disciplinary approach that combines genetics, immunology, and chemotherapy has the potential to revolutionize the treatment of CRC and other types of cancer as well. One of the major challenges in cancer treatment is the heterogeneity of tumors, which can make it difficult to develop effective therapies. However, by understanding the molecular mechanisms underlying cancer and the role of the immune system in cancer development and progression, researchers can develop personalized treatment approaches that target the specific characteristics of each patient's tumor (18). Genetic factors are important influencing factors of CRC. Research shows that approximately 5% of CRC is caused by chromosomal variation, which is hereditary (19). Previous studies have reported many loci associated with the risk of CRC (20–22). However, the specific molecular mechanism of CRC has not been fully understood. There are still a large number of loci that may affect the risk of CRC that have not been reported. Therefore, further exploring the relationship between gene SNPs and CRC risk is much more significant and useful for the specific diagnosis on CRC. As a tumor suppressor associated with fragile sites, *C10orf90* is involved in DNA damage-induced carcinogenesis. *C10orf90* overexpression significantly enhances the sensitivity of non-small cell lung cancer (NSCLC) cells to cisplatin, and is related to the overall survival rate (23). In this study, we analyzed the association between genetic polymorphisms of *C10orf90* and the risk of CRC in 1,339 Chinese people. The results displayed that the genetic polymorphisms of *C10orf90* were significantly associated with the risk of CRC, especially SNP rs12412320. Here, we had reported for the first time that *C10orf90* rs12412320 was associated with a

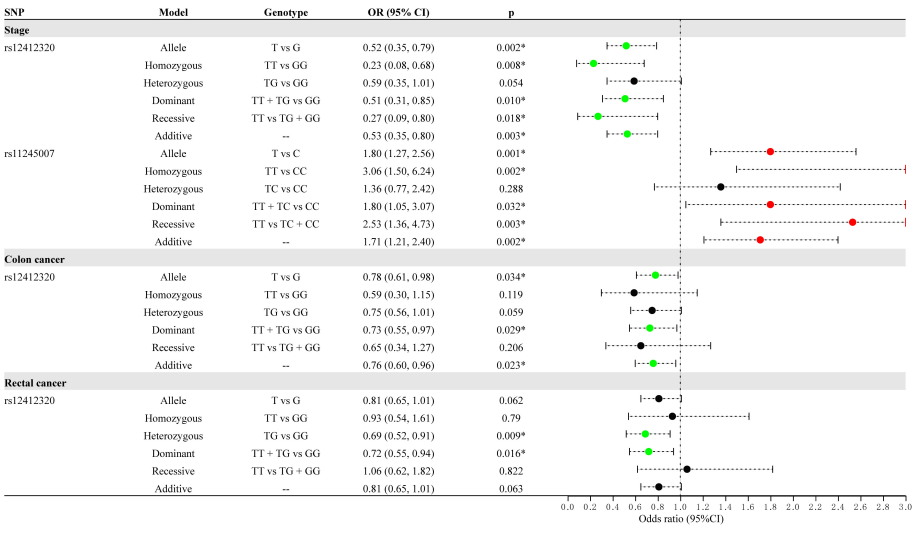

FIGURE 3
Forest map for the stratification analysis by clinical features (cancer type and stage) for the association between *C10orf90* variants and colorectal cancer (CRC) risk.

reduced risk of CRC in the Chinese Han population. There are currently few reports on this locus. Bioinformatics analysis revealed that these SNPs may be related to promoter/enhancer histone marks, and protein-bound motifs changed the binding of TFs and the action of DNase. This indicates that *C10orf90* rs12412320 may affect the risk of CRC by affecting the expression of the gene.

At present, it is universally recognized that the occurrence of CRC is related to immutable risk factors, including age, sex, genetic factors, environment, and lifestyle (6, 7, 24). CRC usually appears after 50 years of age, and the incidence rate of CRC in women is low, usually accounting for one-third of the total incidence rate (25). The combination of tobacco and alcohol increases the risk of cancer. Smoking increases the susceptibility to CRC in a dose-dependent manner with intensity and duration (26). Alcohol consumption and obesity are considered modifiable risk factors for CRC (27, 28). The stratification analysis was explored for the effect of demographic characteristics (age, sex, smoking, drinking, and BMI) on the relationship of three SNPs with CRC. After Bonferroni multiple correction, the relationship of rs12412320 with lower CRC risk was found in people aged >60 years and ≤60 years, women, non-smokers, or non-drinkers. Some studies have suggested that smoking, which created a hypoxic microenvironment that was quite common in solid tumors, might cooperate with genetic polymorphism to produce a superimposed effect on the progression of CRC (29). Previously, possible interactions between GWAS-identified CRC susceptibility SNPs and alcohol consumption were investigated, and genetic polymorphisms were associated with increased risk of CRC among ever drinkers and higher-level alcohol drinkers, suggesting that alcohol consumption could be a possible effect modifier (30). Our study found that *C10orf90* rs12412320 was associated with a reduced risk of CRC overall. The stratification analysis showed that *C10orf90* rs12412320 was also significantly associated with CRC in non-smokers and non-drinkers, but not smokers and drinkers. These results suggested that not smoking or not drinking was found to reduce the likelihood of CRC risk among the population who carried *C10orf90* rs12412320-T allele. Moreover, rs11245008 in people aged ≤60 years and rs11245007 among men had a higher CRC susceptibility after Bonferroni multiple correction. Functional analysis demonstrated that rs11245007, a functional variant of *C10orf90*, can modulate p53 activation, resulting from the more pronounced polyubiquitination of p53 by rs11245007-T (mutant allele) (16). Song et al. showed that rs11245007 played a vital role in preventing the occurrence of breast cancer (16). Here, rs11245007 can increase the risk of CRC in men, which is opposite to its role in breast cancer. It may be caused by the different pathogenesis of various diseases, tumor heterogeneity, and so on. Our study provides

TABLE 4 Summary of SNP – SNP interactions on the risk of colorectal cancer analyzed through MDR method.

Model	Training Bal. Acc. (%)	Testing Bal. Acc. (%)	CVC	OR (95% CI)	*p*
rs12412320	0.54	0.54	10/10	1.40 (1.13, 1.75)	**0.0025**
rs12412320, rs11245008	0.54	0.53	5/10	1.42 (1.14, 1.77)	**0.0015**
rs12412320, rs11245007, rs11245008	0.55	0.53	10/10	1.48 (1.20, 1.84)	**0.0003**

MDR, multifactor dimensionality reduction; Bal. Acc., balanced accuracy; CVC, cross–validation consistency; OR, odds ratio; CI, confidence interval.
p values were calculated using Chi-square test, two sided.
Bold indicates statistical significance at P < 0.05.

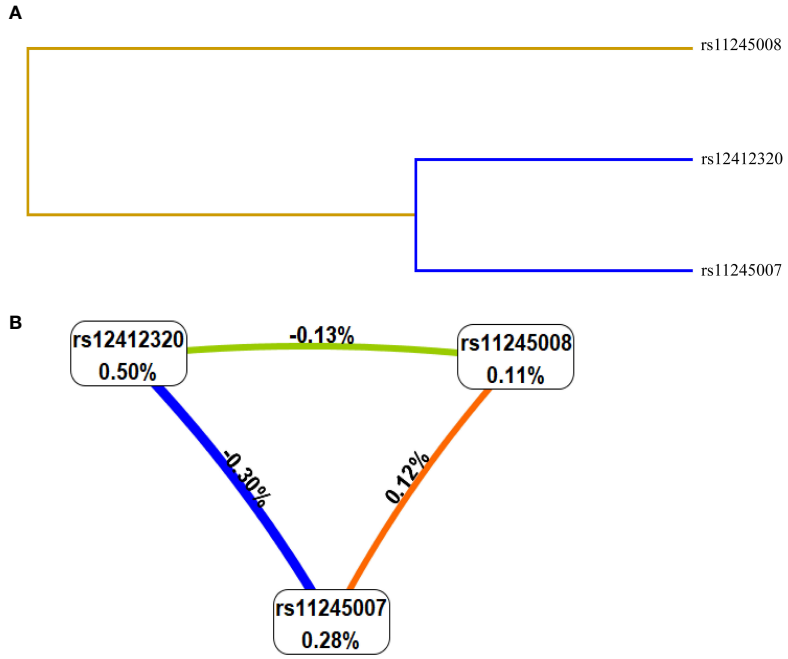

FIGURE 4
Interaction map among single-nucleotide polymorphisms (SNPs) of genes on the risk of colorectal cancer (CRC). Values in nodes represent the information gain (IGs) of individual attribute (main effects). Values between nodes are IGs of each pair of attributes (interaction effects). SNP-SNP interaction dendrogram **(A)** and Fruchterman-Reingold **(B)**.

evidence to clarify that the pathogenic effect on CRC may be partially attributed to the interaction between *C10orf90* variants and age, sex, smoking, and alcohol consumption.

The clinical characteristics of CRC patients are related to prognosis, and the complex interaction between staging, metastasis, and genetic factors plays a role in guiding prognosis, risk stratification, and adjuvant treatment of CRC (31, 32). In the study, stratified analysis by clinical features (stage, lymph node metastasis, and cancer style) for the association between *C10orf90* variants and the risk of CRC was investigated. After Bonferroni multiple correction, rs12412320 was related to the lower risk of advanced stages (III/IV stage), while rs11245007 might be associated with the higher risk of advanced stages (III/IV stage). Moreover, rs12412320 had the most significant relationship with the susceptibility of rectal cancer after Bonferroni multiple correction.

Unavoidably, this study has several limitations. Firstly, the study was conducted in a single hospital in Hainan Province, China, which limits the generalizability of the results to other populations. Secondly, because a proportion of the samples lack information on environmental factors (such as diet, physical activity, and environmental factors) and because of the relatively small sample size, our study did not explain the role of the interaction between *C10orf90* variants and environmental factors on CRC risk. In the future, we would like to increase the sample size and complete the environmental factors to evaluate the relationship and to verify our findings. Thirdly, only three SNPs of *C10orf90* were studied in this study, and other genetic variants that may play a role in CRC susceptibility were not investigated. Experimental design will continue to explore the correlation of other loci on this gene with CRC risk in the future. Fourthly, the mechanism of these SNPs is only predicted through bioinformatics analysis; therefore, functional experiments are needed to further explore the function of *C10orf90* loci in CRC etiology. Fifthly, CRC patients' tissues and normal tissues had not been explored in protein expression studies. In subsequent research, we plan to collect enough CRC patients' tissues and normal tissues to examine them *via* immunohistochemistry (IHC) using protein expression studies and to conduct functional research of these SNPs in CRC.

Conclusion

In summary, this study is the first to report the relationship between *C10orf90* gene polymorphisms and CRC risk in Chinese people, which suggests that *C10orf90* rs12412320 might play a crucial role in preventing CRC occurrence. It provides the foundation for the study on the mechanism of *C10orf90* in CRC and supplies the basis for personalized treatment of CRC patients.

Data availability statement

The original contributions presented in the study are included in the article/Supplementary Material. Further inquiries can be directed to the corresponding author.

Ethics statement

The studies involving human participants were reviewed and approved by Hainan Cancer Hospital. The patients/participants provided their written informed consent to participate in this study.

Author contributions

JS and KW wrote the manuscript, ZC and DZ processed and analyzed the results, LL and LG prepared Figure 1 and collected data, and SY designed the research ideas and plans. All the authors reviewed the manuscript. All authors contributed to the article and approved the submitted version.

Funding

This work was supported by 2020 Hainan Province Major Science and Technology Plan Project (ZDKJ202005) and supported by the specific research fund of The Innovation Platform for Academinicians of Hainan Province(YSPTZX202029).

Acknowledgments

The authors thank all participants and volunteers in this study.

Conflict of interest

The authors declare that the research was conducted in the absence of any commercial or financial relationships that could be construed as a potential conflict of interest.

Publisher's note

Supplementary material

The Supplementary Material for this article can be found online at: https://www.frontiersin.org/articles/10.3389/fonc.2023.1192378/full#supplementary-material

References

1. Sung H, Ferlay J, Siegel RL, Laversanne M, Soerjomataram I, Jemal A, et al. Global cancer statistics 2020: GLOBOCAN estimates of incidence and mortality worldwide for 36 cancers in 185 countries. *CA: Cancer J Clin* (2021) 71(3):209–49. doi: 10.3322/caac.21660

2. Li N, Lu B, Luo C, Cai J, Lu M, Zhang Y, et al. Incidence, mortality, survival, risk factor and screening of colorectal cancer: a comparison among China, Europe, and northern America. *Cancer Lett* (2021) 522:255–68. doi: 10.1016/j.canlet.2021.09.034

3. Huang RL, Liu Q, Wang YX, Zou JY, Hu LF, Wang W, et al. Awareness, attitude and barriers of colorectal cancer screening among high-risk populations in China: a cross-sectional study. *BMJ Open* (2021) 11(7):e045168. doi: 10.1136/bmjopen-2020-045168

4. Deng X, Gao F, Li N, Li Q, Zhou Y, Yang T, et al. Antitumor activity of NKG2D CAR-T cells against human colorectal cancer cells *in vitro* and *in vivo*. *Am J Cancer Res* (2019) 9(5):945–58.

5. Wang H, Wang P, Liu X, Li L, Xiao X, Liu P, et al. Factors predicting the colorectal adenoma detection rate in colonoscopic screening of a Chinese population: a prospective study. *Medicine* (2019) 98(15):e15103. doi: 10.1097/MD.0000000000015103

6. Thanikachalam K, Khan G. Colorectal cancer and nutrition. *Nutrients* (2019) 11(1):164. doi: 10.3390/nu11010164

7. Baidoun F, Elshiwy K, Elkeraie Y, Merjaneh Z, Khoudari G, Sarmini MT, et al. Colorectal cancer epidemiology: recent trends and impact on outcomes. *Curr Drug Targets* (2021) 22(9):998–1009. doi: 10.2174/1389450121999201117115717

8. O'Sullivan DE, Sutherland RL, Town S, Chow K, Fan J, Forbes N, et al. Risk factors for early-onset colorectal cancer: a systematic review and meta-analysis. *Clin Gastroenterol Hepatol* (2022) 20(6):1229–1240.e1225. doi: 10.1016/j.cgh.2021.01.037

9. Rebuzzi F, Ulivi P, Tedaldi G. Genetic predisposition to colorectal cancer: how many and which genes to test? *Int J Mol Sci* (2023) 24(3):2137. doi: 10.3390/ijms24032137

10. Quistrebert J, Orlova M, Kerner G, Ton LT, Luong NT, Danh NT, et al. Genome-wide association study of resistance to mycobacterium tuberculosis infection identifies a locus at 10q26.2 in three distinct populations. *PloS Genet* (2021) 17(3):e1009392. doi: 10.1371/journal.pgen.1009392

11. Kenawy N, Kalirai H, Sacco JJ, Lake SL, Heegaard S, Larsen AC, et al. Conjunctival melanoma copy number alterations and correlation with mutation status, tumor features, and clinical outcome. *Pigment Cell melanoma Res* (2019) 32(4):564–75. doi: 10.1111/pcmr.12767

12. Zhang X, Zhang Q, Zhang J, Qiu L, Yan SS, Feng J, et al. FATS is a transcriptional target of p53 and associated with antitumor activity. *Mol Cancer* (2010) 9:244. doi: 10.1186/1476-4598-9-244

13. Yan S, Qiu L, Ma K, Zhang X, Zhao Y, Zhang J, et al. FATS is an E2-independent ubiquitin ligase that stabilizes p53 and promotes its activation in response to DNA damage. *Oncogene* (2014) 33(47):5424–33. doi: 10.1038/onc.2013.494

14. Zhang TM, Zhang J, Zhou DJ, Wang CL. [Expression of FATS in non-small cell lung cancer and its relationship with prognosis]. *Zhonghua zhong liu za zhi [Chinese J oncology]* (2019) 41(11):826–30. doi: 10.3760/cma.j.issn.0253-3766.2019.11.005

15. Zhang J, Wu N, Zhang T, Sun T, Su Y, Zhao J, et al. et al: the value of FATS expression in predicting sensitivity to radiotherapy in breast cancer. *Oncotarget* (2017) 8(24):38491–500. doi: 10.18632/oncotarget.16630

16. Song F, Zhang J, Qiu L, Zhao Y, Xing P, Lu J, et al. A functional genetic variant in fragile-site gene FATS modulates the risk of breast cancer in triparous women. *BMC Cancer* (2015) 15:559. doi: 10.1186/s12885-015-1570-9

17. Yoshino T, Argilés G, Oki E, Martinelli E, Taniguchi H, Arnold D, et al. Pan-Asian adapted ESMO clinical practice guidelines for the diagnosis treatment and follow-up of patients with localised colon cancer. *Ann Oncol* (2021) 32(12):1496–510. doi: 10.1016/j.annonc.2021.08.1752

18. Derakhshani A, Hashemzadeh S, Asadzadeh Z, Shadbad MA, Rasibonab F, Safarpour H, et al. et al: cytotoxic T-lymphocyte antigen-4 in colorectal cancer: another therapeutic side of capecitabine. *Cancers* (2021) 13(10):2414. doi: 10.3390/cancers13102414

19. Heinimann K. [Hereditary colorectal cancer: clinics, diagnostics and management]. *Therapeutische Umschau Rev therapeutique* (2018) 75(10):601–6. doi: 10.1024/0040-5930/a001046

20. Yu J, Feng Q, Wong SH, Zhang D, Liang QY, Qin Y, et al. Metagenomic analysis of faecal microbiome as a tool towards targeted non-invasive biomarkers for colorectal cancer. *Gut* (2017) 66(1):70–8. doi: 10.1136/gutjnl-2015-309800

21. Fernandez-Rozadilla C, Timofeeva M, Chen Z, Law P, Thomas M, Schmit S, et al. Deciphering colorectal cancer genetics through multi-omic analysis of 100,204 cases and 154,587 controls of European and east Asian ancestries. *Nat Genet* (2023) 55(1):89–99. doi: 10.1038/s41588-022-01222-9

22. Huyghe JR, Bien SA, Harrison TA, Kang HM, Chen S, Schmit SL, et al. Discovery of common and rare genetic risk variants for colorectal cancer. *Nat Genet* (2019) 51(1):76–87. doi: 10.1038/s41588-018-0286-6

23. Tian Y, Zhang J, Yan S, Qiu L, Li Z. FATS expression is associated with cisplatin sensitivity in non small cell lung cancer. *Lung Cancer (Amsterdam Netherlands)* (2012) 76(3):416–22. doi: 10.1016/j.lungcan.2011.11.009

24. Kim SE, Paik HY, Yoon H, Lee JE, Kim N, Sung MK. Sex- and gender-specific disparities in colorectal cancer risk. *World J Gastroenterol* (2015) 21(17):5167–75. doi: 10.3748/wjg.v21.i17.5167

25. Hultcrantz R. Aspects of colorectal cancer screening, methods, age and gender. *J Internal Med* (2021) 289(4):493–507. doi: 10.1111/joim.13171

26. Botteri E, Borroni E, Sloan EK, Bagnardi V, Bosetti C, Peveri G, et al. Smoking and colorectal cancer risk, overall and by molecular subtypes: a meta-analysis. *Am J Gastroenterol* (2020) 115(12):1940–9. doi: 10.14309/ajg.0000000000000803

27. Lauby-Secretan B, Scoccianti C, Loomis D, Grosse Y, Bianchini F, Straif K. Body fatness and cancer–viewpoint of the IARC working group. *N Engl J Med* (2016) 375 (8):794–8. doi: 10.1056/NEJMsr1606602

28. Zhou X, Wang L, Xiao J, Sun J, Yu L, Zhang H, et al. Alcohol consumption, DNA methylation and colorectal cancer risk: results from pooled cohort studies and mendelian randomization analysis. *Int J Cancer* (2022) 151(1):83–94. doi: 10.1002/ijc.33945

29. Fu Y, Zhang Y, Cui J, Yang G, Peng S, Mi W, et al. SNP rs12982687 affects binding capacity of lncRNA UCA1 with miR-873-5p: involvement in smoking-triggered colorectal cancer progression. *Cell Communication Signaling CCS* (2020) 18 (1):37. doi: 10.1186/s12964-020-0518-0

30. Song N, Shin A, Oh JH, Kim J. Effects of interactions between common genetic variants and alcohol consumption on colorectal cancer risk. *Oncotarget* (2018) 9 (5):6391–401. doi: 10.18632/oncotarget.23997

31. Chen K, Collins G, Wang H, Toh JWT. Pathological features and prognostication in colorectal cancer. *Curr Oncol (Toronto Ont)* (2021) 28(6):5356–83. doi: 10.3390/curroncol28060447

32. Patel SG, Karlitz JJ, Yen T, Lieu CH, Boland CR. The rising tide of early-onset colorectal cancer: a comprehensive review of epidemiology, clinical features, biology, risk factors, prevention, and early detection. *Lancet Gastroenterol Hepatol* (2022) 7 (3):262–74. doi: 10.1016/S2468-1253(21)00426-X

Frontiers in Oncology

Advances knowledge of carcinogenesis and tumor progression for better treatment and management

The third most-cited oncology journal, which highlights research in carcinogenesis and tumor progression, bridging the gap between basic research and applications to imrpove diagnosis, therapeutics and management strategies.

Discover the latest Research Topics

See more →

Frontiers

Avenue du Tribunal-Fédéral 34
1005 Lausanne, Switzerland
frontiersin.org

Contact us

+41 (0)21 510 17 00
frontiersin.org/about/contact